ARMEL PICQUENARD

RADIO WAVE PROPAGATION

Philips Technical Library

RADIO WAVE PROPAGATION

Philips Technical Library

RADIO WAVE PROPAGATION

ARMEL PICQUENARD

MACMILLAN EDUCATION

ISBN 978-1-349-01396-8 ISBN 978-1-349-01394-4 (eBook)
DOI 10.1007/978-1-349-01394-4

Softcover reprint of the hardcover 1st edition 1974 978-0-333-13312-5

SBN 333 13312 9

First published 1974 by
THE MACMILLAN PRESS LTD
London and Basingstoke
Associated companies in New York Melbourne
Dublin Johannesburg and Madras

Library of Congress
Catalog No: 72-2046

PHILIPS

CONTENTS

INTRODUCTION

While it is possible to build transmitters, receivers and antennae with defined characteristics, radio waves are submitted during their travel between transmitter and receiver to physical laws over which we have no control.

The practical results of these laws are so important that they affect the circuit quality to a far greater extent than do the terminal equipments. If the designers did not take these laws into account, the link would often be impossible to build, and even if it were possible, excessive capital investment would be needed.

Assuming the technical specification of transmitter and receiver, the location and performance of the antennae, we would have an ideal situation if we could forecast for every instant the quality of the resultant communication circuit. This ideal situation cannot at this present time, and most probably will never, be attained.

A great number of external factors act on the wave propagation (the various states of atmosphere and ionosphere); the effect of these factors depends on the characteristics of the installation (frequency, antennae, mode of modulation). The external factors are random variables in time and location. Finally, in addition to the waves intentionally produced by the transmitter, the receiver is also affected by a number of noise sources.

The problem is very intricate indeed, and since Hertz's original work, the best scientists of all countries have made every effort to formulate usable laws from the apparent chaos of experimental results. Moreover, these laws are usually of a statistical nature, i.e. the results have a larger or smaller probability of happening. This fact does not reduce their practical application, but it makes their interpretation more critical. We can say in general that a very high probability implies high certainty of continuous communication, while a very low probability implies a possible interference.

Like all the phenomena of physics, wave propagation may be studied from two complementary standpoints.

The physicist attempts to isolate the causes, to study them and to deduce their effects. In this way he obtains universal laws, which not only apply to the known facts, but also to those that will be subsequently discovered. The main subjects to be studied are the ground, the atmosphere, the ionosphere and noise. Unfortunately, it is very difficult to isolate the effect of any individual factor, and while the majority of these factors are well appreciated, it is generally difficult to relate them to the observed effects, except by very general and rather indefinite rules.

The engineer prefers to measure the effects and deduce from them more or less empirical laws, which may only be valid over a narrow field, but which can be used immediately. However, field experiments are expensive and time-consuming, and do not allow one to reproduce all the possible conditions—far from it.

Consequently, a merging of both methods is required. Experience will supply an indisputable basis for theoretical study, as well as a check of its accuracy, while theory will extend the field of application of the obtained results more widely, as well as foresee new ones.

Roughly, this double method will be followed in the present book by discussing the main factors affecting wave propagation, and the semi-empirical rules allowing the calculation of a communication circuit.

In the first chapters of the book, it has been attempted to summarize the present state of our knowledge of wave propagation as far as it concerns the telecommunications engineer. In order to keep this book to a reasonable size, discussion is often limited to more or less heuristic basics.

This part is followed by a few chapters giving graphs which can be used for the calculation of the principal parameters of communication circuits, together with detailed instructions for the use of these graphs.

An Appendix gives a brief review of those concepts of mathematical physics required for the comprehension of the theoretical discussions, together with the method of calculating the signal-to-noise ratio in radio links. This will make it unnecessary for the reader to have to refer to various textbooks for the information he requires. On the other hand, an extensive and easily accessible bibliography will enable the reader to go more deeply into the points which interest him most.

The author's aim will have been attained if this book helps engineers to a better understanding of the complex phenomena connected with the propagation of radio waves, and to use this knowledge to improve understanding between men, which surely is the whole purpose of telecommunications.

CHAPTER 1

PROPAGATION OF RADIO WAVES IN A DIELECTRIC

From a physical standpoint it is evident that the waves radiated by an antenna propagate in all directions in space, since the wave surfaces are closed. However, at a sufficiently large distance from the source, and when considering only the behaviour of the waves in the vicinity of the receiving antenna, we are dealing with plane waves.

1.1 PROPAGATION OF PLANE WAVES

1.1.1 PROPAGATION IN A VACUUM

1.1.1.1 **Radio waves of any type**

In a vacuum, $\sigma = 0$ and $\varepsilon_r = 1$. Equations (A.1) of the Appendix become:

$$\left.\begin{aligned} \nabla \times \boldsymbol{E} &= -\mu_0 \frac{\partial \boldsymbol{H}}{\partial t} \\ \nabla \times \boldsymbol{H} &= \varepsilon_0 \frac{\partial \boldsymbol{E}}{\partial t} \\ \nabla . \boldsymbol{E} &= \nabla . \boldsymbol{H} = 0 \end{aligned}\right\} \tag{1.1}$$

Differentiating the first equation with respect to time:

$$\nabla \times \frac{\partial \boldsymbol{E}}{\partial t} = -\mu_0 \frac{\partial^2 \boldsymbol{H}}{\partial t^2}$$

taking the curl of the second equation:

$$\nabla \times (\nabla \times \boldsymbol{H}) = \varepsilon_0 \times \frac{\partial \boldsymbol{E}}{\partial t} = -\varepsilon_0 \mu_0 \frac{\partial^2 \boldsymbol{H}}{\partial t^2}$$

using the well-known equality

$$\nabla \times (\nabla \times \boldsymbol{A}) = \nabla(\nabla . \boldsymbol{A}) - \nabla^2 \boldsymbol{A}$$

(where $\nabla^2 \boldsymbol{A}$ represents the Laplacian of vector $\boldsymbol{A}$) and taking into account the third equation of (1.1), we find:

$$\nabla^2 \boldsymbol{H} = \varepsilon_0 \mu_0 \frac{\partial^2 \boldsymbol{H}}{\partial t^2} \tag{1.2}$$

We can deduce in the same way:

$$\nabla^2 \boldsymbol{E} = \varepsilon_0 \mu_0 \frac{\partial^2 \boldsymbol{E}}{\partial t^2} \tag{1.2a}$$

Equations (1.2) and (1.2a) are of the same type, and are called 'equations of wave motion' (or sometimes, incorrectly, Laplace equations).

A general solution[2] of this type of equation consists of an infinity of plane waves propagating in all directions at a velocity:

$$\frac{1}{(\varepsilon_0 \mu_0)^{1/2}} = 3 \times 10^8 \,\mathrm{ms}^{-1} = c \quad \text{(the speed of light)}$$

This result is interesting because of its general character, since we have not made any assumption with regard to the nature of the wave (shape of surfaces of equal phase, type of polarization, frequency). It proves that a vacuum is a non-dispersive medium for electromagnetic waves.

We shall now specify the conditions of propagation for the types of wave encountered in practice.

1.1.1.2 Plane monochromatic waves of linear polarization

A wave is monochromatic if its frequency is constant; it possesses linear polarization if the direction of the electric field is fixed.

Using complex terms[1], we can write, at a point in the space:

$$\begin{aligned} \boldsymbol{E} &= \boldsymbol{E}_0 \, \mathrm{e}^{\mathrm{j}(\omega t + \varphi)} \\ \boldsymbol{H} &= \boldsymbol{H}_0 \, \mathrm{e}^{\mathrm{j}(\omega t + \psi)} \end{aligned} \tag{1.3}$$

where $\boldsymbol{E}_0$ is a vector of constant direction.

We relate the space to rectangular references axes $0X$, $0Y$ and $0Z$, being the unit vectors $\boldsymbol{k}$, $\boldsymbol{l}$ and $\boldsymbol{m}$ respectively, and make plane $X0Y$ coincide with the plane of the wave. Since the waves are plane, the $\boldsymbol{E}$ and $\boldsymbol{H}$ vectors are equal at all points on this plane at a given instant. We have:

$$\frac{\partial \boldsymbol{E}}{\partial x} = \frac{\partial \boldsymbol{E}}{\partial y} = \frac{\partial \boldsymbol{H}}{\partial x} = \frac{\partial \boldsymbol{H}}{\partial y} = 0 \tag{1.4}$$

and therefore:

$$\begin{aligned} \nabla \times \boldsymbol{E} &= \boldsymbol{m} \times \frac{\partial \boldsymbol{E}}{\partial z} \\ \nabla \times \boldsymbol{H} &= \boldsymbol{m} \times \frac{\partial \boldsymbol{H}}{\partial z} \end{aligned} \tag{1.5}$$

Taking into account equation (1.3), the first two equations of (1.1) now become:

$$\left.\begin{aligned} \boldsymbol{m} \times \frac{\partial \boldsymbol{E}_0}{\partial z} &= -\mathrm{j}\omega\mu_0 \boldsymbol{H}_0 \, \mathrm{e}^{\mathrm{j}(\psi-\varphi)} \\ \boldsymbol{m} \times \frac{\partial \boldsymbol{H}_0}{\partial z} &= \mathrm{j}\omega\varepsilon_0 \boldsymbol{E}_0 \, \mathrm{e}^{\mathrm{j}(\varphi-\psi)} \end{aligned}\right\} \tag{1.6}$$

The result is that vectors $\boldsymbol{E}$ and $\boldsymbol{H}$, both perpendicular to $\boldsymbol{m}$, are in the plane of the wave.

Rotating the axis in such a way that the direction $0X$ coincides with that of $\boldsymbol{E}$, we can put:

$$\boldsymbol{E}_0 = E_0 \boldsymbol{k}$$

The first equation of (1.6) then becomes:

$$\boldsymbol{m} \times \boldsymbol{k} \frac{\partial E_0}{\partial z} = -\mathrm{j}\omega\mu_0 \boldsymbol{H}_0 \, \mathrm{e}^{\mathrm{j}(\psi-\varphi)}$$

or:

$$\boldsymbol{l} \frac{\partial E_0}{\partial z} = -\mathrm{j}\omega\mu_0 \boldsymbol{H}_0 \, \mathrm{e}^{\mathrm{j}(\psi-\varphi)} \tag{1.7}$$

The magnetic field $\boldsymbol{H}$ is therefore parallel to $0Y$ and hence perpendicular to the electric field $\boldsymbol{E}$.

Making $\boldsymbol{H}_0 = H_0 \boldsymbol{l}$, equations (1.6) become:

$$\left.\begin{aligned} \boldsymbol{m} \times \frac{\partial \boldsymbol{E}_0}{\partial z} &= \mathrm{j}\omega\mu_0 H_0 \boldsymbol{l} \, \mathrm{e}^{\mathrm{j}(\psi-\varphi)} \\ \boldsymbol{m} \times \frac{\partial \boldsymbol{H}_0}{\partial z} &= \mathrm{j}\omega\varepsilon_0 E_0 \boldsymbol{k} \, \mathrm{e}^{\mathrm{j}(\varphi-\psi)} \end{aligned}\right\} \tag{1.8}$$

Remembering that the partial derivatives of $\boldsymbol{E}_0$ and $\boldsymbol{H}_0$ with respect to X and Y are zero (equation (1.4)), we see that the spatial derivatives of $\boldsymbol{E}_0$ and $\boldsymbol{H}_0$ are parallel to the corresponding vector. The result is that the directions of fields $\boldsymbol{E}$ and $\boldsymbol{H}$ are constant throughout the space.

We shall now discuss the scalar values E_1 and H_1 of E and H, from the $X0Y$ plane.

Substituting E_0 and H_0 by E_1 and H_1 in equation (1.7), and putting $\boldsymbol{H}_1 = H_1 \boldsymbol{l}$, we have:

$$\frac{\partial E_1}{\partial z} = -\mathrm{j}\omega\mu_0 H_1 \, \mathrm{e}^{\mathrm{j}(\psi-\varphi)} \tag{1.9}$$

In the same way:

$$\frac{\partial H_1}{\partial z} = -\mathrm{j}\omega\varepsilon_0 E_1 \, \mathrm{e}^{\mathrm{j}(\varphi-\psi)} \tag{1.9a}$$

Differentiating the above equations with respect to z, and substituting one in the other, we find:

$$\left.\begin{aligned}\frac{\partial^2 E_1}{\partial z^2} &= -\omega^2 \varepsilon_0 \mu_0 E_1 = -\frac{\omega^2}{c^2} E_1 \\ \frac{\partial^2 H_1}{\partial z^2} &= -\omega^2 \varepsilon_0 \mu_0 H_1 = -\frac{\omega^2}{c^2} H_1\end{aligned}\right\} \tag{1.10}$$

Indeed, $\varepsilon_0 \mu_0 = 1/c^2$, where c = speed of light; see Appendix 1.1.

The solution of these equations is obvious[1, 2]. Noting that they must reduce to E_0 and H_0 for $z = 0$, we have

$$\left.\begin{aligned}E_1 &= E_0 \, e^{\pm j(\omega z/c)} \\ H_1 &= H_0 \, e^{\pm j(\omega z/c)}\end{aligned}\right\} \tag{1.11}$$

and finally, by means of (1.2):

$$\begin{aligned}E &= E_0 \, e^{j[\omega(t \pm z/c) + \varphi]} \\ H &= H_0 \, e^{j[\omega(t \pm z/c) + \psi]}\end{aligned} \tag{1.12}$$

The waves therefore propagate along the Z-axis. Since we have proved above that vectors $\boldsymbol{E}$ and $\boldsymbol{H}$ are parallel to the plane $X0Y$, the waves are transverse. The plus and minus signs correspond to propagation towards a decreasing value of z and an increasing value of z respectively.

Substituting in (1.9) the values of E_1 and H_1 found in (1.11), we have:

$$\pm E_0 = \mu_0 c H_0 \, e^{j(\psi - \varphi)}$$

Two important conclusions emerge from the above equation:

$$\psi - \varphi = 0$$

which means that the electric and magnetic fields are in phase, and

$$\frac{E_0}{H_0} = Z_0 = \mu_0 c = 377\,\Omega$$

Z_0 is called the intrinsic impedance of free space.

1.1.1.3 **Elliptically polarized waves**

If we were dealing with an elliptical oscillation, we would have found similar results. The axes of the ellipse described by each component of the field would remain in a constant direction, and would be perpendicular to the corresponding axes of the ellipse described by the other component. These results can be obtained directly by splitting the elliptical oscillation into two linear ones with a phase difference of $\pi/2$.

The elliptical oscillation may be clockwise or counterclockwise, depending on the sense of rotation of the field vector. A particular case is circular oscillation, where the field vector remains constant when rotating around the direction of propagation with a frequency equal to that of the wave.

1.1.1.4 Non-monochromatic waves

Since a vacuum is non-dispersive (Section 1.1.1.1), the propagation of a non-monochromatic wave is similar to that of a monochromatic wave.

1.1.2 PROPAGATION IN A DIELECTRIC

Here we still have $\sigma = 0$, but $\varepsilon_r > 1$. The previously stated results apply with the following modifications, which can be easily obtained by replacing ε_0 by $\varepsilon_0\varepsilon_r$ everywhere:

(a) The velocity of propagation is:

$$v = \frac{1}{(\varepsilon_0\varepsilon_r\mu_0)^{\frac{1}{2}}} = \frac{c}{\varepsilon_r^{\frac{1}{2}}} \tag{1.13}$$

In analogy with optics we put:

$$\varepsilon_r^{\frac{1}{2}} = n \quad \text{(refractive index)} \tag{1.14}$$

(b) The ratio of the fields becomes:

$$\frac{E_0}{H_0} = \frac{Z_0}{\varepsilon_r^{\frac{1}{2}}} = \frac{Z_0}{n} = Z_c \tag{1.15}$$

where Z_c = intrinsic impedance of the medium, or wave impedance. Measured in ohms, it is equal to $377/n$.

Since the E and H fields are in phase, the same relation applies at all points for their instantaneous values:

$$\frac{E}{H} = Z_c = \frac{Z_0}{n} \tag{1.16}$$

This means that the velocity of propagation, as well as the ratio of the electric field to the magnetic field are inversely proportional to the square root of the dielectric constant, i.e. to the refractive index. They are therefore smaller than in free space.

1.1.3 ENERGY PROPAGATION

Equations (A.3) and (A.3a) of the Appendix give the total energy per unit volume in a space under the influence of a magnetic field.

$$W = \tfrac{1}{2}(\varepsilon_0\varepsilon_r E^2 + \mu_0 H^2) = \varepsilon_0\varepsilon_r E_{\text{rms}}^2 + \mu_0 H_{\text{rms}}^2$$

Using equation (1.16) we can write:

$$W = EH(\varepsilon_0\varepsilon_r\mu_0)^{\frac{1}{2}}$$

As fields E and H propagate along $0Z$ at a velocity v, the same occurs for every function of these fields, in particular the energy.

Let us now consider an elemental cylinder of height $\mathrm{d}x$ in the direction of propagation with a cross-section equal to the unit area. The energy in this cylinder will be:

$$\mathrm{d}w = EH(\varepsilon_0\varepsilon_r\mu_0)^{\frac{1}{2}}\,\mathrm{d}x$$

Propagating at a velocity v, this quantity of energy will have traversed the unit area in the direction of propagation after a time:

$$dt = \frac{dx}{v}$$

The power traversing the unit area will then be:

$$P = \frac{dw}{dt} = \frac{v\,dw}{dx} = vEH(\varepsilon_0\varepsilon_r\mu_0)^{\frac{1}{2}}$$

or, taking into account equation (1.13):

$$P = EH$$

which is a particular case of Poynting's theorem[4, 15]. This equation relates to instantaneous power. Since E and H are sinusoidal, we have for the mean power:

$$P_{\text{mean}} = \frac{E_0 H_0}{2} = E_{\text{rms}} H_{\text{rms}} \tag{1.17}$$

Using again equation (1.12), we can write:

$$P_{\text{mean}} = \tfrac{1}{2}E_0^2/Z_c = E_{\text{rms}}^2/Z_c \tag{1.17a}$$

and

$$P_{\text{mean}} = \tfrac{1}{2}Z_c H_0^2 = Z_c H_{\text{rms}}^2 \tag{1.17b}$$

We notice the analogy of these equations to those representing Joule's Laws.

1.2 SPHERICAL WAVES

The waves radiated by an antenna are in fact not plane waves but cylindrical waves. We must of course consider them as such when studying the radiation of an antenna as a whole, instead of the behaviour of waves in the vicinity of a point at a large distance from the antenna.

1.2.1 ENERGY PROPAGATION BY SPHERICAL WAVES

As a consequence of the law of conservation of energy, all energy radiated by a source will traverse a closed surface surrounding this source.

In particular, if the source radiates continuously, the radiated power will continuously traverse any closed surface surrounding the source. If the source is located in a dielectric, equations (1.17), (1.17a) and (1.17b) allow us to write:

$$P = \iint_S \frac{EH}{2}\,dS = \iint_S \frac{E^2}{2Z_c}\,dS = \iint_S \frac{Z_c H^2}{2}\,dS \tag{1.18}$$

where S is a closed surface surrounding the source, and located at several wavelengths from the latter, E and H are the amplitudes of the fields on the surface under consideration.

1.2.2 FIELD PRODUCED BY A GIVEN POWER

Conversely, if the radiation pattern of a source is known, we can calculate the value of the field in a given direction as a function of the radiated power. Some cases are of particular interest as the results are frequently used in propagation calculations.

1.2.2.1 **Antenna in free space**

An antenna may be considered as being in free space if it is situated a large number of wavelengths above the ground.

Isotropic antenna

An ideal antenna which—like an optical point source—would radiate an equal field in all directions is called an isotropic antenna. Such an antenna cannot be realized, and in fact would not be of any interest; it can however be used as a mathematical reference model for evaluating the properties of a given antenna.

For this antenna, with E = amplitude of the (constant) electric field it radiates, we have:

$$P = \iint_S \frac{E^2}{2Z_0}\,\mathrm{d}S = \frac{E^2 S}{2Z_0}$$

because E = constant.

At the surface S of a sphere of radius d, we have:

$$P = \frac{4\pi E^2 d^2}{2 \times 120\pi} = \frac{E^2 d^2}{60}$$

$$E = 60^{\frac{1}{2}} \frac{P^{\frac{1}{2}}}{d} \tag{1.19}$$

and

$$E_{\mathrm{rms}} = \frac{E}{2^{\frac{1}{2}}} = 30^{\frac{1}{2}} \frac{P^{\frac{1}{2}}}{d} \tag{1.20}$$

Elemental dipole, which is short in relation to the wavelength

We take for the surface S a sphere of radius d. If the dipole is aligned along the axis $0Y$, and making E_0 the field in the equatorial plane, we have for the geometry of Fig. 1:

$$E = E_0 \cos\theta$$

$$\mathrm{d}S = d^2 \cos\theta\,\mathrm{d}\varphi\,\mathrm{d}\theta$$

and hence:

$$P = \iint_S \frac{E_0^2 \cos^2\theta}{2Z_o} d^2 \cos\theta\,\mathrm{d}\varphi\,\mathrm{d}\theta = \frac{E^2 d^2}{90}$$

$$E_0 = 90^{\frac{1}{2}} \frac{P^{\frac{1}{2}}}{d} \tag{1.21}$$

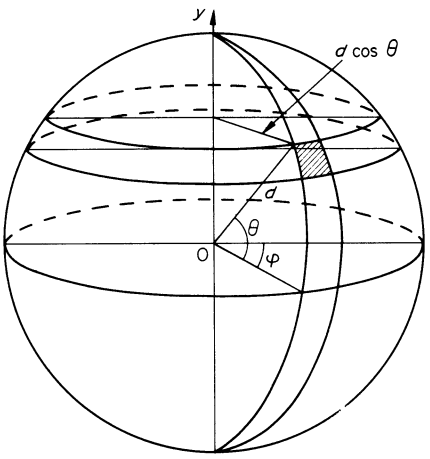

Fig. 1

and $$E_{\text{rms}} = 45^{\frac{1}{2}} \frac{P^{\frac{1}{2}}}{d} \tag{1.22}$$

Half-wave dipole

In this case, the field in a direction subtending an angle θ to the equatorial plane is:

$$E = E_0 \frac{\cos(\pi/2 \sin \theta)}{\cos \theta}$$

A calculation similar to the previous one gives:

$$P = \frac{E_0^2 d^2}{240} S_1(2\pi)$$

where $S_1(x)$ = modified cosine integral.

Since $S_1\ (2\pi) = 2{\cdot}44$, we have finally:

$$E_0 = \frac{240}{2{\cdot}44} \frac{P^{\frac{1}{2}}}{d} = 9{\cdot}93 \frac{P^{\frac{1}{2}}}{d} \tag{1.23}$$

$$E_{\text{rms}} = 7{\cdot}03 \frac{P^{\frac{1}{2}}}{d} \tag{1.24}$$

1.2.2.2 Antenna at short distance from a perfectly conducting ground

Generally speaking, the radiation pattern of an antenna on location near the ground will be modified, and it is necessary to refer to antenna theory for field calculation.

There are however two types of antenna whose radiation pattern in the air has the same shape as the upper half of the free-space pattern, when

they are very near the ground: the isotropic antenna and the vertically polarized short dipole.

Since the power is only radiated into one hemisphere, the power density in a given direction is in both cases multiplied by 2. As it is proportional to E^2, the field is multiplied by $2^{\frac{1}{2}}$.

We therefore have:

For an isotropic antenna:

$$E_0 = 120^{\frac{1}{2}} \frac{P^{\frac{1}{2}}}{d} \tag{1.25}$$

$$E_{\text{rms}} = 60^{\frac{1}{2}} \frac{P^{\frac{1}{2}}}{d} \tag{1.26}$$

For a very short vertical dipole:

$$E_0 = 180^{\frac{1}{2}} \frac{P^{\frac{1}{2}}}{d} \tag{1.27}$$

$$E_{\text{rms}} = 90^{\frac{1}{2}} \frac{P^{\frac{1}{2}}}{d} \tag{1.28}$$

1.2.2.3 **Practical equations**

In practice, P is expressed in kW, d in km and E_{rms} in μV m^{-1}, so that we obtain:

For a half-wave dipole in free space:

$$E_{\text{rms}} = 2{\cdot}22 \times 10^5 \frac{P[\text{kW}]^{\frac{1}{2}}}{d[\text{km}]} [\mu\text{Vm}^{-1}] \tag{1.29}$$

This field has been standardized by CCIR[138, 139] as the reference field for metre and decimetre waves under the term of 'field in free space'.

For a very short vertical dipole near the ground:

$$E_{\text{rms}} = 3 \times 10^5 \frac{P[\text{kW}]^{\frac{1}{2}}}{d[\text{km}]} \tag{1.30}$$

This field has been standardized by CCIR[214] as the reference field for kilometre, hectometre and decametre waves under the term of 'non-attenuated field'.

If the reference antenna has to be changed, it is sufficient to note that the gain in the equatorial plane, referred to an isotropic antenna is: for an elemental dipole, 1·8 dB; and for a half-wave dipole, 2·15 dB.

The field of a spherical wave in free space always decreases as the reciprocal of the distance. This is a fundamental fact in the study of propagation.

1.2.3 THE $\Psi(r)$ FUNCTION

The following function is often used to represent the variations in phase and amplitude of a spherical wave:

$$\Psi(r) = \frac{e^{-j\frac{\omega}{c}r}}{r} \tag{1.31}$$

The electric field can now be written:

$$E(r) = E_0\Psi(r) \tag{1.32}$$

and the magnetic field:

$$H(r) = H_0\Psi(r) \tag{1.33}$$

The above expressions offer the advantage that they include in a single equation the variations in phase and amplitude with distance.

If $r = 0$, we obtain infinite values for $\Psi(r)$, but if we study the radiation of antennae more closely[9], we see that the equations given in the present chapter are valid only for values of r larger than a few wavelengths (which is always the case in propagation problems). Consequently, equations (1.32) and (1.33) will always be valid in the physical problems we shall discuss.

CHAPTER 2

TROPOSPHERIC PROPAGATION

The troposphere is defined as the lower part of the atmosphere, in which the temperature decreases with altitude. It is limited at its upper boundary by the tropopause, a zone where the temperature remains more or less constant. The thickness of the troposphere is of the order of 10 km. It is the least sophisticated of the propagation media. Its dielectric constant is very near unity and its conductivity is practically zero.

The refractive index in the troposphere decreases on average with altitude. This variation produces curvature of radio waves, which is very important for communication using metre, decimetre or centimetre waves (v.h.f., u.h.f., s.h.f.). 'Inversion layers' are sometimes present, in which the refractive index increases with altitude.

Viewed more critically, the troposphere is not homogeneous; its refractive index varies randomly from one point to another around the mean value determined by altitude. This produces two kinds of result: strong and unstable propagation, due to specific meteorological conditions of short duration, which cannot be used for regular communication, but is responsible for interference, especially to TV or radio broadcasting; and a weak but permanent propagation, due to ever present small irregularities causing tropospheric scattering.

2.1 PROPAGATION IN A STANDARD ATMOSPHERE

2.1.1 DEFINITION OF A STANDARD ATMOSPHERE

The dielectric constant of the atmospheric air, and consequently its refractive index, are always very close to unity. If the atmosphere were homogeneous, its presence would only reduce the propagation velocity of radio waves to a negligible extent, as well as the relation between their electric and magnetic fields.

However, the atmosphere is not homogeneous. Its temperature drops on average by 1 °C for each 150 m of altitude, the pressure is reduced to one half at an altitude of 5800 m, and the partial pressure of the water vapour is reduced to one half at an altitude of 2100 m.

The atmospheric refractive index is given by the equation[21, 151]

$$N = (n-1)10^6 = \frac{77{\cdot}6}{T}\left(P + \frac{4\,810\,e}{T}\right) \tag{2.1}$$

where

n = refractive index

N = difference between the refractive index and unity, or co-index. Since this difference is always very small, it is expressed in millionth parts (N-units) in order to give numbers that are easier to remember and to handle.

T = absolute temperature ($T = t+273$, where t is the temperature in degrees Celsius)

P = atmospheric pressure in millibars

e = partial pressure of water vapour in millibars.

The decreases in temperature, pressure and humidity with altitude all cause a variation in the refractive index.

Direct measurement of the refractive index at any point of the atmosphere is possible by mounting a refractometer in an aircraft[116, 152]. This refractometer compares the resonant frequencies of two cavities, one of them evacuated, and the other one filled with ambient air. The natural frequency of this last cavity depends on the refractive index of the air it contains.

It has been ascertained that the average variation of the refractive index per metre of altitude (vertical gradient of the index) near the ground is:

$$\frac{dn}{dh} = -0{\cdot}039 \times 10^{-6} \quad \text{per metre}$$

or -39 N-units per km.

The value of the refractive co-index at an altitude of h km is given by:

$$N = (n-1)10^6 = 289\,e^{-0{\cdot}136\,h} \quad N\text{-units} \tag{2.2}$$

Small as it may be, this variation in the refractive index strongly affects wave propagation.

We shall define the standard atmosphere as a horizontally homogeneous atmosphere in which the refractive index varies with altitude according to equation (2.2).

The term 'standard' should not be misinterpreted. The standard atmosphere is an ideal atmosphere that only represents the mean condition in the actual atmosphere. For a more detailed discussion of the various model atmospheres proposed by various authors, it is useful to consult the literature[145, 151, 164].

2.1.2 RAY TRACING

Let us consider in Fig. 2 a plane of equal phase and take as reference plane a vertical plane which is perpendicular to the first one. Let AB be a line in the plane of equal phase and h the difference in altitude between A and

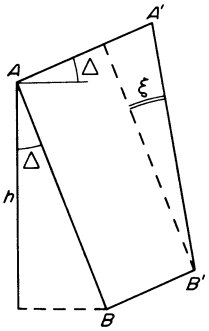

Fig. 2

B. After a time $\mathrm{d}t$, the defined plane will be at $A'B'$. If n is the refractive index at altitude B, we have:

$$BB' = \frac{c}{n}\,\mathrm{d}t$$

$$AA' = \frac{c}{n + h\dfrac{\mathrm{d}n}{\mathrm{d}h}}\,\mathrm{d}t$$

$$AB = \frac{h}{\cos\Delta}$$

where Δ is the angle of the radio ray with the horizontal plane.

The radius of curvature of the path is by definition:

$$\rho = \frac{\mathrm{d}s}{\varepsilon} = \frac{AA'}{\dfrac{AA' - BB'}{AB}} = \frac{AB \cdot AA'}{AA' - BB'} = \frac{\dfrac{h}{\cos\Delta} \cdot \dfrac{c}{n + h\dfrac{\mathrm{d}n}{\mathrm{d}h}}\,\mathrm{d}t}{\dfrac{c}{n} - \left(\dfrac{c}{n + h\dfrac{\mathrm{d}n}{\mathrm{d}h}}\right)\mathrm{d}t}$$

$$= -\frac{h}{\cos\Delta}\,\frac{1}{n + h\dfrac{\mathrm{d}n}{\mathrm{d}h}}\,\frac{n\left(n + h\dfrac{\mathrm{d}n}{\mathrm{d}h}\right)}{h\dfrac{\mathrm{d}n}{\mathrm{d}h}}$$

$$\rho = -\frac{n}{\cos\Delta}\,\frac{\mathrm{d}h}{\mathrm{d}n} \approx -\frac{1}{\cos\Delta}\,\frac{\mathrm{d}h}{\mathrm{d}n} \qquad (2.3)$$

We see that ρ is nearly independent of Δ if this angle is small (for example $< 20°$) and that for larger values ρ increases with Δ, being infinite (linear path) for $\Delta = 90°$ (vertical path).

In the case of large angles of elevation, the curvature of the path has little effect on communication links operating by ionospheric reflection, and on ground-to-air communication. In the former case, the directivity of the antenna is not very great, and propagation uses an ionized layer whose height is not accurately known, so that a precise knowledge of the wave paths is not required. A similar case exists for mobile reception. The same is true for fire control radar because the range is short, so that the effect of the curvature of the path is in general negligible. A discussion of rays with a great elevation angle will be found in the literature[21, 145].

On the other hand, knowledge of the path is extremely important in the case of small elevation angles, because these are encountered in very important classes of communication links.

For example, in the case of moving satellites, it is necessary to align the antenna as soon as the angle of sight reaches a few degrees; this can be done with the necessary accuracy only by taking into account atmospheric refraction. The same is true of a radio link between ground based stations, which may be very distant one from the other, and which have antennae of high directivity. This is so for early warning radar, especially when the antenna's radiation pattern is used for measuring the altitude of the target.

We shall now consider this important case.

2.1.3 RAYS EMERGENT AT A SMALL ANGLE OF ELEVATION

2.1.3.1 **Path**

If the angle of elevation Δ is small, $\cos\Delta$ practically equals unity, and we have:

$$\rho = -\frac{\mathrm{d}h}{\mathrm{d}n} \tag{2.4}$$

The path is an arc of a circle, whose radius does not depend on the elevation angle if the latter is small. Particularly in the case of the standard atmosphere we have:

$$\rho = \frac{10^6}{39} = 25\,600\,\mathrm{km}$$

2.1.3.2 **Equivalent earth radius**

For the study of a radio link, it is particularly useful to draw the radio rays as straight lines. We can obtain this result by transformation of co-ordinates, which in fact is a geometric inversion.

In Fig. 3, 0 is a radio station. Note the axes $0X$ (horizontal) and $0Y$ (vertical), as well as the angle of elevation Δ.

Making α the angle at the centre of the earth's surface (always very small), we have for the equation of the reference surface:

$$x \approx a\alpha$$

$$y = -a(1-\cos\alpha) \approx -\frac{a\alpha^2}{2}$$

and therefore:

$$y = -\frac{x^2}{2a} \tag{2.5}$$

Assuming that Δ is small enough for

$$\sin\Delta \approx \Delta \qquad \cos\Delta \approx 1$$

the equation of the radio ray will be:

$$y = \Delta x - \frac{x^2}{2\rho} \tag{2.6}$$

To convert the radio ray to a straight line, we must add $x^2/2\rho$ to y. Equation (2.5) now becomes:

$$y = -\frac{x^2}{2}\left(\frac{1}{a}-\frac{1}{\rho}\right) = -\frac{x^2}{2Ka} \tag{2.7}$$

where:

$$K = \frac{1}{1-\dfrac{a}{\rho}} = \frac{1}{1+a\dfrac{dn}{dh}} = \frac{1}{1+6{\cdot}4\times10^{-3}\dfrac{dN}{dh}} \tag{2.8}$$

(a, ρ and h are expressed in kilometres).

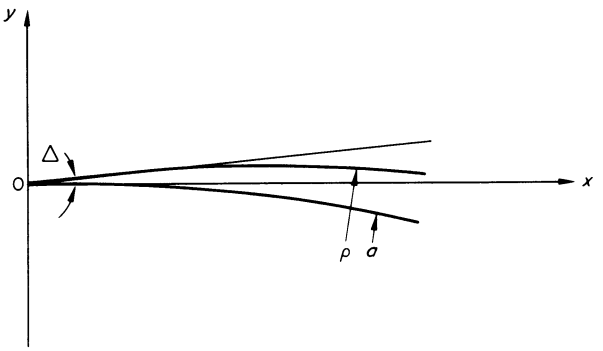

Fig. 3

The expression Ka is called equivalent earth radius. This is the radius of a virtual sphere, whose distance to the straight radio ray is equal to the distance between the actual earth's surface and the actual path of the ray.

For the standard atmosphere we have near the ground (see Section 2.1.1):

$$\frac{dN}{dh} = -39 \quad N\text{-units per km}$$

which gives

$$k \approx 4/3 = 1{\cdot}33$$

and the equivalent earth radius near the ground is:

$$Ka \approx 6\,350 \times 4/3 \approx 8\,500\,\text{km}$$

It is customary in the study of radio links to use ground profiles drawn in relation to the virtual earth surface as defined above. The radio ray is then a straight line and it is very easy to show its position in relation to the earth's surface for various locations of the receiver and source, as well as for various antenna heights.

The apparent reduction of the earth's curvature, which is greater when the variation in refractive index with height is larger, facilitates the communication. Indeed, the horizons of both antennae move away, and consequently we approach the line-of-sight case for the same distance between stations. For the standard atmosphere, the distance of the ratio horizon is given by the following equation, which is derived from (2.7):

$$d = 4{\cdot}13\, h^{\frac{1}{2}} \approx 3(2h)^{\frac{1}{2}} \tag{2.9}$$

where d = distance in km and h = altitude of the antenna in m.

The apparent withdrawal of the horizon in the case of almost horizontal paths exists also for light waves. A rising star can be seen even when still below the geometric horizon. However, the curvature of the rays is not the same for light waves as for radio waves.

2.1.3.3 **Various possible cases**

Table 1 summarizes the considerations relating to paths with a small elevation angle.

2.1.3.4 **Modified index method**

Another method is also used to represent wave propagation in a horizontally stratified atmosphere, which may be either standard or of random form. The actual refractive index is then replaced by the modified index:

$$N = n + \frac{a}{h} \tag{2.10}$$

where h = altitude and a = real earth's radius.

It can be shown that in this case the earth's surface can be represented by a plane, being the distance between the radio ray and the reference plane equal to its altitude above the earth's surface in actual propagation.

The ray path is then represented by a curve, which may be drawn by means of successive arcs, using Snell's law and the value of the modified index at each point.

Though useful for theoretical study, this mode of representation is not very valuable for engineering, where the equivalent earth's radius method is always used.

TABLE 1

Parameters of the path of rays in the atmosphere

dn/dh *N*-units/km	Curvature	ρ (in km)	K	Atmospheric refraction	Virtual earth	Horizontally launched ray
> 0	upwards		< 1	below normal	more convex than actual earth	moves away from the earth
0	nil	∞	1		actual earth	
$0 > \frac{dn}{dh} > -39$	downwards		> 1		less convex than actual earth	
-39		25600	4/3	normal		
$-39 > \frac{dn}{dh} > -157$			$> 4/3$	above normal		
-157		6350 = *a*	∞		plane	remains parallel to earth
< -157			< 0	super-refraction	concave	draws closer to the earth

2.1.4 INTERFERENCE BETWEEN DIRECT AND REFLECTED RAYS; FADING

Using the argument in Section 4.1.5.2 and taking into account the variation in refractive index with altitude, it can easily be shown that very small changes in this variation are sufficient to create either a maximum or a minimum field strength at the receiver. As a matter of fact, both paths, direct and reflected, comprise a very large number of wavelengths, so that a very small variation in refractive index is sufficient to increase or decrease one of these paths by $\lambda/2$.

For example, for a skip of 56 km at 4 GHz (typical CCIR skip at this frequency) the number of wavelengths is $7{\cdot}5 \times 10^5$, so that a variation of 0·66 *N*-units in one of the paths is sufficient to change the resultant from

maximum to minimum. A case like this is the origin of strong fading, which is extremely inconvenient in radio links[181]. This type of fading is mainly produced during the second half of the night, generally for about 25 per cent of the time[175]. Designers attempt to avoid fading:

1. by attenuating the reflected ray in such a way that the minima are less pronounced. This may be done by making the reflecting region a wooded or built up area with a small reflection coefficient (see Section 4.1.4), or if this is impossible (oversea skip) by using an obstacle near one of the antennae to attenuate the reflected ray[171].
2. by using diversity reception with two antennae which are vertically separated by several wavelengths (see Appendix 6.7.1(b)).

2.1.5 ATMOSPHERIC ABSORPTION

Absorption due to rain or fog matters only for very high frequencies (above 6 GHz). Figures 4 and 5 give the approximate values of absorption. However, it is difficult to ascertain the distribution of rain or fog along the path joining two stations[161], so that the practical applications of these curves are rather limited.

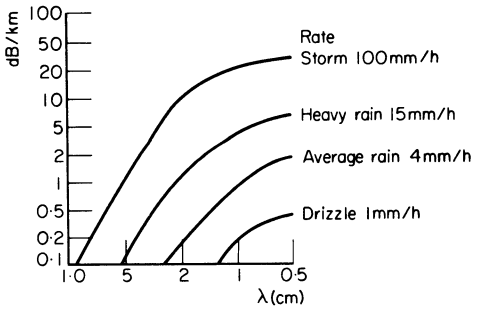

Fig. 4 Rain

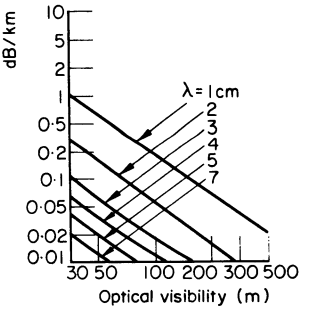

Fig. 5 Fog

As a result of the increasing interest in the use of higher and higher frequency bands (11, 18 and 21 GHz), studies are being carried out to determine the statistical distribution of the attenuation in different climates[173, 175, 177, 182]. The results obtained so far are still too fragmentary to show a clear overall trend. In one particular case[173], it was found that the experimental results agreed with the absorption curves if the height of the rain was multiplied by a reduction factor which could vary between 0·2–0·39.

Rain, and even certain types of cloud, can also cause radar echoes. This property is used in ground based or airborne meteorological radar.

Snow and hail are much less absorbing than water.

Sandstorms and some types of electrically charged rainfalls produce shot noise in the antennae directly bumped by the electrically charged particles. Airborne equipments are especially affected, because they frequently travel through electrically charged clouds. It is possible to provide them with substantial protection by giving the antennae a dielectric coating.

2.1.6 FRESNEL ZONE (see Appendix 8)

Radio ray tracing, made in general on special graphs, using the relevant value of K (see Section 2.2.1.2) allows us to determine whether the source and receiver are in radio visibility of each other.

When this result is achieved, it is possible to calculate the fields as being in free space, on condition that the ray does not pass too close to the ground, i.e. that the first Fresnel zone is cleared.

2.2 PROPAGATION IN A STRATIFIED ATMOSPHERE

2.2.1 PROPAGATION WITHOUT DUCTS OR REFLECTIONS

2.2.1.1 **Actual atmospheric stratification**

As a rule, the actual atmosphere is very different from the standard atmosphere. Along a vertical line, the refractive index gradient varies rather randomly with altitude. It may even become positive in some atmospheric layers (inversion layers—see Section 2.2.1.2). In a horizontal direction,

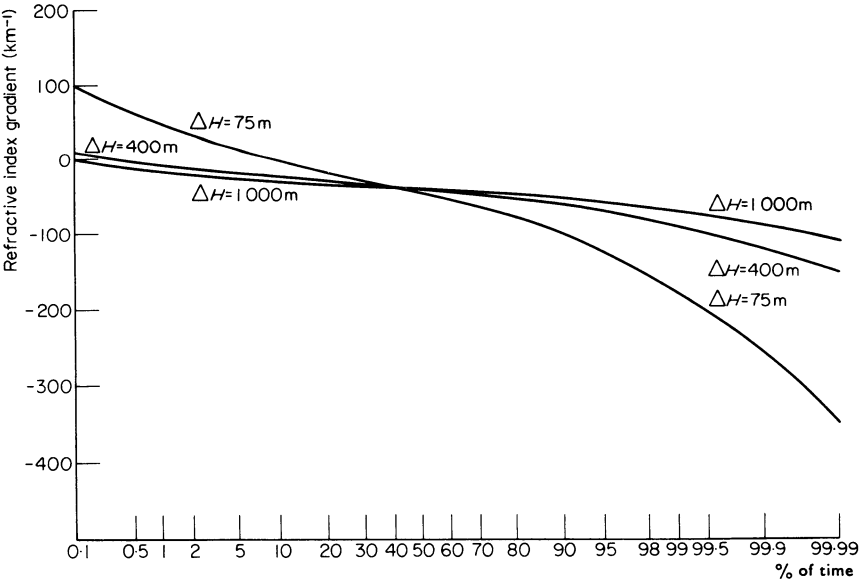

Fig. 6 Refractive index gradient for temperate climate
(Data from France, Japan, U.K., U.S.A.)

one sometimes observes regular stratification extending over a few km, and it is also possible to find weak correlation between refractive indexes at various places at the same altitude.

The refractive index near the ground varies against time over a wide range, but the mean gradient calculated for example over 1 km is much less variable. Figure 6, which summarizes the data communicated to the CCIR by Great Britain, France, Japan and the USA, shows the statistical distribution of the values of K for temperate climates, for three height ranges.

Knowing the vertical and horizontal distribution of the refractive index along the entire wave path, it should be possible to trace the radio rays, which obviously would no longer be circular. In fact, this tracing may be interesting when the atmosphere is regularly stratified (see Sections 2.2.1.2 and 2.2.1.3), but is of no use if the refractive index shows random and variable distribution, especially since the lower part of the atmosphere (the most variable) has the strongest effect on the curvature of the ray[21, 145].

2.2.1.2 Equivalent K coefficient

The effect of a random atmosphere on wave propagation is often characterized by an arbitrary extension of the meaning of equivalent earth radius. In this way, an equivalent K coefficient is defined. It is the K of an atmosphere with linear variation of the refractive index, which would give the radio ray the same total curvature as given by the actual atmosphere.

The equivalent K coefficient represents the propagation properties which are related to the total curvature of the ray, namely the mean distance between the ray and the earth's surface—from which results its general use in diffraction problems. On the other hand, it does not take into account the actual shape of the ray (or rays, in the case of multiple paths).

Due to the permanent variation in meteorological conditions, the equivalent K coefficient is a random function of time, consequently it can be characterized by its median value and statistical distribution.

Median value of K

The simplest hypothesis is to assume that the median value of the refractive index is an exponential function of the altitude. This results in:

$$N_h = N_0 e^{-qh}$$

It has been found[128] that q varies from $-0{\cdot}1177$ to $0{\cdot}2068$, according to meteorological conditions. If, however, it can be accepted that the value of $-0{\cdot}136$ (adopted for the standard atmosphere) is a sufficient approximation[114, 128], it becomes:

$$K = \frac{1}{1 - 8{\cdot}8 \times 10^{-4} N_0}$$

World maps for N_0 have been published[140], which make it easy to use this method. Unfortunately, the referred method gives good results only in temperate climates.

It is also possible to calculate K, using the difference ΔN between the refractive indexes at ground level and at an altitude of 1 km. We find, using equation (2.8):

$$K = \frac{1}{1 - 6{\cdot}4 \times 10^{-3} \Delta N}$$

World maps for ΔN have also been published[140]. However, this method does not seem to be better than the first one.

Statistical distribution of K

The equivalent K coefficient represents by definition a mean of local values of K along the ray path. The variation against time of this coefficient must therefore be smaller as the path becomes longer. This has been confirmed by experimental results.

The most interesting value for engineering is the quasi-minimum value of K, i.e. the value exceeded for a great percentage of the time, e.g. 99·9 per cent. For temperate climates, this value is given as a function of the distance in Fig. 7[171]. Similar curves for other types of climate are not yet available.

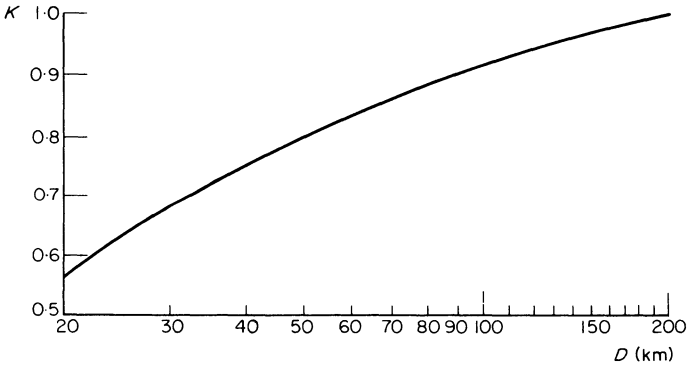

Fig. 7 Minimum value of K for temperate climate

Practical rules

From the present state of knowledge it appears advisable to limit ourselves to a few general rules in the study of a project in radio communication.

1. The median value of K is higher than 1·3 (e.g. of the order of 1·5) in hot and wet climates, equal to 1·3 in temperate climates, and lower than 1·3 in dry climates.

2. Over a distance of approx. 50 km, the values $K = 1$ (wet climates), $K = 0{\cdot}8$ (temperate climates) and $K = 0{\cdot}6$ (desert climates) are exceeded for most of the time (approx. 99·9 per cent). These values are commonly taken as the lower limit in circuit calculations.
3. The quasi-maximum value is 2 or 3 for metre waves (v.h.f.), but can become infinite or even negative for decimetre and centimetre waves (s.h.f. and e.h.f.).

2.2.1.3 **Effect on propagation**

Effect on the hourly median value of the field

In all cases where the ground reflection of the waves (line-of-sight path, reflecting ground) or their diffraction (path not fully clear, over-the-horizon circuits) affect the received field strength, the hourly medians of the field are related to the value of the equivalent K. This is most important when the radio path is nearly tangential to the earth's surface.

For fields weaker than the median value, the distribution of the hourly medians is closely approximated by a log-normal distribution (Appendix 6.3) with a standard deviation σ of the order of 2 or 3 dB. It is possible to calculate σ in an actual case when the values of K which correspond to two probability values (e.g. 50 per cent and 99·9 per cent) are known. This is achieved by calculating the transmission loss in both cases and deducing σ by means of a table of the Gaussian functions (in our example, the difference between the losses, expressed in dB, must be divided by 3·1).

Scintillation

As a result of the irregular structure of the atmosphere, adjacent radio rays may have large phase differences. In this case, Huygens' principle does not apply, and it is necessary to take into account the various rays that reach the receiving antenna.

This fact leads to two results.

1. Since the phases of the various rays are different, the field strength is subjected to rapid variation (scintillation), with a Rayleigh distribution (Appendix 6.1).
2. Since the transit times of the various rays differ one from the other, the bandwidth is limited. We have approximatively:

$$B = 1/\Delta t$$

where $\Delta t =$ maximum difference in transit time.

For line-of-sight radio links, this phenomenon appears mainly during the second half of the night. It is always present in over-the-horizon circuits.

Beam deflection

The variations in the equivalent value of the coefficient K lead to variations in the curvature of the radio waves. This can give rise to a deflection of the beam between directive antennae which can have a certain influence on the gain of very narrow beam antennae used for very high frequencies[174, 175, 179]. The published data do not show very good agreement. However, beam deflections of the order of one degree have been observed in Japan[174].

2.2.2 SUPER-REFRACTION; DUCTS

When coefficient K is negative, 'ducts' are produced.

2.2.2.1 **Duct near the ground**

Let us assume that the curve showing the variation of the refractive index with height is the one shown in the left hand part of Fig. 8. In the vicinity of the ground, dn/dh is negative, with a modulus greater than 157 N-units per km. At an altitude h_0 the gradient then acquires its mean value of -39 (obviously, the actual transition is not so sudden). Below h_0 the curvature of rays launched at small elevation angles is larger than the earth's curvature. Above h_0 the curvature of the rays is smaller than the earth's curvature.

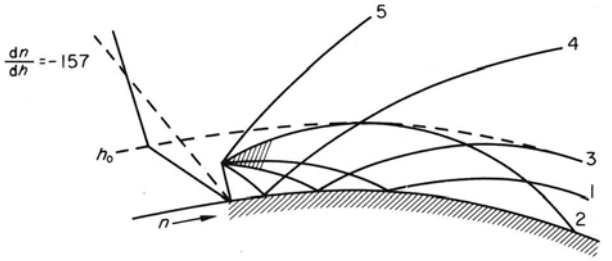

Fig. 8

The shape of the rays is shown on the right hand side of Fig. 8 for a source altitude which is smaller than h_0.

Rays 1, 2 and 3 are trapped between the ground and a virtual sphere located at altitude h_0. Rays 2 and 3 are tangential to this sphere and are the extremes of the trapped beam. Inside this beam, the received energy is very large. Instead of suffering a decrease of $1/d^2$ (as in free space) it decreases only by $1/d$.

Rays 4 and 5 are emitted at a larger angle and are not trapped. Only weakly deviated by the duct, they resume their normal path on exit. The effect of a duct with a large elevation angle is consequently negligible.

2.2.2.2 **Elevated duct**

If the refractive index varies as shown on the left hand side of Fig. 9, i.e. if we first find an 'inversion' (increasing index) from the ground upward to an altitude h_0, followed by a zone of fast decrease in the index (greater than -157 N-units per km) until an altitude h_1, and lastly, above h_1 a zone where the normal gradient is resumed, we see, as in the preceding case, that a wave beam with a small elevation angle emitted by a source at an altitude between h_0 and h_1, is trapped between two spheres of altitudes h_b (which do not coincide with the lower discontinuity of the gradient) and h_1 (higher discontinuity) respectively.

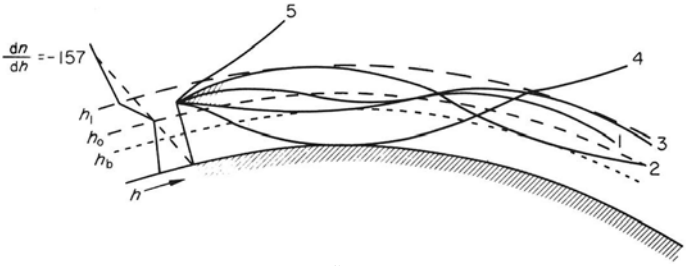

Fig. 9

The same remarks as in the preceding paragraph may be made for the ray emitted at large elevation angles.

2.2.2.3 **Action of ducts**

The ducts are only operative when the altitudes of both the source and the receiver remain within the limits mentioned above. Since the air layers are more or less horizontal, the altitudes of the transmitter and the receiver must be almost the same.

2.2.2.4 **Cut-off frequency**

In the same way as waveguides, ducts have a cut-off frequency. However, since they are not limited by surfaces but rather by zones where the index gradient varies gradually, the cut-off is not sudden.

The maximum wavelength able to be propagated without loss in a duct, is approximatively equal to:

$$\lambda_{max} = 2{\cdot}5\,\Delta h(\Delta n)^{\frac{1}{2}}$$

where Δh = depth of the duct, and Δn = variation of the index inside the duct.

For example, for a duct near the ground, with a depth of 30 m and $\Delta n = 4\times10^{-6}$ (4 N-units) which represent a typical case at average latitudes, we have:

$$\lambda_{max} = 2{\cdot}5\times30\,(4\times10^{6})^{\frac{1}{2}} = 0{\cdot}15\,\text{m}$$

hence $f_{min} = 2000$ MHz.

Ducts will therefore affect mainly radio links and S or X band radar. In the latter case, only early warning radar will be affected, because fire control radar operates usually with elevation angles greater than the limiting angle of the duct. The increase in signal strength is, however, stronger for radar (both ways) than for radio links. This phenomenon can result in plotting errors.

2.2.2.5 **Production of ducts**

A quiet atmosphere is essential for the appearance of ducts. They are mostly encountered in quiet weather conditions, above water or plains. In mountainous areas, atmospheric turbulence and upward motion of air oppose the production of ducts.

The same can be said of sea coasts, but not of those of landlocked seas. The first recorded ducts were observed in Egypt during World War II.

Ducts near the ground

1. A mass of warm air arriving on a cold ground produces a duct near the ground. The probability of this phenomenon occurring is greater when the soil is cold and wet. This type of duct occurs more often at sea near the coast.
2. On the ground, night frost leads to the production of ducts, mainly during the second half of the night. This phenomenon is rather frequent in desert and tropical climates.
3. On tropical seas, the great humidity existing in the lower part of the atmosphere produces almost permanent ducts with a dimension of approx. 10 m and with a strong variation in index (4×10^{-5}), so that the cut-off wavelength is of the order of 15–20 cm.

Elevated ducts

These are mainly caused by subsidence of an air mass in a high pressure zone. When descending, the air is compressed, and thus warmed and dried.

This type of duct occurs mainly above the clouds (up to an altitude of 1 500 m). They affect communications between aircraft in u.h.f., and radio links passing over valleys.

2.2.3 TROPOSPHERIC REFLECTION

In this section we shall deal only with the reflection from very large layers, which do not often occur. The case of small layers will be discussed in Section 2.3 in connection with tropospheric scattering.

If the refractive index varies suddenly, leading to a bend in the path whose radius is smaller than wavelength, and if the reflecting surface is very large, we have a reflection in the optical sense. This case occurs when an heterogeneous layer with a sharp lower border (sudden discontinuity

in the refractive index) is encountered in the atmosphere, in general at the interface of two air masses.

Strong tropospheric reflection occurs mainly at v.h.f. It occurs seldom in the case of microwaves (because the discontinuities of the refractive index are not sudden enough) and in the case of longer waves (because the thickness of the discontinuity layers is not sufficient).

Equation (4.4) enables us to calculate the reflection coefficient when the difference Δn in the indexes is small:

$$R_V = R_H = \frac{1-\left(\frac{2\Delta n}{\sin^2\varphi}+1\right)^{\frac{1}{2}}}{1+\left(\frac{2\Delta n}{\sin^2\varphi}+1\right)^{\frac{1}{2}}} \tag{2.12}$$

where φ = angle between the incident ray and the plane of discontinuity. We observe that R will only have a significant value if $\sin\varphi$ is small (because Δn is assumed small).

The smallest value of $\sin\varphi$ will happen when the rays are tangential to the earth's sphere (see Fig. 10). We find for this case, taking the equivalent earth radius into account:

$$\varphi_{\min} = \left(\frac{2h}{Ka}\right)^{\frac{1}{2}} \tag{2.13}$$

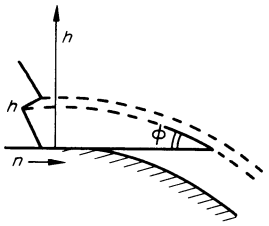

Fig. 10

Recorded typical dimensions for the layers are: horizontal length a few hundred km, vertical depth 30–50 m, altitude 1 000–2 000 m. The deviation of the index is between 20 and 30 N-units.

The reflection coefficient is of the order of a few thousandths. This may be a very small value, but the waves reflected in this way may reach locations well beyond the horizon where, since the field of the ground wave is very weak, the reflected field can be much stronger than the former.

At several hundred kilometres from a powerful metre wave (v.h.f.) transmitter, the field originated by tropospheric reflection may be a hundred times stronger than the normal field. This is therefore a very dangerous source of interference.

2.2.4 RESULTS OF SUPER-REFRACTION AND OF TROPOSPHERIC REFLECTION

2.2.4.1 **Disadvantages of these phenomena**

Super-refraction produces large variations in the received field, whose strength is strongly increased when both the source and the receiver are situated in the duct, and considerably attenuated if only one of them is within the duct. To a lesser degree, tropospheric reflection is also a factor of instability.

On the other hand, by considering random long distance propagation (called 'abnormal propagation') this phenomenon causes interference between stations which do not normally interfere. This allows random undesirable listening, and causes errors in radar and direction finding.

2.2.4.2 **Protection against these phenomena**

It is not possible to suppress abnormal propagation, but it is possible to reduce its effect on field strength for a point-to-point circuit.

Abnormal propagation is related to:

1. Existence of homogeneous and regularly stratified layers.
2. Small elevation angle.

We can reduce their effects:

1. By avoiding as much as possible paths of low altitude above deep valleys, above plains surrounded by hills and above tropical seas.
2. By situating the transmitting and receiving stations at altitudes that are sufficiently different to allow the path to make a rather large angle with the horizontal plane.

2.3 TROPOSPHERIC SCATTERING

The phenomena discussed in the preceding sections are related to the overall atmospheric structure. They give rise to strong fields, sometimes with large but slow variations. Over-the-horizon propagation is only an exceptional case.

However, it has been ascertained since 1950 that metre and decimetre wave transmitters (v.h.f. and u.h.f.) produce a permanent field (however, with a rapid fading rate) well below the horizon. This field is weak, but much stronger than the field calculated by means of the diffraction theory discussed in Chapter 4. It would seem that such a field is related to the fine structure of this atmosphere.

This mode of propagation allows transmission of small capacity multiplex telephony signals over large distances (up to 1 000 km) without relay stations, or transmission of a large number of telephony channels or

of TV programmes over medium ranges (200–300 km). This has become of such great interest that it has given rise to much theoretical and experimental research.

Various theories have been advanced. We shall explain these, limiting ourselves to fundamentals, and attempt to present the basic concepts needed for reading the original papers.

2.3.1 MECHANISM IN A TROPOSPHERIC SCATTERING CIRCUIT

The source E shown in Fig. 11 is equipped with a highly directive antenna and emits a high power density into a narrow cone. The receiver R is also equipped with a high gain, highly directive antenna, which collects the energy scattered by the volume common to the beams of both antennae. Transmission is better when the altitude h of the common volume, as well as the angle θ between both beams, are smaller.

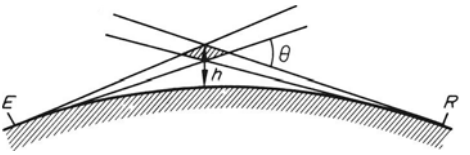

Fig. 11

For a given distance, this will be realized if the horizons of both antennae are completely clear and their beams are tangential to the ground.

The available bandwidth is related to the antenna's radiation pattern. If the pattern is very broad, the paths of the various rays will be very different in length and therefore in transit time. In this case, it is only possible to transmit signals varying so slowly that the difference in transit time becomes irrelevant, which means narrowband signals. To transmit wideband signals, it is necessary to use antennae having such a narrow beam that the difference in transit time for the various points of the common volume remains small in relation to the reciprocal of the desired bandwidth.

Obviously, tropospheric scattering (abbreviated to troposcatter) exists even when the antennae are in line of sight. In this case, the scattered field is generally weak with respect to the main field, and so causes only a small scintillation of the latter. However, during periods of strong fading, the received field can show characteristics similar to those of the troposcatter field.

2.3.2 THEORY OF SCATTERING BY ATMOSPHERIC TURBULENCE

2.3.2.1 **Booker and Gordon's theory**

This theory was the first to appear and still has a number of followers. Our explanation of this theory follows the methods given by the authors[104].

An advantage of this method is that it is based on physical considerations. We shall also discuss its later development.

Atmospheric turbulence

In addition to its large scale characteristics, the atmosphere is in perpetual motion at every point. Eddies appear, move and disappear. This is atmospheric turbulence, and follows variations in temperature and pressure, therefore causing variations in the index of refraction.

The best known manifestation of atmospheric turbulence is the twinkling of stars, even when their elevation above the horizon precludes any interference between reflected or refracted rays by air layers of different indexes.

Representation of atmospheric turbulence

The basic idea is that of the elementary volume. In a turbulent medium, the dielectric constant varies from one point to another, and at each point it varies with time. At two very close points, the dielectric constant will permanently have a very closely related value, while at very distant points the dielectric constants will be uncorrelated.

In other words, the coefficient of correlation between the dielectric constants at two points is a function of their separation. In addition, the authors mentioned above assume that it depends only on this separation (isotropic turbulence) and state for the length of the turbulence scale height:

$$l_0 = \int_0^\infty C(r)\,\mathrm{d}r$$

where $C(r)$ = coefficient of correlation, equal to unity for $r = 0$, and to zero for $r = \infty$. In the initial form of their theory, the authors have put:

$$C(r) = \mathrm{e}^{-r/l_0}$$

The length l_0 defined above is the radius of a virtual sphere inside which the dielectric constant would have at every instant the same value at every point ($C(r) = 1$), while outside this sphere it would vary randomly ($C(r) = 0$).

Imagine an atmosphere as consisting of an assembly of spheres with a radius l_0, where the dielectric constant of each sphere differs by a small value $\Delta\varepsilon$ from the mean value in the atmosphere under consideration.

Various methods for determining l_0 have resulted in values ranging from a few metres to a few hundred metres. Moreover, elementary volumes of various sizes are encounted in the atmosphere, and the statistic distribution of length l_0 plays an important part in the troposcatter mechanism.

Measurements made on board aircraft[116] seem to be the most reliable and have given values ranging from 7 m to 190 m, with a mean value of 68 m.

Effect of waves on an inhomogeneous atmosphere

Incident waves cause polarization of the elementary volumes, converting them to electrical dipoles, which in turn radiate energy.

Elementary dipoles

It is well known[4, 15] that a dielectric sphere which is merged in a dielectric medium having a different permittivity and subjected to an electric field, acquires a polarization, which transforms it into an electrical dipole, prototype of the elementary antenna.

Under the effect of the electric field of the incident wave, all elementary volumes are converted to antennae, which will radiate in all directions. However, since they are dipoles, radiation will take place mainly in directions at a small angle to that of the incident wave, either forward (forward scatter) or backward (back scatter).

Overall radiation

The fields originating from the elementary dipoles (randomly scattered in space) are not in phase, because the dipoles are located at different distances from the source. The assembly of these dipoles forms a kind of three dimensional network of antennae, whose radiation is maximum in the direction opposite to that of the incident waves, and decreases rapidly when the direction diverges from it.

The thus produced beam has, however, an aperture of a few degrees, which allows us to receive the wave outside that part of the space which is limited by optical geometry.

Putting these concepts in numerical form by calculation, we find that the density of power in the radiation cone is proportional to:

$$\delta^2 = \left\langle \left(\frac{\Delta\varepsilon}{\varepsilon} \right)^2 \right\rangle$$

Values ranging from 4×10^{-14} to $6{\cdot}4 \times 10^{-12}$ have been found for this parameter. The values resulting from direct measurements aboard aircraft, which appear to be the most reliable, range from $0{\cdot}4 \times 10^{-12}$ to $6{\cdot}4 \times 10^{-12}$.

Obviously, as the altitude increases, the atmosphere becomes less and less dense, ε tends towards unit and $\Delta\varepsilon$ tends towards zero. The lower part of the atmosphere is therefore the most favourable for scattering.

Scattering parameter

It is possible to show that the scattered power:

1. per unit solid angle,
2. per unit incident power density, and
3. per unit scattering volume

is proportional to the scattering parameter.

$$\sigma = \frac{\left\langle \left(\frac{\Delta\varepsilon}{\varepsilon}\right)^2 \right\rangle}{l_0} = \frac{\delta^2}{l_0}$$

Measurements of field strength cannot therefore give us separate values of l_0 and δ. Measurements with a refractometer[116] have given values of σ ranging from 10^{-14} to 10^{-17}, usually decreasing with altitude.

Variants of Booker and Gordon's theory

In the above explained original form, Booker and Gordon's theory offers some difficulties:

1. The coefficient of correlation $C(r) = e^{-r/l_0}$ is the same in all directions, although the vertical should play a special part. Furthermore, the choice of an exponential function is somewhat arbitrary.
2. The statistical distribution of the turbulence height l_0 has a strong effect on the variation with frequency of the scattered field. Booker and Gordon have used an old theory of turbulence, which is no longer accepted in aerodynamics.
3. The law of variation with altitude for the scattering parameter strongly modifies the value of the received field as a function of distance.

Various variants of the theory have been proposed[105, 121], dealing with the correlation function to be used, with the statistical distribution of the turbulence scale height, and with the variation with altitude of the diffraction parameter.

2.3.2.2. **Modern forms of turbulence theory**

Modern turbulence theory is based on the work of Kolmogoroff and Obukoff[111, 119, 122, 126, 132].

If we consider a part of a fluid, approximately spherical with a diameter l and rotating because of turbulence, the energy of this mass may be dissipated in two ways: it drives other parts of the fluid, thus creating smaller eddies, and it generates heat by viscous friction.

Large volumes possess great kinetic energy, and as their surface is small in relation to their mass, the viscous frictional forces are rather unimportant. They are said to be in the inertial range. Very small volumes, on the other hand, possess a reduced kinetic energy, and as their surface is large in relation to their mass, they dissipate their energy by producing heat. It is said that they are included in the dissipation range.

The motion must be maintained by some power source. We can consider two kinds of source: large fluid masses in motion, for example winds; or

the prior existence of a temperature or pressure gradient inside the fluid, for example by the mixing of two air masses.

Thermodynamic and aerodynamic reasoning allows us to determine the processes of the exchange of energy between the various parts of the fluid, and the distribution of the latter as a function of their size[119, 125]. Instead of the diameter l, it is preferable to use its reciprocal $K = 1/l$, and the distribution of K is expressed by a function $S(K)$, which represents the number of elementary volumes included in a small interval centred on K. By optical analogy, this function is called the spectrum $S(K)$ of the relevant distribution. With the two types of energy supply mentioned above, we reach the two schematic representations of the spectrum $S(K)$ as a function of K (Figs 12 and 13).

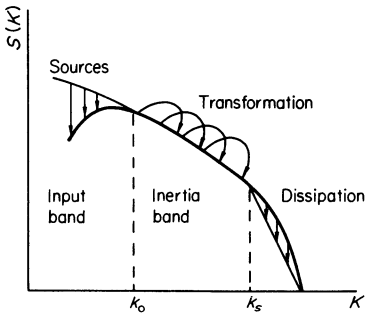

Fig. 12

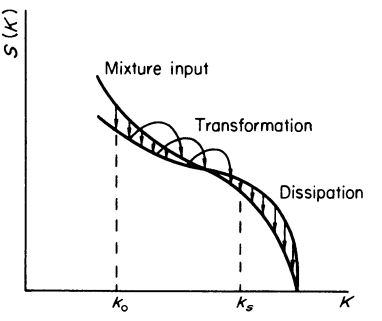

Fig. 13

In the troposphere, length $l_0 = 1/K_0$ is of the order of 1 km. Length $l_s = 1/K_s$ is approx. 0·65 mm. Air masses reacting in the propagation of waves used for tropospheric propagation (metre and decimetre waves; v.h.f. and u.h.f.) will therefore always remain in the inertial range (see p. 39). In this band, the first of the spectra we have contemplated is proportional to $K^{-11/3}$, while the second is proportional to K^{-5}.

In turbulence theory, troposcatter is caused by variations in the dielectric constant of an air mass. These variations are caused by variations in temperature, pressure and humidity, and these are in turn caused by variations in velocity. Each individual air mass considered in the study of turbulence will therefore have its own dielectric constant, which will be slightly different from the mean value.

The spectrum of dielectric inhomogeneities is therefore the spectrum of the turbulence, multiplied by a constant factor.

Correlation function and spectrum of dielectric inhomogeneities; Scattering vector

Distribution of ε_r

ε_r varies with the time t and with the point P in the space. We can therefore write exactly:

$$\varepsilon_r = \varepsilon_r(P \cdot t)$$

In fact, the variation in time of ε_r only affects slow signal variations, as we shall see later. It is therefore sufficient to consider the values of ε_r at the same time at the various points P in the space, and to put:

$$\varepsilon_r = \varepsilon_r(P) = \langle \varepsilon_r \rangle + \Delta\varepsilon_r(P)$$

The quadratic mean of the inhomogeneities in the common volume V is defined by:

$$\langle (\Delta\varepsilon_r)^2 \rangle = \frac{1}{V} \overset{3}{\int_V} (\Delta\varepsilon_r)^2 \, \mathrm{d}V \tag{2.14}$$

Correlation function of $\Delta\varepsilon_r$

This function is defined by the equation:

$$C(\boldsymbol{r}) = \frac{1}{V\langle (\Delta\varepsilon_r)^2 \rangle} \overset{3}{\int_V} \Delta\varepsilon_r(P) \cdot \Delta\varepsilon_r(P') \, \mathrm{d}V \tag{2.15}$$

where vector $\boldsymbol{r} = P' - P$.

If the scattering medium is isotropic, $C(\boldsymbol{r})$ is a function of $|\boldsymbol{r}| = r$ only.

Spectrum of $\Delta\varepsilon_r$

This is the product of the mean value of $(\Delta\varepsilon_r)^2$ by the spatial Fourier transform of $C(\boldsymbol{r})$ (see Appendix 7).

$$S(K) = \langle (\Delta\varepsilon_r)^2 \rangle \int_{-\infty}^{+\infty} \iiint C(\boldsymbol{r}) \cdot \mathrm{e}^{\mathrm{j}\boldsymbol{K} \cdot \boldsymbol{r}} \, \mathrm{d}^3 r \tag{2.16}$$

We thus have:

$$\langle (\Delta\varepsilon_r)^2 \rangle C(\boldsymbol{r}) = \frac{1}{8\pi^3} \int_{-\infty}^{+\infty} \iiint S(K) \, \mathrm{e}^{\mathrm{j}\boldsymbol{K} \cdot \boldsymbol{r}} \mathrm{d}^3 K \tag{2.17}$$

Scattering vector $\boldsymbol{K}$

Consider in the scattering volume V a point P chosen as the origin, and another point P', so that $P' - P = \boldsymbol{r}$ (see Fig. 14).

We now attempt to calculate the phase difference between the rays passing through P and P', linking a source and a receiver, which are both

very distant from the scattering volume. If R_E and R_R are the distances from P to the source and the receiver respectively, we have, by putting:

$$k = \frac{\omega}{c} = \frac{2\pi}{\lambda}$$

and using the geometry of Fig. 14:

$$\begin{aligned}\Delta\Phi &= -k(|\boldsymbol{R}_E - \boldsymbol{r}| - |\boldsymbol{R}_E| + |\boldsymbol{R}_R - \boldsymbol{r}| - |\boldsymbol{R}_R|) \\ &= -kr(\sin\theta_1 - \sin\theta_2) \end{aligned} \tag{2.18}$$

We now consider two vectors $\boldsymbol{K}_1$ and $\boldsymbol{K}_2$ with the same modulus:

$$|\boldsymbol{K}_1| = |\boldsymbol{K}_2| = k \tag{2.19}$$

and with the direction of the incident and the scattered ray respectively. We define the scattering vector by:

$$\boldsymbol{K} = \boldsymbol{K}_2 - \boldsymbol{K}_1 \tag{2.20}$$

Projecting this equality on vector $\boldsymbol{r}$, and using equation (2.18), we find:

$$\Delta\Phi = -\boldsymbol{K}_1 \cdot \boldsymbol{r} + \boldsymbol{K}_2 \cdot \boldsymbol{r} = \boldsymbol{K} \cdot \boldsymbol{r} \tag{2.21}$$

It will be easily seen in Fig. 14 that:

$$|\boldsymbol{K}| = 2k \sin\theta/2 \tag{2.22}$$

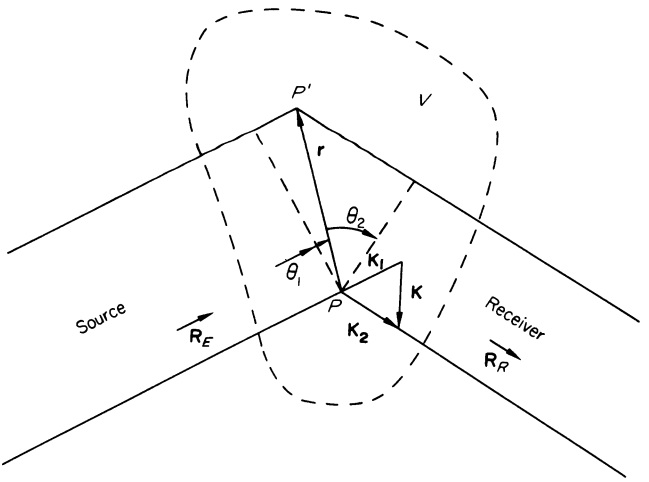

Fig. 14

Effect of an electric field on an inhomogeneous medium

The scattering medium with a dielectric constant:

$$\langle \varepsilon_r \rangle + \Delta\varepsilon_r$$

is affected by the field:

$$\boldsymbol{E} = \boldsymbol{E}_0 + \boldsymbol{E}_1$$

where $\boldsymbol{E}_0$ = primary field, and $\boldsymbol{E}_1$ = scattered field.

The second equation (Appendix 3.1) may now be written (noting that $\sigma = 0$, but that ε_r is a function of time):

$$\nabla \times \boldsymbol{H} = \varepsilon_0 \frac{\partial}{\partial t}[(\langle \varepsilon_r \rangle + \Delta\varepsilon_r)(\boldsymbol{E}_0 + \boldsymbol{E}_1)]$$

$$= \varepsilon_0(\langle \varepsilon_r \rangle + \Delta\varepsilon_r)\left(\frac{\partial \boldsymbol{E}_0}{\partial t} + \frac{\partial \boldsymbol{E}_1}{\partial t}\right) + (\boldsymbol{E}_0 + \boldsymbol{E}_1)\varepsilon_0 \frac{\partial \Delta\varepsilon_r}{\partial t}$$

The last term of this expression can obviously be disregarded, owing to the slowness of the variations in $\Delta\varepsilon_r$ (related to the meteorological variations, while $\boldsymbol{E}_0$ and $\boldsymbol{E}_1$ vary with the frequency of the incident wave).

We can also disregard $\boldsymbol{E}_1$ in comparison to $\boldsymbol{E}_0$, which means disregarding multiple scattering, whose effect is in fact very small, because $\boldsymbol{E}_1$ is always much smaller than $\boldsymbol{E}_0$. This latter approximation is called the Born approximation. We now have:

$$\nabla \times \boldsymbol{H} = \varepsilon_0 \varepsilon_r \frac{\partial \boldsymbol{E}_0}{\partial t} + \varepsilon_0 \Delta\varepsilon_r \frac{\partial \boldsymbol{E}_0}{\partial t}$$

$$= \mathrm{j}\omega\varepsilon_0\varepsilon_r \boldsymbol{E}_0 + \mathrm{j}\omega\varepsilon_0 \Delta\varepsilon_r \boldsymbol{E}_0 \tag{2.23}$$

Comparing this equation with (3.1) of the Appendix:

$$\nabla \times \boldsymbol{H} = \varepsilon_0 \varepsilon_r \frac{\partial \boldsymbol{E}}{\partial t} + \sigma \boldsymbol{E} = \mathrm{j}\omega\varepsilon_0\varepsilon_r \boldsymbol{E} + \sigma \boldsymbol{E}$$

we see that the inhomogeneities in the dielectric constant have the same effect as would have a system of currents having a density:

$$\boldsymbol{i} = \sigma \boldsymbol{E} = \mathrm{j}\omega\varepsilon_0 \Delta\varepsilon_r \boldsymbol{E}_0 \tag{2.24}$$

Radiation from the scattering medium

Radiation from the scattering medium outside the straight line linking the source and the receiver is caused by the system of currents discussed above.

An element of volume $\mathrm{d}V$ in this scattering medium, with a length $\mathrm{d}l$ in the direction of the incident field, and a cross-section $\mathrm{d}S$ in the perpendicular plane, will have a moment:

$$\mathrm{d}\boldsymbol{M} = \boldsymbol{I}\,\mathrm{d}l = \boldsymbol{i}\,\mathrm{d}S\,\mathrm{d}l = \boldsymbol{i}\,\mathrm{d}V$$

$$= \mathrm{j}\omega\varepsilon_0 \Delta\varepsilon_r \boldsymbol{E}_0\,\mathrm{d}V \tag{2.25}$$

Following the theory of the electric dipole, the field radiated at a distance R_R by this element in a direction forming an angle θ with the incident wave, will be:

$$\mathrm{d}\boldsymbol{E} = -\mathrm{j}\frac{60\pi\,\mathrm{d}\boldsymbol{M}}{\varepsilon\lambda}\Psi(R_R)\sin\theta$$

where:

$$\Psi(r) = \frac{e^{-j\frac{\omega}{c}r}}{r}$$

Substituting dM by its value (2.25) we find:

$$dE = \frac{k^2}{4\pi} E_0 \Delta\varepsilon_r \Psi(R_R) \sin\theta \, dV \tag{2.26}$$

We must now sum the contributions dE of all parts of the common volume V. The problem can be simplified by assuming that the dimensions of this volume are small compared to distances R_E and R_R of the source and the receiver respectively. It can then be assumed that E_0 possesses a constant amplitude throughout the scattering volume, and that R_R is constant in the denominator of the function $\Psi(R_R)$. This is Fraunhofer's approximation.

Nevertheless, these calculations are rather intricate[104]. Using P_0 for the power density supplied by the source to the scattering volume, P_R for the power density received, and X for the angle between the direction of the electric field in the scattering volume and the direction of the receiver, we find:

$$\frac{P_R}{P_0} = \left(\frac{k^2 \sin X}{4\pi R_R}\right)^2 I \tag{2.27}$$

where:

$$I = \int_V^3 \int_V^3 \Delta\varepsilon_r \Delta\varepsilon_r' \cdot e^{j\mathbf{K}\cdot\mathbf{r}} d^2V \tag{2.28}$$

where ε_r' and ε_r = dielectric relative constants at two points in the scattering volume (Booker and Gordon used the absolute dielectric constants $\varepsilon = \varepsilon_0\varepsilon_r$. They therefore used $\Delta\varepsilon/\varepsilon$ instead of $\Delta\varepsilon_r$). We note on the one hand that angle X is equal to $\pi/2$ for horizontal polarization, and to $(\pi/2 \pm \theta)$ for vertical polarization. Since θ is always small, we can put $\sin X = 1$.

On the other hand we derive from equation (2.15):

$$\int_V^3 \Delta\varepsilon_r \Delta\varepsilon_r' \, dV = V\langle(\Delta\varepsilon_r)^2\rangle C(\mathbf{r})$$

and therefore:

$$I = V\langle(\Delta\varepsilon_r)^2\rangle \int_V^3 C(\mathbf{r}) e^{j\mathbf{K}\cdot\mathbf{r}} dV \tag{2.29}$$

In fact we can expand the integral to infinity because $C(\mathbf{r})$ rapidly reduces to zero outside the scattering volume, and we have (2.16):

$$I = V \cdot S(\mathbf{K}) \tag{2.30}$$

and

$$\frac{P_R}{P_0} \quad \left(\frac{k^2}{4\pi R_R}\right)^2 V S(\boldsymbol{K}) \tag{2.31}$$

The scattering parameter σ as defined on page 33 is equal to the ratio P_r/P_0 per unit volume and per unit solid angle. Therefore:

$$\sigma = \frac{P_R}{P_0}\frac{R_R^2}{V} = \left(\frac{k^2}{4\pi}\right)^2 S(\boldsymbol{K}) \tag{2.32}$$

This equation allows one to compare the experimentally ascertained values of σ to the values of $S(\boldsymbol{K})$ resulting from the various theories[132].

Isotropy

It seems a well established fact[127] that atmospheric turbulence is not isotropic. As could be expected, the vertical plays an important part in the distribution of inhomogeneities. However, due to the complexity of calculation in the case of anisotropic turbulence, the hypothesis of isotropic turbulence is often used—as proposed by Booker and Gordon in their original paper[104].

In this case the correlation between the dielectric fluctuations at two points in the scattering volume is only a function of the distance. We can therefore replace $C(\boldsymbol{r})$ by $C(r)$, and according to (equation 2.22), $S(\boldsymbol{K})$ by $S(K) = S(2k \sin \theta/2)$. Equations (2.16) and (2.32) then become:

$$S(K) = \langle(\Delta\varepsilon_r)^2\rangle \cdot \frac{4\pi}{K}\int_0^\infty r \cdot C(r) \sin K_r \, dr$$

$$\sigma = \left(\frac{k^2}{4\pi}\right)^2 S\left(2k \sin\frac{\theta}{2}\right) \tag{2.33}$$

or in practice (because θ is very small):

$$\sigma \approx \left(\frac{k^2}{4\pi}\right)^2 S(k\theta) \tag{2.34}$$

Equation (2.34) shows that the only inhomogeneities acting on the scattering of waves having a frequency f will be those with equivalent dimensions given by:

$$\frac{1}{l} = k\theta = \frac{\omega}{c}\theta$$

or

$$l = \frac{c}{2\pi f \theta} \tag{2.35}$$

For the commonly used frequency range (150–4000 MHz) and scattering angle (10–60 mrad) the length varies between 30 m and 20 cm, and therefore lies in the inertial range. This would still be true in the case of anisotropic turbulence—even with a rather high anisotropy factor.

Effect of frequency

In the inertial range (see page 33) the spectrum can be represented by the following equation:

$$S(K) = \propto K^{-\alpha}$$

We have for a constant scattering angle θ:

$$S(K) = \propto k^{-\alpha}$$

and by means of equation (2.34):

$$\sigma \propto k^{(4-\alpha)} \propto f^{(4-\alpha)} \tag{2.36}$$

Booker and Gordon[104] have adopted:

$$C(r) = \mathrm{e}^{-r/l_0} \tag{2.37}$$

an equation which makes calculation particularly easy. The spectrum is then:

$$S(K) = \frac{8\pi\langle(\Delta\varepsilon_r)^2\rangle l_0^3}{(1+K^2 l_0^2)^2} \tag{2.38}$$

With this spectrum, $\alpha = 4$ and σ is independent of frequency. A great number of accurate observations have shown that, other factors being equal, the scattered energy depends on frequency. Though the results show different values[142], it is generally agreed that σ is inversely proportional to frequency, which requires $\alpha = 5$.

The value $\alpha = 5$ is that given by the theory of mixing of air masses (see page 34) and is found by adopting the following equation for the correlation coefficient:

$$C(r) = \frac{r}{l_0} K_1\left(\frac{r}{l_0}\right) \tag{2.39}$$

where $K_1(z)$ = modified Bessel function of the second order, of the first order[1, 2].

The spectrum is now:

$$S(K) = \frac{6\pi^2\langle(\Delta\varepsilon_r)^2\rangle l_0^3}{(1+K^2 l_0^2)^{\frac{5}{2}}} \tag{2.40}$$

Effect of distance

In the study of tropospheric propagation, the effect of troposcatter is usually expressed by the difference between the actual loss and the loss that would occur if both source and receiver were in free space. This difference is called the loss related to free space.

The same as for σ, the loss related to free space depends on $S(K)$ and therefore on the scattering angle θ, as well as on the quadratic mean of the inhomogeneities $\langle(\Delta\varepsilon_r)\rangle^2$. This last quantity depends in turn on the altitude where scattering takes place, because ε_r (and therefore $\Delta\varepsilon_r$) decreases with altitude (equation (2.2)).

Though a considerable amount of mathematical work has been carried out in this field, a satisfactory theory has not yet been found.

For medium distances (150–300 km), the received power decreases more or less as $d^{-5\cdot5}$, when the axes of both the source and receiving antenna beams are horizontal. If they are above the horizon, a supplementary decrease in h^{-2} is observed (h is the mean altitude of the scattering volume). This latter phenomenon has a very strong effect, so that it is very important that the horizon of the antennae is quite clear.

Nomograms giving the mean value of the loss related to free space will be found in Chapter 8. The proposed method of calculation takes into account the altitude of the scattering volume.

Effect of climate

It has been shown in Section 2.2.1 that the refractive index gradient affects the ray curvature. The latter reduces both the scattering angle and the altitude of the scattering volume, thus increasing the scattered field. On the other hand, the refractive index gradient is obviously related to the meteorological conditions. There must therefore exist a relation between the meteorological conditions and the field. Unfortunately it is very difficult to express this relation in a quantitative form.

The most obvious idea, which is still widely applied, is to use either the index of refraction near the ground, or the index gradient calculated over the first 1 000 m of altitude[114, 140, 142, 145, 149, 155]. The former method gives correct results in temperate climates[171]. Generally speaking, it is not valid in other climates[164]. However, it would appear that in climates with a high refractive index, the mean value of transmission loss is lower than in climates where this index is low. For want of something better, we can therefore use the rules given by CCIR[140]. For this purpose, a map giving the mean monthly value of the refractive index near the ground is shown in Fig. 224, Chapter 9.

A new parameter, based on the mean value, g_e, of the gradient between the ground and the common volume, and on the gradient at the base of the common volume, g_c, seems to be more satisfactory[172].

This parameter is defined as:

$$T = -3/8\, g_e - 5/4\, g_c$$

The attenuation between isotropic antennae is thus:

$$A = 110{\cdot}5 + 30 \log d + 30 \log f + T$$

The values of g_e and g_c are deduced from meteorological sondes. Unfortunately, there are not many weather stations where such sondes are used, and the hours of sonding are limited, which restricts the scope of the method quite considerably.

Experimental curves of field strength

A purely experimental method which can also be used consists in using different field curves for each climate. Various experimental curves[118, 139, 166] have been proposed for calculating the median field strength (or the median loss). Different authors have published different results, even for zones for which numerous experimental results are available (Europe and North America). The uncertainty is still greater for those climatic zones where propagation study is scarce.

Graphs derived from CCIR Report 241–1[139] and from the curves issued by the French CNET[166] will be found in Figs 221 and 222, Chapter 9.

Barsis, Norton and Rice[159] consider that the standard deviation between calculations and experiments is of the order of 3·6 dB. This value is certainly optimistic, especially outside temperate regions.

It is of course possible to attempt improving the accuracy of the calculations in every particular case by carrying out field measurements. However, these measurements must be carried out over a long period of time to give sufficient certainty[159].

Antenna-to-medium coupling loss

Even when transmitting and receiving antennae have large beams, the common volume is limited. Downwards it is limited by the shadow of the earth. Upwards and on the sides, it is practically limited to a region corresponding to small values on the scattering angle θ, while σ decreases very steeply when θ increases.

However, when the free space gain of the antennae becomes very great, their beam becomes very narrow, and it can no longer cover the entire volume considered above. In this case, the antenna suffers a reduction in free-space gain (antenna-to-medium coupling loss). This reduction in gain increases with the normal gain of the antennae used, and probably with distance. A very interesting study on this subject has been published by Staras[127] who has studied the case of anisotropic turbulence. The principle of his method is as follows: he makes the ratio

$$r = \frac{l_0 \text{ vertical}}{l_0 \text{ horizontal}}$$

the anisotropy coefficient. He first calculates the reduction in gain for an antenna having a narrow beam in the vertical direction, and then for an antenna having a narrow beam in the horizontal direction. He assumes that the gain reduction for an actual antenna (which commonly possesses the same beam width in both directions) is equal to the product of both

reductions in gain calculated in this manner. He gives the symbol Ω_1 to the 3 dB beam width of the transmitting antenna, and Ω_2 to the corresponding angle of the receiving antenna. He defines an angle Ω_0 by means of the equation:

$$\frac{1}{\Omega_0^2} = \frac{1}{\Omega_1^2} + \frac{1}{\Omega_2^2}$$

The results are expressed as a function of θ_0/Ω_0, where θ_0 = scattering angle.

Starting from an analysis of the published results, Boithias and Battesti[163] have proposed a different theory, according to which, for distances between 150 and 500 km, and for frequencies ranging from 400–10 000 MHz, the reduction in gain depends solely on the free space gain of the antennae. The corresponding curve is reproduced in Fig. 222, Chapter 9.

This question is still highly controversial and it is difficult to state a definite preference for any of the proposed methods.

Available bandwidth

The various paths linking the transmitter and the receiver traverse various points in the scattering volume. They have therefore different lengths, producing differences in transit time. If Δt is the difference in transit time between the shortest and the longest ray, the available bandwidth is defined by:

$$B = \frac{1}{\Delta t}$$

If the antenna possesses a broad pattern, the farthest rays and hence the bandwidth, are not related with them, but with the characteristics of the medium, as mentioned in the preceding paragraph. It is possible to reduce the deviation of the farthest rays—thus increasing the bandwidth—by using antennae possessing very narrow beams.

The available bandwidth has been calculated for both cases by Gerks[117]. A nomogram based on this study is given in Fig. 194, Chapter 8. Starting from similar calculations, Shaft[158] has constructed more complete nomograms.

Variations in the received signal

Due to the random motion of the atmosphere, the received signal varies erratically in both time and space.

Cyclical variations of the mean field with time

Our data on the cyclical variation of the median field are still inadequate. This is probably due to the fact that most observations have been too short.

In temperate climates, where the greatest number of observations have been made, a maximum appears in summer and a minimum in winter, with a difference of 8–10 dB between the mean values. A diurnal minimum seems to occur in the afternoon as well. Most published observations show that these cyclical variations have a smaller effect on small field values, i.e. fields which are exceeded during a large percentage of the time. The field values for the 'worst' month of the year are the most interesting[155, 166].

Random variations in the field. These have been studied by Rice[410], who applied the same physical considerations as used by Booker and Gordon[104]. Silverman[126] has rigorously related the variations in the field with modern turbulence theory.

Taking into account the simplifications introduced by Rice at the end of his calculations, we can confirm his results in the following way:

Suppose that the geometry is as in Fig. 14, and that:

1. The coordinates of the vector have a gaussian distribution, with an r.m.s. value of l following every axis;
2. The speeds of the scattering elements P'_n have a gaussian distribution, with an r.m.s. value U following every axis.

Result (a)

According to equation (2.21), we have, putting P_z for the vertical axis passing through P

$$\Delta\Phi = \mathbf{K}\cdot\mathbf{r} = 2kz \sin\frac{\theta}{2} = \frac{4\pi fz}{c}\sin\frac{\theta}{2}$$

whence

$$\Delta f = \frac{1}{2\pi}\frac{\mathrm{d}(\Delta\Phi)}{\mathrm{d}t} = \frac{2f}{c}\sin\frac{\theta}{2}\frac{\mathrm{d}z}{\mathrm{d}t} = \frac{2f}{c}\sin\frac{\theta}{2}V_z$$

V_z being the speed of P'_n in the vertical direction. As V_z is a gaussian variable, the same is true for Δf, and for the sum of the contributions of all the points of the scattering volume. Thus, we can take the r.m.s. value of both sides.

$$(\Delta f)_{\text{r.m.s.}} = \sigma_a = \frac{2fU}{c}\sin\frac{\theta}{2}$$

Rice[404] has shown that for this type of wave, the number of maxima per second of the envelope is given by

$$2{\cdot}52\,\sigma_a = \frac{5{\cdot}04fU}{c}\sin\frac{\theta}{2}$$

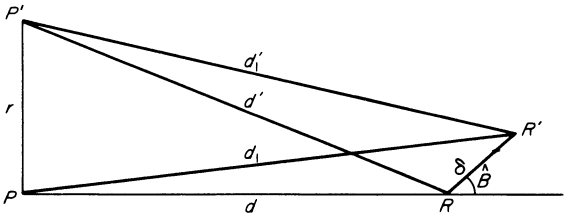

Fig. 14a

Result (*b*) (see Fig. 14a)

If $\rho \ll d$ and $\delta \ll d$, we can find

$$\Delta^2 d = (d_1' - d_1) - (d' - d) \approx -\frac{r\delta \sin \hat{B}}{d}$$

whence

$$\Delta^2 \Phi = \frac{2\pi \Delta^2 d}{\lambda} \approx -\frac{2\pi r\delta \sin \hat{B}}{\lambda d}$$

The phase relation will be the same as in the receiving location R if

$$\frac{2\pi r\delta |\sin \hat{B}|}{\lambda d} = 2\pi$$

or:

$$\frac{1}{\delta} = \frac{r|\sin \hat{B}|}{\lambda d}$$

This is again a gaussian variable, and we can write

$$\left(\frac{1}{\delta}\right)_{\text{r.m.s.}} = \sigma_b = \frac{l|\sin \hat{B}|}{\lambda d}$$

The number of maxima per metre will be $2{\cdot}52\sigma_b$, and the distance between maxima will be

$$\frac{1}{2{\cdot}52\,\sigma_b} = \frac{\lambda d}{2{\cdot}52\, l|\sin \hat{B}|}$$

According to this formula, the distance between the maxima would be infinite when travelling along the direction of propagation. However, using a closer approximation, it is easy to prove that in this case we have

$$\frac{1}{\sigma_b'} = \frac{2\lambda d^2}{(3)^{\frac{1}{2}} l^2}$$

Result (*c*)

From (2.21)

$$\Delta\Phi = \mathbf{K}\cdot\mathbf{r} = \frac{4\pi fz}{c} \sin \frac{\theta}{2}$$

we deduce that the phase relation will be the same for two frequencies with a difference Δf given by

$$\frac{4\pi z \Delta f}{c} \sin\frac{\theta}{2} = \pm 2\pi$$

or

$$\pm \frac{1}{\Delta f} = \frac{2z \sin\frac{\theta}{2}}{c}$$

whence

$$\left(\frac{1}{\Delta f}\right)_{\text{r.m.s.}} = \sigma_c = \frac{2l \sin\frac{\theta}{2}}{c}$$

The number of maxima per hertz will then be

$$2{\cdot}52\,\sigma_c = \frac{5{\cdot}04\,l \sin\frac{\theta}{2}}{c}$$

and the frequency difference between two maxima will be

$$\frac{1}{2{\cdot}52\,\sigma_c} = \frac{c}{5{\cdot}04\,l \sin\frac{\theta}{2}} \text{ Hz}$$

As pointed out by Rice, these results suppose a scattering mechanism based on scattering centres with a gaussian distribution, which is questionable. They do not have an absolute value, but they agree with the experimental data on the following points.

1. The speed of fading is proportional to the carrier frequency.
2. The correlation distance between the field in two points is much greater following the direction of propagation than in the perpendicular direction.
3. The frequency difference giving correlated fields is inversely proportional to the dimensions of the scattering volume.

Among the published results about fading, we must also point out those of Wright[144] and Vigants[433] on the duration of fadings.

Measurements have shown, as for the other modes of propagation, that there are two distribution laws, one for short time intervals and the other for long intervals.

Short time intervals. Measured over a short period (e.g. 1–5 min) the field strength obeys Rayleigh's law with remarkable accuracy. This allows the easy calculation of the effect of diversity reception (see A.6.7.1 and A.6.7.2 of the Appendices). The phase of the received field also varies randomly, with a constant density distribution.

Long period fading. It is often difficult to know whether the authors of papers on tropospheric scattering have distinguished in the published results between the part played by cyclical variations and that played by long period random variations. Nevertheless, the hourly mean values of

the fields seem to have an approximately log-normal distribution, at least for weak fields (which are the only ones of interest for the calculation of communication circuits).

The standard deviation σ of this distribution depends on distance and climate. Analysis of the experimental results[159] has proved that in temperate climates σ at first increases with the scattering angle and reaches a maximum for $\theta = 15$ mrad, then decreases and remains practically constant for $\theta > 60$ mrad.

CCIR[139] has published provisional curves of statistical distribution for other climates. Values of σ deduced from these curves and from those issued by the French CNET[166] are given in Fig. 222, Chapter 9.

Spatial correlation of long period fading. The hourly median values of the field are almost identical over large regions. This makes it impossible to compensate their variations by space diversity.

Spatial correlation of short period fading. A relation exists between the field strength received at the same instant at two points, which is covered by the correlation coefficient of these fields. This coefficient equals unity if the points are extremely close to each other, and tends towards zero as the points move infinitely apart.

It has been found (and it can be proved) that the correlation coefficient remains significant for a much greater displacement in the sense of propagation than in a perpendicular sense. Antennae that are spaced perpendicularly to the direction of propagation must therefore be used for space diversity.

For frequencies above 1 GHz, and for temperate climate, the following formulas have been proposed by the Deutsche Bundespost for the minimum distance between antennae used for space-diversity reception:

$$\text{Horizontal: } \Delta y = 0{\cdot}36\,(D^2+1600)^{\frac{1}{2}}$$
$$\text{Vertical: } \Delta z = 0{\cdot}36\,(D^2+225)^{\frac{1}{2}}$$

Δy and Δz = antennae distance, metres

D = antenna diameter, metres.

Frequency correlation of the fading. The difference in the length of the rays scattered by the different parts of the diffusing volume (measured in wavelengths) depends on the frequency. The relation between the field strength and the frequency difference may thus be defined by a correlation coefficient[175,183]. The correlation of the long term fading extends over a very wide frequency range[175], so that multiple frequency reception will not deal with this type of fading. However, this measure is very effective in dealing with short term fading. As it avoids the use of two receiving antennae, it is very widely used.

Mode of modulation

As the received field varies greatly and very rapidly, frequency modulation would appear to be the most practical method. Small modulation indexes (1–2) are used to avoid an excessive increase in receiver bandwidth, which would lead to an increase in the required transmitted power.

It has also been proposed to use d.s.b. (double sideband without carrier) or i.s.b. (with reduced or suppressed carrier wave). This latter method can only be used for the lower frequencies of the allowed band, because of the necessary frequency accuracy. On the other hand, this method is much more strongly affected by selective fading.

2.3.3 THEORY OF MULTIPLE REFLECTION

We have discussed in Section 2.2.3 the case of tropospheric reflection by large layers with a refractive index that can differ rather appreciably from the mean value. These layers are related to stable atmospheric conditions and occur only rarely. They are responsible for most TV interference, and cannot be used for establishing regular radio communications. On the contrary, meteorological observations, measurements made with airborne refractometers, and observations carried out with specially designed radar equipment, have shown that lamellae are permanently present in the atmosphere, whose refractive index does not differ very much from the mean value. These lamellae are able to produce partial reflections, which are necessarily very weak. The power reflected by the various lamellae are added at the receiving station, producing a fluctuating but always present field. Various authors[130, 131, 133, 134, 141, 142, 146] think that the existence of a rather strong field beyond the horizon is due to these lamellae.

2.3.3.1 **Characteristics of lamellae**

The horizontal dimensions of these lamellae are of the order of a few km. Their thickness varies from a few metres to 20 m, their altitude from 300–3 000 m, and the corresponding Δn from 5–10 N-units at ground level (it decreases with increasing altitude).

The angle of incidence on the lamella φ, calculated by means of equation (2.13) then varies from 8 to 27 mrad.

2.3.3.2 **Calculating the reflection coefficient**

It is obvious that the refractive index varies progressively at the input into the lamella, as well as at the output. By selecting a given function as representing the curve of variation in the index, a complete calculation of the reflection coefficient of the lamella can be carried out[130, 133, 134, 141]

We have already established the following equation (2.12) which gives the reflection coefficient for a small value of Δn:

$$R = \frac{1-\left(\frac{2\Delta n}{\sin^2\varphi}+1\right)^{\frac{1}{2}}}{1+\left(\frac{2\Delta n}{\sin^2\varphi}+1\right)^{\frac{1}{2}}}$$

Since φ is small, this equation can be simplified to:

$$R = \frac{1-\left(\frac{2\Delta n}{\varphi^2}+1\right)^{\frac{1}{2}}}{1+\left(\frac{2\Delta n}{\varphi^2}+1\right)^{\frac{1}{2}}}$$

or, noting that in our case

$$\frac{2\Delta n}{\varphi^2} \ll 1$$

$$R \simeq \frac{\Delta n}{2\varphi^2} \tag{2.41}$$

Supposing that the vertical gradient of the index is represented by:

$$g(h) = \frac{\mathrm{d}n}{\mathrm{d}h}$$

the reflection coefficient of a thin horizontal slab at an altitude h will be:

$$\mathrm{d}R = \frac{g(h)}{2\varphi^2}\mathrm{d}h \tag{2.42}$$

The phase difference between the two slabs can be calculated by means of equation (2.21):

$$\Delta\Phi = \boldsymbol{K}\cdot\boldsymbol{r}$$

Substituting $\boldsymbol{h}$ for $\boldsymbol{r}$, noting that $\boldsymbol{K}$ and $\boldsymbol{h}$ are parallel, and putting K for the modulus of $\boldsymbol{K}$, the phase difference will be:

$$\Delta\Phi = Kh \tag{2.43}$$

if we take the phase at $h = 0$ as the origin.

Finally, combining equations (2.42) and (2.43) we find for the total reflection coefficient of a random layer:

$$R = \frac{1}{2\varphi_2^2}\int_{h_0}^{h_1} g(h)\mathrm{e}^{-\mathrm{j}Kh}\mathrm{d}h \tag{2.44}$$

This means that $2\varphi^2 R$ is the Fourier transform (see Appendix 7) of the gradient of the index, $g(h)$. For example, for a linear layer, defined by:

$$g(h) = \frac{\Delta n}{\Delta h} = \text{constant} \qquad \text{for } h_0 \leqslant h \leqslant h_0+\Delta h$$

we have:

$$R = \frac{\Delta n}{2\varphi^2} \frac{\sin \frac{K\Delta h}{2}}{\frac{K\Delta h}{2}} \tag{2.45}$$

For a parabolic layer, defined by:

$$g(h) = \Delta n\left(1 - \frac{h}{\Delta h}\right) \qquad \text{for } h_0 \leqslant h \leqslant h_0 + \Delta h$$

$$R = \frac{\Delta n}{2\varphi^2}\left(\frac{\sin \frac{K\Delta h}{2}}{\frac{K\Delta h}{2}}\right)^2 \tag{2.46}$$

For small values of φ we have furthermore approximately, using equation (2.22) and noting that $\theta = 2\varphi$:

$$K = 2k\varphi \tag{2.47}$$

Comparing R in the extreme conditions of frequency, altitude of reflection, layer thickness and Δn, and assuming $g(h)$ constant throughout the layer, we find values from 10^{-1} to 10^{-4}, the higher value of course being the less frequent.

2.3.3.3 **Reflection by a small surface**

When the dimensions of a reflecting surface greatly exceed the area illuminated by the source antenna as seen by the receiving antenna, the reflected power will be equal to the received power, multiplied by the square of the reflection coefficient R^2.

If the reflecting surface is small, it is necessary as in optics to apply Fresnel's diffraction theory. The problem can be slightly simplified by assuming a plane, horizontal and rectangular lamella with the following dimensions:

- b in the direction of propagation, and
- c in the perpendicular direction (see Fig. 15). Under these conditions, the diffraction parameters will be, putting a for half the distance between source and receiver:

In the direction of propagation:

$$u = \frac{c}{(\lambda a)^{\frac{1}{2}}} \tag{2.48}$$

In the perpendicular direction:

$$v = \frac{b\varphi}{(\lambda a)^{\frac{1}{2}}} \tag{2.49}$$

The ratio of reflected power to incident power is:

$$\frac{P_R}{P_0} = 4[C^2(u) + S^2(u)][C\ (v) + S^2(v)]R^2 \tag{2.50}$$

where $C(x)$ and $S(x)$ are the Fresnel integrals:

$$C(x) = \int_0^x \cos\left(\frac{\pi x^2}{2}\right) dx$$

$$S(x) = \int_0^x \sin\left(\frac{\pi x^2}{2}\right) dx$$

When x is very large, both integrals tend towards 0·5. When x is small, $C(x)$ tends towards x and $S(x)$ towards $\pi x^3/6$; it is therefore negligible when compared to $C(x)$.

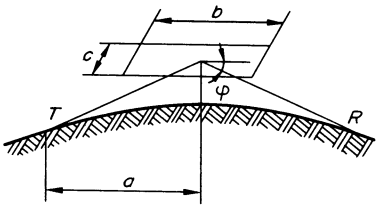

Fig. 15

It is normal to assume $c = b$. When comparing equations (2.48) and (2.49) with the orders of magnitude given in Section 2.3.1, we see that in practice u may be considered as large and v as small. Finally, it is convenient to put $d = 2a$ (distance between source and receiver). Equation (2.50) then becomes:

$$\frac{P_R}{P_0} = 4\frac{b^2\varphi^2}{\lambda d} R^2 \tag{2.51}$$

Assuming the lamellae being of the linear type (the simplest one), the value of R is given by equation (2.45) and we have:

$$\frac{P_R}{P_0} = \frac{b^2}{4\pi^2}\left(\frac{\Delta n}{\Delta h}\right)^2 \frac{1}{d\varphi^4} \lambda \sin^2 \frac{K\Delta h}{2} \tag{2.52}$$

2.3.3.4 **Effect of corrugation in the lamellae**

If the shape of the surface is so irregular that Rayleigh's criterion (Section 4.1.4.1) is no longer satisfied, the reflection coefficient decreases. With the values of angle φ under consideration, this occurs for a depth of irregularities equal to 2–8 wavelengths. At the same time part of the reflection will be scattered, so that the lamellae radiate energy in directions not foreseen in our former reasoning.

2.3.3.5 Reflection by a set of lamellae

Each lamella pertaining to the common volume will afford a contribution given by equation (2.52) and as the phases of the received field are random, the powers will be added. For the same reason the $\sin^2$ factor must be replaced by its mean value, i.e. $\frac{1}{2}$. We then have:

$$\frac{P_R}{P_0} = \frac{\lambda}{8\pi^2 d} \sum_i \frac{b_i^2}{\varphi_i^4} \left(\frac{\Delta n}{\Delta h}\right)_i^2 \tag{2.53}$$

Effect of frequency

We observe that for a lamella of linear type, the received power is proportional to λ and therefore inversely proportional to the frequency—which agrees with experimental results.

Effect of distance

This may be deduced from the terms:

$$\frac{1}{d} \sum_i \frac{b_i^2}{\varphi_i^4} \left(\frac{\Delta n}{\Delta h}\right)_i^2$$

Other things being equal, angle φ is proportional to the distance. On the other hand, the reflection altitude h is proportional to the square of the distance and $\Delta n/\Delta h$ depends on h. It is possible, by a suitable choice of the laws of variation for these quantities, to rediscover the experimental law of variation in $d^{-5.5}$ or d^{-6}.

Other characteristics

The other characteristics of the received field (antenna-to-medium coupling loss, available bandwidth, received signal fluctuations) are explained in the same way as in turbulence theory because of the similarity of the propagation mechanisms, though the number of scattering centres is smaller. In particular, this does not prevent the rapid fluctuations of the field from obeying Rayleigh's law[411, 413].

2.3.4 NORMAL MODE THEORY

Caroll[115, 129] has proposed a theory explaining tropospheric propagation well beyond the horizon, using the theory of propagation by diffraction around the earth, amended to take into account the variations in the refractive index with altitude. In this theory, turbulence would only intervene for explaining field fluctuation.

Earlier studies assumed a linear decrease of the index up to a given altitude, where it becomes zero. Field calculations have given acceptable values, but it has been observed that this was due to the index gradient discontinuity at the instant the index became zero.

This discontinuity does not exist in natural media. New calculations were therefore carried out, assuming a parabolic profile of the index, linking up without discontinuity. The newly calculated fields were about 60 dB below the first evaluation and could no longer explain the observed field. Anyhow, this theory does not give an explanation of most of the field characteristics observed well beyond the horizon (antenna-to-medium coupling loss, limitation of bandwidth and rapid fading).

2.3.5 CONCLUSIONS

Explanations of tropospheric scattering propagation, either by atmospheric turbulence or by reflections from small lamellae, are based on experimental results. It remains probable that, according to the meteorological conditions, they coexist in variable proportions.

However, they do not allow the calculation of either the received fields or their variations with the accuracy required for practical applications. A long period of experimental work will still be necessary before accurate predictions in the various regions of the earth will have been achieved.

It is hoped that this research will include not only the effects, but also the causes, especially micro-meteorology. This will allow improvement of the theories and perhaps the achievement of fully satisfactory explanations of the observed phenomena.

CHAPTER 3

WAVE PROPAGATION IN THE GROUND

3.1 TERRESTRIAL ELECTRIC CONSTANTS

The earth's surface consists of seawater and soils of different compositions. These media are conductors (although rather poor ones) and possess a rather high dielectric constant. They will therefore behave towards radio waves in a way between conductors and dielectrics. The values of conductivity for seawater range from 4–5 S/m; those for the ground range from 0·01–0·001 S/m. The relative dielectric constant of seawater is 80, and of earth 4–20, according to the degree of humidity. CCIR Report No. 229[227] gives a survey of measurement methods for ground conductivity.

To simplify propagation calculations, they are usually carried out for only three media: seawater, good ground and poor ground, the last being the worst conductor. Different authors give different definitions of these media. The American Army Radio Propagation Unit has adopted the following standard values:

	S/m	ε_r
Sea	5	80
Good ground	10^{-2}	10
Poor ground	10^{-3}	4

The characteristics of 'good ground apply to thick layers of arable soil, clay soil, and the lowest parts of humid valleys. 'Poor ground' will be found in rocky terrain, dry sand and deserts.

3.2 ELECTRICAL BEHAVIOUR OF IMPERFECTLY CONDUCTING BODIES*

An elementary cube of a conducting body having unit height and section is submitted to an electric field E. The resulting conduction current is:

$$I_C = \sigma E \tag{3.1}$$

* The term 'semiconductor', found in older books, is incorrect, because semiconductors now form a well defined class of their own, having nothing to do with the earth's surface.

In the case of a dielectric, the conventional formula of the parallel plate capacitor gives us a displacement current:

$$\boldsymbol{I}_D = C\frac{\mathrm{d}\boldsymbol{E}}{\mathrm{d}t} = \varepsilon_0\varepsilon_r\frac{\mathrm{d}\boldsymbol{E}}{\mathrm{d}t} \tag{3.2}$$

Similarly, we have in the case of an imperfect conductor:

$$\boldsymbol{I} = \boldsymbol{I}_C + \boldsymbol{I}_D = \sigma\boldsymbol{E} + \varepsilon_0\varepsilon_r\frac{\mathrm{d}\boldsymbol{E}}{\mathrm{d}t} \tag{3.3}$$

In radio problems, $\boldsymbol{E}$ is a sinusoidal field of an angular frequency ω, so that equation (3.3) can be written:

$$\boldsymbol{I} = (\sigma + \mathrm{j}\omega\varepsilon_0\varepsilon_r)\boldsymbol{E} \tag{3.4}$$

We now put:

$$\left|\frac{I_C}{I_D}\right| = \frac{\sigma}{\omega\varepsilon_0\varepsilon_r} = q \tag{3.5}$$

If $q \gg 1$, the medium is practically a pure conductor. If $q \ll 1$, the medium is practically a pure dielectric.

We see therefore that at sufficiently low frequencies imperfectly conducting bodies behave as pure conductors, while they act as pure dielectrics for very high frequencies.

The frequency for which $q = 1$ is 1 100 MHz for seawater, 18 MHz for 'good ground' and 4·5 MHz for 'poor ground'.

3.3 PROPAGATION OF A PLANE SINUSOIDAL WAVE OF CONSTANT FREQUENCY IN AN IMPERFECTLY CONDUCTING MEDIUM

3.3.1 GENERAL EQUATIONS

Propagation phenomena in an imperfectly conducting medium are of a complex nature, and there are many possible waveforms. Apart from the case of communication with submarines, or the use of buried antennae, there are no other applications of this type of propagation. We shall therefore only mention the simplest case, namely the case of a plane sinusoidal wave of constant frequency.

We can write for the fields:

$$\boldsymbol{E} = \boldsymbol{E}_0\,\mathrm{e}^{\mathrm{j}\omega t}$$

$$\boldsymbol{H} = \boldsymbol{H}_0\,\mathrm{e}^{\mathrm{j}\omega t}$$

Amplitudes $\boldsymbol{E}_0$ and $\boldsymbol{H}_0$ depend on x exclusively.

Equations A.1 in the Appendix then become:

$$\left.\begin{aligned}\nabla\times\boldsymbol{E}_0 &= -\mathrm{j}\mu_0\omega\boldsymbol{H}_0\\ \nabla\times\boldsymbol{H}_0 &= (\sigma + \mathrm{j}\omega\varepsilon_0\varepsilon_r)\boldsymbol{E}_0\\ \nabla.\boldsymbol{F}_0 &= \nabla.\boldsymbol{H}_0 = 0\end{aligned}\right\} \tag{3.6}$$

The conversions used in Chapter 1 lead to:

$$\left.\begin{aligned}\nabla^2 \boldsymbol{E}_0 + \mu_0\omega(\omega\varepsilon_0\varepsilon_r - \mathrm{j}\sigma)\boldsymbol{E}_0 = 0\\ \nabla^2 \boldsymbol{H}_0 + \mu_0\omega(\omega\varepsilon_0\varepsilon_r - \mathrm{j}\sigma)\boldsymbol{H}_0 = 0\end{aligned}\right\} \tag{3.7}$$

As $\mu_0\varepsilon_0 = 1/c^2$, we can write:

$$\left.\begin{aligned}\nabla^2 \boldsymbol{E}_0 + \frac{\omega^2}{c^2}\left(\varepsilon_r - \frac{\mathrm{j}\sigma}{\omega\varepsilon_0}\right)\boldsymbol{E}_0 = 0\\ \nabla^2 \boldsymbol{H}_0 + \frac{\omega^2}{c^2}\left(\varepsilon_r - \frac{\mathrm{j}\sigma}{\omega\varepsilon_0}\right)\boldsymbol{H}_0 = 0\end{aligned}\right\} \tag{3.7a}$$

3.3.2 COMPLEX MEDIUM CHARACTERISTICS

The quantity

$$\varepsilon_r' = \varepsilon_r - \frac{\mathrm{j}\sigma}{\omega\varepsilon_0} = \varepsilon_r(1 - \mathrm{j}q) \tag{3.8}$$

which in equation (3.7a) plays the part of ε_r in the case of a dielectric, is called the complex relative dielectric constant of the medium at frequency ω.

Similarly we define the complex index of refraction as:

$$n = \beta - \mathrm{j}\alpha = (\varepsilon_r')^{\frac{1}{2}} = [\varepsilon_r(1 - \mathrm{j}q)]^{\frac{1}{2}} \tag{3.9}$$

We should note that both ε_r and n are variable complex quantities, dependent on ω.

We can now write equation (3.7a) as:

$$\left.\begin{aligned}\nabla^2 \boldsymbol{E}_0 + \frac{\omega^2 n^2}{c^2}\boldsymbol{E}_0 = 0\\ \nabla^2 \boldsymbol{H}_0 + \frac{\omega^2 n^2}{c^2}\boldsymbol{H}_0 = 0\end{aligned}\right\} \tag{3.10}$$

This is an equation of the 'wave equations' type with a complex propagation velocity:

$$v = \frac{c}{n}$$

Contrary to what happens in dielectrics, this velocity is frequency dependent.

The same as in Chapter 1, it can be shown that the waves are transverse, that the electric and magnetic fields are mutually perpendicular, and that the state of wave polarization is the same at all points.

3.3.3 CALCULATING THE FIELDS; PENETRATION

On the other hand, the fields are no longer in phase and the difference in phase between $\boldsymbol{H}$ and $\boldsymbol{E}$ is given by:

$$\tan 2\varphi = q \tag{3.11}$$

Their ratio is:

$$\frac{E_0}{H_0} = \frac{Z_0}{|n|} = \frac{Z_0}{[\varepsilon_r(1+q^2)^{\frac{1}{2}}]^{\frac{1}{2}}} \tag{3.12}$$

According to the above, assuming that we are dealing with a plane wave travelling in the direction $0x$, the field of the wave can be written as:

$$\left.\begin{aligned} E_y &= E_{0y}\, e^{j\omega(t-nx/c)} \\ H_z &= H_{0z}\, e^{j[\omega(t-nx/c)+\varphi]} \end{aligned}\right\} \tag{3.13}$$

Equation (3.12) gives the relation between E_{0y} and H_{0z}. Using equation (3.9) we can write, when separating the real and imaginary components of n:

$$\left.\begin{aligned} E_y &= E_{0y}\, e^{-\omega\alpha x/c} e^{j\omega(t-\beta x/c)} \\ H_z &= H_{0z}\, e^{-\omega\alpha x/c} e^{j[\omega(t-\beta x/c)+\varphi]} \end{aligned}\right\} \tag{3.14}$$

We are therefore in the presence of a plane wave, whose phase plane travels at a velocity c/β and whose amplitude is reduced exponentially. This amplitude is divided by e = 2·718 each time that x is increased by:

$$p = \frac{c}{\omega\alpha} \tag{3.15}$$

α is called the extinction coefficient or extinction index, and p the depth of penetration.

We easily derive:

$$\alpha^2 = \varepsilon_r \frac{(1+q^2)^{\frac{1}{2}} - 1}{2} \tag{3.16}$$

Equation (3.5) has shown that q and therefore α tend towards zero when ω increases indefinitely. The attenuation per wavelength travelled diminishes and the medium has a tendency to become transparent, which is only natural, because it approaches the properties of a dielectric.

However, for practical purposes, p plays a far more important part than α. Indeed, the only cases where ground propagation has any importance, are those of a buried antenna and on board a submarine; in both cases the depth is fixed in advance.

It is easy to verify by means of equations (3.15) and (3.16) that:

1. when ω increases indefinitely, p will approach a fixed limit:

$$p(\omega \to \infty) = \frac{2c\varepsilon_0\varepsilon_r^{\frac{1}{2}}}{\sigma} \tag{3.17}$$

The boundary value is of the order of 10 m in the case of poor ground, which explains the good reception obtained with antennae buried in the sands of desert regions. The order of magnitude is only 1 cm in seawater, which prohibits the use of high frequencies in communication with submarines.

2. when ω becomes very small, we find however:

$$p(\omega \to 0) = c\left(\frac{2\varepsilon_0}{\sigma\omega}\right)^{\frac{1}{2}} \tag{3.18}$$

This value increases therefore when ω decreases. In the case of wavelengths of the order of 30 km ($f = 10$ kHz) in seawater, it is about 2 m, i.e. an attenuation of 4·34 dB/m of immersed passage. This explains the use of waves of great length for this type of communication.

3.4 WAVE PROPAGATION IN THE GROUND

The obvious conclusion of the above discussion is that, generally speaking, the ground is too opaque to radio waves to be used as a medium of propagation.

However, there are two cases where ground propagation becomes necessary despite its poor efficiency.

We have already mentioned the case of a submerged submarine. The emitting station is then at ground level. Very low frequencies are used, necessitating enormous antennae and very powerful transmitters. Moreover, a single station is sufficient for providing coverage over a wide area, because, as we shall see in Sections 6.2.1.1 and 7.1.2.2, the attenuation of the field received varies slowly in relation to the distance.

On the other hand, stimulated by the danger of a nuclear war, the possibility of communication between underground command posts and bomb stores has been examined, using exclusively buried antennae[216, 218, 229].

One can use horizontal dipoles buried in the upper stratum. The waves then emerge from the earth, travel by tropospherical modes (earth wave and wave guided by the ionosphere) and return to earth. The attenuation equals that between antennae erected in the air, increased by a quantity which is practically independent of distance. Quite large ranges are thus possible.

It is also possible to use vertical dipoles in bore-holes—well below the upper stratum. In this case, the range will be only a few kilometres. It is sometimes possible to attain 100 km with low frequencies (10 kHz) when the antennae are situated in the waveguide formed by the upper stratum and the earth's inner shell—the moderately conductive plastic layer situated below crystalline rocks.

CHAPTER 4

WAVE PROPAGATION CLOSE TO THE EARTH'S SURFACE

Wave propagation in the atmosphere can be studied by means of simple reasoning, using geometric optics. The determination of the wave planes and the plotting of the radii are both easy. Planes of equal phase are confused with planes of equal amplitude.

Nothing similar applies to wave propagation close to the earth.

One of the theories of geometric optics—the reflection theory—obviously applies when we choose a point in the line of sight and at least a few wavelengths away from the earth. But even in this case, we are dealing with an extremely complex phenomenon because—as we have seen in Chapter 3—the terrestrial surface is neither a perfect conductor nor a perfect dielectric.

Waves in the immediate proximity of the ground acquire specific properties, which are unknown in optics because the carrying out of experiments at a distance of a few wavelengths from a reflector is obviously impossible.

Finally, the theory of diffraction by the earth's surface is extremely complex because of the great dimensions of the diffracting sphere compared to the wavelength, and the necessity of meeting Maxwell's boundary equations at this imperfectly conducting sphere. Apart from considerable mathematical argument, the solution demands a very delicate discussion of possible approximations.

It will therefore be necessary to summarize the problem and to discuss at least the simplest cases in some detail.

4.1 WAVE REFLECTION FROM THE EARTH'S SURFACE

4.1.1 PLANE WAVES; FLAT UNIFORM GROUND

Without going into the details of the calculation, let us indicate its principle. We can write the incident plane wave as:

$$A_i = A_{0i} e^{j\omega[t - 1/c(\alpha x + \beta y + \gamma z)]} \tag{4.1}$$

where α, β and γ are the cosines of the angles of the normal of the wave

plane to $0x$, $0y$ and $0z$. Taking plane $z = 0$ as the ground plane, we have at this plane:

$$A_i = A_{0i} e^{j\omega[t - 1/c(\alpha x + \beta y)]} \tag{4.2}$$

Due to the continuity of physical phenomena, the reflected (R) and transmitted (T) waves must have expressions of the same form at this plane, irrespective of t, x and y. This requires (when giving the symbol n to the complex refractive index of the ground):

$$\left.\begin{aligned} \omega_i &= \omega_R = \omega_T \\ a_i &= \alpha_R = n\alpha_T \\ \beta_i &= \beta_R = n\beta_T \end{aligned}\right\} \tag{4.3}$$

hence:

$$\frac{\alpha_i}{\beta_i} = \frac{\alpha_R}{\beta_R} = \frac{\alpha_T}{\beta_T}$$

4.1.1.1 **Descartes' laws**

We can conclude from the above that:

1. Frequency is not modified either by reflection or refraction. Its symbol simply remains ω.
2. Ratio α/β, which is the same for the three waves, determines a plane, called the incident plane. We can take this plane for plane $y0z$. We then have $\beta = 0$ and in the plane $x0z$:

$$\alpha_i = \cos \Delta_i$$
$$\alpha_R = \cos \Delta_R$$
$$\alpha_T = \cos \Delta_T$$

whence according to equation (4.3):

$$\Delta_i = \Delta_R \qquad \text{(Descartes' first law)}$$

We can therefore put:

$$\Delta_i = \Delta_R = \Delta$$

Still according to equation (4.3), we have:

$$\cos \Delta = n \cos \Delta_T \qquad \text{(Descartes' second law)}$$

4.1.1.2 **Calculating the reflection coefficient**

Figure 16 represents the disposition of the fields for vertical polarization (vertical electric field, horizontal magnetic field). A similar disposition occurs in the case of horizontal polarization (the electric and magnetic fields changing place).

In the case of oblique polarization, separation in two components—horizontal and vertical—will be necessary.

We can state that:

1. Tangential field components are continuous at the interface.
2. Electric and magnetic fields are related by equation (3.12).
3. Normal components of the displacement current and of the magnetic displacement are continuous.

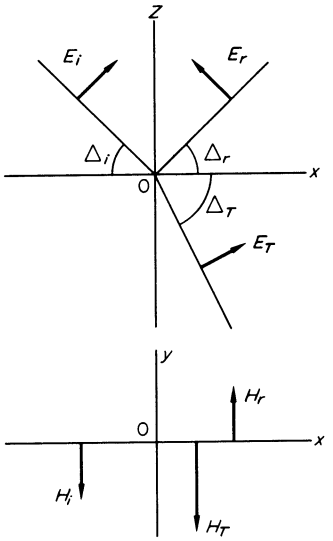

Fig. 16

We thus obtain for the electric field*

$$\left.\begin{aligned} R_V &= \frac{n^2 \sin\Delta - (n^2 - \cos^2\Delta)^{\frac{1}{2}}}{n^2 \sin\Delta + (n^2 - \cos^2\Delta)^{\frac{1}{2}}} \\ R_H &= \frac{\sin\Delta - (n^2 - \cos^2\Delta)^{\frac{1}{2}}}{\sin\Delta + (n^2 - \cos^2\Delta)^{\frac{1}{2}}} \end{aligned}\right\} \qquad (4.4)$$

which, when combined with equation (3.9)

$$n = \beta - j\alpha$$

allows one to calculate the planar reflection coefficient in all cases. This coefficient is a complex quantity whose modulus (always less than unity) is the ratio of the amplitude of the reflected wave to that of the incident wave, and whose phase is the phase difference introduced by reflection.

The resultant equations are so complex that they cannot be used unless plotted as graphs. Burrows has constructed very complete graphs; some of them have been published[3, 8]. Figures 17–20 give a summary reproduction in linear coordinates to provide a better idea of these phenomena.

* Some authors use the minus sign in front of R_H, which is in accordance with the definition of the reflection coefficient, but which obliges one to use different signs for the two polarization directions in equations for field strength.

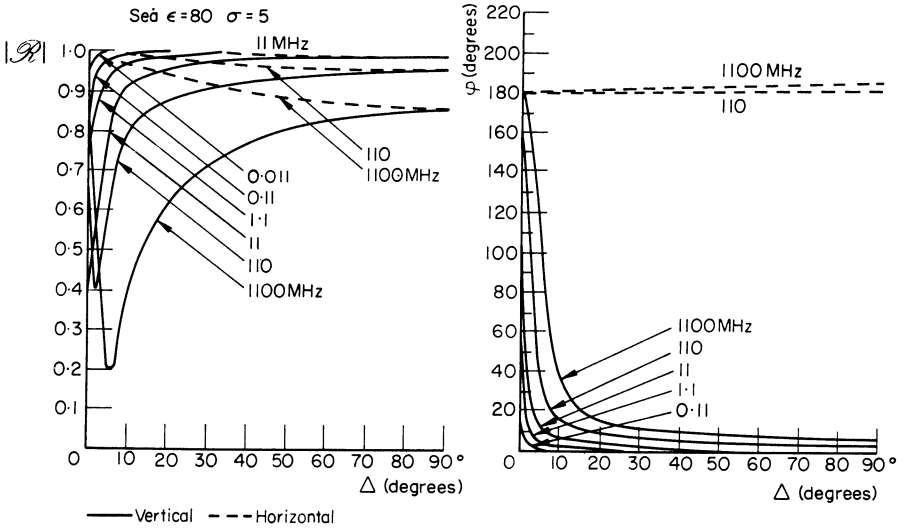

Fig. 17

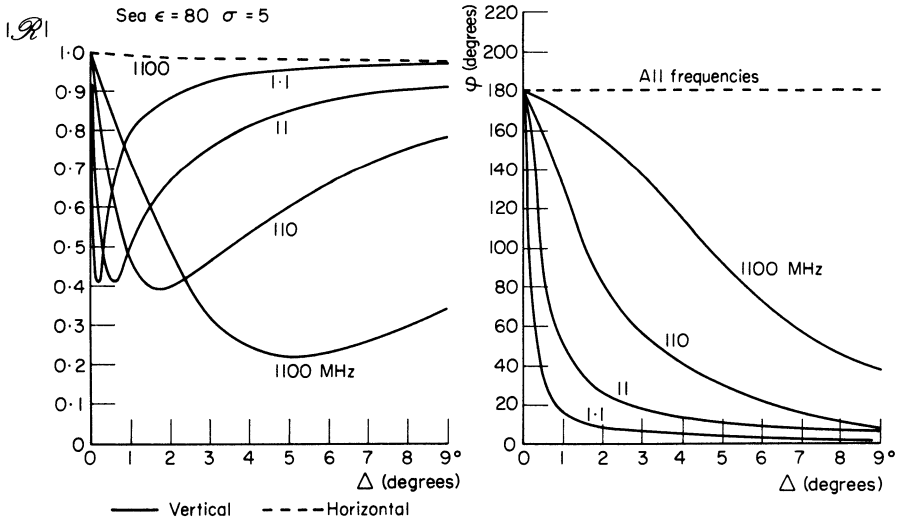

Fig. 18

These figures show that:

1. For horizontal polarization:

(a) the modulus of the reflection coefficient decreases regularly with increasing angle Δ and increasing frequency. The modulus will be higher when the ground conductivity is greater.

(b) the phase of the reflection coefficient is always in the proximity of 180° and slightly higher than this value (with our sign convention for R_H).

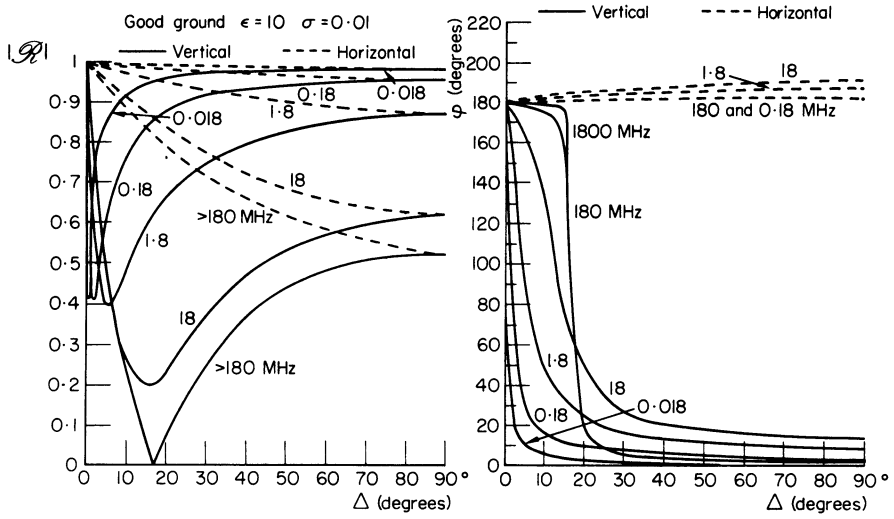

Fig. 19

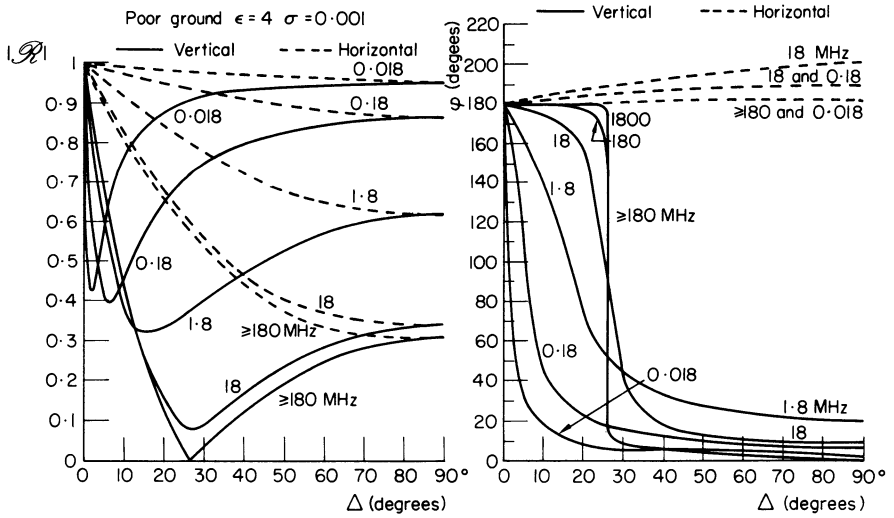

Fig. 20

2. For vertical polarization:

(a) the modulus of the reflection coefficient first decreases with increasing

angle Δ, until this angle has attained a critical value called 'pseudo-Brewster incidence'. The modulus then passes through a minimum, after which it gradually increases towards normal incidence to the ground plane.

(b) the angle Δ corresponding to the minimum value of R will be still smaller when the frequency is smaller and conductivity greater.

(c) the phase of the reflection coefficient starts at 180° for grazing incidence, then rapidly decreases in the neighbourhood of the pseudo-Brewster incidence, after which it continues to decrease slowly and finally attains a small positive value for the normal incidence to the ground plane.

(d) as the phase difference due to reflection is not the same for both the horizontal and vertical components, an incident wave with inclined linear polarization gives rise to a reflected wave with elliptical polarization.

4.1.2 SPHERICAL WAVES

In the case of spherical waves it has been shown by extremely complex calculations[5] that the spherical reflection coefficient tends towards the planar reflection coefficient:

1. when the curvature of the wave surface becomes very small (great distance from source)
2. when coefficient q of equation (3.5):

$$q = \frac{\sigma}{\omega \varepsilon_0 \varepsilon_r}$$

is much smaller than unity,

3. or when the waves are close to grazing.

4.1.3 SMOOTH SPHERICAL GROUND

As will be seen from Fig. 21, the beam reflected by the terrestrial sphere

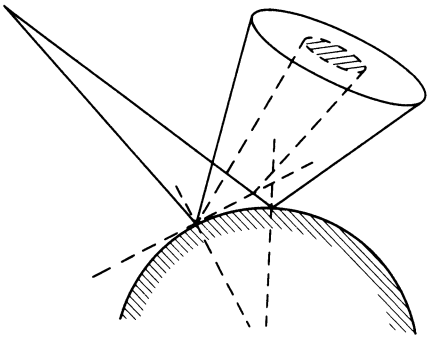

Fig. 21

possesses after reflection a section that is larger than that of the same beam reflected by the plane tangential to this sphere.

In virtue of the principle of conservation of energy, the energy density per unit surface is therefore smaller. We take this decrease in energy into account by multiplying the field by the divergence coefficient—a quantity which solely depends on the shape of the terrestrial surface and not on its electrical properties.

This coefficient will be smaller when the source is situated higher above the ground and the beam is more at grazing incidence.

4.1.4 IRREGULAR GROUND

4.1.4.1 **Effect on regular reflection**

It will be easily seen that the greater the irregularities, the smaller will be the reflection coefficient. Lord Rayleigh has defined this point by considering the phase difference introduced by surface irregularities. Figure 22 shows the value of this phase difference:

$$\frac{2\pi}{\lambda}.2h\sin\Delta = \frac{4\pi h\sin\Delta}{\lambda}$$

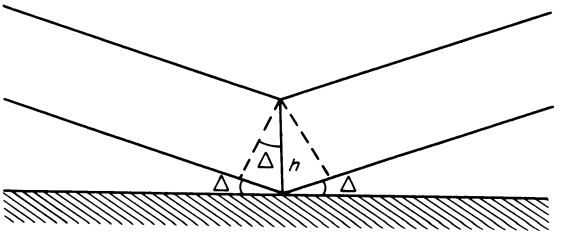

Fig. 22

He has shown that the surface can be considered as smooth (regular reflection) when the phase differences introduced by the various points are well below $\pm\pi/2$. If they are higher, the surface is rough (diffuse reflection). This is Rayleigh's criterion, which is used in two different forms.

1. We admit that the reflection coefficients calculated for smooth ground are valid for phase differences up to $\pi/4$. This gives the following value for the maximum height of the obstacles or irregularities of the terrain:

$$h_{max} = \frac{\lambda}{16\sin\Delta} \tag{4.5}$$

In the case of greater heights, the reflection coefficient decreases rapidly and tends towards $0{\cdot}2$[16].

2. We define the quantity:

$$R = \frac{4\pi h \sin \Delta}{\lambda} \tag{4.6}$$

(Rayleigh's criterion) and try to establish a relation between this quantity and the reflection coefficients or the strength of the field received.

Although other methods for taking irregularities of the terrestrial surface into account have been proposed, the results achieved so far are too divergent to be of any practical value.

4.1.4.2 **Diffuse reflection**

The ground surface always presents enough irregularities for part of the incident energy to be diffused in all directions. This may be likened to an illuminated imperfectly polished surface. The diffused field is much weaker than the regularly reflected field if equation (4.5) is satisfied. However, the phenomenon is used in the study of the ionosphere (see Section 6.1.3.3).

4.1.5 APPLICATION OF REFLECTION THEORY

4.1.5.1 **Validity of the theory**

Reflection theory can only be applied when diffraction is of a minor effect, i.e. when the waves are not too grazing.

The following value is usually taken as the minimum limit of reflection angle Ψ (see Fig. 23):

$$\Psi = \left(\frac{\lambda}{2\pi K a}\right)^{\frac{1}{3}}$$

where a = terrestrial radius, K = coefficient defined in Section 2.1.3.2, and whose mean value equals 4/3.

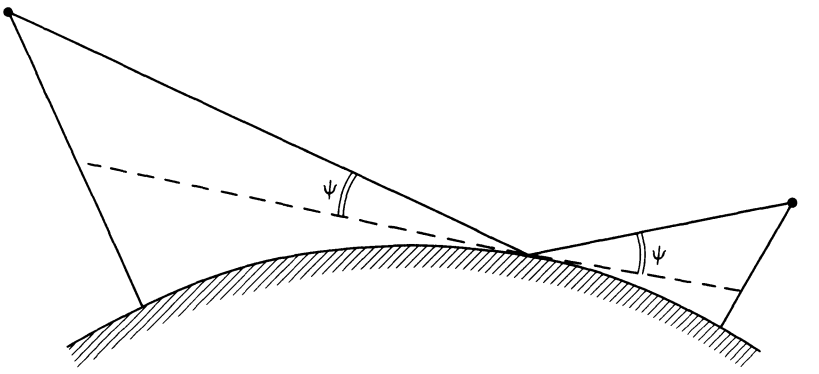

Fig. 23

The curve in Fig. 24 shows the value of the limiting angle against frequency for $K = 4/3$.

We see that, in the case of high frequencies, the propagation can be calculated by the methods used in geometric optics—practically to the horizon.

When the reflection angle is smaller than the limiting angle, the field must be calculated by using diffraction theory (Section 4.3); this is however very difficult in the neighbourhood of the radio horizon.

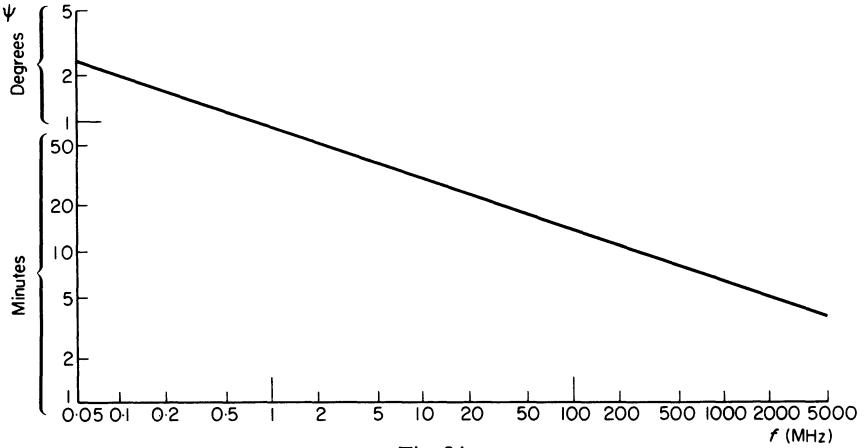

Fig. 24

4.1.5.2 Effects of reflection

Horizontally polarized plane wave, which is reflected at a small angle on flat ground

This represents the simplest case. It occurs in line-of-sight communication with horizontal polarization over short distances (e.g. line-of-sight radio links) and also for radar.

We assume that reflection angle Δ is greater than the limiting value Ψ defined in Section 4.1.5.1, but small enough to ensure a reflection coefficient of approximately -1.

The difference in length between the direct ray and the reflected ray will be:

$$l = \frac{2h_1h_2}{d} \qquad (h_1, h_2 \ll d)$$

and hence:

$$\begin{aligned} E &= E_0\left[\sin\omega t - \sin\left(\omega t - \frac{4\pi h_1 h_2}{\lambda d}\right)\right] \\ &= 2E_0 \sin\frac{2\pi h_1 h_2}{\lambda d}\cos\left(\omega t - \frac{2\pi h_1 h_2}{\lambda d}\right) \end{aligned} \tag{4.7}$$

We have therefore a series of maxima equal to twice the field in free space when:

$$\frac{h_1 h_2}{\lambda d} = \frac{2k+1}{4} \qquad (k = 0, 1, 2\ldots) \tag{4.8}$$

and a series of zeros when:

$$\frac{h_1 h_2}{\lambda d} = \frac{k}{2} \qquad (k = 1, 2\ldots) \tag{4.9}$$

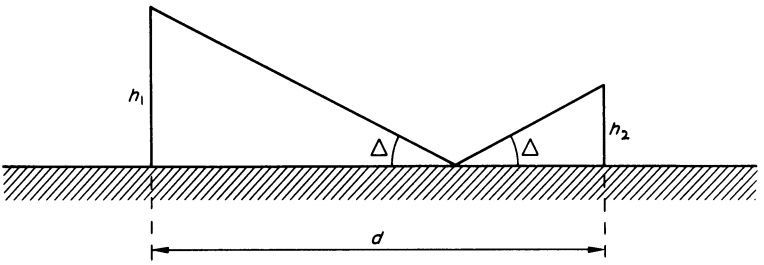

Fig. 25

The value $K = 0$ is excluded because we have assumed $\Delta > \Psi$. We shall see, however, in Section 4.3 that the field tends towards zero when h_1 and h_2 tend towards zero.

We can therefore conclude that:

1. If $h_1 h_2 < \lambda d/2$, which will usually be the case for communication between fixed stations, zero will not be observed, except at ground level.
2. Nevertheless, in the case of short wavelengths, this inequality may not be satisfied; if reception is weak or negligible in this case, the height of one of the two antennae should be modified.
3. In the case of radio beams of decimetre or centimetre waves passing over the sea, the variations of the refractive index due to different meteorological conditions for the two rays give serious fading by the same mechanism, which is combated by using multiple reception with two antennae of different heights (Section 2.1.4).
4. In the case of search radar we usually have:

   $$h_1 \ll h_2$$

   because the height of the antenna of a radar station is very much smaller than that of an aircraft.

   Therefore:

   $$\Delta \approx \frac{h_2}{d}$$

and

$$\Delta \approx \frac{(2k+1)\lambda}{4h_1} \quad \text{for the maxima} \tag{4.10}$$

$$\Delta \approx \frac{k\lambda}{4h_1} \quad \text{for the minima} \tag{4.11}$$

The space is therefore graduated in angles by conical beams of maximum field, separated by zeros of equidistant angles.

Other cases

If, in the case of horizontal polarization, angle Δ becomes considerable, the modulus of the refractive index decreases. Instead of zeros, there will be less pronounced minima.

In the case of vertical polarization, the phenomena occurring at small angles will be similar to those described above. As soon as the angle increases a little, the phenomena become involved because the phase angle of the refractive coefficient and its modulus vary rapidly in the proximity of pseudo-Brewster incidence.

For a spherical wave, analogous phenomena will occur because the spherical reflection coefficient differs little from the planar reflection coefficient.

If the distance is great, the divergence factor must be taken into account. The phenomena show the same qualitative aspect as for smooth ground.

Rayleigh's criterion (Section 4.1.4.1) can be taken into acount when obstacles of a well defined height (trees, houses, etc.) are present on otherwise smooth ground.

It is sometimes possible in mountainous regions, when using metre or shorter waves in conjunction with directional antennae, to use a vertical wall as a reflector to permit communication between two stations which are not in line of sight.

General behaviour of field values

The behaviour of field variations is usually similar to that shown in Fig. 26, which corresponds to the following conditions:

1. horizontal polarization
2. transmitted power 1 kW
3. average ground
4. antenna heights 10 m and 300 m.

The interference fringes begin to appear closer to the horizon when the antennae and the frequencies are higher.

4.1.5.3 Calculating reflection effects

This calculation must take into account the curvature of the direct ray and that of the reflected ray, due to the variation of the refractive index at different altitudes (Section 2.1.3.1).

These calculations are so long and complex that it is generally not left to the user to carry them out. They are carried out in advance for:

1. radiation diagrams of antennae in the presence of ground
2. graphs giving the field strength for line-of-sight paths.

It is obvious that these diagrams and graphs cannot take into account:

1. modifications of the reflection coefficient due to obstacles on the ground
2. terrain that slopes towards the antennae
3. nearby obstacles that can cause interference fringes.

When using these diagrams and graphs it should be remembered that they only give a mean field value, and that the actual value may vary around this mean value when moving the antenna not more than one wavelength. If, in a practical case, the received field is too weak, one can always try such a displacement.

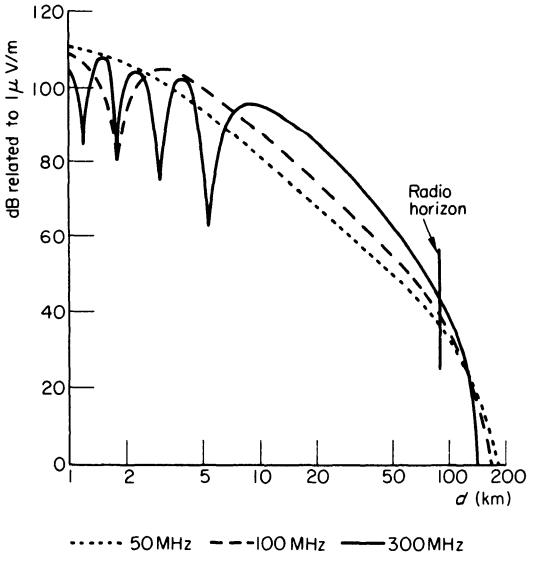

Fig. 26

More complex methods, such as the Matsuo method[103], give a greater accuracy in evaluating the irregularities of the ground, but they are rather difficult to apply and then only to certain forms of terrain.

4.2 WAVE BEHAVIOUR NEAR THE GROUND

4.2.1 ZENNECK WAVE

As we have seen in Section 4.1.5.1 the reflection theory does not apply in the immediate proximity of the ground. And yet this zone is very important because it often contains the antennae.

Let us first pose the following simple problem, which was first formulated by Zenneck: 'To define a plane vertically polarized wave which satisfies Maxwell's equations at ground level and its immediate proximity'.

Since the wave is assumed to be plane, the equations obtained only apply at large distance of the source, and over a rather small region, in order that there will be no appreciable variation in this distance and the wave direction. This will give us a 'local' theory, which is nevertheless very interesting because it shows several important facets of the propagation mechanism in the proximity of the ground.

Assuming a horizontal magnetic field and a vertical electric field, we can write for each of the two media:

$$\boldsymbol{E} = \boldsymbol{E}_0 \, e^{j\omega[t - n/c(\alpha x + \beta z)]} \tag{4.12}$$

and a similar equation for $\boldsymbol{H}$.

Quantities α_1 and β_1 (for the air) and α_2 and β_2 (for the ground) are complex quantities. The value of n is 1 in the air; its value in the ground is given by equation (3.9) where two letters have been changed in order to prevent confusion:

$$n = \nu - j\kappa = \left(\varepsilon_r - \frac{j\sigma}{\omega\varepsilon_0}\right)^{\frac{1}{2}} = \varepsilon_r^{\frac{1}{2}}(1 - jq)^{\frac{1}{2}}$$

Substituting equation (4.12) and the similar equation for $\boldsymbol{H}$ in Maxwell's equations, and taking into account that:

$$H_x = H_z = E_y = 0$$

we find:

$$\left.\begin{aligned} \frac{n}{c}(\beta E_{0x} - \alpha E_{0z}) &= H_{0y} \\ \frac{\beta}{c} H_{0y} &= -\varepsilon_0 n E_{0x} \\ \frac{\alpha}{c} H_{0y} &= -\varepsilon_0 n E_{0z} \end{aligned}\right\} \tag{4.13}$$

4.2.2 PROPERTIES OF ZENNECK WAVE

We shall not completely resolve these equations but make some deductions:

4.2.2.1 **Calculation of the cosines**

We first have by definition:

$$\alpha_1^2+\beta_1^2 = 1 \tag{4.14}$$

and

$$\alpha_2^2+\beta_2^2 = 1 \tag{4.15}$$

For $z = 0$ we must preserve the continuity of the tangential field components. This requires:

$$\alpha_1 = n\alpha_2 \tag{4.16}$$

For the same reason:

$$H_{01y} = H_{02y}$$

$$E_{01x} = E_{02x}$$

We then deduce from the second of equations (4.13):

$$\beta_2 = n\beta_1 \tag{4.17}$$

Equations (4.14), (4.15), (4.16) and (4.17) give:

$$\alpha_1^2 = \frac{n^2}{n^2+1} \qquad \beta_1^2 = \frac{1}{n^2+1}$$

$$\alpha_2^2 = \frac{1}{n^2+1} \qquad \beta_2^2 = \frac{n^2}{n^2+1}$$

Zenneck's theory is generally used for waves of a frequency of less than 1 MHz. Under these conditions, q is greater than unity, and we can put in first approximation:

$$n^2 \simeq -\mathrm{j}q\varepsilon_r$$

Therefore:

$$\left.\begin{aligned} \alpha_1^2 = \beta_2^2 &\simeq 1-\frac{\mathrm{j}}{q\varepsilon_r} \\ \alpha_2^2 = \beta_1^2 &\simeq \frac{\mathrm{j}}{q\varepsilon_r} \end{aligned}\right\}$$

and

$$\left.\begin{aligned} \alpha_1 = \beta_2 &\simeq 1-\frac{\mathrm{j}}{2q\varepsilon_r} \\ \alpha_2 = \beta_1 &\simeq -\frac{1+\mathrm{j}}{(2q\varepsilon_r)^{\frac{1}{2}}} \end{aligned}\right\} \tag{4.18}$$

We have therefore in the air:

$$\boldsymbol{E} = \boldsymbol{E}_0\, \mathrm{e}^{-\omega/c[x/2q\varepsilon_r + z/(2q\varepsilon_r)^{1/2}]}\mathrm{e}^{\mathrm{j}\omega[t-1/c(x-(z/(2q\varepsilon_r)^{1/2}))]} \tag{4.19}$$

These waves weaken exponentially during propagation (vanishing waves)

The planes of equal amplitude:

$$\frac{x}{2q\varepsilon_r}+\frac{z}{(2q\varepsilon_r)^{\frac{1}{2}}} = \text{constant}$$

or:

$$x + z(2q\varepsilon_r)^{\frac{1}{2}} = \text{constant}$$

are normal to the planes of equal phase:

$$x - \frac{z}{(2q\varepsilon_r)^{\frac{1}{2}}} = \text{constant}$$

In this case, we speak of a dissociated wave.

The planes of equal phase subtend to the vertical in the direction of propagation an angle which is given by:

$$\tan\theta = \frac{1}{(2q\varepsilon_r)^{\frac{1}{2}}} \tag{4.20}$$

In the ground it is interesting to determine the decrease in field with depth. If we approximate:

$$\beta_2 = 1$$

the coefficient of z in the exponent is:

$$-\mathrm{j}\frac{\omega n}{c} = -\mathrm{j}\frac{\omega}{c}(-\mathrm{j}q\varepsilon_r)^{\frac{1}{2}} = -\frac{\omega}{c}\left(\frac{q\varepsilon_r}{2}\right)^{\frac{1}{2}}(\mathrm{j}+1)$$

The penetration is therefore:

$$p = \frac{c}{\omega}\left(\frac{2}{q\varepsilon_r}\right)^{\frac{1}{2}} = \frac{c}{\omega}\cdot\frac{1}{\kappa}$$

a value we have already determined in equation (3.15).

4.2.2.2 **Field polarization in air**

Dividing the last two equations of (4.13) one by the other, we find:

$$\frac{E_{0z}}{E_{0x}} = \frac{\alpha_1}{\beta_1} = n = \nu - \mathrm{j}\kappa \tag{4.21}$$

Since this ratio is complex, fields E_{0z} and E_{0x} will not be in phase.

The electric field therefore possesses elliptical polarization in a vertical plane. From this we can make two important deductions:

1. When comparing the moduli, we obtain:

$$\frac{|E_{0x}|}{|E_{0z}|} = \frac{1}{|n|} = \frac{1}{[\varepsilon_r(1+q^2)^{\frac{1}{2}}]^{\frac{1}{2}}} \tag{4.22}$$

and because

$$q = \frac{\sigma}{\omega\varepsilon_0\varepsilon_r}$$

the horizontal field will possess a greater relative value when the ground is less conducting and the frequency higher. Over the sea, it is very weak and usually negligible.

2. The elements of the polarization ellipse:
   (a) ratio of the axes: K
   (b) angle of the major axis to the vertical: θ

depend on the conductivity and to a lesser extent on the dielectric constant of the ground. These elements can be measured quite easily by means of a portable screened receiver provided with a short dipole antenna. This is one of the best methods for measuring ground conductivity at high frequencies. The most practical manner is to use the field of a nearby radio transmitter; lacking this, a portable transmitter situated about 10 km away may be used. Measurement is more accurate at not too high frequencies.

Figure 27 has been calculated by Norton and permits one to calculate conductivity by starting from the measured results.

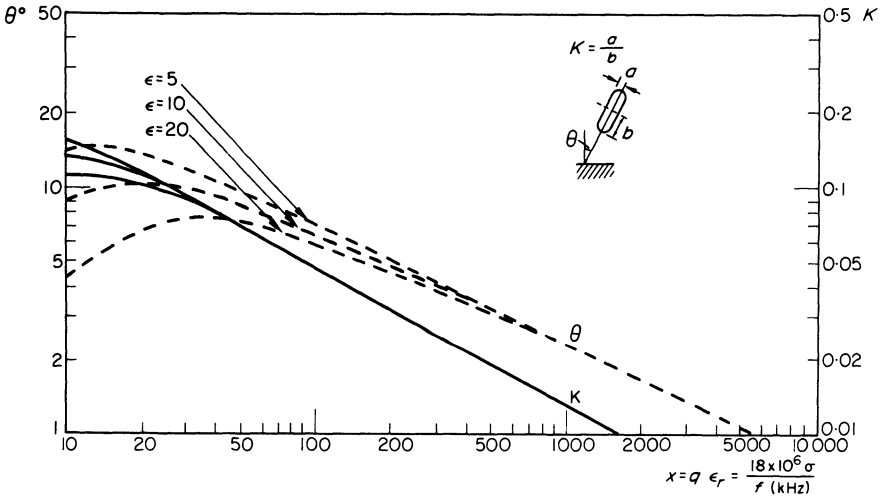

Fig. 27

4.3 FIELD VALUE ON FLAT GROUND: SURFACE WAVE

It is possible to calculate accurately the field produced on flat ground by an electric dipole when the heights above the ground of the antennae are too small for reflection theory to apply. The first calculation of this kind was carried out by Sommerfeld. Van der Pol[202] has confirmed Sommerfeld's results by using a very elegant method.

The complete development of this theory is beyond the scope of this book. We shall therefore content ourselves with stating the reasoning and the most important results.

4.3.1 THEORY

Let us first give a very schematic definition of the source. The latter is assumed to consist of a vertical electric dipole, situated at the origin and directed along $0z$. This dipole of a very small length l, consists of two charges $+q$ and $-q$ with:

$$q = q_0 e^{j\omega t}$$

It is equivalent to a conductor of length l through which passes a current:

$$I = \frac{dq}{dt} = j\omega q_0 e^{j\omega t}$$

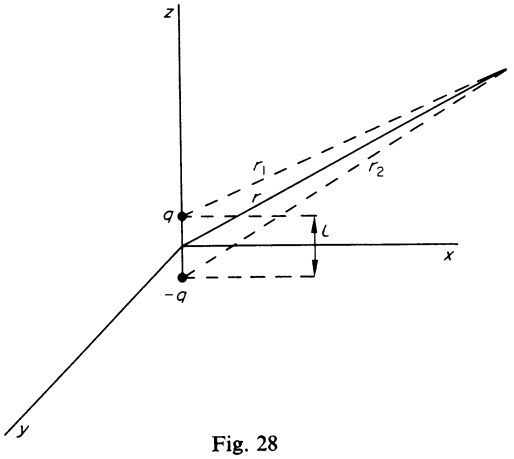

Fig. 28

The moment of the dipole is the quantity:

$$M = lq_0 e^{j\omega t} = M_0 e^{j\omega t} = -j\frac{lI}{\omega} \tag{4.23}$$

We assume that l tends towards zero and that the moment M_0 remains constant. We now calculate the potentials from which the fields are derived by means of equations (A.5) of the Appendices, noting that $\int i\, dv = lI$, and that for each charge $\int \rho\, dv = q$. We find:

$$V = \frac{q}{4\pi\varepsilon_0}[\Psi(r_1) - \Psi(r_2)] = -\frac{ql}{4\pi\varepsilon_0}\frac{\partial \Psi(r)}{\partial z} = -\frac{M}{4\pi\varepsilon_0}\frac{\partial \Psi(r)}{\partial z} \tag{4.24}$$

$$A = \frac{lI\Psi(r)}{4\pi} = \frac{j\omega M \Psi(r)}{4\pi}$$

We can combine these two equations into a single one by introducing the Hertzian vector Π. Since we have, according to the first equation of (A.7):

$$A = \frac{\partial \Pi}{\partial t}$$

we can write the radio vector as:

$$\Pi = \frac{M\Psi(r)}{4\pi} \tag{4.25}$$

The same as vector M, vector Π is everywhere vertical. When we know its value, we can determine the electric and magnetic fields at each point by means of equations (A.8).

The use of this vector considerably simplifies calculations, because instead of defining two fields, E and H, we only have to define the modulus of a vector Π, which is everywhere vertical.

We now change the conditions to the relative field boundaries:

1. E and H are zero at infinity
2. tangential field components are continuous at ground level
3. electric and magnetic displacements are continuous

in equivalent conditions for Π.

Finally we separate Π into two components:

1. the primary field, which in the air is identical with that of the source in free space (therefore infinite at the point of transmission) and zero in the ground.
2. the secondary field, taking into account the presence of the ground, which is finite in the entire system.

4.3.2 PRACTICAL RESULTS

4.3.2.1 **Field value**

Although the theory may appear complex, the results are rather simple and easy to interpret. The field is expressed by the equation:

$$E = 3 \times 10^5 \frac{p^{\frac{1}{2}}}{d} AF(h_1)F(h_2) \tag{4.26}$$

where P is in kW and d is in km.

Factor A is equal to or less than unity and is called the attenuation factor. Factors $F(h)$ are the height factors of the antennae; they are both greater than unity.

We can calculate these various factors by means of graphs or equations, starting from:

1. the wave polarization
2. the electric constants of the ground
3. the distance and heights of the antennae.

This calculation is carried out via auxiliary variables: the numerical distance (resulting from a transformation of the distance) and the numerical heights (resulting from the transformation of the antenna heights).

Without going into the details of these calculations, we shall mention a few important results.

4.3.2.2 Effect of the principal factors

Conductivity of the ground

The numerical distance (and hence the attenuation of the waves) will be smaller when the conductivity of the ground is greater.

Polarization

When the elevation of the antennae above ground is small, the field value of waves with vertical polarization is much greater than that of waves with horizontal polarization. The latter approaches zero when the height of the antenna approaches zero.

When the height above ground level of the antennae attains 3 or 4 wavelengths, the direction of polarization has no longer any practical importance.

Frequency

The field strength will be greater when the frequency is lower.

Distance

At small distances, $A = 1$, and the field varies as $1/d$. When the distance increases sufficiently, A becomes proportional to $1/d$, so that the field becomes proportional to $1/d^2$. This law of damping characterizes the Sommerfeld region, and remains valid as long as the terrestrial curvature plays a negligible part.

Height of antennae

When increasing the distance from the ground (Fig. 29), the height factor $F(h)$ starts by being equal to, or even slightly smaller than unity, until we have attained a boundary height h_1. Many authors call this constant field near ground level the 'surface wave'. Sommerfeld made the assumption (which is not mathematically exact) that this was a wave guided by the earth's surface. The height factor then increases in proportion to the height of the antenna, in any case as long as the zone where the reflection theory applies (Section 4.1.5) is not reached.

The boundary height h_1 is approximately defined by the graph in Fig. 30, which is derived from an equation by Bullington[101].

Equivalent conductivity of built-up ground

When the ground is covered with vegetation or buildings, its absorption will be greater. The Sommerfeld equation can still be applied, provided

that one takes as conductivity value an equivalent conductivity which is lower than the actual conductivity. In towns, values of σ between 10^{-3} and 10^{-4}S/m have been found.

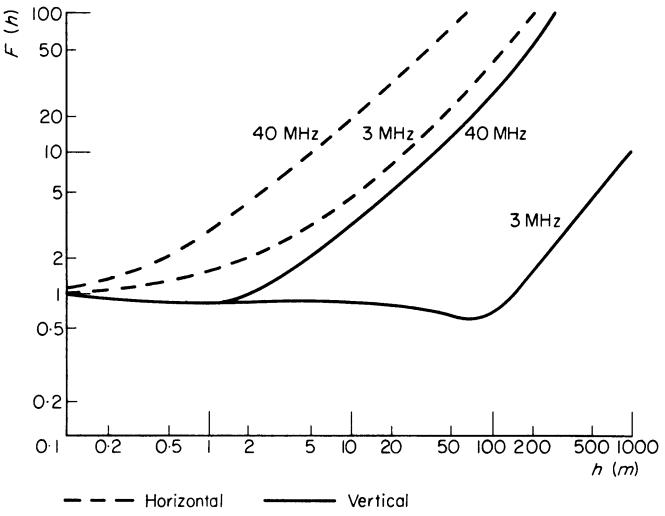

Fig. 29

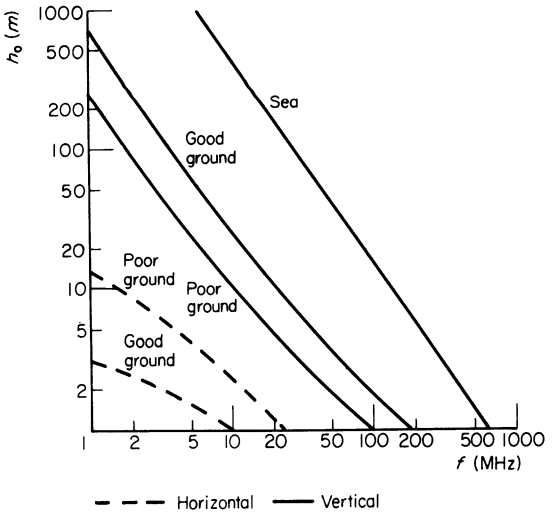

Fig. 30

4.4 CALCULATING THE FIELD ON SPHERICAL GROUND

This is obviously the most interesting calculation, because it corresponds to actual conditions. Unfortunately, it is extremely complex and we must restrict ourselves to a survey of the methods used.

4.4.1 METHOD OF GEOMETRIC OPTICS

When antennae are in line of sight, when they are sufficiently high to ensure that the angle between the reflected ray and the ground is greater than the limiting value Ψ given in Section 4.1.5.1, and when the direct ray does not pass too closely to the horizon, we simply apply the reflection laws defined in Section 4.1, as if we were dealing with a problem of geometric optics.

4.4.2 CALCULATING DIFFRACTED WAVES

Should the above conditions not be satisfied, we can calculate directly the wave diffraction by the earth's surface by using Maxwell's equations. This method has led to magnificent mathematical arguments, which unfortunately are almost impossible to summarize[5, 11, 200, 201, 203, 204].

The same as in the case of level ground, we define an Hertzian vector, which is usually taken as radial[5]. The problem is thus converted to a scalar one.

The boundary conditions are given, just as in the case of level ground, and the radio vector is once again separated into primary and secondary fields.

The formal resolution of the problem is comparatively easy when developing the field into a series of Legendre polynomials. Poincare has given the equations of this first part of the problem in 1897. Unfortunately, the resultant series are not amenable to numerical summation because:

1. it is very difficult to calculate the terms (the coefficients contain four Bessel functions)
2. the series converges very slowly (several thousand terms are required[204]).

Watson showed in 1918 that, by taking a curvilinear integral along a convenient path, one can transform this series into a series of residuals, which converges rapidly (the number of terms necessary varies between 2 and 18). Van der Pol and Bremmer[5, 204] have perfected this method of calculation, which is the only one now in use. They have given equations and graphs that are useful although complex.

Eckersley[201, 203] proposed in 1932 a very general method (which takes into account atmospheric refraction or ionospheric reflection), based on the calculation of eigenvalues, and which he called the phase integral method. Some of his results are of great interest, especially as this method is relatively simple.

Fock and Leontovitch[17] recently introduced a new and simpler method, which consists of the slight modification of the expression of the boundary conditions at ground level.

The height above ground of antennae can in most cases be taken into

account by means of height factors, similar to the ones we discussed with reference to level ground.

4.4.3 PRACTICAL RESULTS

4.4.3.1 **Accurate field calculation**

The calculation methods derived from the theory discussed above are extremely complex. Should their use be absolutely necessary (e.g. when determining the primary coverage zone of a broadcast station, calculation of a very important fixed circuit) one could use one of the following documents, which give very similar results:

1. the nomograms given by Norton in *PIRE* **29,** 623–639, December 1941
2. Termann's method in *Radio Engineers Handbook*, 674–695
3. Bremmer's method in *Terrestrial Radio Waves*, Chapter VI, 105–124.

4.4.3.2 **Effect of the main factors**

The effect is the same as described in Section 4.3.2.2, apart from the following points:

Starting from a distance of approximately:

$$d_1 = \frac{80}{f^{\frac{1}{3}}} \text{ km},$$

where f is in MHz, the effect of earth curvature becomes noticeable and the decrease in the field becomes exponential. The effect of the frequency increases with the distance.

4.4.3.3 **Approximate calculations**

Under normal practical conditions, the field can be determined with sufficient accuracy by means of the graphs given in Chapter 8.

4.5 PROPAGATION OVER IRREGULAR TERRAIN

The surface of the earth is anything but regular because of the nature and ruggedness of the surface, as well as the obstacles it supports. It would be rather difficult to take all these very different irregularities into account. Precise methods for taking into consideration ruggedness have been proposed, especially by Matsuo[103], but they are highly complex and apply only to certain types of terrain.

We shall only examine a few simple cases, where we can obtain results that can be used directly.

4.5.1 EQUIVALENT EARTH SURFACE

Suppose we have drawn, as in Fig. 31, the profile of the terrain between source and receiver. The distances are plotted on the x-axis and the altitudes above sea level on the y-axis, as they are read from a map. Let us

assume that this profile is entirely situated below the straight line between the antennae of source and receiver. In this case, we call the profile concave.

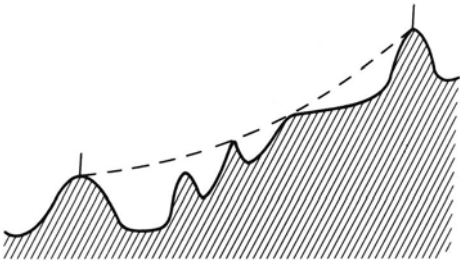

Fig. 31

We now draw a circle through the bases of the two antennae and tangential to the ground. The absorption due to the actual ground will be smaller than that produced by the above defined regular concave ground, because absorption increases very rapidly when the radio wave is close to the ground.

We put for the equivalent ground radius we have drawn:

$$R' = K'a$$

where a = radius of the earth.

The depression of the concave terrain below the plane joining the antenna bases is given by the following equation, which is similar to equation (2.7):

$$y = \frac{x^2}{2K'a}$$

Adding this value to the value given by equation (2.7), and taking atmospheric refraction (coefficient K) into account, we find for the height of the concave terrain above the horizon:

$$y = -\frac{x^2}{2Ka} + \frac{x^2}{2K'a} = -\frac{x^2}{2K''a} \tag{4.27}$$

whence:

$$\frac{1}{K''} = \frac{1}{K} - \frac{1}{K'} \tag{4.28}$$

It is thus possible to calculate a lower limit of the field value by replacing value K which belongs to a spherical terrain by value K'' given by equation (4.28). This method is used in Chapter 8.

4.5.2 COMPOSITE PATHS

In practice one often meets paths covering a number of terrains, each of a different conductivity—especially paths that pass over land and sea.

Millington[206] has given a remarkably simple equation for calculating the attenuation over these paths and which is in very good agreement with experimental results:

When $A_1(d)$ = attenuation due to the distance travelled above medium 1 and $A_2(d)$ = the same value for medium 2, we have:

$$A_{\text{total}} = \left(\frac{A_1(d_1)A_2(d_2)A_1(d)A_2(d)}{A_2(d_1)A_1(d_2)}\right)^{\frac{1}{4}}$$

where d = total distance, d_1 = distance travelled over medium 1, and d_2 = distance travelled over medium 2.

Other authors[212, 223, 226] have treated this problem theoretically and have obtained accurate solutions in some specific cases. Report No. 230 of CCIR[228] contains a survey of the papers published on this subject.

It has also been observed that in the neighbourhood of a seacoast, planes of equal phase are subjected to a kind of refraction that causes errors in radiogoniometry[9, 17].

The nature of the ground near the transmitting station affects not only ground links (maintained by means of 'ground waves') but also the intensity of the ionospheric wave[230] and tropospheric links with aircraft[176].

4.5.3 THIN OBSTACLES

S. O. Rice[208] has shown that an obstacle can be considered as thin and Fresnel's diffraction theory can be applied, when the diffraction angle satisfies the inequality (Fig. 32)

$$\Psi < \tfrac{1}{4}\left(\frac{\lambda}{R}\right)^{\frac{1}{4}}$$

where R = radius at the summit and Ψ is in radians.

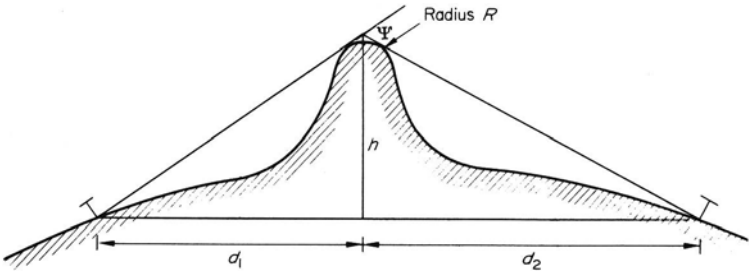

Fig. 32

Bullington[101] has established a simple calculation method for this case, which is based on practical conditions.

One first simplifies the expression of the diffraction parameter:

$$v = h\left[\frac{2}{\lambda}\left(\frac{1}{d_1}+\frac{1}{d_2}\right)\right]^{\frac{1}{2}}$$

Assuming $d_1 \leqslant d_2$, we can put:

$$\frac{1}{d_1}+\frac{1}{d_2}=\frac{\sqrt{2}}{d_1}$$

with an error smaller than $2^{\frac{1}{4}}$. We then have:

$$v \approx 3\times 10^{-3}\, h_m\left(\frac{f}{d_1}\right)^{\frac{1}{4}}$$

where f is in MHz and d_1 is in km.

Since attenuation solely depends on v, a nomograph with aligned points gives an immediate reading of the attenuation as a function of h, f and d_1 (Chapter 8, Fig. 189).

Fresnel's theory usually gives rather accurate results[225].

If there are several successive obstacles, it appears[224] that the most correct method consists of first calculating the attenuation caused by the obstacle that produces the strongest attenuation, then joining the summit of this obstacle to the antennae, and calculating the attenuation caused by the remaining obstacles as if they were situated above the lines thus drawn (see Fig. 191).

When a thin obstacle is surrounded by two plains with good reflection, a stronger field can be obtained by the judicious choice of the height of the two antennae.

In this case there are four paths for the waves to travel from the source to the receiver (Fig. 33):

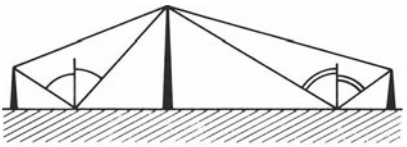

Fig. 33

1. one path without reflection by the ground
2. two paths, each with one reflection
3. one path with two reflections.

We can calculate[217] the attenuation by diffraction of each of the rays and their difference in length and therefore phase, and sum the resultant fields.

We observe that:

1. The field behind the obstacle presents an average value which decreases slowly, but which possesses very pronounced minima for certain distances and heights of obstacles, which however only extend over small distances.

2. The maximum field strength is greater than the one that would be obtained if the obstacle were absent; the ratio of fields with and without obstacles can attain very great values when the distance is great. However, this result requires a phase equilibrium that can be easily destroyed by meteorological variations.

The resultant 'obstacle gain' can reach a value of, say, 90 dB at 250 km at a frequency of 100 MHz. However, the gain is less than the attenuation on regular spheric ground—the more so if the distance is greater—so that the field decreases with distance, as was to be expected.

Since the high value of the field is related to the equilibrium between the phases of the four paths, which in their turn are influenced by the meteorological conditions, fading can be considerable[220].

4.5.4 ROUNDED OBSTACLES

Dougherty and Maloney[221] have extended the work of Rice so as to make it applicable to all types of obstacles found in uneven terrain, for waves in the metre band or shorter. A graph calculated on these principles will be found in Chapter 8 (Fig. 190).

In the case of a number of successive rounded obstacles, the method of Section 4.5.2 for a series of obstacles can be used. If accurate maps are available, excellent results can be obtained.

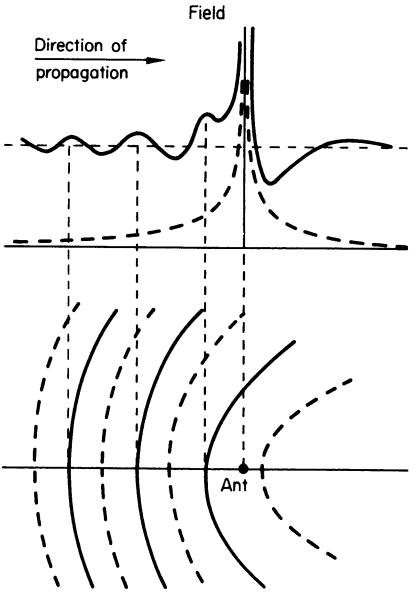

Fig. 34

The coverage zone of an emitter for metre waves or shorter often has to be calculated. To a first approximation, one may make use of the propagation curves of the CCIR[138], which are reproduced in part in Chapter 8 (Figs 109 and 110). More accurate results can be obtained with the aid of more elaborate methods[231], if a computer is available.

4.5.5 ISOLATED VERTICAL OBSTACLES

The simplest case is that of a vertical tuned antenna. This case has been thoroughly investigated by Mesny[9], who found that the field in the neighbourhood of the antenna presents the maxima and minima shown in Fig. 34.

Similar phenomena have been observed at frequencies in the neighbourhood of the $\lambda/4$ resonance of pylons, trees, etc. In these cases, we should establish the maximum field by experiment by displacing the antennae over a distance of approximately one wavelength.

The effect of isolated obstacles can be neglected if they are at great distances of the antennae.

4.5.6 ENCLOSED VALLEYS

Enclosed valleys act like waveguides for vertically polarized waves or for horizontally polarized waves in the direction of the axis.

For these polarizations, only waves whose wavelength is smaller than twice the width of the valley will be propagated. In the case of horizontal polarization perpendicular to the axis of the valley, there is no boundary value for the wavelength, but the ground wave will always be weak.

4.5.7 ARTIFICIAL OBSTACLES

Although this is not really a case of a natural medium, we should mention the interesting use of artificial obstacles, which provide controlled diffraction[220, 222]. These obstacles consist of metal strips comprising elements of diffraction gratings, similar to the ones introduced by Soret in optics. This gives us the facility of passing centimetre waves over an obstacle with reasonable attenuation and very good signal stability.

CHAPTER 5

WAVE PROPAGATION IN IONIZED MEDIA

5.1 CONSTITUTION OF AN IONIZED MEDIUM

In this chapter we shall only discuss gaseous ionized media or plasmas. Several types of these media occur in nature in the shape of external layers of brilliant stars, the ionosphere around our earth, etc. The latter is described in Chapter 6 and plays a very important part in wave propagation between two points on the earth, or between a ground based station and a satellite in space.

We must also mention the artificial plasmas occurring around rockets (engine exhaust) or produced by the re-entry of satellites into the earth's atmosphere. These plasmas are very important for communication with space devices.

A plasma consists of:

1. Electrically charged particles.

1.1. Free electrons with mass $m_e = 9 \times 10^{-31}$ kg and negative charge $\varepsilon = -1{\cdot}6 \times 10^{-19}$ C.

1.2. Ions consisting of an atom or molecules having a positive or negative charge equal to a small multiple of the charge of an electron. The lightest ion, atomic hydrogen, has a mass of 1 837 m_e. The masses of other ions are 1 822 Mm_e where M represents the atomic or molecular mass of the gas in question. This would give 7 293 m_e for atomic helium. Ions of other gases are very much heavier.

2. Atoms and/or neutral molecules. Simple gases at low pressures occur in the atomic form, at high pressures in the molecular form.

If the ratio of ionized particles to the total number of particles is very great, the plasma is said to be strongly ionized. If the ratio is small, the plasma is weakly ionized.

A great many different types of wave can exist in a plasma, especially in the case of strong ionization.

We shall only discuss electromagnetic wave propagation in a weakly ionized plasma, such as the earth's ionosphere. However, we shall give some data on particular cases of wave propagation in more strongly ionized media, such as occur in the polar regions and around satellites on their re-entry into the earth's atmosphere.

5.2 MOTION OF PARTICLES; EFFECT OF ELECTRIC AND MAGNETIC FIELDS

Charged particles are submitted:

1. to the electromagnetic field of the wave. In this case it is sufficient only to consider the effect of the electric field (Appendix 2.1)
2. to the magnetic field of the earth, whose direction and strength are fairly constant at a given point.

5.2.1 EFFECT OF AN ALTERNATING ELECTRIC FIELD

A particle with a charge ε in an electric field $\boldsymbol{E}$ is submitted to a force $\varepsilon\boldsymbol{E}$ by definition of $\boldsymbol{E}$. If the electric field is alternating, we have:

$$m\frac{\mathrm{d}^2x}{\mathrm{d}t^2} = \varepsilon E_0 \mathrm{e}^{\mathrm{j}\omega t} \tag{5.1}$$

Integrating once with respect to time, assuming $V = 0$ at $t = 0$, and suppressing factor $\mathrm{e}^{\mathrm{j}\omega t}$ in the two terms, we obtain:

$$V_0 = \frac{\varepsilon}{m}\frac{E_0}{\mathrm{j}\omega} \tag{5.2}$$

where V_0 = amplitude of velocity.

It can be shown in electricity theory[4] that the motion of an electrically charged particle is equivalent to a current of elementary amplitude:

$$i_0 = \varepsilon V_0 \tag{5.3}$$

Substituting the values of V_0 derived from equation (5.2), we have:

$$i_0 = -\mathrm{j}\frac{\varepsilon^2}{m\omega}E_0$$

Under the effect of an alternating electric field, the charged particles will therefore produce a current in the direction of the field, which is in quadrature with the field, inversely proportional to its frequency, proportional to the ratio ε^2/m, and has the same direction as the field.

When referring to the figures given in Section 5.1, we see that almost the entire current is due to the electrons on account of their small mass. We can therefore base our discussion on the assumption that an ionized medium consists solely of electrons.

5.2.2 EFFECT OF A CONSTANT MAGNETIC FIELD

Let $\boldsymbol{H}$ be the constant magnetic field. A particle with a charge ε and having a velocity $\boldsymbol{V}$, will be subjected to a force:

$$\boldsymbol{F} = \mu_0 \varepsilon \boldsymbol{V} \times \boldsymbol{H}$$

perpendicular to both $\boldsymbol{V}$ and $\boldsymbol{H}$. It can be shown that the corresponding

path is a helical one whose axle is parallel to H, plotted on a circular cylinder with radius ρ, in such a manner that the centrifugal force is in equilibrium with the electromagnetic force. We have therefore:

$$m\omega_H^2\rho = \mu_0\varepsilon H V_n \tag{5.4}$$

where V_n = component of the velocity normal to the field, and
$\omega_H = 2\pi f_H$ = angular frequency of the motion.

We can write:

$$V_n = \frac{2\pi\rho}{T} = \omega_H\rho$$

and therefore:

$$\omega_H = \frac{\mu_0\varepsilon H}{m} = 2\pi f_H \tag{5.5}$$

We find for an electron with the values of ε and m_e given in Section 5.1:

$$f_H = 3{\cdot}56 \times 10^4 H \tag{5.6}$$

This natural rotational frequency of electrons in the earth's magnetic field is called *gyrofrequency* or *cyclotron frequency*.

The earth's magnetic field varies at an altitude of 100 km from 19 At/m at the intersection of the magnetic equator with the small arc of the great circle which joins the magnetic poles, to 53 At/m at the magnetic south pole (George V Land in the Antarctic). At the same time, the gyrofrequency varies between 0·7 and 1·8 MHz (Fig. 35).

5.2.3 EFFECT OF COLLISIONS

If electrons in the ionosphere are only subjected to thermal agitation, the mean value of the current produced by their motion is zero, because both direction and value of V are random. This is not the case if the electrons are subjected to an electric field, because then the mean velocity in the direction of the field is no longer zero, as we have seen in Section 5.2.1.

But if there are also neutral particles present, the electrons in motion will collide with them and the direction of their velocity after the collision will once again be random. Any electron which has collided with a neutral particle will be lost to coordinated displacement, and therefore to the current.

It has been shown in kinetic gas theory[6] that for N particles having an average free path l, the number of particles that will travel distance x without collision is:

$$n = N\mathrm{e}^{-x/l} \tag{5.7}$$

Since $x = V_0 t$ and $l = V_0/\nu$ (ν being the number of collisions per second), equation (5.7) can be written:

$$n = N\mathrm{e}^{-\nu t} \tag{5.8}$$

Assuming that at instant $t = 0$, the N electrons have velocity V_0, each of which will maintain this velocity until the first collision occurs, the current produced will be:

$$I = n\varepsilon V_0 = N\,\mathrm{e}^{-\nu t}\varepsilon V_0 \tag{5.9}$$

We can define an imaginary velocity

$$V = V_0\,\mathrm{e}^{-\nu t} \tag{5.10}$$

in such a manner that if all N electrons had this velocity, they would produce the same current I as before.

The corresponding acceleration is:

$$\gamma = \frac{\mathrm{d}V}{\mathrm{d}t} = -V_0\nu\,\mathrm{e}^{-\nu t} = -\nu V \tag{5.11}$$

and the force acting on the electron would be:

$$\mathbf{f} = m\gamma = -m\nu V \tag{5.12}$$

Therefore, the effect of collisions on electrons from the point of view of the current produced by their displacement is equivalent to that of viscosity force proportional to the number of collisions per second, and to the velocity of these electrons.

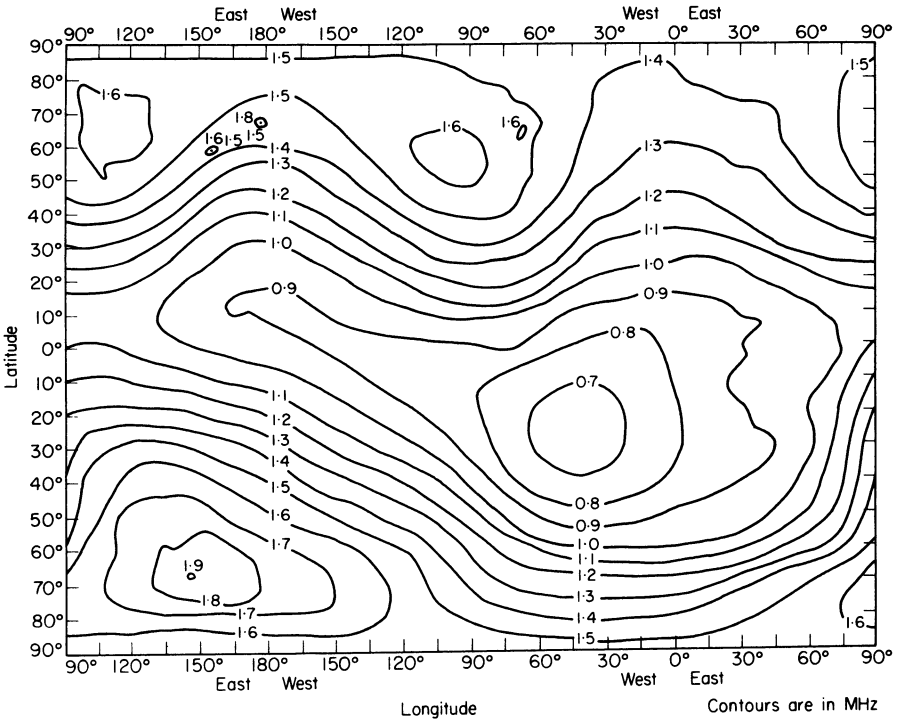

Fig. 35

5.2.4 EQUATION OF ELECTRON MOTION

The preceding results allow us to write the equation of electron motion. In accordance with the system generally used in kinetic gas theory, all electrons are assumed to have the same imaginary velocity, which equals their mean velocity. They are therefore subjected to:

1. the force of inertia: $-m\,\mathrm{d}V/\mathrm{d}t$
2. the viscosity force due to collision: $-mvV$
3. electric field $\boldsymbol{E}$, giving a force: $\varepsilon\boldsymbol{E}$
4. earth's magnetic field $\boldsymbol{H}$, giving a force $\mu_0\varepsilon V\times\boldsymbol{H}$.

We have therefore:

$$\varepsilon\boldsymbol{E}+\mu_0\varepsilon V\times\boldsymbol{H}-m\frac{\mathrm{d}V}{\mathrm{d}t}-mvV=0 \tag{5.13}$$

In this very general form, this equation leads, for the study of propagation, to complex formulae the physical significance of which it is, however, difficult to understand.

We shall discuss more especially two specific cases that lead to solutions of easy interpretation and which cover the majority of practical cases.

5.3 PROPAGATION IN THE ABSENCE OF A MAGNETIC FIELD

Although this case may appear purely theoretical, since the earth's magnetic field is present everywhere in space, it allows nevertheless:

1. the definition of important constants of ionized media
2. to be applied each time that the effect of the earth's magnetic field is weak, which is the case in the ionospheric reflection of waves whose frequency is not too close to a critical frequency we shall discuss later.

5.3.1 COMPLEX DIELECTRIC CONSTANT

As in Section 3.2, we shall discuss a capacitor whose dielectric consists of an elementary cube (1 cubic metre) of unit section and height, filled with an ionized medium containing N electrons.

The current in this capacitor will be the sum of the convection current (due to electron displacement) and the displacement current in vacuo (the relative dielectric constant of rarefied air is very close to unity).

$$\boldsymbol{I}=\boldsymbol{I}_C+\boldsymbol{I}_D$$

The first term is calculated by writing equation (5.13) as:

$$\frac{\mathrm{d}V}{\mathrm{d}t}+vV=\frac{\varepsilon}{m}\boldsymbol{E}_0\,\mathrm{e}^{\mathrm{j}\omega t} \tag{5.14}$$

Let V_0 be the amplitude of V and putting

$$\mathbf{V} = \mathbf{V}_0 \, e^{j\omega t}$$

we have (once equilibrium has been established):

$$\boldsymbol{V}_0 = \frac{\varepsilon}{m} \cdot \frac{\boldsymbol{E}_0}{\nu + j\omega}$$

and according to equation (5.3):

$$\boldsymbol{I}_{0C} = \frac{N\varepsilon^2}{m} \cdot \frac{\boldsymbol{E}_0}{\nu + j\omega} \tag{5.15}$$

where N = number of electrons per m^3.

Moreover, equation (3.2) gives:

$$\boldsymbol{I}_{0D} = j\omega\varepsilon_0 \boldsymbol{E}_0 \tag{5.16}$$

Therefore:

$$\boldsymbol{I}_0 = j\omega\varepsilon_0 \left[1 + \frac{N\varepsilon^2}{jm\varepsilon_0\omega(\nu + j\omega)}\right] \boldsymbol{E}_0 = j\omega\varepsilon_0\varepsilon_r' \boldsymbol{E}_0$$

where

$$\varepsilon_r' = 1 + \frac{N\varepsilon^2}{jm\varepsilon_0\omega(\nu + j\omega)} \tag{5.17}$$

ε_r' is the complex dielectric constant of the ionized medium.

5.3.2 CRITICAL FREQUENCY OR PLASMA FREQUENCY

Let us consider the case where $\nu = 0$. We can write:

$$\varepsilon_r' = 1 - \frac{N\varepsilon^2}{m\varepsilon_0\omega^2} = 1 - \frac{\omega_C^2}{\omega^2} \tag{5.18}$$

where

$$\omega_C^2 = \frac{N\varepsilon^2}{m\varepsilon_0} \tag{5.19}$$

The refractive index of the ionized medium is given by:

$$n = (\varepsilon_r')^{\frac{1}{2}} = \left(1 - \frac{\omega_C^2}{\omega^2}\right)^{\frac{1}{2}}$$

Two cases are possible:

5.3.2.1 **Case 1**

$$\omega > \omega_C \qquad 1 - \frac{\omega_C^2}{\omega^2} > 0 \quad n \text{ is real}$$

In this case, wave propagation takes place.

5.3.2.2. **Case 2**

$$\omega \leqslant \omega_C \qquad 1 - \frac{\omega_C^2}{\omega^2} \leqslant 0 \quad n \text{ is purely imaginary}$$

The waves are vanishing and no wave propagation occurs. Frequency

$$f_C = \frac{\omega_C}{2\pi} = \frac{1}{2\pi}\left(\frac{Ne^2}{m\varepsilon_0}\right)^{\frac{1}{2}} \approx 9(N)^{\frac{1}{2}}\ \text{Hz} \tag{5.20}$$

which separates the two behaviour patterns, is called *critical frequency* or *plasma frequency*.

5.3.3 EQUIVALENT ELECTRIC CHARACTERISTICS OF AN ABSORBENT IONIZED MEDIUM

By introducing the critical frequency and separating the real and imaginary components, equation (5.17) gives:

$$\varepsilon_r' = 1 - \frac{\omega_C^2}{\omega(\omega - \mathrm{j}\nu)} = 1 - \frac{\omega_C^2}{\nu^2+\omega^2} - \frac{\mathrm{j}\omega_C^2\nu}{(\nu^2+\omega^2)\omega} \tag{5.21}$$

Putting the same as in Section 3.3.2 (equation (3.8)):

$$\varepsilon_r' = \varepsilon_r - \frac{\mathrm{j}\sigma}{\omega\varepsilon_0} = \varepsilon_r(1 - \mathrm{j}q)$$

we see that the ionized medium possesses an equivalent dielectric constant:

$$\varepsilon_r = 1 - \frac{\omega_C^2}{\nu^2+\omega^2} \tag{5.22}$$

and an equivalent conductivity:

$$\sigma = \frac{\varepsilon_0 \nu \omega_C^2}{\nu^2+\omega^2} \tag{5.23}$$

Contrary to what took place for the ground, the conductivity and dielectric constant of plasmas depend on frequency. We can consider two extreme cases:

1. If ω tends towards infinity:

   $$\varepsilon_r \to 1 \qquad \sigma \to 0$$

   the effect of ionization disappears. This is indeed what we observe of light waves, which are not affected by passage through the ionosphere.
2. If ω tends towards zero:

   $$\varepsilon_r \to 1 - \frac{\omega_C^2}{\nu^2} \qquad \sigma \to \frac{\varepsilon_0\omega_C^2}{\nu}$$

   Propagation is only possible if $\nu > \omega_C$.

5.3.4 REFRACTIVE INDEX

The refractive index can be defined by the following equation, similar to equation (3.9):

$$n = \beta - \mathrm{j}\alpha = (\varepsilon_r')^{\frac{1}{2}} = \left(\varepsilon_r - \mathrm{j}\frac{\sigma}{\omega\varepsilon_0}\right)^{\frac{1}{2}} = (\varepsilon_r')^{\frac{1}{2}}(1 - \mathrm{j}q)^{\frac{1}{2}}$$

When carrying out the calculations we come across the following equations, which are valid for $\varepsilon_r \geqslant 0$, i.e. for $\omega^2 \geqslant \omega_C^2 - \nu^2$:

$$\beta^2 = \varepsilon_r \frac{(1+q^2)^{\frac{1}{2}}+1}{2}$$

$$\alpha^2 = \varepsilon_r \frac{(1+q^2)^{\frac{1}{2}}-1}{2} \tag{5.24}$$

A general discussion of these equations is rather difficult because of the great number of parameters involved. Let us therefore only discuss the most interesting practical cases.

5.3.4.1 Phase constant

The most interesting case is when absorption is weak. We assume $\nu^2 \ll \omega_C$ and consider two cases:

High frequencies: $\omega^2 \gg \omega_C^2$

Equations (5.22) and (5.23) give:

$$\varepsilon_r \approx 1 - \frac{\omega_C^2}{\omega^2} \qquad \sigma \simeq \frac{\varepsilon_0 \nu \omega_C^2}{\omega^2}$$

whence:

$$q \approx \frac{\nu \omega_C^2}{(\omega^2 - \omega_C^2)\omega} \ll 1$$

and

$$\beta^2 \approx 1 - \frac{\omega_C^2}{\omega^2} + \frac{\omega_C^4}{\omega^4} \frac{\nu^2}{4(\omega^2 - \omega_C^2)}$$

In the case of frequencies that are higher than ω_C, β rapidly tends towards unity and ν has very little effect on the phase constant.

Frequencies close to ω_C

In this case we shall put

$$\Delta\omega = \omega - \omega_C \ll \omega_C$$

From (5.21), we derive:

$$\beta^2 \approx \frac{2\omega_C \Delta\omega + \nu^2 + [(2\omega_C \Delta\omega + \nu^2)^2 + \nu^2 \omega_C^2]^{\frac{1}{2}}}{2(\omega_C^2 + 2\omega_C \Delta\omega + \nu^2)}$$

Since ν is small, the minimum value of β^2 corresponds approximately to $\Delta\omega = 0$, or $\omega = \omega_C$. We have:

$$\beta_{\min}^2 \approx \frac{\nu}{2\omega_C}$$

As this minimum is not zero, there will be no total reflection, but reflection will be more effective when ν is smaller.

In the case of $\nu = 0$, the result will be the same as in Section 5.2.3.

5.3.5 PHASE VELOCITY; GROUP VELOCITY; SIGNAL VELOCITY

The phase velocity or propagation velocity of planes of equal phase is c/n (equation (1.12)).

Assuming zero absorption ($v = 0$) we have:

$$n = (\varepsilon_r)^{\frac{1}{2}} = \left(1 - \frac{\omega_c^2}{\omega^2}\right)^{\frac{1}{2}} \tag{5.25}$$

This quantity is always less than unity, so that planes with equal phase travel at a velocity $V_\varphi = c/n$, higher than the speed of light. This fact appears to be in contradiction with relativity theory.

However, in reality no information can be transmitted by a pure sinusoidal wave. In order to transmit a meaningful signal, the wave must either be modulated or coded. Let us assume that the wave is sine modulated, that the modulation frequency is sufficiently low to be negligible in relation to the carrier wave frequency, and that the variation of the refractive index in the modulation band can be considered as being linear.

Let

$$E = E_0(1 + \sin \Omega t) \sin \omega t \tag{5.26}$$

be the field at à given point. We can write:

$$E = E_0 \sin \omega t + \frac{E_0}{2} [\cos(\omega - \Omega)t - \cos(\omega + \Omega)t] \tag{5.27}$$

The three respective frequency components $(\omega - \Omega)$, ω, $(\omega + \Omega)$ do not travel at the same velocity, because n is frequency dependent, so that we have at a distance x in the direction of propagation:

$$E = E_0 \sin \omega\left(t - \frac{nx}{c}\right) + \frac{E_0}{2} \cos\left[(\omega - \Omega)\left[t - \left(n - \Omega \frac{dn}{d\omega}\right)\frac{x}{c}\right]\right] - \frac{E_0}{2} \cos\left[(\omega + \Omega)\left[t - \left(n + \Omega \frac{dn}{d\omega}\right)\frac{x}{c}\right]\right] \tag{5.28}$$

or, neglecting the terms containing Ω^2 and rearranging the components:

$$E = E_0\left[1 + \sin \Omega\left[t - \left(n + \omega \frac{dn}{d\omega}\right)\frac{x}{c}\right]\right] \sin \omega\left(t - \frac{nx}{c}\right) \tag{5.29}$$

We see therefore that, if the phase velocity of the carrier wave is c/n, the phase velocity of the envelope, or group velocity, is:

$$V_G = \frac{c}{n + \omega \dfrac{dn}{d\omega}} = \frac{c}{\dfrac{d(\omega n)}{d\omega}} \tag{5.30}$$

It is the envelope that will be detected, and the intelligible signal will

therefore travel at this velocity. When combining equations (5.25) and (5.30) we find:

$$V_G = nc = \frac{c^2}{V_\varphi} \tag{5.31}$$

This velocity is lower than the speed of light, as was to be expected.

If absorption is not zero, equation (5.31) must be replaced by a more complex one, but the phenomena will be similar.

Finally, when dealing with a coded signal, its spectrum in theory contains all frequencies, so that a linear variation of n with ω can no longer be assumed in the modulation band. The result is signal distortion. Instead of sudden increases and decreases in amplitude, we have a more gradual change. Indeed, it is never necessary to transmit rigorously square signals, and the signal velocity is practically the same as the group velocity.

5.3.6 ABSORPTION BY IONIZED MEDIA

Considering the electric field of a wave at a distance r from the source, we have:

$$E(r) = \frac{E_0}{r} e^{j\omega(t-nr/c)} = \frac{E_0}{r} e^{-\omega\alpha r/c} e^{j\omega(t-\beta r/c)}$$

α is necessarily positive in the direction of energy propagation. Therefore, during its travel the wave is subjected to exponential attenuation.

As we have mentioned in Section 5.3.4, we must restrict our discussion of this attenuation to the most important specific cases.

5.3.6.1 **High transparency band**

When the frequency increases indefinitely:

$$\varepsilon_r \to 1 \qquad \sigma \to \frac{\varepsilon_0 \nu \omega_C^2}{\omega^2}$$

thus:

$$q \to \frac{\nu\omega_C^2}{\omega^3}$$

$$(1+q^2)^{\frac{1}{2}} \to 1+\frac{q^2}{2}$$

and therefore:

$$\alpha^2 \approx \frac{q^2}{4} \approx \frac{\nu^2\omega_C^4}{4\omega^6}$$

The attenuation per metre (in nepers) is given by:

$$\kappa^2 = \frac{1}{p^2} \approx \frac{\alpha^2\omega^2}{c^2} = \frac{\nu^2\omega_C^4}{4c^2\omega^4} \qquad \kappa \approx \frac{\nu\omega_C^2}{2c\omega^2}$$

It is therefore proportional to ν and tends rapidly towards zero with increasing ω.

This frequency band is always present and is called the high transparency band.

5.3.6.2 Low transparency band

In contrast with the above, this second band is only present when there is a high collision frequency ν, as is sometimes the case in the ionosphere, when, as a result of a solar flare, ionization descends to low altitudes; it can also be produced during the re-entry of a satellite into the earth's atmosphere.

Assuming

$$\nu \gg \omega_C \qquad \text{and } \nu \gg \omega$$

we have:

$$\varepsilon_r \approx 1 \qquad \sigma \approx \frac{\varepsilon_0 \omega_C^2}{\nu} \qquad q \approx \frac{\omega_C^2}{\nu\omega}$$

When ω tends towards zero, q will tend towards infinity, so that we have:

$$\alpha^2 \approx \frac{q}{2} \approx \frac{\omega_C^2}{2\nu\omega}$$

and

$$\kappa^2 = \frac{1}{p^2} = \frac{\alpha^2\omega^2}{c^2} \approx \frac{\omega\omega_C^2}{2c^2\nu} \qquad \kappa \approx \frac{\omega_C}{c}\left(\frac{\omega}{2\nu}\right)^{\frac{1}{2}}$$

Attenuation is therefore reduced when the frequency is reduced, or when the collision frequency increases. This apparent paradox can be attributed to the fact that the electron motion is so small that little energy is removed from the wave[19].

5.3.6.3 Deviative absorption

When ν is small compared to ω_C, and ω differs little from ω_C, the values of β will differ considerably from unity (Section 5.3.4.1). As we shall see in Chapter 6, this results in curvature or deviation of the rays. At the same time, attenuation is present, called deviative absorption.

Similar calculations to those in Section 5.3.4.1 lead to:

$$\kappa^2 = \frac{1}{p^2} = \frac{\omega^2\alpha^2}{c^2} = \frac{\omega^2}{2c^2} \cdot \frac{-2\omega_C\Delta\omega - \nu^2 + [(2\omega_C\Delta\omega + \nu^2)^2 + \nu^2\omega_C^2]^{\frac{1}{2}}}{\omega_C^2 + 2\omega_C\Delta\omega + \nu^2}$$

If ν is small, the maximum absorption is attained at $\omega = \omega_C$.

We should remember that the above equation is only valid when

$$\omega^2 \geqslant \omega_C^2 - \nu^2$$

5.4 PROPAGATION IN THE PRESENCE OF THE EARTH'S MAGNETIC FIELD, WHEN THE LATTER IS PARALLEL TO THE DIRECTION OF PROPAGATION

5.4.1 COMPLEX DIELECTRIC CONSTANT

In this case since the waves are transverse the electric field of the wave is normal to the earth's magnetic field. The same as in Section 5.3.1, we shall assume an elemental capacitor of unity section and height, which is filled with an ionized medium and subjected to both an alternating field $\boldsymbol{E}$ and a constant field $\boldsymbol{H}$, both fields being perpendicular.

The vectorial form of equation (5.13):

$$q\boldsymbol{E}+\mu_0 q\boldsymbol{V}\times\boldsymbol{H}-m\frac{\mathrm{d}\boldsymbol{V}}{\mathrm{d}t}-mv\boldsymbol{V}=0$$

suggests that its solution can be more easily obtained by geometric reasoning than by calculation.

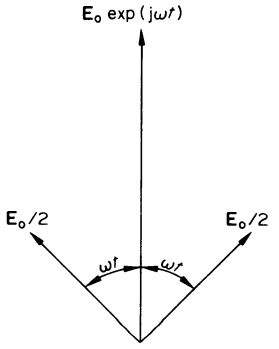

Fig. 36

As it may be seen in Fig. 36 we can replace field $\boldsymbol{E}_0\,\mathrm{e}^{\mathrm{j}\omega t}$ of constant direction and variable amplitude by two fields of constant amplitude $E_0/2$ and circular polarization in reverse directions, which would be normal to magnetic field $\boldsymbol{H}$, the same as the linearly polarized field. Because of the symmetry of the system with regard to $\boldsymbol{H}$, it is obvious that the velocity $\boldsymbol{V}$ received by the electrons from one of these fields will also be a constant vector, which rotates with frequency ω in a perpendicular plane towards $\boldsymbol{H}$. Finally, vector $\boldsymbol{V}\times\boldsymbol{H}$ is by definition perpendicular to both $\boldsymbol{H}$ and $\boldsymbol{V}$.

Arranging the various vectors of the equation in a plane $x0jy$ perpendicular to $\boldsymbol{H}$, we obtain the arrangements shown in Figs 37 and 38.

Moreover, equation (5.13) can be written as:

$$m\frac{\mathrm{d}\boldsymbol{V}}{\mathrm{d}t}+mv\boldsymbol{V}-\mu_0 q\boldsymbol{V}\times\boldsymbol{H}=q\boldsymbol{E} \tag{5.32}$$

Representing vectors $\mathrm{d}V/\mathrm{d}t$ and $V \times H$ by their imaginary values, and taking the direction of rotation into account, we have:

$$j m\omega V + mvV \pm j\mu_0 qHV = q\frac{E_0}{2} \tag{5.33}$$

where the plus and minus signs correspond to the two directions of rotation.

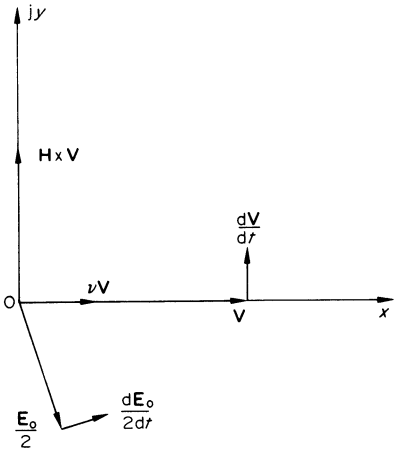

Fig. 37 Right-hand rotation

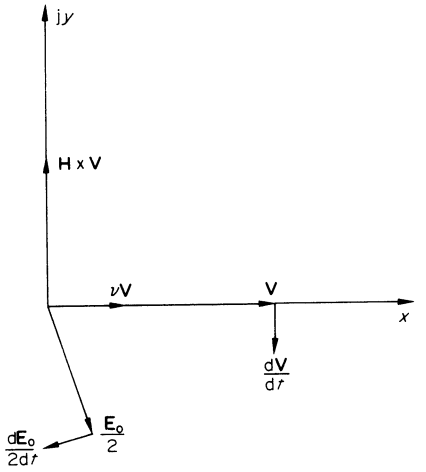

Fig. 38 Left-hand rotation

We now derive from equation (5.5):

$$V(j\omega + v \pm j\omega_H) = \frac{q}{m}\frac{E_0}{2}$$

or

$$\boldsymbol{V} = \frac{q}{m}\frac{1}{\mathrm{j}(\omega \pm \omega_H)+\nu}\frac{\boldsymbol{E}_0}{2} \tag{5.34}$$

The conduction current is therefore:

$$\boldsymbol{I}_C = NqV = \frac{Nq^2}{m}\cdot\frac{1}{j(\omega \pm \omega_H)+\nu}\cdot\frac{\boldsymbol{E}_0}{2} \tag{5.35}$$

As will be seen from the diagram, we also have:

$$\boldsymbol{I}_D = \frac{\varepsilon_0}{2}\frac{\mathrm{d}\boldsymbol{E}_0}{\mathrm{d}t} = \mathrm{j}\omega\varepsilon_0\frac{\boldsymbol{E}_0}{2} \tag{5.36}$$

whence:

$$\boldsymbol{I} = \mathrm{j}\omega\varepsilon_0\left(1-\frac{\omega_C^2}{\omega(\omega \pm \omega_H - \mathrm{j}\nu)}\right)\frac{\boldsymbol{E}_0}{2} \tag{5.37}$$

The complex relative dielectric constant of the ionized medium is therefore:

$$\varepsilon_r' = 1-\frac{\omega_C^2}{\omega(\omega \pm \omega_H - \mathrm{j}\nu)} \tag{5.38}$$

If the earth's field equals zero, equation (5.5) gives:

$$\omega_H = \frac{\mu_0 q\boldsymbol{H}}{m} = 0$$

and we find again equation (5.21) by adding the two waves with circular polarization, which in this case remain in phase.

5.4.2 EFFECT ON PROPAGATION

It would be easy to repeat the discussion of Sections 5.2.4, 5.2.4.1 and 5.2.4.2. The only difference would be that the equations would be slightly more complex.

However, it is sufficient to compare the following equations:

$$\varepsilon_r' = 1-\frac{\omega_C^2}{\omega(\omega-\mathrm{j}\nu)} \tag{5.17}$$

and

$$\varepsilon_r' = 1-\frac{\omega_C^2}{\omega(\omega \pm \omega_H - \mathrm{j}\nu)} \tag{5.38}$$

to be able to deduce the effect of the magnetic field on propagation.

Incident waves are divided upon entering an ionized medium into two waves with circular polarization in reverse directions. The complex dielectric constants corresponding to these two waves are given by the two signs of the denominator of equation (5.38). In analogy with optics, the wave corresponding to the plus sign is called ordinary wave, and the one corresponding to the minus sign extraordinary wave.

In order to obtain in equation (5.17) the same value of ε_r as in equation (5.38), ω must be replaced by:

$$[\omega(\omega+\omega_H)]^{\frac{1}{2}} > \omega \text{ for the ordinary wave, and by}$$
$$[\omega(\omega-\omega_H)]^{\frac{1}{2}} < \omega \text{ for the extraordinary wave.}$$

Referring to the results of Sections 5.3.4.1, 5.3.6.1 and 5.3.6.3, we see immediately that:

1. The ordinary wave has a smaller phase velocity and a greater group velocity than the extraordinary wave.
2. The ordinary wave is less attenuated in its travel through the ionosphere than the extraordinary wave. More specifically, if the frequency of the incident wave equals the gyrofrequency, the extraordinary wave will be very strongly absorbed. Only the ordinary wave will be received, which will have circular polarization—to the left in the Northern hemisphere, and to the right in the Southern hemisphere. This phenomenon constitutes one of the experimental proofs of the existence of ionized layers.

The two waves recombine upon leaving the ionized medium. They then have different amplitudes and phases, so that the result of this recombination will be an elliptically polarized wave. This is a characteristic phenomenon of ionospheric propagation.

If absorption is very small, there will simply be a rotation of the plane of polarization (Faraday rotation).

5.5 COMPLETE EQUATION AND APPROXIMATIONS

It is possible by means of rather complex calculations to establish an equation that gives the complex dielectric constant in the most general case where the magnetic field subtends a random angle to the direction of wave propagation.

The symbols have the following meaning:

ω_C = critical frequency

ω_H = gyrofrequency corresponding to the earth's magnetic field

ω_L = gyrofrequency corresponding to the component of this field in the direction of propagation

ω_T = gyrofrequency corresponding to the component normal to the direction of propagation.

We thus arrive at Appleton-Hartree's formula:

$$\varepsilon_r' = 1 + \frac{2}{\dfrac{2\omega(\omega+\mathrm{j}\nu)}{\omega_C^2} - \dfrac{\dfrac{\omega^2\omega_T^2}{\omega_C^4}}{1+\dfrac{\omega(\omega+\mathrm{j}\nu)}{\omega_C^2}} \pm \left[\dfrac{\dfrac{\omega^4\omega_T^4}{\omega_C^8}}{\left(1+\dfrac{\omega(\omega+\mathrm{j}\nu)}{\omega_C^2}\right)^2} + \dfrac{4\omega^2\omega_L^2}{\omega_C^4}\right]^{\frac{1}{2}}} \tag{5.39}$$

This exact equation is obviously not suitable for practical calculations. It can be simplified for practical purposes by assuming that field $\boldsymbol{H}$ is solely transverse (quasi-transverse approximation) or solely longitudinal (quasi-longitudinal approximation).

When examining the various possibilities, it has been observed[8] that when the wave frequency is greater than 1 or 2 MHz (which is always the case for transmissions by ionospheric wave) the quasi-longitudinal approximation can be used in most cases, and it is this approximation on which the application calculations are based[7].

If the direction of propagation subtends an angle θ to the earth's field, we obviously have:

$$\boldsymbol{H}_L = \boldsymbol{H}\cos\theta$$

and therefore (equation (5.5)):

$$\omega_L = \omega_H \cos\theta$$

so that equation (5.38) can now be written as:

$$\varepsilon_r' = 1 - \frac{\omega_C^2}{\omega(\omega \pm \omega_H \cos\theta - \mathrm{j}\nu)} \tag{5.40}$$

This equation is sufficiently accurate and simple for practical applications. However, recent publications[317, 318, 343] have shown the possibility of using more rigorous methods.

CHAPTER 6

IONOSPHERIC PROPAGATION

The propagation of waves in the ionosphere can be studied by the same methods as used for examining the effect of the earth's surface, where ionosphere is an imperfectly conducting sphere. This is the theory proposed by Eckersley[203] and more recently by Bremmer[5], Wait[321, 322], Budden[320] and other workers.

However, more intuitive methods, akin to those used in optics, permit us to present the main results for the prediction of radio communication by way of the ionosphere. It is these methods we shall now discuss.

Despite these simplified methods, the study of propagation in the ionosphere is much more complex than the corresponding investigation of the atmosphere; this is due to variations in conductivity of the medium with frequency, and especially to double refraction, caused by the earth's magnetism. A brief theoretical account of these phenomena has been given in Chapter 5. The importance of communication by means of ionospheric propagation justifies a more detailed discussion of the complex mechanism of this mode of propagation.

6.1 THE IONOSPHERE

6.1.1 EXISTENCE OF THE IONOSPHERE

The great ranges attained by decametre waves cannot be explained solely by referring to atmospheric refraction and diffraction around the earth as discussed in Chapters 2 and 4. Certainly, atmospheric refraction can occasionally cause great ranges, but it is a rare phenomenon that never stretches beyond an area with uniform meteorological conditions—which of course can never be the case for ranges of several thousand kilometres. With regard to diffraction, this produces a weaker field when the frequency is higher; the exponential decrease of the field of a diffracted wave absolutely prevents large ranges. Moreover, the field strength of the waves of these two modes of propagation varies continuously with frequency. On the contrary, propagation of decametre waves is characterized by sudden field discontinuities at certain frequencies.

These observations caused Heaviside to assume the existence in the upper atmosphere of layers of ionized—and therefore conductive—air. In 1902, when this hypothesis was advanced, the only actual proof was the existence

of the Northern Lights. More recently it has been confirmed by direct measurement carried out by means of rockets.

6.1.2 PHYSICAL ORIGIN OF THE IONOSPHERE

Ionization of layers in the upper atmosphere is essentially caused by radiation from the sun; however, a not inconsiderable contribution is also made by meteorites travelling through this atmosphere.

The action of the sun consists mainly of photo-ionization, i.e. solar radiation of short wavelength and large quantum energy causes the ionization of molecules in the upper atmosphere. This effect is linked with the intensity of solar radiation, i.e. time of day, season, geographic latitude and solar activity. The sun also emits electrically charged particles which reach the earth in the neighbourhood of the two magnetic poles; this effect is therefore related to the geomagnetic latitude. The electrically charged particles modify electric currents in the upper atmosphere and therefore the earth's magnetic field (magnetic storms). Ions are also produced when these particles are slowed down upon entering the earth's atmosphere.

6.1.2.1 **Solar activity**

Various indexes are used to indicate solar activity in the study of the ionosphere[354, 358].

Sunspot number

The oldest of these indexes is the relative Zurich sunspot number, also called Wolf number:

$$R = k(10g + f) \tag{6.1}$$

where g = number of sunspot groups

f = number of observable individual spots

k = correction factor ≈ 1, used to equalize the results from different observers and equipments.

The sunspot number varies from year to year according to a cycle whose mean duration is about 11 years. Routine observations have been carried out since 1749 and have shown 19 cycles of 11 years (the first started in 1755) with a duration of between $7\frac{1}{2}$ and $14\frac{1}{2}$ years. The values of the sunspot number at the maxima are spread from 46 in 1816 to 175 in 1957, those at the minima from 0 in 1810 to 11 in 1766. The period of growth (average $4\frac{1}{2}$ years) is usually much shorter than the period of decline (average $6\frac{1}{2}$ years)[14].

Prediction of the sunspot number is difficult. It is usually sufficiently accurate during periods of increasing and decreasing solar activity, but the determination of the period and the value of the maxima and minima

remains uncertain. This problem has been most thoroughly discussed by Waldmeier[14] and Mayot[302, 303, 308]. Halley and Gervaise[348] have recently proposed a new method. They prove that the mean times of the minima are indicated by the following formula:

$$t' = 11{\cdot}15r + 1\,774{\cdot}31$$

and those of the maxima by

$$T' = 11{\cdot}08r + 1\,749{\cdot}42$$

where r = number of the cycle. These authors then consider a secondary cycle of 170 years, which results in a correction to the mean times in order to obtain times of a defined cycle.

Most parameters used in the study of the ionosphere are linked with the sunspot number in a simple and rather accurate manner. This fact emphasizes the great importance of knowing the sunspot number for establishing ionospheric predictions.

Predictions of the value of the sunspot number are published in the *Journal de l'UIT* (Berne) and in the *CRPL Ionospheric Predictions* of the NBS in Washington. These predictions are made three months in advance.

Index I_{F2}

This index was introduced in 1955 by Minnis[344, 358]. Strictly speaking this is not an index of solar activity but a radioelectric index, which permits one to predict the critical frequency of the F_2 layer at noon. This prediction can be made 6 months in advance. The index is published by the Radio and Space Research Station at Slough in Buckinghamshire (U.K.).

Index Φ

This index was introduced by Covington in 1947 and is a measure of the radioelectric emission from the sun at 2800 MHz. It is expressed in $W/m^2/Hz.10^{-22}$. It appears to be capable of medium-term prediction (6–9 months) to a better approximation than the one obtained from the other indexes[358].

Sliding averages

The sunspot number is subject to wide variations from month to month because of the discontinuity of solar activity. The characteristics of the ionosphere do not follow these variations. In order to ensure better correlation, a sliding average over 12 months is therefore used, which is defined by:

$$R_{12} = \frac{1}{12}\left[\tfrac{1}{2}(R_{n-6} + R_{n+6}) + \sum_{n=-5}^{n=+5} R_n\right]$$

The value of this average is, by definition, only known 7 months after the last recorded observation.

Correlation between indexes

Because of the recent introduction of indexes Φ and I_{F2}, the study of their correlation with R_{12} is still in its infancy[358].

It has been found:

$$\Phi = R_{12} + 46 + 23\, e^{-0.05\, R_{12}}$$

On the other hand, I_{F2} shows a less simple relationship with the two other indexes. For the same relative value of R_{12} or Φ, the value of I_{F2} is smaller in the ascending part of the cycle than in the descending one.

6.1.2.2 Effect of time of day, season and latitude

These three factors modify the angle subtended by the sun to the zenith at the place of observation. The energy received by a given ground surface is proportional to the cosine of the zenith angle, indicated by χ.

6.1.2.3 Solar electromagnetic radiation

The exact nature of electromagnetic radiation from the sun is not fully known. As a matter of fact, observations made at ground level—which obviously are the most numerous—are modified by the strong absorption of the earth's atmosphere. Observations by rockets or satellites do not offer this disadvantage, but are not permanent, and each launch only allows the study of a few preselected characteristics.

The spectrum of the radiation from the sun contains a continuous background, which is observed from radio waves of 20 MHz (longer waves are reflected or absorbed by the ionosphere) to light, X- and γ-rays. The total calorific radiation received from the sun at the upper part of the earth's atmosphere seems to be of the order of magnitude of $3{\cdot}5.10^3$ W/m^2. Most of this radiation does not contribute to ionization (because of the weak quantum energy of its photons) but plays an important part in the behaviour of ionized layers, because of its action on the equilibrium of atmospheric gases.

Brilliant lines appear on this background. The most powerful are[19, 330, 360] as shown in Table 6.1.

TABLE 6.1

Lα		(hydrogen)	1 216 Å	10^{-4}–9×10^{-3} W/m^2 (average 3×10^{-4})
Lβ		(hydrogen)	1 026 Å	$4{\cdot}8 \times 10^{-5}$ W/m^2
O	V	(oxygen)	630 Å	$2{\cdot}8 \times 10^{-5}$ W/m^2
He	I	(helium)	584 Å	$3{\cdot}4 \times 10^{-5}$ W/m^2
He	II	(helium)	304 Å	$1{\cdot}7 \times 10^{-4}$ W/m^2

Between 170 and 930 Å, the energy flux is about 2×10^{-3} W/m^2 at the period of minimum solar activity, and several times this value at the maximum[360].

X-rays are of particular interest to the ionosphere; their spectrum corresponds to a temperature of 5×10^5 K, with an intensity of between $1{\cdot}3 \times 10^{-4}$ and 10^{-3} W/m^2.

6.1.2.4 Absorption of solar radiation by the atmosphere

Figure 39 schematically indicates the transmission characteristics of the atmosphere to different solar radiations (Friedman[330]). The wavelengths from 170–930 Å are absorbed between 120 and 175 km and create an ionized layer, called the *F*-layer. Line Lβ and X-rays of a wavelength between 10 and 32 Å, which are absorbed between 100 and 120 km, give rise to the ionized *E*-layer. Line Lα and X-rays of a short wavelength (about 2·5 Å) are only absorbed in the neighbourhood of 80 km; they produce the ionized *D*-layer. Line Lα, and especially X-rays of short wavelength are submitted to a suddenly increased intensity during chromospheric eruptions. At 70 km, where no X-rays are found during periods of relative solar inactivity, the intensity of these rays can attain 10^{-7} to 2×10^{-5} W/m^2 (average 5×10^{-6}). A considerable increase in the ionization of the *D*-layer will then take place.

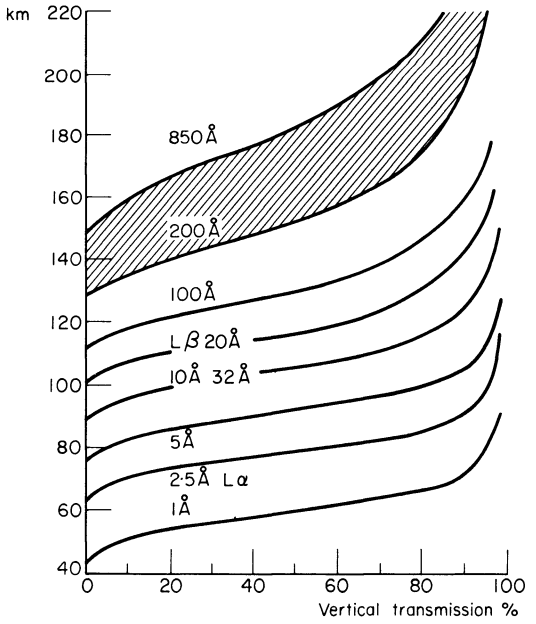

Fig. 39

These effects occur about ten minutes after the chromospheric eruption has started; this is the travelling time of the electromagnetic radiation from the sun to the earth—to which should be added the time required to increase ionization. The annual number of chromospheric eruptions is closely proportional to the sunspot number.

6.1.2.5 Formation of ionized layers by absorption of solar radiation

Description of the phenomena involved

When a photon pertaining to an electromagnetic radiation collides with a molecule, it can force an electron out of the molecule if the energy of the photon is greater than the ionization energy of the molecule. The energy of a photon equals hv, where h is Planck's constant ($h = 6{\cdot}625 \times 10^{-34}$ J s) and v represents the radiation frequency. Radiation will therefore have a greater ionizing power when the frequency is higher. Ionization is accompanied by absorption of the incident radiation, in accordance with the principle of conservation of energy. The ionization process gives rise to the simultaneous appearance of one liberated electron and one positive ion.

As we have seen in Chapter 5 (Section 5.2.1), the electrons have much more influence on the propagation than the ions. We shall therefore try to calculate the electron density in the plasma, which results from an equilibrium between the rate of production of the electrons and their rate of disappearance.

The electrons can disappear according to a number of different mechanisms, which lead to different equations for the equilibrium.

Let $N(h, t)$ be the number of electrons per m^3 at altitude h and time t, and $q(h)$ be the number of electrons produced per m^3 per second at the altitude h.

In the case of direct recombination between electrons and positive ions, the rate of disappearance will be proportional to the number of electrons and the number of ions, both equal to N. We thus have:

$$\frac{dN}{dt} = q - \alpha N^2 \tag{6.2}$$

putting α for the recombination coefficient, i.e. the number of m^3 of ionized plasma recombining per second.

The electron can also *attach* itself to a neutral molecule, to give a negative ion. Since the number of molecules is much greater than that of electrons (10^2–10^3 as many), the rate of disappearance in this case will be proportional to N, so that we may write:

$$\frac{dN}{dt} = q - \beta N \tag{6.3}$$

Finally, the electrons, ions and neutral molecules can undergo various *reactions* before the ions produced are electrically neutralized. These

reactions obey equations like equations (6.2) and (6.3)[19, 360], but the coefficients α and β will be different, giving a wider choice of parameters for the explanation of certain properties of the ionized layers.

Chapman's formula[301]

This formula, the first to be derived to deal with the problem, gives a very accurate explanation of the formation of the layers E and F_1.

Rate of production of the electrons

Let: S_∞ be the density of the solar energy above the absorbing layer, expressed in W/m^2

S be the same quantity at an arbitrary point

n be the number of particles (molecules or atoms) of the gas per m^3

n_0 be the same number at the altitude h_0

H be the 'scale height' of the gas in the layer, assumed to be isothermal (H = constant)

σ be the effective cross-section of the gas particles

η be the number of electrons produced by the absorption of one Joule

h be the altitude

h_0 the altitude at which $n_0\sigma H = 1$

and let us put $z = (h-h_0)/H$.

Now it follows from the laws of gaseous equilibrium that:

$$n = n_0\,[\exp(-z)] \tag{6.4}$$

Let us suppose that the sun is at its zenith. If we consider a column 1 m^2 in cross-section, we may write:

$$\mathrm{d}S = \sigma S n\,\mathrm{d}h = S\exp(-z)\,\mathrm{d}z \tag{6.5}$$

$$\frac{\mathrm{d}S}{S} = \exp(-z)\,\mathrm{d}z$$

$$\log_e \frac{S}{S_\infty} = \int_\infty^z \exp(-z)\,\mathrm{d}z = -\exp(-z)$$

$$S = S_\infty \exp[-\exp(-z)] \tag{6.6}$$

It now follows from equation (6.5) that:

$$\frac{\mathrm{d}S}{\mathrm{d}z} = S_\infty \exp\,[-z-\exp(-z)]$$

now:

$$q = \eta\frac{\mathrm{d}S}{\mathrm{d}h} = \frac{\eta}{H}\frac{\mathrm{d}S}{\mathrm{d}z} \tag{6.7}$$

The maximum value of q, which we shall call q_0, is reached when $dq/dh = 0$. Now it follows from equations (6.6) and (6.7) that:

$$\frac{dq}{dh} \propto \exp[-z-\exp(-z)][1-\exp(-z)]$$

which is zero when $z = 0$. Again making use of equations (6.6) and (6.7), we find:

$$q_0 = \frac{\eta}{eH} S_\infty \tag{6.8}$$

whence:

$$q = q_0 \exp[1-z-\exp(-z)] \tag{6.9}$$

If the solar rays make an angle χ with the vertical, we find in the same way:

$$q = q_0 \exp[1-z-\exp(-z)\sec\chi] \tag{6.10}$$

The maximum ion production is thus found at a height corresponding to $z = \log_e(\sec\chi)$, and is equal to $q_0 \cos\chi$.

The electron density

It is found experimentally that the variation of the electron density is so slow that we can assume without excessive error that dN/dt in equation (6.2) is zero. It follows that:

$$N_{max} = \left(\frac{q}{\alpha}\right)^{\frac{1}{2}} = \left(\frac{q_0 \cos\chi}{\alpha}\right)^{\frac{1}{2}} \tag{6.11}$$

With the aid of equation (5.20) of Chapter 5, we may thus write:

$$f_{C\,max} \propto \cos^{\frac{1}{4}}\chi \tag{6.12}$$

This relation is characteristic of Chapman's layers. Measurements generally confirm that the value of the exponent of $\cos\chi$ in this equation is very close to 1/4.

Let us now assume that the production of ions in an ionized layer is suddenly stopped, as actually occurs in the case of a total eclipse of the sun. Substituting N_{max} for N in equation (6.2) we have:

$$\frac{dN_{max}}{dt} + \alpha^2 N_{max}^2 = 0 \tag{6.13}$$

which gives:

$$N_{max} = \frac{N_{0\,max}}{N_{0\,max}\alpha t + 1} \tag{6.14}$$

The quantity

$$\tau = \frac{1}{2\alpha N_{max}} \tag{6.15}$$

is called the time constant of the layer. The smaller this value is, the more rapidly will the layer density N_{max} follow the variations in ion production.

Martyn's theory[336]

Chapman's formula is completely invalid in the case of the highest ionized layer, *F*. Here Martyn assumes that a displacement of ionized plasmas takes place from one part of the atmosphere to another under the effect of:

1. wind. In this case the transport of ionized particles is almost parallel to the earth's magnetic field,
2. electric fields due to charges, which, in combination with the earth's magnetic field, submit the electrified particles to electromagnetic forces,
3. gravity,
4. partial pressure of the various components of the atmosphere.

Martyn replaces equation (6.2) by:

$$\frac{\partial N}{\partial t} = q - \beta N - \nabla . VN \tag{6.16}$$

where V = velocity

β = a coefficient acting as a recombination coefficient.

The quasi-stationary behaviour corresponding to equation (6.3) can then be written as:

$$q = \beta N - \nabla \cdot VN \tag{6.17}$$

Recent theories

More elaborate theories have been worked out of recent years, in particular to explain the peculiarities of the F_2 layer[360]. These are based on the theories of Chapman and Martyn, but assume other disappearance mechanisms for the electrons. On the hypothesis that two disappearance mechanisms operate simultaneously, these theories can explain in particular the fact that the F region is split into two layers, F_1 and F_2, starting from a single electron producing layer.

Many points in these new theories remain highly hypothetical.

6.1.2.6 Meteoric ionization

Meteors are small bodies, most of which orbit the sun. Their orbital velocity lies between 11·3 km/s (minimum velocity for a solar orbit) and 72 km/s (the velocity required to escape solar gravity). The measured mean velocity is 40 km/s. On the other hand, the orbital velocity of the earth is approximately 30 km/s.

At 06.00 h local time at the point of observation, the orbital velocity of the earth is directed towards the zenith, and the relative velocity of meteors in relation to the atmosphere lies between 41 and 102 km/s, with

a mean value of 70 km/s. At 18.00 h local time at the point of observation, the orbital velocity of the earth is directed towards the nadir, and some meteors are unable to catch up with it, while others arrive at velocities between 0 and 42 km/s with a mean value of 10 km/s.

Therefore, the number of meteors encountered and their velocity are considerably greater at 06.00 h than at 18.00 h.

The deceleration of meteors by the relatively low layers of the atmosphere produces intense heat, which causes their combustion at a greater height and more rapidly if their initial velocity was greater. The combustion products are ionized and form a meteoric trail that is capable of reflecting radio waves. Very thick trails can be seen with the naked eye at the moment of their formation (shooting stars).

Radar measurement assists in identifying a great number of small trails, but it is certain that there does exist a still far greater number of very small trails, which reveal themselves by the scattering of waves in the ionosphere.

Meteoric ionization occurs at altitudes between 80 and 100 km, with a maximum at about 90 km[315].

The detailed mechanism of meteoric reflection is rather complex and its discussion would exceed the scope of this book[335].

We distinguish between underdense trails, containing less than 10^{14} electrons per metre, and overdense trails, containing more than 10^{14} electrons per metre. In the first case, the contributions made by all the electrons to the scattering of waves are simply added together. In the second case, there is a strongly ionized nucleus through which the waves cannot travel. Furthermore, we must take account of the wave scattering from one electron to another, with the result that the equations become less simple.

Maximum ionization occurs immediately after the trail has been formed; the trail then begins to expand and to diffuse outwards. Its electron density decreases and it is no longer capable of reflecting high frequencies. At the same time, the trail is distorted by atmospheric disturbances.

In the case of a large meteor, the head of the trail reflects a considerable amount of energy. Because of the motion involved, this reflection occurs with a change in frequency due to the Doppler effect (Appendix A.9). Waves reflected by the head of the trail interfere with those reflected by the body of the trail, thereby producing a whistling noise that starts at the top of the audio range and falls throughout the range, then ascends again. This phenomenon is called whistling atmospherics or just whistlers.

Table 6.2 schematically presents the principal characteristics of meteors.

The mean interval of usable strikes represents the interval between two strikes occurring in a spherical radius of 480 km around the point of observation. The reflection coefficient is defined as the ratio of the field received by the meteoric trail to the field reflected by that trail.

TABLE 6.2

Mass (kg)	Radius (m)	Number of strikes per day	Number of strikes per m^2 and per s	Mean interval of usable strikes	Ionization in trail (electrons per metre)	Maximum coefficient of reflection at 150 km, for 30 MHz	Duration at 30 MHz	Stellar magnitude
10	8.10^{-2}	10						-12
1	4.10^{-2}	10^2						-10
10^{-1}	2.10^{-2}	10^3						-7
10^{-2}	8.10^{-3}	10^4	$1{\cdot}6.10^{-16}$		10^{18}			-5
10^{-3}	4.10^{-3}	10^5	$1{\cdot}6.10^{-15}$	16h	10^{17}	$7{\cdot}7.10^{-3}$	4h	-2
10^{-4}	2.10^{-3}	10^6	$1{\cdot}6.10^{-14}$	100m	10^{16}	$4{\cdot}4.10^{-3}$	25s	0
10^{-5}	8.10^{-4}	10^7	$1{\cdot}6.10^{-13}$	10m	10^{15}	$2{\cdot}4.10^{-3}$	2·5s	2
10^{-6}	4.10^{-4}	10^8	$1{\cdot}6.10^{-12}$	60s	10^{14}	$9{\cdot}1.10^{-4}$	0·5s	5
10^{-7}	2.10^{-4}	10^9	$1{\cdot}6.10^{-11}$	6s	10^{13}	$1{\cdot}6.10^{-4}$	0·5s	7·5
10^{-8}	8.10^{-5}	10^{10}	$1{\cdot}6.10^{-10}$	6.10^{-1}s	10^{12}	$1{\cdot}6.10^{-5}$	0·5s	10
10^{-9}	4.10^{-5}		$1{\cdot}6.10^{-9}$	6.10^{-2}s	10^{11}	$1{\cdot}6.10^{-6}$	0·5s	12·5
10^{-10}	2.10^{-5}		$1{\cdot}6.10^{-8}$	6.10^{-3}s	10^{10}	$1{\cdot}6.10^{-7}$	0·5s	15
10^{-11}	8.10^{-6}				10^9	$1{\cdot}6.10^{-8}$	0·5s	

visible with the naked eye

h = hour m = minute s = second

6.1.2.7 **Corpuscular radiation**

A sunspot is a kind of vortex from which emanates a multitude of electrically charged particles. If the latter are ejected in the right direction (i.e. when the spot is situated in the proximity of the solar equator and on the central meridian) they arrive at the earth after 24–48 hours. Here they are deviated from a linear path by the earth's magnetic field and travel towards the auroral regions which enclose the magnetic poles, where they give rise to strong magneto-currents. The very strong ionization produced by these very fast particles causes aurorae (e.g. Northern Lights), whilst the particle currents modify the earth's magnetism and cause a magnetic storm. The structure of the ionosphere is simultaneously modified over the entire earth[329].

6.1.3 METHODS FOR STUDYING THE IONOSPHERE

The ionosphere was first studied by means of radio methods by ground stations. These methods are still the most frequently used and have the advantage of supplying continuous information at many points of observation; these data are suitable for the immediate prediction of the propagation of radio waves. Unfortunately, a great many assumptions have to be made before the actual constitution of the ionosphere can be deduced. The

use of rockets permits direct, but discontinuous observation (several minutes per rocket). Moreover, the high cost of these observations restricts their use.

Satellites allow a much longer and much wider observation, but they can only remain permanently in orbit in extra-ionospheric orbits. Moreover, as in the case of terrestrial observation, a great many hypotheses are required for the interpretation of the observed results.

6.1.3.1 **Vertical soundings**

A series of brief pulses (30 of 100 μs duration) at a rate of 30–120 pulses per second are transmitted by a wideband aerial beamed in a vertical direction. A nearby receiver receives the initial pulse, its echo from the ionosphere and possibly other successive echoes originating from reflections by the ground and by the ionosphere.

These pulses modulate a cathode ray oscillograph. The echoes received are recorded—on a known time scale—on photographic film by means of a calibrated timebase or a rotating mirror.

One control simultaneously varies the transmitted frequency, the tuning of the receiver, and transports the film over a distance that corresponds to the frequency. One thus obtains a family of curves as shown in Fig. 40.

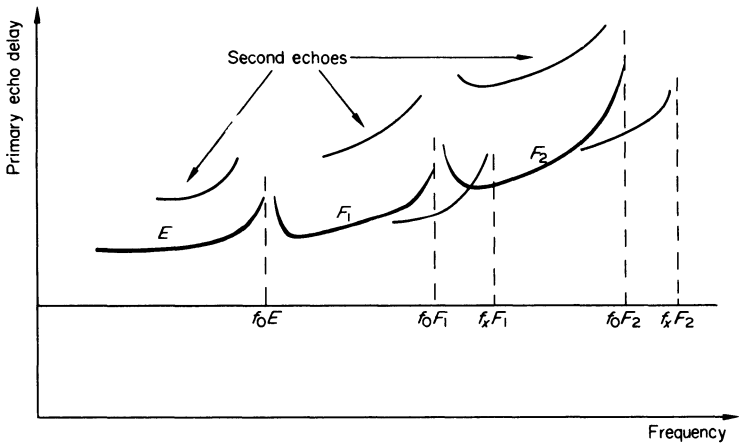

Fig. 40

This presentation suggests that the ionosphere consists of a number of successive layers with different critical frequencies (Section 5.3.2), while the discontinuities in the recording correspond to these critical frequencies.

The division of the curve on the side of high frequencies illustrates the existence of two different critical frequencies for ordinary and extra-ordinary rays (Section 5.4.2).

The fact that the curves corresponding to higher frequencies show a greater delay—or time of travel—indicates that layers having the highest critical frequencies are the farthest away from the ground.

We have seen in Section 5.3.5 that a pulse is propagated practically at the group velocity, which is given by equation (5.30):

$$V_G = \frac{c}{\frac{d(\omega n)}{d\omega}}$$

When the critical frequency is approached, the phase constant decreases very rapidly (Section 5.3.4.1) and therefore also the group velocity. This explains the sudden rise in the curves in the vicinity of this frequency, because the signal takes a long time travelling the ionosphere.

The virtual height is the height at which a signal would be reflected if it always travelled at the speed of light. This height is always greater than the actual height of reflection because the group velocity is always lower than the speed of light. We shall see below that it is sufficient to know the virtual height for resolving practical propagation problems.

Summing up we can state that the vertical sounding method is most frequently used and permits us to know at a given instant and a given location:

1. the number of existing layers
2. their virtual height
3. their critical frequencies.

By measuring the relation between the intensities of the first and second echoes, the reflection coefficient of the ionosphere can be calculated by taking absorption into account. This calculation is however rather difficult. Figure 41 shows a schematic example of some results obtained with vertical sounding.

6.1.3.2 **Oblique soundings**

For this purpose we use a receiver separated from the transmitter; their frequencies are varied simultaneously.

When the separation is small, we can simultaneously receive the ground wave and the wave reflected by the ionosphere. Since these two waves have travelled different distances, they will have some phase difference to each other. The phases are additive at certain frequencies, while at others they are subtractive. The difference in distances travelled and hence the height of the reflecting layer, can be deduced from the maxima and minima observed.

For a great separation between the two terminals of the system the local oscillators must be well synchronized and calibrated (usually by frequency

standards based on atomic resonance) in order to determine the duration of the travel and its variations with frequency, which are always very small. In this case, the method is obviously very difficult, and very few paths have been studied in this manner. However, the results obtained have been most interesting because they have allowed one to determine the different paths followed by the waves between transmitter and receiver (reflections from different ionized layers and from the ground). Some results were exactly as predicted by the classical theory of the constitution of the ionosphere, while others appear to obey propagation laws whose paths lie outside the plane of the great circle passing through the transmitter and the receiver[19].

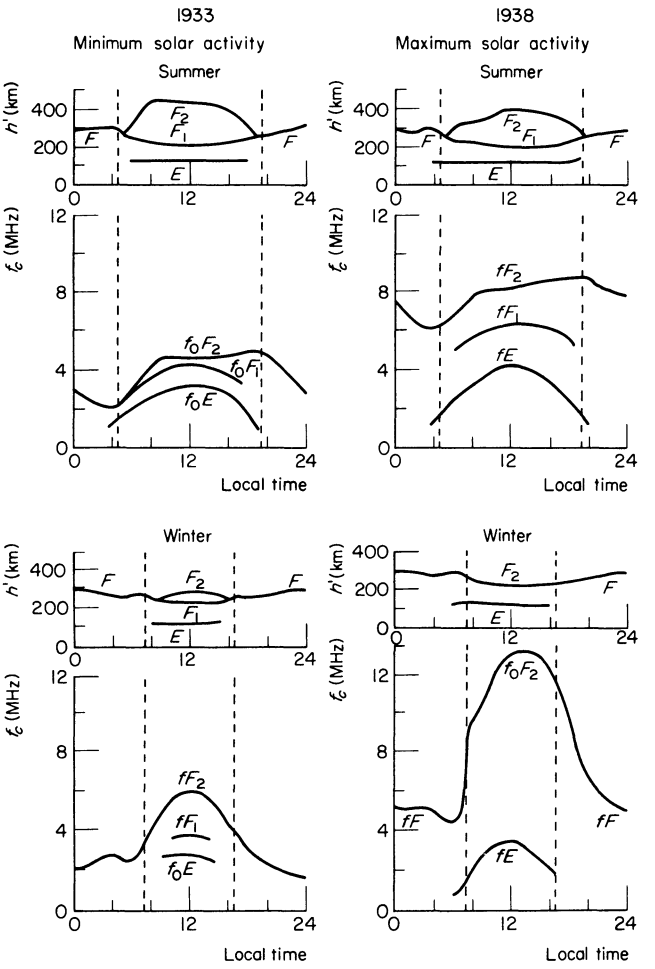

Fig. 41

6.1.3.3 Soundings by back scattering

In this case the pulses are transmitted at a fixed frequency by means of a rotating directional antenna. Waves reflected from the ionosphere strike the ground, which in view of its irregularities scatters these reflected waves in all directions including in the direction whence they came (see Fig. 42).

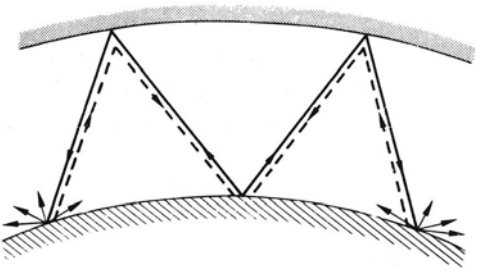

Fig. 42

The receiver is placed in the vicinity of the transmitter. From the duration of travel of the pulses and the virtual height, the areas on the earth which could be reached by waves of the frequency used can be deduced. Sounding devices having four frequencies based on this principle were installed at a great number of stations on the occasion of the International Geophysical Year[338].

The advantage of this method lies in the fact that the results can be immediately used for the establishment of short wave communications. COZI (Communication Zone Indicator) of the U.S. Army is based on this principle. Investigations are being carried out to realize this type of sounding with any transmitter, without interfering with its normal operation.

6.1.3.4 Extra-terrestrial study

Investigation by means of rockets[330, 333]

The NRL (National Radio Laboratory) method consists in effecting the transmission by a rocket of two signals—one at 7 754 kHz and the other at six times this frequency, i.e. 46 254 kHz.

The greatest critical frequencies encountered during solar activity maxima are less than 20 MHz, so that the relative dielectric constant of the ionized layers for waves of 46 254 kHz (given by equation (5.21)) differs little from unity. These waves are hardly affected by their transit through the ionosphere. This is however not the case for waves of 7 754 kHz, where both the dielectric constant and the refractive index are clearly different from unity.

The Doppler effect (Appendix A.9) only depends on the refractive index of the medium surrounding the source, and therefore has different values for these two wavelengths. This difference can be measured by receiving the

two frequencies at ground level, multiplying the lowest by 6, and observing the interference between the two waves of about 46 MHz. Assuming that the refractive index for original frequency 46 MHz equals unity, the conventional calculation of the Doppler effect gives:

$$f_B = \frac{6fv}{c}(1-n)$$

where f = 7754 kHz

v = radial velocity of rocket

c = speed of light

n = refractive index of medium surrounding the rocket at frequency 7754 kHz

f_B = frequency of the observed interference.

We can calculate n from this equation. The number of electrons per cubic metre can then be calculated quite easily from n and f.

This is an interesting method as it allows one to plot a complete profile of the ionization during the entire flight of the rocket. On the other hand, the radial velocity of the rocket must be known at every instant; it is sometimes difficult to know this velocity to the required degree of accuracy.

The AFCRC (Air Force Cambridge Research Centre) uses a rocket transmitting a pulse at 200 MHz, immediately followed by one at 10 MHz. The first pulse remains unaffected when travelling through the ionosphere, but the second pulse is delayed. The total electron density between the rocket and the point of observation can be calculated from this delay.

The DOVAP (DOppler Velocity And Position) method consists in transmitting a signal at 38 MHz from the ground to the rocket. The latter doubles the frequency and re-emits the signal. The ground station also transmits a signal at twice the frequency: 76 MHz. A number of ground stations observe the interference between the two frequencies, and the trajectory of the rocket can be plotted from these data. As long as the rocket has not reached the ionosphere, this trajectory is the true trajectory, and can be extended into the ionosphere by applying ballistic laws. In the ionosphere we observe an apparent trajectory, which is modified by refraction. The electron densities can be determined by comparing the two trajectories.

Finally, we can directly measure the ion density in the space through which the rocket travels by using an ion trap consisting of a spherical mesh cage carrying an electrode whose potential is negative with respect to the sphere[333]. The ions penetrating the sphere produce a current, and the rocket transmits the intensity of this current. However, despite all possible

precautions, there is no certainty that the results are not affected by the potential difference between the rocket and the ionosphere.

Investigation by satellite

Satellites only traverse the ionosphere just after having been launched and again during their final orbits before re-entry. It is therefore not possible to make direct measurements with them. The evaluation of the measurements that have been carried out is rather difficult[350].

We have seen in Section 5.4.2 that when a wave with linear polarization travels through the ionosphere without being noticeably absorbed, its polarization plane is subjected to Faraday rotation.

Let n_e and n_o be the refractive indexes for the ordinary wave and extraordinary wave respectively, we have for the Faraday rotation:

$$d\Omega = \frac{f(n_e - n_0)}{2c} dr$$

where c = speed of light

r = distance between satellite and observer.

Since n_e and n_o are both dependent on electron density, the latter may be deduced from the rotation measured. It has been shown[328] that rotation is usually proportional to the total electron density between observer and satellite.

It has been shown that the part of the ionosphere above the ionization maximum contained by day three times as many electrons than the lower part, and by night five times as many[19].

The 'rising' and 'setting' of a satellite borne transmitter depend on the ionospheric refraction for the transmitted frequency, in the same manner as the rising and setting of heavenly bodies depends on atmospheric refraction. The total electron density can be determined by the observation of the instants of appearance and disappearance of the signals.

Similar results have been obtained by comparing the radio sighting of a satellite with its optical sighting.

It is also possible to calculate electron density from the Doppler effect by means of rather complex calculations.

When a number of observation stations are available, the shape and dimensions of the irregularities of ionized layers in the horizontal direction can be easily calculated.

Finally, it has been possible to perform ionospheric soundings of the part of the ionosphere above the altitude of maximum ionization by means of satellite-borne sounding devices (e.g. on the Canadian Alouette satellite), complementing the curves supplied by ground-based sounding devices[362].

6.1.4 DESCRIPTION OF THE NORMAL IONOSPHERE

6.1.4.1 General considerations

A now universally accepted model of the ionosphere has been calculated as a result of the various methods discussed above and the numerous theoretical studies on the constitution of the actual ionosphere. Divergencies between experts only relate to a few points of detail and to the explanation of some phenomena, whose statistical laws are well known in other respects.

The accepted theory is that the ionosphere consists of three regions: *D*, *E* and *F*. Each region consists of one or more layers. An ionospheric layer is almost spherical and concentric with the earth, so that ionization increases with altitude up to a maximum value, then decreases or at least remains constant until the appearance of the upper layer.

On rising through the ionosphere, the maximum electron density in each layer increases. The number of molecules, and therefore the number of collisions, decreases at the same time.

All layers vary in altitude and density according to the solar cycles (daily, annual and of about 11 years), but these variations do not always have the same sense in the different layers.

It is interesting to illustrate the physical properties of the earth's atmosphere in the ionospheric region. Figure 43 shows the principal known characteristics[19, 337].

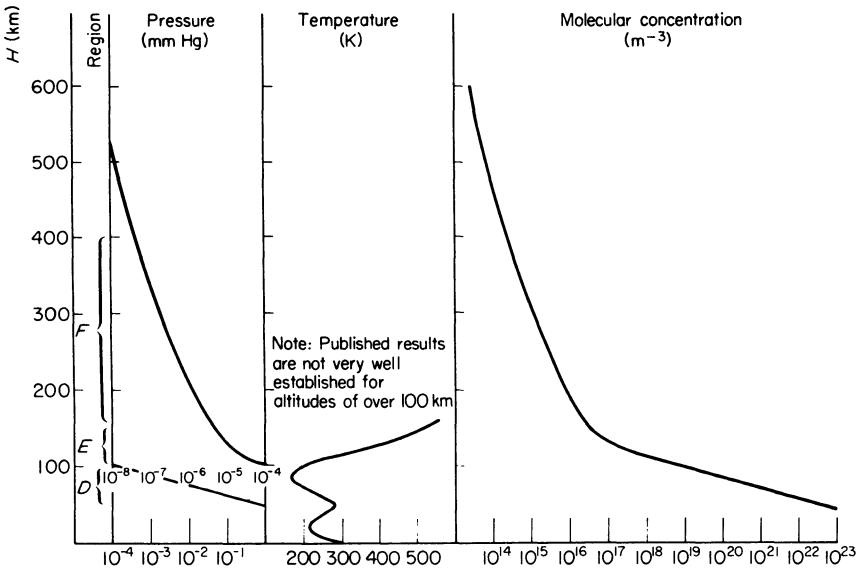

Fig. 43 Main characteristics of the upper atmosphere

We note the extremely rapid decrease of molecular density with altitude. The calculation of pressure and temperature at these very great altitudes presents considerable difficulties and the results are as yet inconclusive.

The composition of the higher layers of the atmosphere is not very different from its composition on the ground. The oxygen and nitrogen molecules O_2 and N_2 are progressively replaced by their respective atoms at increasing altitudes. There is also a small proportion of NO, due to the combination of oxygen and nitrogen as the result of electrical discharges. Despite its small proportion, this gas plays an important part in the ionization of the upper atmosphere because of its small ionization potential of 9·4 eV.

6.1.4.2 *D*-region

The *D*-region is usually defined as the whole of the ionized layers between 60 and 90 km altitude. This region is not recorded by current soundings because its critical frequency (100–700 kHz) is too low.

The *D*-region is investigated:

1. by means of a small number of special sounding devices[323]
2. by measuring the absorption of decametre waves that travel through it before and after being reflected by higher layers
3. by measuring the reflection altitude of v.l.f. waves, that are reflected by the *D*-region at a grazing angle of incidence
4. by studying the propagation of low frequency waves produced by electrical discharges.

The *D*-region is characterized by:

1. a high molecular concentration of the order of 10^{20} molecules/m^3
2. a small electron concentration (10^8–10^{10} electrons/m^3)
3. a very high collision frequency between electrons and molecules (5×10^5–5×10^6 per m^3/s). This region is therefore highly absorbent to radio waves (Section 5.3.6)
4. a high recombination coefficient (of the order of 10^{-12}–10^{-13} m^3/s). The time constant given by equation (6.15) is of the order of 1 min, i.e. the ionization of the *D*-region follows variations in solar illumination very rapidly.

The *D*-region occasionally contains two layers: D_1 and D_2.

Figure 44 shows the approximate values of certain parameters for the *D*- and *E*-regions:

1. electron density N_e according to Houston[323] when the sun is at its zenith
2. collision frequency ν per m^3/s[352]

3. recombination coefficient α in m^3/s in the *D*-region and the lower part of the *E*-region[323].

However, in view of the very considerable divergencies between figures given by different authors, Fig. 44 should only be considered as a guide.

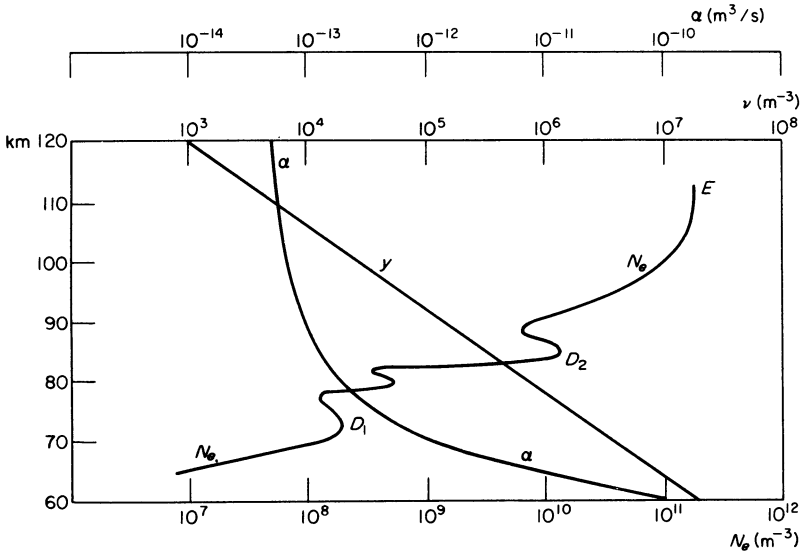

Fig. 44

6.1.4.3 The-*E* region

The *E*-region extends from 100–150 km altitude. It contains three main layers:

Sporadic *E*-layers (E_s)

At low and average altitudes we are dealing with ionospheric lamellae of a small thickness (2 km) which are discontinuous and suffer displacement at great velocities. These are situated at an altitude in the neighbourhood of 100 km and are capable of reflecting high frequencies. The exact nature of these lamellae has not been established. It is generally assumed that they are strongly ionized clouds in the lowest part of the *E*-region. The other explication that has been advanced is that the observed phenomena are caused by whirlwinds which provoke intense turbulence in the *E*-region and therefore strong diffraction of the waves striking this turbulence. However, this latter explanation does not appear very probable in view of the fact that rocket soundings have shown the existence of ionized clouds that correspond to E_s[333, 353].

The E_s-layer is usually continuous in the vicinity of the magnetic poles, and often shields the higher layers because of its heavy absorption.

The E_1-layer

This is the best example of a Chapman layer. The thickness of the layer varies between 20 and 40 km. Maximum ionization is found at an altitude of approximately 120 km. The maximum electron density exceeds 10^{11} per m^3 at noon. It can attain 2.10^{11} when the sun is at its zenith, which corresponds to a critical frequency of 4 MHz.

As a function of the zenith angle of the sun χ, the variation is similar to that of equation (6.11), but the exponent of the right hand side only equals $\frac{1}{2}$ at average latitudes. It varies between 0·44 at the poles and 0·6 at the equator.

The critical frequency at a given location at noon is linked with the solar activity by the following equation[327]

$$(f_0E)^2 = a_n(1+0{\cdot}004\,R)$$

where a_n = coefficient corresponding to the number n of the month

R = sunspot number.

One can also use the following approximate equation[19] which is valid for any time of day and any season:

$$f_0E = 0{\cdot}9[(180+1{\cdot}44\,R)\cos\chi]^{0.25}$$

A certain amount of ionization persists by night, due to imperfect ion recombination and to meteoric ionization[315], but the critical frequency is low: 0·25 MHz during the period of a solar minimum and 0·5 MHz during the period of a maximum, corresponding to an electron density of the order of $10^9/m^3$.

The number of collisions between electrons and molecules is rather large (5.10^3–2.10^4 per m^3/s) so that there is still a great deal of absorption.

The recombination coefficient is also high (of the order of $5.10^{-14}\,m^3/s$), corresponding to a time constant of about 2 min. The E_1-layer therefore rapidly follows variations in illumination.

The E_2-layer

The E-layer often splits into two, giving rise to an adjacent layer at 140 km, the E_2-layer, whose ionization is slightly greater.

6.1.4.4 The F-region

The F-region extends from 160–450 km. It consists of two layers with very different patterns of behaviour.

The F_1-layer

The F_1-layer is situated at an altitude of about 200 km and is a Chapman layer, the same as the E-layer. Its maximum density is given by[336]:

$$N = 2{\cdot}5 \times 10^{11}(1 + 0{\cdot}0062\,R)$$

where R = sunspot number.

It rather exactly obeys equation (6.11) as a function of the zenith angle χ. The following equation[19] has been proposed; it is valid for any time of day and for any season:

$${}_0F_1 = (4{\cdot}3 + 0{\cdot}01\,R)\cos^{0{\cdot}2}\chi$$

Absorption is small. The recombination coefficient α is approximately 10^{-13} m^3/s, and the time constant is of the order of 4 min.

The F_2-layer

The altitude of the F_2-layer is situated at about 300 km; its behaviour is completely different from that of the other layers. Martyn's theory (Section 6.1.2.5) suggests an explanation, in any case a qualitative one, of its principal characteristics[336].

The critical frequency varies in the same sense as the solar activity, but no satisfactory formula has been established to correlate these two variables. It increases with solar activity and is stronger by day than by night (with a lag on the zenith angle of the sun). The critical frequency is higher in the winter than in the summer, particularly in the northern hemisphere.

Figure 45 shows a few charts in geomagnetic coordinates. They give some idea of the behaviour of the F_2-layer during a maximum (1947) and during a minimum (1943–44) of solar activity.

It is interesting to note that:

1. The minimum critical frequency occurs around 06.00 h or slightly earlier
2. The highest critical frequencies are usually centred around 15.00 or 16.00 h, and not at noon
3. The geomagnetic equator corresponds to a minimum of the frequencies
4. The critical frequencies vary considerably from day to day
5. Electron density can attain values as high as 3.10^{12} per m^3.

Coefficient β of equation (6.16) acts as recombination coefficient. Its value is:

$$\beta = 10^{-4}\,e^{[300 - h/50]}$$

where h is expressed in km.

It is very difficult to deal with the behaviour of the F_2-layer theoretically in an adequate manner, or to represent it accurately in formulae. The

behaviour of this layer differs very much from that of the other layers[360]. In particular, it exhibits a *seasonal anomaly* (its critical frequency is higher in the winter than in the summer) and an *annual anomaly* (the critical frequency for the layer as a whole is higher in the summer of the northern hemisphere). Since these two anomalies are in phase in the northern hemisphere, the variations in the critical frequency there are particularly pronounced. In the southern hemisphere, they are in opposition, which gives rise to a biannual anomaly. All explanations for these phenomena are still at the hypothetical stage.

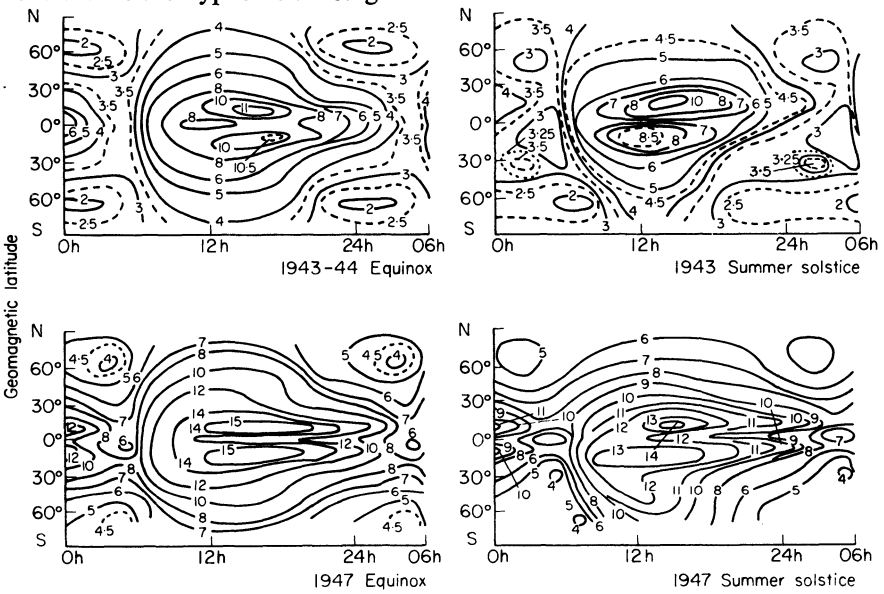

Fig. 45

For a given station and a given month, the critical frequency at noon obeys the relation:

$$(f_0F_2)^2 \propto 1+0{\cdot}02\,R.$$

Table 6.3 shows the altitude of maximum ionization:

TABLE 6.3

R	Great or average latitudes				Magnetic equator	
	Noon			Midnight	Noon	Midnight
	Equinox	Winter	Summer			
0	220	210	240	320	350	300
maximum	250	240	270	350	420	370

6.1.4.5 **Motions of ionosphere**

Very violent winds occur in the ionosphere. A large number of papers have been published on the subject of winds in the lower part of the ionosphere; they usually follow the displacement of the E_s-layer or meteoric trails. The mean velocity has been found to be approximately 30 m/s (110 km/h), practically horizontal. By day, the wind direction changes from west to east in the northern hemisphere, and from east to west in the southern hemisphere. At the same time, the wind velocity varies periodically from 7–40 m/s[335].

There also appear to exist in the ionosphere solar and lunar tidal motions, which cause variations in the critical frequencies.

Finally, very strong turbulence takes place in the ionosphere, in any case in the lower part of the *E*-layer. This appears to be due to the mixing of large masses of air having different characteristics. This turbulence is made apparent by the scattering of radio waves.

6.2 IONOSPHERIC PROPAGATION

The ionosphere affects the propagation of all waves, in any case up to a frequency of approximately 50 MHz. Frequencies lower than approximately 30 MHz are propagated by reflection, while frequencies between 30 and 50 MHz are propagated by scattering.

6.2.1 PROPAGATION BY REFLECTION

6.2.1.1 **Long waves (frequency less than 500 kHz)**

The wavelength being very great, the wave meets a rather large electronic density, before the ray has travelled one wavelength above the lower limit of the layer. The ionospheric layer therefore behaves like a sudden discontinuity and the laws of optical reflection apply with reflection coefficients that can attain a value of 0·9 for the longest waves.

True ionospheric reflection therefore takes place, followed by reflections from the ground, whose reflection coefficient for long waves is also high (Section 4.1.1.2). Ground reflection produces divergence in the wave beams (Section 4.3). On the other hand, reflection from the concave surface of the ionosphere produces convergence (or focusing), that increases the energy density.

We thus simultaneously find at the receiving station rays that have been subjected to 1, 2, 3. . . n reflections from the ionosphere. Since the phases of these rays are not mutually related, the energies received must be added, i.e. the field received is:

$$E = \left(\sum_{j=1}^{n} |E_j|^2 \right)^{\frac{1}{2}}$$

For example, Fig. 46 shows the results for a wave of 300 kHz which is reflected by the *E*-layer at night. The figures indicate the number of reflections from the ionosphere.

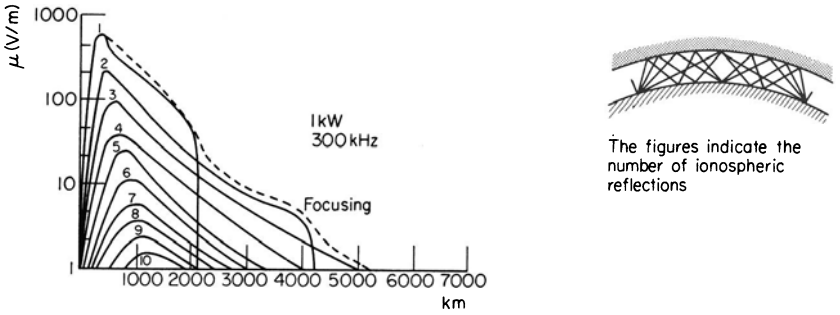

Fig. 46

If we only consider the overall result (dotted curve), this is a rather slow exponential decrease of the field. A still more regularly exponential decrease would be found for longer waves (e.g. 30 kHz), which would also be slower (2 dB for 1 000 km instead of 5 dB in the example of Fig. 46). The first investigators of wave propagation were misled by this exponential appearance, and attempted to explain it by diffraction, which gives a law of the same form (Section 4.4.3.2). There is excellent agreement between present day theory and results[321, 322]. The theory predicts the existence of an absorption band in the vicinity of 3 kHz; this has been confirmed by experiment.

6.2.1.2 **Medium waves (0 5–1·5 MHz)**

The proximity of the gyrofrequency strongly complicates the phenomena. As we have seen in Section 5.4.2, the extraordinary ray is almost entirely absorbed. Even the ordinary ray is subjected to such an amount of absorption in daytime that it is usually very weak, but at night its reflection occurs in a way similar to that which occurs for short waves.

6.2.1.3 **Short waves (frequencies exceeding 1·5 MHz)**

Contrary to what occurs for long waves, short waves usually penetrate into ionized layers by several wavelengths, because on the one hand their wavelength is shorter, and on the other hand they can only be subject to pseudo-reflection from media with a high critical frequency, and which are therefore situated close to the centre of the ionized layer. This is no longer true reflection, but progressive refraction. However, it can be shown that this phenomenon is the equivalent of normal reflection; hence the use of expressions like 'reflected wave' and 'ionospheric reflection', which—though incorrect—are in general use.

Moreover, the waves travel through ionized layers or parts of ionized layers before, during and after their reflection, thus undergoing absorption of energy.

To consider all ionospheric layers would be too involved for the practical study of propagation. We therefore usually restrict ourselves to a simplified model of the ionosphere:

1. the D-region is replaced by an absorption coefficient
2. an E-layer, whose virtual height is fixed at 105 or 110 km, represents the effects of the E, E_2 and F_1-layers, which have a similar diurnal evolution
3. the virtual height of the F_2-layer is often fixed at 320 km
4. the sporadic E_s-layers are sometimes taken into account by considering them as having the same height as the E-layer, and a given critical frequency and probability of occurrence.

The following simplications may also be introduced:

1. the effect of the curvature of the rays in the earth's atmosphere is neglected (Section 2.1.2) because this effect is negligible compared to the inexactitude of the data concerning the ionosphere
2. to a first approximation, the effect of the earth's curvature and that of the ionosphere are neglected, as well as that of the earth's magnetic field. These two phenomena can be taken into account by using corrective terms.

Ionospheric reflection

Flat earth condition

1. *General behaviour of the phenomena.* Ionization increases from the lower part to the upper part of the ionized layer. According to equation (5.20) we can write:

$$f_C = 9N^{\frac{1}{2}} \tag{6.18}$$

On rising, the critical frequency increases therefore with N.

The index is given by equation (5.25):

$$n = \left(1 - \frac{\omega_C^2}{\omega^2}\right)^{\frac{1}{2}} \tag{6.19}$$

if absorption can be neglected.

The index therefore decreases on rising; it can be proved (as in Section 2.1.2) that the rays curve back towards the ground. However, the variations in the index are much greater this time, and the return of the ray to the ground, which was the exception in tropospheric propagation, is here the general case.

2. *Snell's law* (see Fig. 47). Since the index decreases continuously with height, Snell's law, applied at a point where the angle of the ray with the vertical is i and the index is n, gives:

$$\frac{\sin(i+\mathrm{d}i)}{\sin i} = \frac{n-\mathrm{d}n}{n}$$

or

$$1+\cot i\,\mathrm{d}i = 1-\frac{\mathrm{d}n}{n}$$

which gives after integration:

$$\log n = -\log\sin i+\log K$$

or

$$n = \frac{K}{\sin i}$$

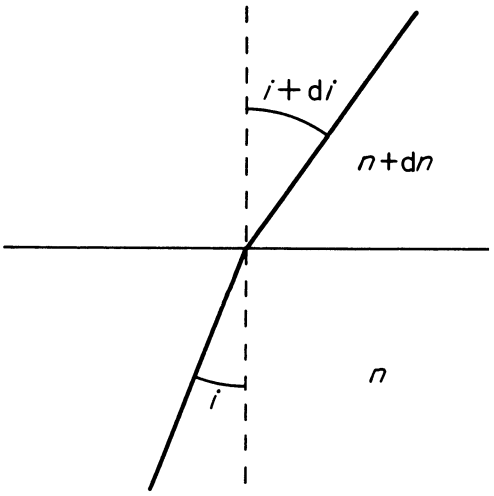

Fig. 47

Upon entering the layer, n very nearly equals unity, and i has a fixed value i_0. Therefore:

$$K = \sin i_0$$

so that Snell's law can be written for a medium whose index varies continuously:

$$n\sin i = \sin i_0 = \text{constant} \qquad (6.20)$$

3. *Secant law* (*Martyn's law*). If the rays become horizontal at a point (see Fig. 48) we have at this point:

$$\sin i = 1$$

and hence, according to equations (6.19) and (6.20):

$$n = \left(1 - \frac{\omega_C^2}{\omega^2}\right)^{\frac{1}{2}} = \sin i_0$$

$$\frac{\omega_C^2}{\omega^2} = 1 - \sin^2 i_0 = \cos^2 i_0$$

and

$$\omega = \frac{\omega_C}{\cos i_0} = \omega_C \sec i_0 \tag{6.21}$$

At a point where the critical frequency is ω_C, an ionized layer can reflect waves of a frequency higher than ω_C, and the higher according as the angle of incidence upon entering the layer is smaller.

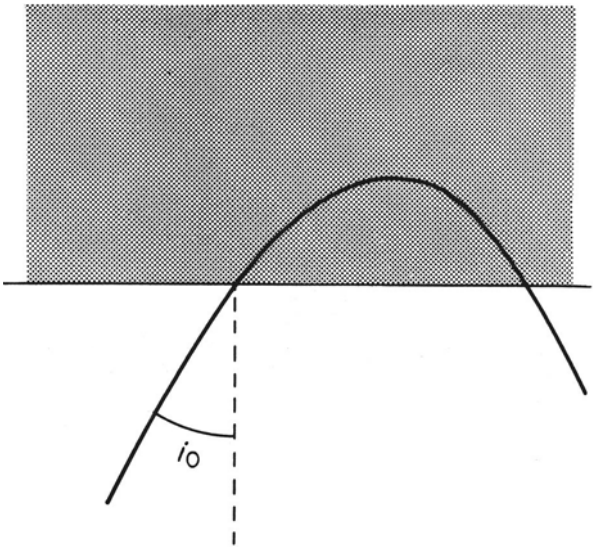

Fig. 48

4. *Equivalent relationship between virtual and real heights.*

Theorem of Breit and Tuve. Let *ABFDE* in Fig. 49 be the real path of a ray and a virtual path be *ABCDE* in which the ray travels in a straight line through the ionosphere and is subjected to optical reflection at *C*. We shall prove that we can also assume that the virtual path is travelled at the speed of light.

We want to establish the duration of travel by both the real and the virtual paths on the two elements ds and $d\sigma$ which correspond to the same horizontal distance dx.

We have on the virtual ray:

$$dt = \frac{d\sigma}{c} = \frac{dx}{c \sin i_0}$$

and on the real ray:

$$dt' = \frac{ds}{V_G} = \frac{ds}{cn} = \frac{dx}{cn \sin i}$$

Equation (6.20) states:

$$n \sin i = \sin i_0$$

and this gives:

$$dt = dt'$$

Therefore, the velocity of travel of a signal on the virtual path can be taken to be the speed of light without introducing any error.

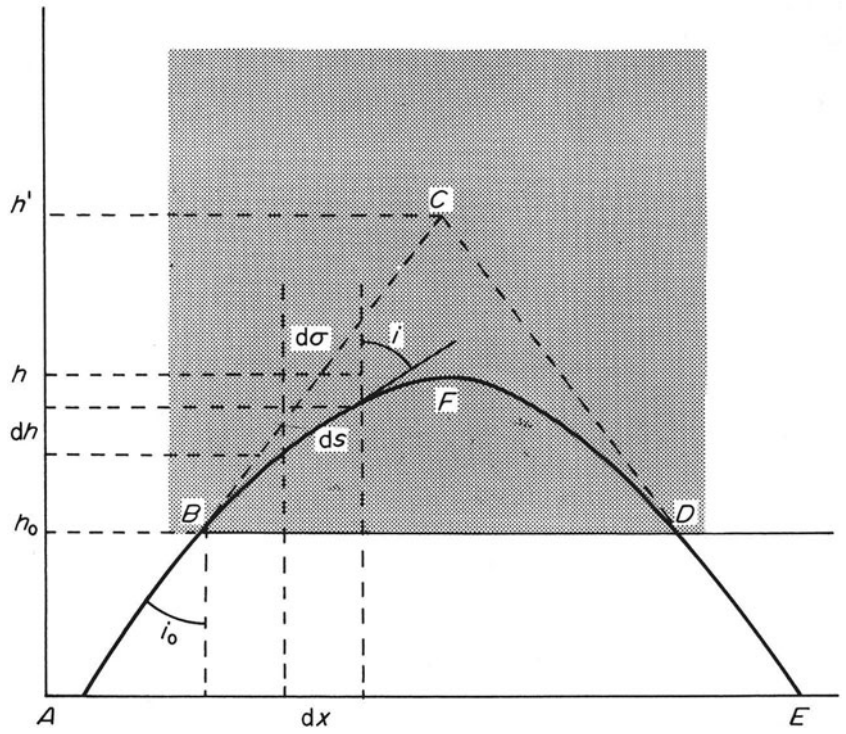

Fig. 49

5. *Equivalence relationships of heights*

The duration of virtual travel *BC* considered above is:

$$\tau' = \frac{h' - h_0}{c \cos i_0} \tag{6.22}$$

where h' = virtual reflection height.

On the other hand, the duration of real travel BF is:

$$\tau = \int_0^s \frac{ds}{nc} = \frac{1}{c}\int_0^s \frac{ds}{n} = \frac{1}{c}\int_0^h \frac{dh}{n\cos i} \tag{6.23}$$

According to equations (6.19) and (6.20):

$$n\cos i = (n^2 - \sin^2 i_0)^{\frac{1}{2}} = \left(\cos^2 i_0 - \frac{\omega_C^2}{\omega^2}\right)^{\frac{1}{2}} \tag{6.24}$$

$$= \frac{1}{\omega}(\omega^2\cos^2 i_0 - \omega_C^2)^{\frac{1}{2}}$$

If, on the other hand, Ω_C be the critical frequency at the summit of the path, we can write equation (6.21) as:

$$\omega = \frac{\Omega_C}{\cos i_0}$$

Introducing this value in equation (6.24) we obtain:

$$n\cos i = \frac{\cos i_0}{\Omega_C}(\Omega_C^2 - \omega_C^2)^{\frac{1}{2}}$$

and equation (6.23) becomes:

$$\tau = \frac{\Omega_C}{c\cos i_0}\int_{h_0}^{h} \frac{dh}{(\Omega_C^2 - \omega_C^2)^{\frac{1}{2}}} = \frac{\Omega_C}{c\cos i_0}\varphi(h) \tag{6.25}$$

$\varphi(h)$ equals the integral which depends on h for its upper limit and on ω_C. We have seen that $\tau' = \tau$ and can therefore write:

$$h' = h_0 + \Omega_C\varphi(h) \tag{6.26}$$

Therefore, the virtual reflection height is the same for all waves that correspond to the same real refraction height.

The above equivalence relationships are valid for any vertical distribution of ionization. They allow the replacement of the real ray by a virtual ray that travels in a medium with index 1 and is optically reflected from a plane situated at the virtual height.

The existence of these relationships justifies the term 'reflection from the ionosphere' and makes it much easier to solve the problems of ionospheric propagation.

Spherical condition

A detailed study of the corrections necessary to take the earth's curvature into account would exceed the scope of this book. They are in fact incorporated in the practical propagation nomograms and never need be calculated by the user.

The earth's curvature increases the apparent critical frequency for oblique incidence. Instead of equation (6.21) we now have:

$$\omega = \omega_C K \sec i_0 \tag{6.27}$$

$K \sec i_0$ is called the corrected secant.

Coefficient K is greater than unity and depends in a rather complex manner on the distance and vertical distribution of the ionization. It can be calculated by graphical methods.

Effect of the earth's magnetic field

When taking the earth's magnetic field into account, equation (6.19):

$$n = \left(1 - \frac{\omega_C^2}{\omega^2}\right)^{\frac{1}{2}}$$

is replaced in the case of longitudinal travel by the following equation, which is obtained by putting $\nu = 0$ in equation (5.38):

$$n = \left[1 - \frac{\omega_C^2}{\omega(\omega \pm \omega_H)}\right]^{\frac{1}{2}} \tag{6.28}$$

In the frequency band that interests us, $\omega > \omega_H$, so that the correction is rather small; it becomes negligible for the higher bands of frequencies, except those in the proximity of the critical frequency.

We have for a vertically travelling wave at the point of reflection and in the absence of a magnetic field:

$$\omega_C = \omega$$

If a magnetic field is present, we have:

1. for the ordinary ray:

$$\omega_C^2 = \omega(\omega + \omega_H) > \omega^2$$

2. for the extraordinary ray:

$$\omega_C^2 = \omega(\omega - \omega_H) < \omega^2$$

The ordinary ray will therefore be reflected at an altitude where ω_C is greater, i.e. at a greater altitude than the one reflecting the extraordinary ray (which is in fact observed on sounding).

The same applies to oblique incidence, so that the ordinary ray is closer to the vertical than the extraordinary ray. We shall see that this results in less absorption of the ordinary ray.

Geometry of the path

Since it is possible by means of equivalence relationships to replace the real path by a virtual path with optical reflection from a surface situated at the virtual height, the geometry of the wave path becomes very simple indeed.

All that is necessary is to consider a series of concentric reflecting layers, which can be reduced by means of the practical model of the ionosphere discussed in Section 6.2.1.3 to:

1. the earth's surface
2. the E-layer
3. the F_2-layer.

According to their frequency, their angle of elevation and the critical frequencies of the layers, the waves can travel along different paths, or by different ionospheric modes. Figure 50 shows a few of these modes.

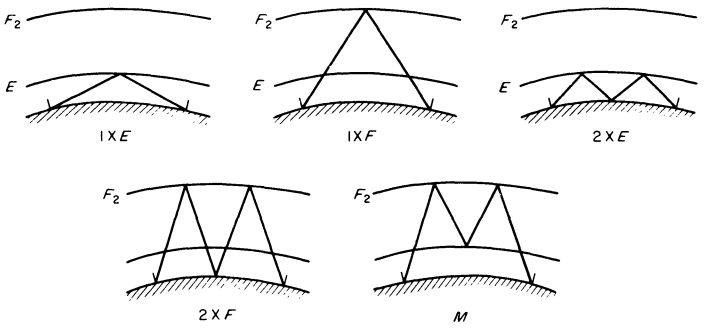

Fig. 50

We shall now examine the possibility for existence of these different modes. Assuming that they are possible, the most important parameter for each of them is the angle of departure Δ. Figure 51 shows this value for the most frequently encountered cases.

Figure 51 also allows one to determine the point where a ray reflected from the F_2-layer meets the E-layer. This is done by determining the elevation angle for the given range and for the F_2-layer; one then reads off for this angle Δ the range that corresponds to the E-layer. The ray meets the E-layer at half the distance read off (Fig. 52) at either the beginning or the end of the path. We shall later make use of this fact. The modes shown in Figs 50 and 51, as well as all those that can be derived from them by multiplying the reflections from the ground and from the permanent layers of the ionosphere, are the 'normal' modes. Many others will be found when analysing oblique soundings (Section 6.1.3.2). These abnormal modes usually give rise to intense propagation of little permanency. They originate from reflections by the sporadic E_s-layers, ionized nuclei, the ground—outside the plane of the great circle that joins the source to the receiver, etc.[19]. For distances below 2000 km, the modes can be identified and the experimental results agree with theory[363].

Maximum usable frequency

Transmission by ionospheric reflection is characterized by the existence of an operational maximum usable frequency, abbreviated to MUF; transmission above this value is impossible. In view of the great number of possible transmission modes, especially over great ranges, the predetermination of the MUF is a very complex affair. Highly ingenious methods have been developed for its determination, but their detailed discussion would exceed the scope of this book. We shall therefore only give a few general indications.

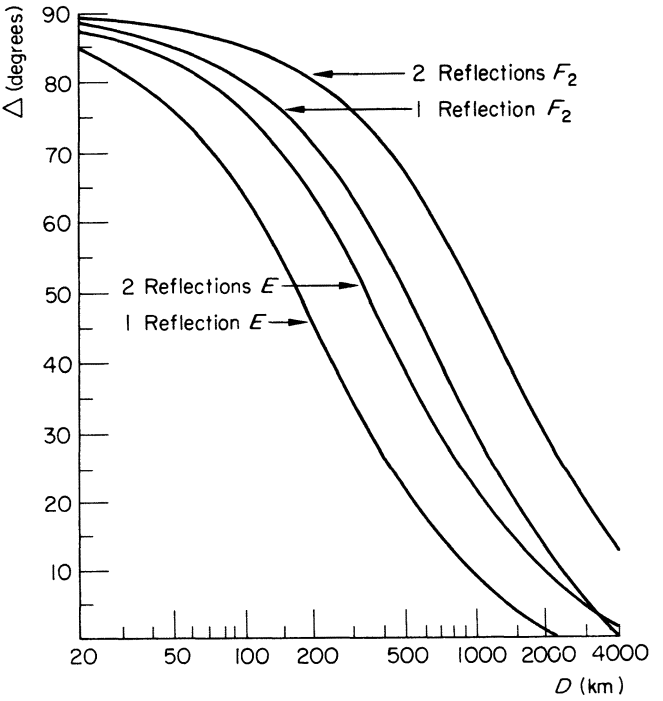

Fig. 51

We shall only discuss the standard MUF (also called Estimated Junction Frequency, EJF), i.e. the highest frequency that can be used for 50 per cent of the time between two given points at a given time of day. The operational MUF, which takes into account all possible modes of propagation, even the sporadic ones, is usually higher[19].

Single ionized layer; short transmission range. In the case of vertical incidences, the existence of a maximum frequency is obvious from the ionospheric soundings themselves. The mechanism can be easily explained. The wave rises into the ionized layer and encounters regions of decreasing index, until it arrives at an altitude where its frequency is the same as the

critical frequency of the medium: $\omega = \omega_c$. At this point, both the index and the group velocity are null, and since no further propagation is possible, the wave is reflected towards the ground. Since the ionization of a layer has a maximum at some given height, the critical frequency at this height

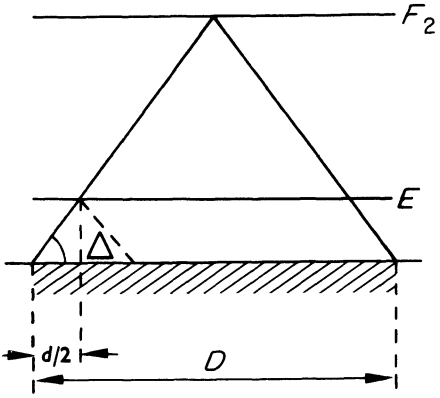

Fig. 52

is then also the maximum usable frequency. Ordinary and extraordinary waves have different refractive indexes (equation (5.38)). We thus have two values of the MUF, one for the ordinary, and one for the extraordinary ray. The case of vertical incidence is of no practical interest because it corresponds to a zero transmission range.

In the case of oblique incidence, the secant law must be applied (equation (6.21)):

$$\omega = \omega_c \sec i_0$$

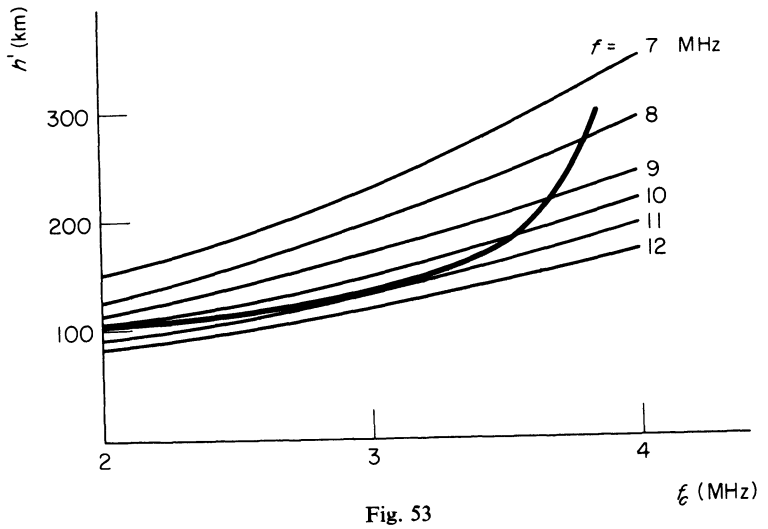

Fig. 53

In virtue of the equivalence relationships we have for the plane condition:

$$\tan i_0 = \frac{D}{2h'} \tag{6.29}$$

where h' = virtual height corresponding to frequency ω_C.

On the other hand, the sounding curve yields:

$$h' = \varphi(\omega_C)$$

We can find h' and ω_C as functions of ω by eliminating i_0 from these three equations.

Starting from the first two equations we are now able to plot a family of curves that give h' as a function of ω_C for each value of ω. Superimposing an echo sounding on the family of curves thus established, we may obtain, e.g. for the E-layer and a range of 1000 km, a figure similar to the one shown in Fig. 53. We observe that frequencies lower than 11 MHz are reflected at two different virtual heights (110 and 180 km for 10 MHz), giving rise to two rays: the low angle ray and the high angle (or Pedersen) ray. The 11 MHz frequency is only reflected at a single altitude (140 km) and represents the MUF because still higher frequencies can no longer be reflected since the corresponding curve no longer intersects curve $h' = \varphi(f_C)$ given by the sounding. It is also named junction frequency, as for this frequency both high and low rays join together. The path of the rays corresponding to 10 and 11 MHz waves is shown in Fig. 54.

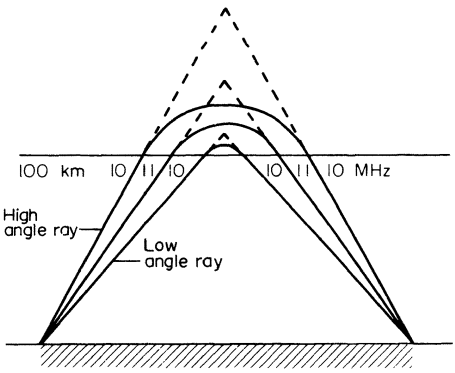

Fig. 54

In the case of waves with frequencies lower than the MUF, the high angle ray travels a much longer path in the ionosphere than the low angle ray. It is therefore very strongly attenuated, the more so when the frequency is lower. It is usually not necessary to take this ray into account. Similarly, as the sounding curves for the ordinary and extraordinary rays are different (see Fig. 40) the values of the MUF might be calculated for these

two rays. However, as the attenuation of the extraordinary ray is higher, the MUF is, as a rule, calculated only for the ordinary ray.

The earth's curvature can easily be taken into account by using equation (6.27) and by substituting a slightly more complex equation for equation (6.29).

The MUF increases with distance for the same ionization value, as will be seen when plotting the families of curves corresponding to several distances for the same sounding. This increase is due to the fact that angle i_0 increases with distance for the same virtual reflection height.

Two ionized layers; short transmission range. The $1 \times E$-layer path (see Fig. 50) is only possible when the frequency is lower than the MUF of the E-layer (E-MUF) for the range under consideration. In the same way, the path by the $1 \times F_2$-layer is only possible when the frequency is lower than the F_2-MUF.

However, this second condition is not sufficient in itself, because it is also essential that the waves reach the F_2-layer without being first reflected by the E-layer (see Fig. 55).

In order to know whether this condition is met, we determine the elevation angle corresponding to a given distance (D) by means of Fig. 51. Distance d corresponding to the same angle for the E-layer can then be determined for the same elevation angle on the same nomogram. The E-MUF for this last range is the lower limit of the frequencies that can traverse the E-layer and be reflected from the F_2-layer. This frequency is called the E-layer cut-off frequency.

In the case that the F_2-MUF of the range considered is higher than the E-MUF (as usually the case) the paths shown in Table 6.4 will be possible.

TABLE 6.4

Wave frequency	Possible paths
Lower than the E-layer cut-off frequency	$1 \times E$
Between the E-layer cut-off frequency and E-MUF	$1 \times E$ and $1 \times F_2$
Higher than E-MUF	$1 \times F_2$
Higher than F_2-MUF	none

If, on the contrary, the E-MUF were the higher, we would have the paths shown in Table 6.5.

TABLE 6.5

Wave frequency	Possible paths
Lower than the E-layer cut-off frequency	$1 \times E$
Between the E-layer cut-off frequency and F_2-MUF	$1 \times E$ and $1 \times F_2$
Between F_2-MUF and E-MUF	$1 \times E$
Higher than E-MUF	none

The MUF for a given path is therefore the highest of the MUFs for the layers under consideration.

Great transmission range. Here, a great number of modes is possible and the problem becomes extremely complex. It is not practicable to ask the user to examine every possible case in order to determine the MUF for a given path. We must therefore adopt an approximating method.

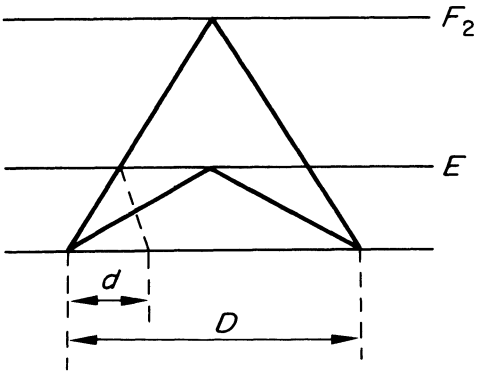

Fig. 55

The American CRPL method makes use of a semi-empirical process that consists in determining separate MUF values for the *E*- and *F*-layers at a 'control point' in the centre of the path, or, for long paths, at two 'control points' situated 1 000 km (*E*-layer) or 2 000 km (*F*-layer) from the terminal points of the paths. For each layer, the MUF is taken as equal to its lowest value at any control point, and the highest of the two MUF values (*E* and *F*) is then taken as the MUF of the path. The same method is used by the Radio Research Station at Slough in Buckinghamshire (U.K.).

Variation of the MUF. Apart from its variations with distance (mentioned above) the MUF varies with time and with the position of the observation stations. With time, the MUF follows—just as does the ionization of the layers from which it is derived—the daily and annual cycles as well as the 11 year solar activity cycle.

Its maximum is usually attained between local noon and 16.00 h; its minimum between 03.00 and 05.00 h. The MUF varies with the season and is highest during maxima of solar activity.

The MUF usually increases from the poles to the equator. When it is given by the F_2-layer, it also varies with longitude, i.e. that for the same local time and same latitude, the MUF does not have the same value at all parts on the globe. Because of this effect, we must use ionization charts for studying the F_2-MUF, which represent the state of ionization of the ionosphere for the entire globe at a certain hour in Universal Time (UT).

The charts are published either monthly (ESSA) or for all time (RRS, CCIR). In the latter case, the activity of the sun is taken into account by a numerical coefficient.

Skip distance

We have seen above that the MUF increases with distance. If the frequency used is higher than the MUF for vertical incidence, i.e. for zero distance (zero MUF), the transmitted wave can only be reflected after having travelled a sufficient distance to ensure that the corresponding MUF is at least equal to its own frequency. This distance is called the skip distance.

There will be a zone of silence around the transmitter, whose radius is equal to the skip distance (Fig. 56). We should mention that this zone of silence does not exist when the wave frequency is lower than the zero MUF.

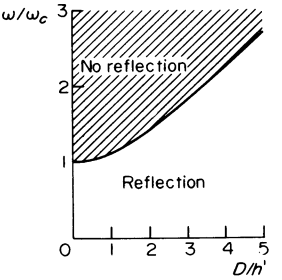

Fig. 56

Satellites; diaphragm effect and deviation

Waves emitted by a satellite situated above the ionosphere can only reach the earth if the angle between the radio ray and the normal to the ionosphere is smaller than the angle of total reflection, defined by:

$$\sin \varphi = n_{\max} \simeq \left(1 - \frac{\omega_{C\,\max}^2}{\omega^2}\right)^{\frac{1}{2}}$$

The ionosphere therefore acts as a diaphragm. On the other hand, in view of birefringence by the ionosphere due to the magnetic field, we have two radio images of the satellite, and for each of them the direction of arrival of the waves will be different from the geometric direction of the satellite.

Ionospheric absorption

As we have seen in Section 5.3.6, ionized media absorb waves—the more so when the collision frequency ν is greater. We also mentioned that the study of ionospheric absorption is very complex when starting from the conventional equations. We must therefore attempt to find simpler methods.

Absorption can occur:

1. when waves traverse one of the lower layers (D, E or F_1) and are reflected at a higher layer. In this case the path of the waves is little affected by traversing the layer, and—in accordance with Snell's law—re-emerge parallel to the incident direction. This is called non-deviative absorption. Absorption is weaker for the high angle ray, whose path through the layer is shorter
2. during pseudo-reflection by a layer. In this case absorption is stronger for the high angle ray (whose path through the layer is then much longer) than for the low angle ray. This is called deviative absorption.

Dependence on the zenith angle of the sun

Since absorption is proportional to the collision frequency in layers through which the waves pass, it therefore depends to a first approximation on their electron density and hence on the zenith angle of the sun. Starting from experimental data, CRPL has adopted the formula:

$$K = 0{\cdot}142 + 0{\cdot}858 \cos \chi$$

which defines a coefficient equal to unity when the sun is at its zenith. Muggleton[359] has proposed another formula, which gives practically the same results:

$$A = A_0(\cos \chi)^n.$$

In periods of solar calm, $n = 0{\cdot}80$ in the summer and $0{\cdot}86$ in the winter.

Absorption for vertical incidence

If ionospheric reflection took place without absorption, the field received, as we have seen in Section 1.2, would be:

$$E_0 = K \frac{P^{\frac{1}{2}}}{2h'}$$

where K = coefficient depending on the antenna used

h' = virtual height of reflection

However, when vertical ionospheric soundings are carried out, a smaller field E_1 is observed. We can therefore define an absorption index:

$$\alpha = \log \frac{E_0}{E_1} \tag{6.30}$$

We see that this index varies in a similar manner as the one shown in Fig. 57 (the dotted curves refer to the extraordinary ray; they can be observed only for certain parts).

The frequencies for which absorption is very pronounced are the gyro-frequency and the critical frequencies of the layers.

Neglecting these frequencies, obviously of little interest, and limiting ourselves to frequencies higher than 2 MHz, we have in very good approximation:

$$\alpha = \frac{\alpha_1}{(f \pm f_H \cos\theta)^2} \tag{6.31}$$

where α_1 = a constant

f_H = gyrofrequency

θ = angle of the earth's magnetic field to the direction of propagation.

Sign + corresponds to the ordinary ray; sign − to the extraordinary ray.

We can therefore state that when the frequencies are higher than the gyrofrequency, absorption—all other factors being equal—increases approximately as the inverse of the square of the frequency.

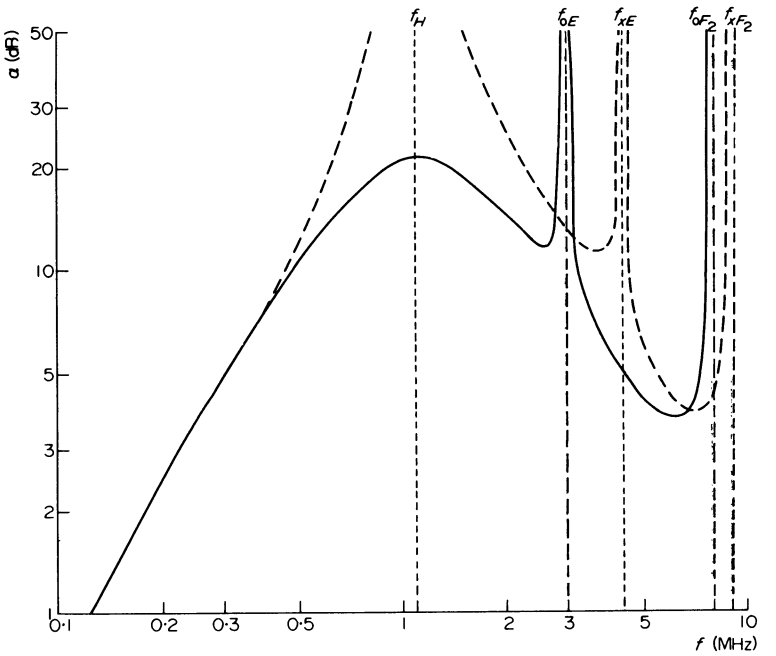

Fig. 57

Short transmission ranges

With frequencies far from the MUF, only the low angle ray is of importance; its penetration into the reflecting ionized layer is very small, so that the only important absorption is the non-deviative one due to the lower layers. The absorption coefficient is proportional to the length of the path

in the absorbing layer or layers. Their refractive index is very close to unity, so that we have in good approximation (see Fig. 58):

$$\alpha' = \frac{\alpha}{\cos i_0} \tag{6.32}$$

However, when approaching the critical frequency, particularly in the E-layer which has a rather great number of molecular collisions, absorption increases and more complex equations have to be used. In any case, as propagation by the E-layer occurs at a greater angle of incidence, absorption will be greater than in the case of propagation by the F_2-layer. For the same reason, the extraordinary ray which originates as a smaller angle will be more attenuated than the ordinary ray. More elaborate methods of computation, making use of a digital computer, allow the absorption to be calculated with good accuracy[366].

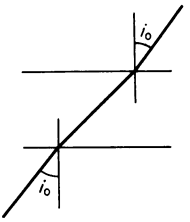

Fig. 58

Great transmission ranges

Above 3 000 km there is hardly any propagation by the E-layer because the absorption for the corresponding modes is too strong.

We have for F_2 propagation for great transmission ranges in the case of a plane condition (Fig. 59):

$$\cos i_0 = \sin \Delta \simeq \frac{h'}{D}$$

so that:

$$\alpha' = \frac{\alpha}{\cos i_0} = \frac{\alpha D}{h'} \tag{6.33}$$

The absorption coefficient is therefore proportional to the distance.

This formula remains approximately accurate for paths containing several reflections ($D > 4\,000$ km), provided we make α the mean value of all absorption coefficients over the entire path.

Multiple paths and telegraphy speed

We can deduce from what we have said above that there are usually a number of different modes operating simultaneously in a communication by the ionosphere. Each of these modes corresponds to a different travelling

time. The most unfavourable case, that only occurs at the greatest ranges, is when the signal arrives via both arcs of the great circle joining the transmitter and the receiver.

The existence of multiple signals, or echoes, limits the telegraphy speed of transmitted signals to a value:

$$V \leqslant \frac{1}{\Delta t} \text{ bauds}$$

where Δt = difference between the travelling times.

The increasing importance of high speed data transmission has led to research into the requirements of short wave circuits in order to be able to transmit these signals[19,365].

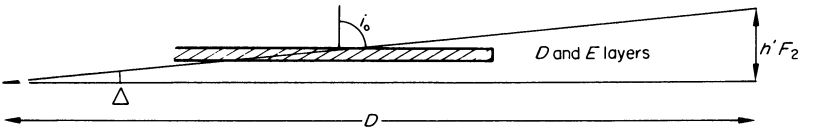

Fig. 59

It has been observed that for distances between 1 000 and 4 000 km, and using a frequency higher than or equal to the FOT, the difference between the travelling times is normally less than 5.10^{-4} s, which permits a telegraphy speed of 2 000 bauds.

At the same frequency the useful telegraphy speed decreases rapidly with decreasing transmission range and slowly with increasing range.

Using any frequency, the most favourable transmission ranges are between 2 000 and 8 000 km. Telegraphy at 300 bauds will always be possible at these ranges. At 200 km the maximum practical speed falls to 125 bauds.

6.2.2 PROPAGATION BY SCATTERING

The lower part of the ionosphere is capable of scattering radio waves by means of a mechanism similar to that described in Section 2.3. At frequencies below 25 or 30 MHz, scattering is completely masked by reflection, which produces much stronger signals. In contrast, at frequencies between 30 and 50 MHz, reflection occurs only sporadically, while permanent scattering can be easily observed.

6.2.2.1 **Origin of ionospheric scattering**

It appears certain that ionospheric scattering is caused by two facts: meteoric ionization and turbulence in the lower part of the ionosphere.

Meteoric ionization

We discussed this subject in Section 6.1.2.6 and saw that meteoric ionization is strongest around 06.00 h. The same applies to ionospheric scattering[316, 319].

Ionospheric turbulence

The lower part of the ionosphere is a region of rapid motion (Section 6.1.4.5) which is probably due to the mixing of gases having different degrees of ionization and which thus creates strong turbulence.

The effects of this turbulence can be calculated in the same way as tropospheric turbulence[119]. The refractive index of the ionosphere depends on the degree of ionization in the same manner as the refractive index of the troposphere depends on pressure and humidity. All other factors being equal, fluctuations in the index will therefore be stronger when the atmosphere is more strongly ionized, i.e. about noon.

Combination of the two causes

Figure 60 shows the contributions made by these two causes and gives an approximate account of the degree of phenomena observed.

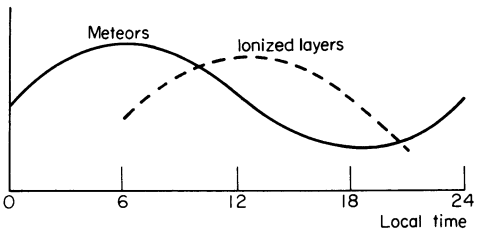

Fig. 60

6.2.2.2 Characteristics of ionospheric scattering

General characteristics

Altitude of scattering medium

Although tropospheric scattering can occur at any altitude (provided only that the air is not too rarefied), ionospheric scattering occurs at a well defined altitude, namely between 70 and 80 km by day, and between 85 and 90 km by night[323]. This property affects the characteristics of the antennae as well as the possible ranges.

Useful frequency band

The strength of the propagated field decreases rapidly with increasing frequency. The band of useful frequencies is restricted:

1. at low frequencies by the appearance of phenomena of ionospheric absorption, particularly sudden ionospheric disturbances (SIDs, see Section 6.4.2.1) which make it impossible to use frequencies lower than 25 MHz
2. at high frequencies by the very rapid decrease in field strength with frequency, the stronger fading, and the added interference due to large meteors, which create a Doppler effect.

The best frequency band appears to lie between 30 and 40 MHz. If we want to be totally free from sudden ionospheric disturbances (SIDs), we may go to 50 or even 60 MHz, but the transmission powers must then be much greater.

Range

The range is also limited:

1. lower limit: by the necessity to limit the angle between the rays emitted by the source and the scattered rays to a small value. Due to the altitude of the scattering layer the minimum range is in the neighbourhood of 1 200 km
2. upper limit: by the necessity to cover the whole path in a single skip, which limits the range to about 2000 km.

Variations in the field received

Cyclic variations

The value of the field received presents three kinds of cyclic variation:

Time of day. The minimum occurs between 19.00 and 21.00 h (local time at the centre of the path). This minimum appears to be caused by the coincidence of weak meteoric ionization and a low density in the *E*-layer.

Annual variations. At average latitudes, the field is minimum at the equinoxes and maximum at summer and winter solstices. In the auroral zones, there is only one annual maximum, namely in the summer.

Sunspot cycle. The medium value of the field received around noon, expressed in dB, appears to be a linear function of the sunspot number (Section 6.1.2.1).

Irregular variations

These are due to well defined causes that appear in a random fashion.

Sporadic E_s*-layer* (*Section* 6.1.4.3). Due to this layer, the field received increases sporadically to values several times greater than normal during a

period that may be between a few minutes and several hours. At average latitudes, these increases occur—like the E_s-layers' appearance—particularly in daytime and during the summer. They are significantly noticeable at nightfall in the auroral zones.

Sudden ionospheric disturbances (SID). During the occurrence of SIDs, signals transmitted at 50 MHz are increased because of the higher degree of ionization in the lower part of the *E*-layer. But signals transmitted at 25 MHz are suppressed, due to the higher absorption in the *D*-layer. The same phenomenon occurs in the auroral zones during polar blackouts.

Sputter. This is the rapid modulation of a signal by noise. It appears to be caused by the reflection from large columns of meteoric ionization, or when an auroral display is in evolution. The variations in ionization in time and space are sufficient to convert a carrier wave into a group of components with different, irregularly distributed frequencies that cause noise.

When this phenomenon occurs, ionospheric sounding shows a considerable extension of the trace of the *E*-layer at the high frequency end, and at greater than normal altitudes ('oblique *E*-layer'). The path of the waves during the sounding then presents a triangle, one corner of which is occupied by the auroral display or the large meteoric columns, one corner by the station which carries out the sounding, and the third corner by a point in the *E*-layer. The *E*-layer is no more affected perpendicularly, and is able to reflect waves of a frequency higher than the normal MUF.

Meteors. The passage of large meteors produces a considerable increase in the field, accompanied by a Doppler effect; the variation in frequency can attain a value of 6 kHz. This effect is due to the displacement of the head of the ionization column. If normal scatter continues, the Doppler shift produces a whistling noise of variable pitch, due to the interference between the two waves. This phenomenon occurs very often during a meteoric shower.

Random variations

These are irregular variations due to non-discriminated causes.

Short term fading. The duration of rapid fading is between 0·2 and 5 s. The distribution of the fields over a short period of time obeys Rayleigh's law, unless there are unusual increases.

Slow fading. The distribution of fields smaller than the mean value follows an approximately log-normal law with a standard deviation of 6 dB. The strong fields have distinctly higher values than the ones given by this law, even when eliminating irregular increases.

Correlation in space

The correlation coefficient of fields at two adjacent points decreases

rather slowly when the separation between these points increases. It is still 0·4 for a separation of 5 wavelengths in a direction normal to that of propagation, or 60 wavelengths in the direction of propagation.

The distance between two receiver antennae for space diversity reception must be greater than 20 wavelengths, measured in the direction normal to that of propagation.

Antenna-to-medium coupling loss

The reduction in gain of the receiver antenna is more important when the signals are weaker. Even when larger rhombic antennae are used, one cannot expect an overall gain (transmitting and receiving antennae) exceeding 14 dB for 99 per cent of the time.

Transmitted bandwidth

The transmitted bandwidth is restricted by the possibility of multiple paths. Meteors only very rarely produce differences in travelling time greater than 1 ms.

The sporadic E_s-layer, the oblique E-layer (which causes sputter), the back scattering from ionized masses or from irregularities on the ground, all can lead to much greater differences in travelling time.

Use of antennae with strong directivity, whose secondary lobes are as small as possible can reduce the differences in travelling time, or at least attenuate the waves having important phase differences. With ideal antennae, it would be possible to use transmitted bandwidths of several tens of kHz. In practice, however, the available bandwidth is no more than a few kHz.

6.2.2.3 **Practical data**

Equipment characteristics

Emitted power

This should be as great as possible, usually between 10 and 30 kW.

Antennae

The antennae used are large rhombic antennae (up to 600 m), Beverage antennae, or very large reflectors.

The elevation angle Δ between the waves and the ground is calculated so as to obtain an altitude of 85 km at the centre of the path, i.e. 7° for 1 200 km, and 1° for 2 000 km. It is extremely difficult to realize these very small values.

It can be shown for the plane condition[335] and it has been confirmed by experiment that the received field is stronger when the source and receiver antennae are directed—not towards the centre of the path—but to the 'hot

spots' where meteor ionization is strongest, taking the direction of the earth's motion into account.

For a path from east to west, the antenna should be directed slightly north of the great circle joining the source and the receiver from midnight to noon, and slightly south of the same great circle from noon to midnight.

For a path from north to south, they must be directed east of the great circle in daytime, and west by night.

In view of the difficulty of shifting the beam of the very large antennae used, one employs antennae with two lobes, each at a slight angle to the direction towards the receiver.

Since the angle of departure of the waves is very small, the terrain should be very flat and entirely free from obstacles in the direction of the receiver, and this over a considerable length. Similarly, the height of the horizon must also be very low. In view of the relatively low frequencies used and the weakness of the fields received, the receiving antenna must be situated at a place that is completely free from industrial noise.

Modulation

The useful transmitted bandwidth is narrow because of the small correlation value between the fields received at different frequencies, and because of the necessity for limiting the bandwidth of the receiver as much as possible in order to reduce noise.

Four telegraph channels can be transmitted in carrier-shift, or one telephone channel in SSB.

Moreover, telegraphy reception requires very complex equipment for signal reconstruction. Synchronized systems of telegraphy are used instead of start-stop systems.

Modes of application

We can use either permanent links with very great emitted powers (10–50 kW) or discontinuous links.

In this last case (the JANET system) a sounding transmitter situated in the proximity of the receiver, is received by an auxiliary receiver close to the main transmitter. When this auxiliary receiver receives the sounding transmitter, the main transmitter will be modulated. Modulation ceases when the auxiliary receiver does not receive further signals. While using the best periods of propagation, this method allows one to operate at much smaller source powers (usually 500 W).

6.2.3 PROPAGATION IN THE EXOSPHERE

The existence of long range missiles and earth satellites has drawn the attention to communications outside the ionosphere. Very few results have been published in this respect.

One of the best means for studying the exosphere is the investigation of whistling atmospherics produced by low frequency waves originating from lightning discharges or specialized sources[332]. The wavetrains have a frequency of several kHz and travel from one hemisphere to the other along the magnetic flux lines of the earth's field. They are only very slightly attenuated by their propagation in a medium that is practically loss free because of its very low density; they are reflected from the ground and their passage can be heard a number of times.

The relevant propagation theory[331] consists of equations also applied to propagation in the ionosphere, but at these extremely great altitudes, the values of electron density and of the earth's magnetic field are very different from those encountered in the ionosphere. The number of electrons has been estimated at 1.8×10^8 m^{-3} at a distance of 6 earth radii from the centre of the earth, and appears to lie between 1·5 and $4{\cdot}5 \times 10^7$ m^{-3} in outer space.

There are also waves of a very low frequency that are produced by the arrival into the earth's magnetic field of electrically charged particles originating from the sun. These waves are produced by the interaction between the particles and a region in space where the wave propagation velocity is low and close to that of the particles. Their propagation mode is similar to that of whistling atmospherics.

Reference 349 comprises an excellent bibliography and descriptions of the various types of observed phenomena.

6.3 IONOSPHERIC PREDICTIONS

Many international radio communications make use of the ionosphere. This also applies to nearly all internal radio communications in many countries. However, these communications can only function properly if their frequencies are selected having regard to the state of the ionosphere. That makes it imperative to know in advance what this state will be. This is the purpose of ionospheric predictions.

General predictions, which give the monthly median values of the MUF and of absorption, are usually published 3 or 6 months in advance.

However, a number of organizations now publish short term predictions, based on the observation of the sun or on back scattering. These data are transmitted by radio.

We shall only discuss the first mentioned type of prediction.

6.3.1 PREDICTIONS

Predictions are published by a number of services, who use complex and more or less empirical methods[18, 326, 340, 344]. We shall not go into details but can sum up the processes as follows:

6.3.1.1 Predicting the index of solar activity

This is the most complicated and most uncertain part of the prediction as we have seen in Section 6.1.2.1. However, in periods far from the maxima and minima of the solar cycle, prediction with a certain accuracy is possible several months in advance.

6.3.1.2 Determining ionization at each point

Partly theoretical and partly experimental methods allow us to deduce the probable ionization of the various layers at each point in the ionosphere and for any time from the index of solar activity.

6.3.1.3 Establishing prediction documents

Whatever their form, prediction documents show in a rapidly usable manner the monthly median values of the MUF (and sometimes of absorption) as a function of time and the terminal points of the path for a given month.

They are always deduced from the ionization values expected at each point of the globe at a given time. These values have in turn been derived from observations during previous years by stations performing ionospheric soundings.

However, the manner of establishing and presenting these documents, as well as their instructions for use, vary considerably from one country to another.

U.S.A.

A complete set of ionospheric maps, covering the whole solar cycle, is contained in the following document:

OT/TRE 13. Telecommunication Research and Engineering Report 13. Ionospheric predictions. Vol. 1, 2, 3, and 4. D. of C., Office of Telecommunication, Institute for Telecommunication Sciences, Boulder, Colorado, September, 1971.

CCIR

A similar document has been issued by the CCIR:

CCIR Report 340. CCIR Atlas of Ionospheric Characteristics. Oslo, 1966. ITU, Geneva, 1967.

Both documents must be used as indicated in Chapter 8, item 8.2.3.1. Some complementary graphs for field strength calculation can be found in the referred Chapter.

These documents leave it to the user to calculate the MUF and the absorption for the various modes E and F, and to combine them. Calculating absorption, in particular, means a rather intricate computation.

Other documents

Other countries outside the U.S.A. publish ionospheric predictions.

In Great Britain, the Radio and Space Research Station at Slough has published a collection of permanent ionization maps for the calculation of the MUF, as well as a handbook for their use[344]. A monthly sheet gives—six months in advance—the prediction of index I_{F2}, the only periodic element necessary for using these predictions.

In France, the DPI (Division de Propagation Ionosphérique) publishes documents for certain regions of the globe and for certain paths; only very simple calculations are required for their use.

There are still other documents[326]. All these documents lead in practice to the same results.

6.3.2 PRACTICAL VALUE OF PREDICTIONS

With regard to the MUF and the FOT:

1. Predictions concerning the E-layer are remarkably accurate
2. Predictions concerning the median MUF for the F_2-layer are usually exact with a margin of more or less than 10 per cent. The greatest degree of accuracy is obtained in regions having the greatest number of sounding and radio stations.

The predicted median MUF is sometimes lower, but very seldom higher, than the median MUF observed (operational MUF), so that this prediction can be used in all safety.

Predictions concerning absorption are much less accurate. They are also less precise, as we have seen above. However, in view of the necessary margin for taking fading into account, this lack of precision is of little practical importance.

Provided we do not ascribe an absolute character to these predictions (which they do not possess), they are an indispensable tool for the establishment of any communication by means of the ionosphere.

6.4 RANDOM VARIATIONS IN THE IONOSPHERE

Ionospheric predictions are established from the cylic variations of the ionized layers. But these layers are also subject to random variations which do not appear to obey any known law.

Two kinds of deviation are therefore possible between prediction and observation:

1. The monthly averages given by the predictions can be erroneous. However, one can always attempt to minimize this source of error by improving the method of calculation.
2. At a given instant, the state of the ionosphere may differ (sometimes considerably) from the monthly average. In this case we are faced with random problems we cannot hope to minimize. Random variations of the ionosphere can be divided into three groups:
   (a) Random fluctuations from day to day or for a short time.
   (b) Large variations in the characteristics during a period regarded as abnormal or perturbed.
   (c) Spatial variations.

6.4.1 RANDOM FLUCTUATIONS

We shall only consider variations in a random direction and without apparent laws of the characteristics of the ionosphere on unperturbed days. We shall not discuss variations in the virtual height of the layers, which are of little interest to the user.

6.4.1.1 **Variations from day to day**

In view of the yearly and solar cycle period of solar activity, the state of the ionosphere at a given instant and a given place, should vary continuously and rather slowly from day to day.

This is in fact confirmed by the observations of the critical frequencies of the E- and F_1-layers, but not as regards the critical frequency of the F_2-layer, nor the absorption.

Critical frequency of F_2; optimum working frequency (FOT)

The critical frequency of F_2 changes rather considerably from day to day. This obviously also applies to the F_2-MUF, which is derived from it.

We define an hourly median value—the median value during the hour under consideration over one month (short in relation to the annual cycle, but long enough for the daily cycle)—and observe that during 90 per cent of the hours the F_2-MUF is higher than about 85 per cent of its median value (a more accurate relation between F_2-MUF and F_2-FOT can be found in CCIR report 252-2[368]).

If the MUF over a given path is determined by the F_2-layer, we call the frequency calculated as above the optimum working frequency FOT (after the French initials); this value offers sufficient certainty for sure communication. This term can be explained by the fact that this is the highest, and therefore the least absorbed, frequency that can be used for sure transmission.

If the MUF of the path is determined by the *E*-layer, whose MUF is not subject to daily variations, the FOT equals the *E*-MUF.

Absorption

In the same way we can define an hourly median value of the absorption. We observe that at a given time of day, during 90 per cent of the days, the field will be stronger than half the value (−6 dB) corresponding to the median absorption value, and that during 10 per cent of the days, it will be stronger than twice the value (−6 dB) corresponding to the median value of the absorption.

6.4.1.2 Short term variations; ionospheric fading

Seen on a large scale, the ionosphere consists of concentric and homogeneous layers; but, like our atmosphere, it presents when observed in detail, certain inhomogeneities, and is in animated motion, which is the cause of the fact that the layers are not permanently horizontal, but are being continuously displaced with regard to the ground.

This means that a receiver can usually receive a transmitted signal via a number of paths (Section 6.2.1.3). Since these paths are not all of the same length, interference will occur between the various rays. The path lengths vary continuously and the phases of the various rays are distributed at random—resulting in a continuous fluctuation of the resulting field received. These short term fluctuations (from a fraction of a second to several minutes[325]) are called 'fading'. Fading is usually of shorter duration according as the frequency is raised.

The field obeys Rayleigh's law when observed over a short period of, say, 5 min (under constant ionospheric conditions). But it obeys the normal logarithmic law when observed for 15–60 min. The deviation is $13 \pm 3{\cdot}2$ dB between the fields that correspond to the probabilities of 10 and 90 per cent[325]). This corresponds to a standard deviation $\sigma = 5 \pm 1{\cdot}2$ dB.

Interference fading is usually selective, because the difference in path lengths, expressed in wavelengths, varies with frequency. If there is a considerable difference in path lengths and for a short wavelength, adjacent frequencies—even those that are part of the same communication channel —will not be affected by fading in exactly the same way at the same instant, with the result that voice communication will be distorted in a most incoherent manner (selective fading). This type of fading produces the 'scintillation' of satellite sources.

On the other hand, we have seen in Section 5.4.2 that because of the earth's magnetic field, waves reflected from the ionosphere possess elliptical polarization. But the receiver antennae normally possess linear

polarization. The two axes of the polarization ellipse fluctuate independently of each other and the antenna will only receive the field in a proportion of $2^{\frac{1}{2}} = 0{\cdot}707$ (−3 dB).

On the whole, the presence of fading forces us to use greater transmitted power—greater by about 13 dB, i.e. 20 times more powerful than would be necessary if fading did not exist. Moreover, fading reduces the quality of the received signal, especially for radiotelephony.

Figure 61 shows the approximate percentage of the time availability for ionospheric communication for long distance transmission as a function of the increased transmitted power, expressed in dB, and taking fading into account.

An ionospheric link of average quality functions for 90 per cent of the time. If a reliability of 99 per cent is required, the power must be increased by 18 dB, i.e. 63 times greater.

On the other hand, it will still function for 10 per cent of the time when the power is 34 dB below its nominal value (2 500 times weaker). This explains the very great ranges one sometimes obtains with very small powers.

6.4.2 IONOSPHERIC DISTURBANCES

This is due to a sudden increase in solar activity (Section 6.1.2).

6.4.2.1 **Sudden ionospheric disturbance (SID)**

This kind of perturbance is caused by a sudden increase in the ultraviolet and X-radiation from the sun, due to chromospheric eruption (solar flare). It causes an equally sudden increase in the ionization of the *D*-layer over the entire illuminated hemisphere (Section 6.1.2.4), gradually returning to normal after a period of time which may vary between a few minutes and one hour. Electron densities of up to $2{\cdot}5.10^{10}$ m^{-3} have been observed at an altitude of about 80 km.

The propagation of waves of a frequency lower than 500 kHz improves during these disturbances (better reflection from the *D*-layer). On the other hand, the absorption of short waves becomes so strong that all communication is often impossible.

6.4.2.2 **Magnetic storms**

Magnetic storms are caused by the emission of electrically charged particles from the sun (Section 6.4.2.7). They have the following effects on propagation[334].

1. The critical frequency f_{CF2} of the F_2-layer is modified

High latitudes	Summer—Fall at all times
	Winter—Sharp fall, centred around noon
	Equinox—Rather slow fall, centred around noon
Low latitudes	Usually a small rise (rarely a fall)
Average latitudes	In general: Summer—a fall
	Winter—a rise

These effects are generally strongest on the first day.

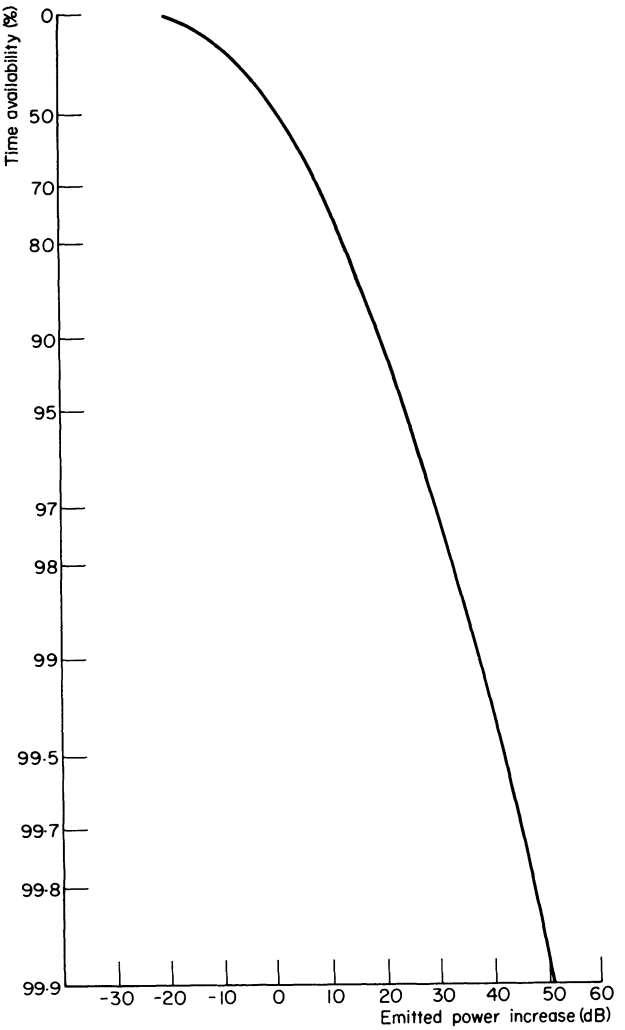

Fig. 61

2. The altitude of the F_2-layer seems to increase by approximately 30 km over a period of a few hours, centred around 04.00 or midnight. Martyn's theory of ionization transfer (Section 6.1.2.5) gives the best account of the phenomena observed. The beginning is gradual, but the increase is more rapid according as the magnetic storm is stronger. The phenomenon starts nearly simultaneously at all longitudes, but travels from the poles to the equator at a velocity of 180 km/h. Magnetic storms last from one to several days. There is a gradual return to normal.

6.4.2.3 **Polar blackout**

Blackout periods occur in the polar regions which have nothing in common either with aurorae borealis or with magnetic storms. They appear to be caused by the expulsion of high energy protons by the sun. This phenomenon commences one or several hours after a solar flare and it lasts from one to ten days (three days on average). Strong ionization descends to an altitude of 70 or even 50 km, causing extremely strong absorption. This is called polar cap absorption.

6.4.3 VARIATIONS IN SPACE

Apart from the sporadic E_s-layers we discussed in Section 6.1.4.3, volumes of ionized particles are constantly present in the ionosphere, which are often of important dimensions, not homogeneous with the remainder of the layers, and which cause scattered reflection over a large frequency spectrum. The behaviour of these particles in the ionosphere is in certain ways the same as that of clouds in the atmosphere.

It is impossible at present to state categorically whether these scattering nuclei are clouds whose ionization is stronger than that of the remainder of the layer, or whether they are regions where ionospheric turbulence is particularly strong.

The existence of these nuclei becomes particularly apparent by the nuisance they cause to radio direction finding. They reflect waves in all directions and allow paths outside the vertical plane containing transmitter and receiver. The direction of arrival of these waves can therefore be totally random, so that the direction finder will determine the direction of the scattering mass instead of that of the transmitter. This lateral deviation can take a maximum value of 2–5° for great ranges, depending on the paths.

Equatorial transmission is encountered rather often; this provides a north–south propagation across the equator of waves of a frequency of 50 MHz or more. This phenomenon is particularly prevalent during the autumn, in the course of the evening and the night. The mass of ionized nuclei that permits this type of propagation has a width (north–south) of the order of 1 km, a thickness of about 10 m and a length (east–west) which may attain 1 000 km.

6.4.4. ABNORMAL PROPAGATION

The existence on certain unpredictable and rather rare occasions of nuclei or very strongly ionized layers cause so-called abnormal (or anomalous) propagation, which cannot be used for transmission purposes and which is a source of interference between stations which do not normally interfere.

The investigation of these phenomena is far from complete. However, CCIR[324] has summarized the chances of interference because of ionospheric propagation in the Table 6.6, based on observations made in a number of countries.

Table 6.6

Cause of interference	Zone of latitude	Period of severe interference	Upper frequency limit (MHz)	Lower frequency limit (MHz)	Distance interval (km)
Regular reflections from F_2-layer	temperate	Day. Equinox and winter–solar maximum	50	60	east–west: 3 000–6 000
	low	Afternoon–evening. Solar maximum	60	70	north–south: 3 000–10 000
Reflections from sporadic E_s-layers	aural	Night	70	90	500–2 000
	temperate	Summer days and evenings	60	90	
	equatorial	Day	60	90	
Scattering by sporadic E_s-layers	low	Evening–midnight	60	90	up to 2 000
Reflections from meteoric ionization	all	Especially during meteoric showers	May be important at all points in the band		up to 2 000
Reflections from columns of auroral ionization aligned to the magnetic field	auroral	End of afternoon and night			
Scattering by low F-region		Evening–midnight Equinox	60	80	1 000–4 000
Special trans-equatorial effect	low	Evening–midnight	60	80	4 000–9 000

CHAPTER 7

PRINCIPLES OF CALCULATING A RADIO LINK

In order to determine whether radio communication is possible and what its quality will be, we must first calculate the field received, then the field required for a communication of the desired type and quality, and finally ensure that the first result is higher than the second.

7.1 FIELD RECEIVED

The discussions of the preceding chapters have shown the manner of wave propagation in various media. Actually all waves travel through the atmosphere, the ground and the ionosphere, so that the different propagation modes we have discussed so far are all superimposed in any situation. But they are not of equal importance in each practical situation; usually, one of them is so predominant that the others can be neglected. The problem is then reduced to calculating the field received by the predominant mode.

In this chapter we shall give only some general indications. Numerical data and practical calculation methods will be found in Chapter 8.

7.1.1 RELATIVE IMPORTANCE OF THE VARIOUS PROPAGATION MODES

In order to judge the relative importance of the various modes, we must look at the problem from two complementary viewpoints:

1. the conditions under which a given mode occurs effectively
2. the most important modes in each part of the frequency spectrum.

These two viewpoints obviously lead to the same conclusions, but each allows us a different view of the propagation problem, resulting in a better general picture.

7.1.1.1 **Applicability of the various modes**

Combined fields

When the field received is due to several different modes, the component fields will combine into a single one, taking the different phases into account. Usually, these phases are independently and continuously

variable. In this case, the energies received will be summed, i.e. the squares of the amplitudes.

For example, if two fields with independent phases are received simultaneously, the mean value of the field received will be

$$E = (E_1^2 + E_2^2)^{\frac{1}{2}}$$

or

$$E = E_1(1+\alpha^2)^{\frac{1}{2}}$$

where $\alpha = E_2/E_1$. As soon as α is less than 0·5, the mean field received practically equals E_1, the strongest field (see Fig. 62).

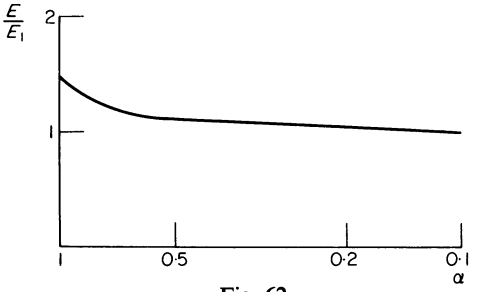

Fig. 62

We can therefore state that two fields of different modes will combine only when their ratio lies between 2 and 0·5. In the opposite case, only the strongest mode will prevail, which will be affected by fading caused by interference between the two modes, which is variable in time.

If the strength of the two fields is almost the same, their combination will give rise to particularly strong fading, especially:

1. with hectometre or decametre waves, when the stable diffracted wave combines with the unstable ionospheric wave
2. with metre or decimetre waves, when the direct ray and the ray reflected by a flat ground or by the sea are perturbed by meteorological phenomena.

If there are many fields available for the combination (multiple reflection) the result will be more complex. But even here we can neglect all components whose mean value is well below that of the others (e.g. scattered field against the field reflected by the ionosphere). When the strengths of a great number of components are more or less the same, statistical cancellation will occur, and the resulting field will vary less than in the case of only two components. This is a case of Rayleigh distribution (Appendix A.6.1).

Stability of the various modes

The characteristics of variation in time differ greatly according to the modes under consideration.

The most stable fields are produced by propagation along the ground of diffracted waves that are emitted and received by rather low antennae. Ground characteristics do not vary all that much, nor is the effect of the atmosphere very noticeable.

The field of tropospheric waves between antennae in line of sight is subjected to rapid and important variations, especially at night. The field of ionospheric waves undergoes considerable variations both with long or short periods, because of variations in the ionosphere.

Fields obtained by tropospheric or ionospheric scattering continuously show rapid fluctuations. Long period fluctuations are smaller.

Finally, some propagation modes produce very strong fields which, however, are so irregular as to be of no use in communications. These are the 'abnormal' propagations, which may be tropospheric (Section 2.2) or ionospheric (Section 6.4.4). We should nevertheless attach some importance to these modes because they occur quite frequently, in any case during certain times of the year, and the interference they cause is the more intense because, when existing, these are excellent modes of propagation.

Utilization of regular modes

Each of the modes that can be used for communication purposes has its own field of application, which is determined by the range and the frequencies at which it gives a sufficiently strong field.

We can describe the various modes of propagation as follows.

Tropospheric propagation

Line-of-sight communication. The field received between antennae having a given gain is inversely proportional to frequency and separation, i.e. the field strength decreases rather slowly as the separation is increased. This mode of propagation is restricted only by the conditions of radio visibility. It is the mode used for radar. It can also be used for communication between ground and aircraft. Stations for land communication must be located on the highest points of the terrain, which involves increased cost (service, connection to supplies, security, etc.).

Very stable radio links can be realized with metre and decimetre waves at reduced powers of a few tenths of a watt to several watts.

Apart from some isolated cases, a line-of-sight communication is always accompanied by reflection from the ground or the sea, which will cause interference fading.

Tropospheric scattering (*troposcatter*). This mode is used only for waves of more than 50 MHz, which cannot be reflected by the ionosphere, and has the advantage of not having to incur the increased cost connected with stations at high altitudes, as well as possessing a large range of more than

500 km. On the other hand, the emitted power must be great (100 W–10 kW) and the antennae must have a high gain, which implies great dimensions.

Propagation in the proximity of the earth's surface

Reflection. Reflection from the ground does not constitute an independent mode. Reflection intervenes in line-of-sight links. It modifies the radiation diagram of the antennae for ionospheric links. Reflection occurs only when the height of the antennae above the ground is sufficient (Section 4.1.5.1).

Diffraction around the earth's curvature. The effect of diffraction strongly depends on frequency; the field at a given distance will be stronger accordingly as frequency is lower.

For frequencies lower than 500 kHz, diffraction plays a more predominant part at short and average ranges. At great ranges, the ionospheric field becomes the dominant factor.

For frequencies between 500 kHz and 1·5 MHz diffraction produces useful fields up to a range of about 100 km on land and a few hundred km at sea. In daytime this is the only possible mode of propagation of medium waves.

For frequencies between 1·5 and 50 MHz diffraction is the normal method for short range links, e.g. military links from the battlefield.

For still higher frequencies diffraction allows links over the horizon, which will be shorter according as the frequency is higher. For example, this mode is used for metre wave links with vehicles, and for television and f.m. broadcasts.

Diffraction caused by obstacles. Knife edge obstacles are sometimes used for the realization of great ranges for metre waves without relay stations.

Ionospheric propagation

Ionospheric reflection plays a fundamental part in the propagation of waves at a frequency lower than the MUF of the path (which is rarely higher than 30 MHz). This mode of propagation involves very little attenuation and is therefore the preferred method for transmission over average and great ranges.

Ionospheric scattering only enters the picture for frequencies that are not subject to regular reflection. The useful frequency spectrum appears to lie between 30 and 100 MHz with useful ranges between 900 and 2000 km.

Effect of antenna on the relative importance of the various modes

When several modes are capable of efficient transmission of energy, the angle of departure is in general not the same for each of them.

If the antenna is sufficiently directional, energy transmitted by one of the possible modes may be much more powerful than that propagated by the other or others. In that case the preferred mode can become distinctly predominant.

The most typical case is a short range link by hectometre or decametre waves. The two possible propagation methods are:

1. the ground wave with an angle of departure equal to zero.
2. the ionospheric wave which departs almost vertically.

The use of a vertical antenna gives a vertically polarized wave with a strong ground wave. On the other hand, the radiation of the antenna in the vertical zone will be very weak, and the same will apply to the ionospheric wave. Communication will be effected by means of ground waves.

Anti-fading antennae for radio transmission on medium wavelengths are based on this principle.

When using a horizontal antenna whose altitude is smaller than $\lambda/4$, the ground wave can be neglected because of horizontal polarization. On the other hand, maximum radiation will take place in the neighbourhood of the vertical, and only ionospheric waves will be propagated.

7.1.1.2 Modes used at different frequencies

Long waves (less than 500 kHz)

Antennae are always ground based and their altitude is smaller than one wavelength. Polarization is vertical. Transmission takes place by diffraction and multiple reflection from the ground and ionosphere; diffraction is preponderant at small ranges (up to a few hundred km). The transition between the two modes is imperceptible. There is little variation in time of the field, mainly at lower frequencies.

Medium waves (500–1 500 kHz)

Links between ground based stations

In this case as well, the altitude of the antenna is smaller than one wavelength; antenna polarization is vertical.

1. By day all propagation is by diffraction because the ionospheric wave is heavily absorbed and therefore negligible. The field is very stable.
2. By night ionospheric and ground waves coexist:
   (a) at short ranges, the diffracted wave is predominant and the field is stable. There is a zone of good reception or of 'primary coverage' of radio transmitters.
   (b) at medium ranges (between 100 and 150 km over average ground) the mean values of the two waves are very close. Fading is very strong and radio reception is poor.

(c) at great ranges only the ionospheric wave remains and is subjected to rather pronounced fading. This is the 'secondary coverage zone' of radio transmitters.

Links between ground and aircraft

In this case, the altitude above ground of one of the antennae is great enough to create interference fringes between direct and reflected waves. However, since the wavelength is great, this phenomenon will be present only at very short ranges (equations (4.10) and (4.11)), but medium wave links are seldom used for short ranges.

Apart from this exceptional case, propagation occurs like that between land based stations, but, since one of the antennae is situated so high, the field of the ground wave will be considerably stronger.

Decametre waves (1·5 MHz–30 MHz)

Links between ground based stations

As the antenna altitudes are not very great, reflection does not enter the picture, except that it affects the radiation patterns of the antennae.

1. At short ranges and vertical polarization, ground diffraction dominates and the link is stable, although depending on the profile of the terrain. With horizontal polarization there would be an appreciable ground wave.
2. At medium and great ranges with vertical polarization, and at every range for horizontal polarization, the ionospheric wave is the prevailing mode. It is rather unstable against time, but does not depend on the profile of the terrain. When the frequency exceeds the zero-MUF at the place of transmission, the ionospheric wave will only exist from the skip distance. At this distance it appears at maximum strength, and will subsequently decrease slowly.
3. At intermediate ranges we can observe:
   (a) either coexistence of the two modes, with very strong fading if their mean values are identical
   (b) or a silent zone, because the ground wave has become negligible and the ionospheric wave has not yet appeared.

Links between ground and aircraft

In the line-of-sight zone, interference fringes between direct and reflected rays start earlier than in the case of intermediate waves, because the wavelength is shorter.

Apart from the above case, the same phenomena occur as between ground based station, but the direct wave is much stronger.

Metre waves (30–300 MHz)

Links between ground based stations

Small antenna altitude. Only vertical polarization can be used in this case, giving a useful diffracted wave effective up to a few dozen km. The field is stable, but depends heavily on obstacles in the terrain, especially in the neighbourhood of the antennae. This is for example the case for vehicles equipped with v.h.f. radio.

Great antenna altitudes (several wavelengths). In the case of line-of-sight links we have not only to deal with the direct wave, but also with its reflection, primarily by the ground and also be isolated obstacles in the proximity of the antennae. The field is stable in time, except in the case of super-refraction or tropospheric reflection, but varies over a few metres in space because of interference due to reflection by obstacles.

Not in line of sight; the relatively easy diffraction of these waves allows them to travel round isolated obstacles and to penetrate into the shadow zone caused by the earth's surface. The field is stable. When using great emitted powers, tropospheric scattering permits one to attain ranges of several hundred km. Finally, ionospheric scattering—at the cost of a reduced passband and considerable powers—allows one to attain ranges of between 1 000 and 2 000 km. The resultant fields are unstable over short periods, but the average and quasi-minimum fields are stable over long periods.

We should also mention diffraction by sharp mountain ridges and reflection from mountain sides: These are very exceptional modes.

Links between ground and aircraft

In line of sight, propagation occurs by direct waves and by reflection, usually with interference fringes at small ranges. Outside the region of line of sight, the diffracted field induces relatively great ranges because of the altitude of one of the antennae. In the case of modern aircraft, flying at high altitudes, we can attain considerable ranges by using high power transmitters, so that the use of decametre waves becomes unnecessary.

Microwaves (greater than 300 MHz)

In this case, a link between ground based stations is only possible in line of sight or at a small distance over the radio horizon, unless great powers are used in conjunction with tropospheric scattering.

Links between ground and aircraft as well as television broadcast are established in the lower part of this spectrum (u.h.f.) under the similar conditions as those met with metre waves.

7.1.2 METHODS FOR CALCULATING THE FIELD RECEIVED (OR THE POWER RECEIVED)

For practical reasons one usually prefers to calculate the field received for decametre and longer waves, and the power received at the input of the receiver for metre and shorter waves.

The calculation is based on three factors:

1. radiated power
2. antenna gain
3. transmission loss.

The radiated power is always smaller than the power supplied to the antenna, because antenna efficiency is always smaller than unity. In the case of long wave antennae, or antennae mounted on vehicles, efficiency may be very low—even as low as 10 per cent.

Antenna gain for different frequencies and in different directions is given by graphs or equations. It is expressed either in relation to an isotropic antenna, to an elemental dipole, or in relation to a half-wave dipole. We have seen in Section 1.2.2.3 that the gain of an elementary dipole is 1·8 dB compared to an isotropic antenna, and that of a half-wave dipole is 2·15 dB.

7.1.2.1 **Ground wave**

Different zones

Retreating from a transmitter, we find the following zones, or at least some of them:

1. illuminated zone (transmitter and receiver in line of sight)
2. zone in the proximity of the radio horizon
3. Sommerfeld's zone, where the ground may be considered as being flat
4. diffraction zone.

The boundaries of the illuminated zone are defined by geometric considerations (Section 4.1.5.1). Those of the other zones are not clearly defined because there is no discontinuity between them.

In the case of antennae in the immediate proximity of the ground, the first two zones are replaced by a zone of direct radiation, where the waves travel as in free space. Here, the boundaries are approximately defined by Fig. 63. We observe that:

1. the boundary of the diffraction zone does not depend on the nature of the ground
2. on the other hand, the boundary between the zone of direct radiation and Sommerfeld's zone depends on the nature of the ground
3. Sommerfeld's zone does not exist at sufficiently low frequencies; one goes immediately from direct radiation to the diffraction zone.

Calculating the field in the various zones

The field in the illuminated zone is not subject to loss, apart from loss due to imperfect reflection (Section 4.1.1.2) and to decrease by $1/d$ produced by beam divergence (Section 1.2.2). Its strength is calculated in the same manner as in geometric optics.

In the other zones, the diffraction theory (Sections 4.3 and 4.4) allows us to calculate the field. This calculation becomes more complicated when one comes closer to the boundary of the illuminated zone.

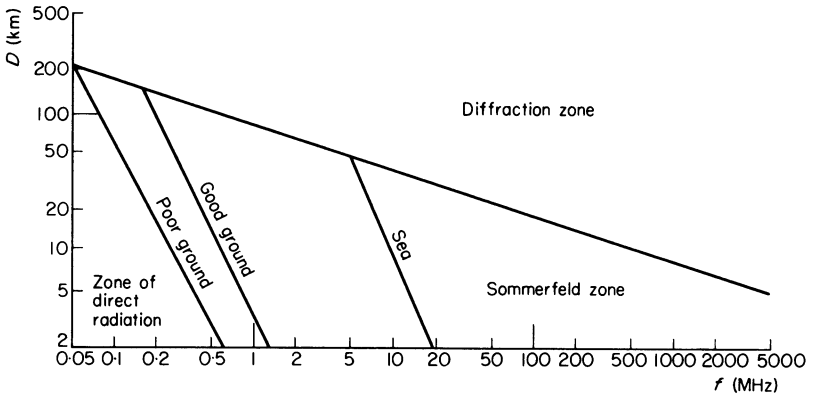

Fig. 63

The field decreases approximately as $1/d^2$ in Sommerfeld's zone, while its decrease is exponential in the diffraction zone.

Practical diagrams

The form of diagrams is simpler for decametre or longer waves (when the antenna altitude is always in practice a fraction or a small multiple of the wavelength) than for metre or shorter waves (in which case the antenna altitudes may be a considerable number of wavelengths).

Decametre or longer waves

The diagrams used give the field in dB in relations to $1\mu V/m$ against distance for 1 kW radiated by a short vertical dipole close to the ground and for various frequencies.

The actual power and antenna in use are taken into account by adding the power and antenna gain values (in dB) to the field given by the graph.

At greater antenna altitudes, the corresponding height factors should be included as well, but this is normally not necessary for the wavelengths we now consider.

On the other hand, it is useful to consider the loss due to diffraction from

obstacles situated between transmitter and receiver. This loss can be calculated by means of special graphs.

Metre and shorter waves

Here the number of factors to be included is greater. We have to take account of the antenna altitudes, terrain profiles, and factor K, determining the equivalent earth's radius (Section 2.1.3.2).

In the case of low antennae (on vehicles) or sound or television transmission, we can use the CCIR curves[138], which take the altitude of the transmitter antenna into account. However, these curves only provide mean values while the value of the field at a given point can differ considerably from this mean value.

The problem is highly complex in the general case. A number of methods have been proposed for its solution, and many graphs have been published. All these methods are based on the same principles:

1. by selecting, wherever possible, a certain domain, obtained by limiting the variation of one or more variable (e.g. distance, frequency or antenna altitude limits) in such a manner that the field can be calculated by means of a single and sufficiently simple equation (as long as one remains within the limits of the combination)
2. by establishing the graphs corresponding to these combinations in the case of the spherical earth. Because of the large number of variables involved, these graphs usually take the form of alignment nomograms
3. by taking into account the actual shape of the terrain, either by calculating the diffraction for isolated obstacles, by determining the equivalent earth's surface (Section 4.5.1), or by means of more complicated methods[103, 221].

Metre waves also show 'abnormal' tropospheric propagation, which can cause interference, but which are too unstable to be used for regular communication.

7.1.2.2 Ionospheric wave

The calculation methods differ greatly according to the frequencies of the waves used.

Long waves (less than 500 kHz)

The field could be accurately calculated by means of the theory of multiple reflection. In practice, however, one prefers the semi-empirical Austin-Cohen equation:

$$E = K\frac{P^{\frac{1}{2}}}{d}\left(\frac{\theta}{\sin\theta}\right)^{\frac{1}{2}} e^{-\alpha d/\lambda^{\frac{1}{3}}} \tag{7.1}$$

where θ = angle at the centre of the path and where constants K and α

depend on the nature of the ground. Different authors do not agree on the value of these constants.

At sea, we can assume $K = 600$ and $\alpha = 0{\cdot}0015$ if P is expressed in kW, d and λ in km, and E in μV/m. On land, we can assume $\alpha = 0{\cdot}0026$.

Decametre waves (1·5–30 MHz)

MUF

Before calculating field strength, we obviously must first know whether propagation is at all possible. In other words, we must calculate the value of the MUF. This calculation has been explained in Section 6.2.1.3.

Field strength

As far as the strength of the ionospheric field is concerned, there does not exist a synthetic diagram similar to the nomograms of ground wave propagation. The number of variables would in this case be prohibitive. Figures 64 and 65 give an idea of the behaviour of field strength variations.

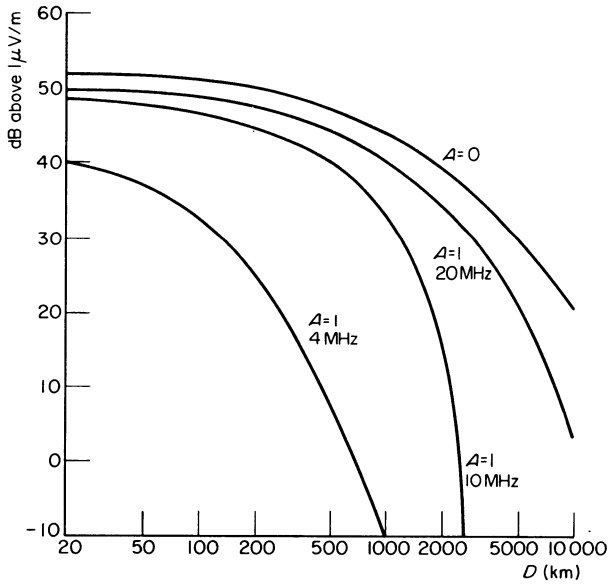

Fig. 64

They are related to a power of 1 kW radiated by a short dipole near to the ground. The curve relating to zeo absorption ($A = 0$) is valid for all frequencies. Absorption value $A = 1$ represents a typical value of absorption at noon.

It is obvious that all curves must discontinue at the MUF.

When comparing these curves with those of the ground wave (Chapter 8),

we observe a much slower variation of the field with distance. On the other hand, in contrast to what happens in the case of the ground wave, the highest frequencies are least attenuated.

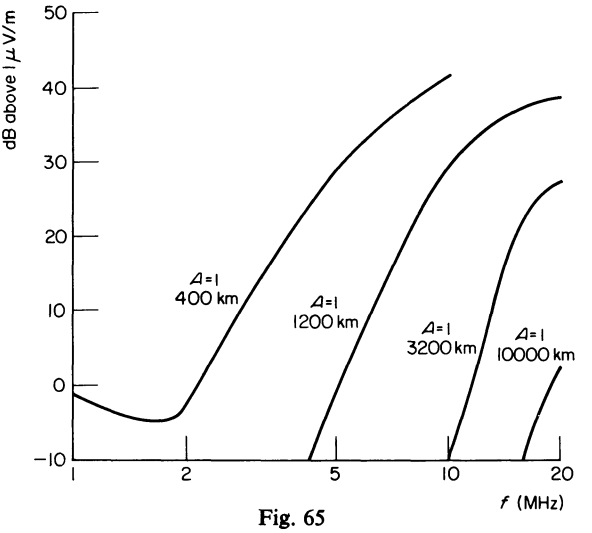

Fig. 65

If there is no absorption (e.g. during the night), the field diminishes as $1/r$ (r = path travelled, which can be derived by means of geometric considerations). It can be assumed that each reflection by the ground produces an additional loss of the order of 4 dB.

If absorption is present, it can be calculated by the methods mentioned in Section 6.2.1.3.

Practical diagrams

In practice, the MUF and the field strength are calculated by means of ionospheric prediction charts, together with complementary graphs. The method of using CCIR and RPU diagrams is described in Chapter 8.

Metre waves

Metre waves do not possess regular ionospheric propagation, but often present 'abnormal' ionospheric propagation; its probability of appearance is discussed in Section 6.4.4. When this type of propagation is present, absorption is low and field strength is great.

7.1.2.3 Scattered waves

The field of tropospheric and ionospheric waves can be calculated by means of graphs, which take into account the scattering angle, the altitude of the scattering medium, etc.

A great many methods have been proposed, but the results do not show too much agreement.

7.2 FIELD REQUIRED

A radio circuit is viable only if the received signal can be distinguished with certainty from the noise present in any electric circuit. We shall therefore now discuss noise.

We should also remember that the required signal-to-noise ratio at the receiver depends on the nature of the transmitted signal. Usually, neither signal nor noise are constant. This makes it necessary to define during which part of the time (time availability—e.g. 90, 99 or 99·9 per cent) the signal-to-noise ratio must be higher than a fixed value (service grade). This requires that the median value of the signal-to-noise ratio (50 per cent of the time) is higher than the necessary minimum value. The difference between these two values constitutes the margin of the link.

The required signal field is obtained by adding the value of the necessary signal-to-noise ratio and the margin to the noise field.

7.2.1 NATURE AND INTENSITY OF NOISE

7.2.1.1 **Thermal antenna noise**

An antenna appears at the receiver input as an impedance whose real component consists of the sum of its ohmic resistance and its radiation resistance. The ohmic resistance of antennae at the lowest frequencies greatly exceeds their radiation resistance. On the other hand, the radiation resistance of high frequency antennae is much greater than their ohmic resistance.

It is known[403, 404] that the maximum noise power that a resistance can produce is

$$P = KTB \tag{7.2}$$

where: P = power in W

K = Boltzmann's constant: $K = 1{\cdot}374 \times 10^{-23}$

T = temperature of resistance in K

B = bandwidth in Hz over which the energy is collected (approximately 3 dB passband of the receiver). The fact that the noise power is proportional to the passband of the receiver is characteristic of white noise, i.e. noise whose spectrum is constant with respect to frequency[1, 404].

The temperature of the ohmic resistance of an antenna is the ambient temperature, i.e. approximately 300 K. On the other hand, the temperature of its radiation resistance is the same as that of the medium from which the

antenna receives radiation. It is rather difficult to determine this latter temperature because the radiation temperature of electrons in the ionosphere is rather high, but they only radiate in the frequency band corresponding to hectometre and decametre waves. On the other hand, certain parts of the sky possess very low temperatures for very short waves. With regard to radio links between two points of the earth's surface, it is generally assumed that the temperature of the radiation resistance is the same as the ambient temperature.

Expressing the noise power in dB in relation to 1 W, we have:

$$P = -204 + 10 \log B \tag{7.3}$$

7.2.1.2 **Background noise in a receiver**

Because of the use of valves, transistors or diodes, any system capable of receiving a signal will produce noise in the form of white noise (shot noise plus partition noise), which is added to the thermal noise across the input resistance[404]. This noise is covered by means of the noise factor.

The noise factor of a receiver has been defined as the ratio of the noise at the output of this receiver to that which would be present at the output of a perfect receiver (without added noise) having the same gain and the same response—both ideally matched to the same dummy antenna at the same temperature.

The noise factor is usually represented by the symbol N, expressed in dB.

Up to a frequency of 100 MHz it is possible to design receivers with not more than 4 dB noise factor, using conventional valves, transistors or diodes. This value can be reduced to 1·5 dB by using field effect transistors. At 300 MHz, the minimum noise factor of well designed receivers is 5 dB, at 900 MHz 8 dB, at 4000–6000 MHz 10 dB. The use of tunnel diodes can give a minimum of 7 dB, even at the highest frequencies. However, the noise factor may be reduced to only 1 dB or even less by using a parametric amplifier before the receiver.

The noise power of an antenna which is correctly matched to the input of the receiver is:

$$P = -204 + 10 \log B + N \qquad \text{dB above 1 W} \tag{7.4}$$

The equivalent noise field E_n can be derived from this equation. If e is the e.m.f. equivalent to the noise, it acts on the total resistance R of the antenna in series with the input resistance of the receiver, also equal to R because the antenna is correctly matched. We have therefore for the power P it supplies to one of these resistances:

$$\frac{e^2}{2R} = 2P$$

On the other hand, if the equivalent noise field is E_n and the antenna effective height h, we have:

$$e = E_n h$$

whence

$$E_n = \frac{2(PR)^{\frac{1}{2}}}{h} \tag{7.5}$$

from which we derive by means of equation (7.4) and expressed in dB:

$$E_n = -78 + 10\log B + 10\log R - 20\log h + N \tag{7.6}$$

dB in relation to 1 μV/m (with B expressed in Hz, R in Ω and h in m).

We have for a $\lambda/2$ antenna isolated in space:

$$R \approx 73\Omega \qquad h = \frac{\lambda}{\pi} = \frac{c}{\pi f}$$

whence, by conversion into dB in relation to 1 μV/m:

$$E_n = -99 + 20\log f + 10\log B + N \tag{7.7}$$

Equations (7.3) and (7.7) are in current use for metre and shorter waves, where the receivers are usually well matched to their antenna, whose efficiency closely approaches unity (the ohmic resistance is negligible in comparison with the radiation resistance).

For decametre and longer waves, antenna efficiency is less good (e.g. whip antenna) and their matching to the receiver is generally poor.

For these wavelengths, the signal field required in the presence of noise, for a given service, is often used instead of the noise field.

7.2.1.3 **Atmospheric noise**

Origin and nature

Atmospheric noise is caused by disturbances in the atmosphere, such as thunderstorms. Except in the case of a local thunderstorm, this type of noise has almost the same spectrum as white noise over not too wide a frequency band (e.g. the passband of a receiver), but its intensity varies considerably over the entire electromagnetic spectrum.

If the thunderstorm is local, the noise has the characteristics of shot noise, where each discharge excites the circuit in an impulse-like fashion.

Thunderstorm characteristics

We have about 50 000 thunderstorms per annum, 2 000 happening at each instant, giving 100 lightning flashes per second, each lightning flash including two discharges.

The discharge current varies between 10 and 100 kA, with a mean value of 20 kA. The altitude of the discharge is between 2 and 4 km, and its damped oscillatory period is of the order of 0·01 ms. We are therefore in

the presence of an irregular sequence of pulses, each having a mean duration of 0·01 ms, and whose maximum power is very great (several tens of GW). The frequency spectrum of these pulses is very extensive, so that a local thunderstorm will produce intensive interference, even in the case of metre waves. However, the radiated energy reaches a maximum at frequencies in the proximity of 10 kHz.

The main thunderstorm centres are situated in the tropical or equatorial regions. A first region extends from Central America to Brazil, a second (and the most intensive) occupies Central Africa, with an additional region in Madagascar. The Far East, Indonesia, New Guinea and the Philippines also have important thunderstorm centres, as well as the mountainous part of Burma during the summer. Figures 66 and 67 show the distribution of thunderstorms during summer and winter, according to Brooks.

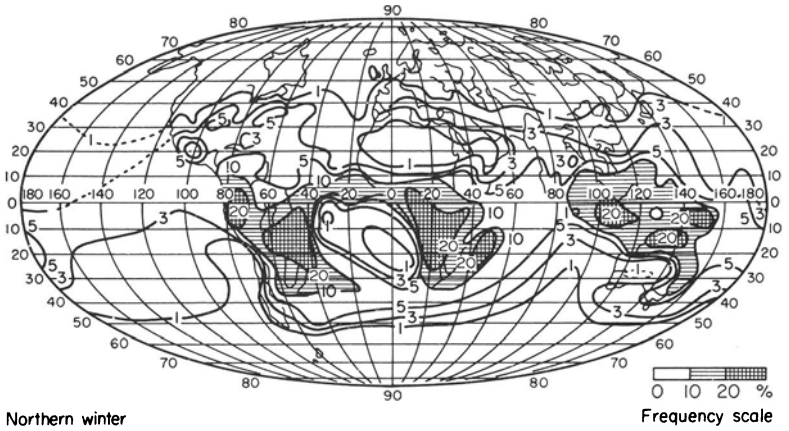

Fig. 66

Propagation of atmospheric noise

Atmospheric noise obeys the same propagation laws as communication signals, but its enormous power allows it to travel by modes that would give communication signals prohibitive attenuation. Multiple paths with various reflections and scattering are the rule, so that the energy from a single discharge arrives at the receiver at different instants. (This is why it was believed for a long time, on the strength of distant recordings, that the discharge had an oscillatory character.) The result is a continuous noise, whose spectrum is similar to that of white noise if the thunderstorm is not confined to the receiver's locality. If the thunderstorm is local, the shot noise must be added.

Since the sources of atmospherics and the laws of propagation are known, one could conceive of the possibility of calculating the noise level observed

at a random point on the globe at a given instant. However, the number of relevant factors is so great that it is only possible to establish very general tendencies, for example the fact that the rapid decline in noise level for frequencies of over 10 MHz, and more particularly of over 30 MHz, is obviously due to the circumstance that these frequencies are only able to travel great distances during specific conditions of the ionosphere.

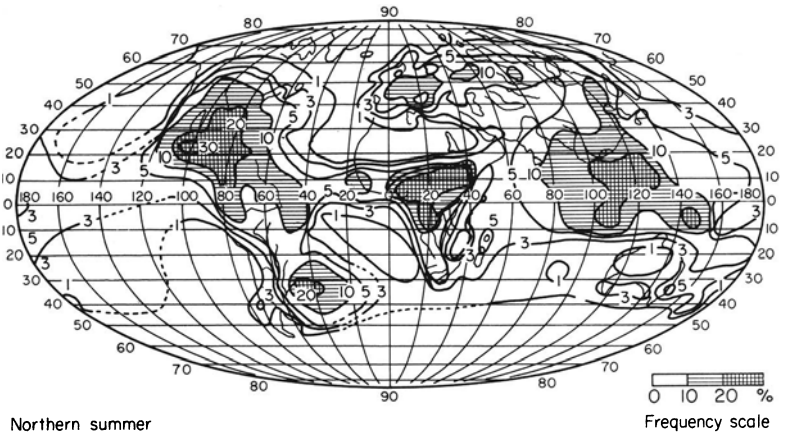

Fig. 67

Measurement methods

We can use two methods for measuring atmospheric noise:

Direct method

With this method we measure the noise field as indicated on a measuring device placed at the output of a receiver, which is connected to a standard antenna.

It is not possible to record the instantaneous value of the noise current (a concept without a precise meaning) because the noise spectrum extends to extremely high frequencies. We must therefore use circuits that integrate noise energy over a given period. Therefore:

1. the indication of the measuring device depends on the integration circuit used
2. the fact that the measuring device gives the same indication twice does not justify the conclusion that the effect on a given receiver will be the same in both cases
3. on the other hand, indications obtained by the direct method are objective and make it easier to carry out a scientific study of the problem.

The quantity measured is usually the r.m.s. value of the noise field over a period of a few minutes for a bandwidth of 1 kHz. This quantity is called the mean quadratic noise.

Indirect method

Let us assume a receiver connected to a standard antenna, which receives signals from a local oscillator whose power can be varied by means of a potentiometer. The oscillator transmits an automatically keyed text at the rate of 10 words per minute. The operator regulates the oscillator power in such a manner that he does not make more than 5 per cent errors when he reads the signal.

A network of stations of this type has been installed over the entire world. Despite the subjective character of this method, the results can be mutually compared. The mean operator error amounts to 3 dB, and the equipment errors also to 3 dB, which gives a total error of about 6 dB. This value is quite acceptable in view of the great variations in noise level.

It has been found that the ratio of the r.m.s. values of signal and noise is -6 dB when the device is set to 95 per cent intelligibility, but this system is generally used to determine not the noise field itself, but the signal field required in the presence of noise.

Value of noise field

The atmospheric noise field depends on:

1. the geographic location of the receiver—the maximum noise will occur in the vicinity of thunderstorm centres
2. the season, the field value being greater during the local summer
3. the time, being stronger during the night than during the day
4. frequency: very strong for frequencies of less than 1 MHz—increasing to 9 MHz and becoming negligible between 15 and 20 MHz
5. bandwidth of receiver; it is proportional to the square root of the passband.

Knowing these rules, we can predict noise in the same manner as we have done in the case of ionospheric predictions. However, in this case the predictions will be much less accurate because of the considerable spread in values. Although on average of the order of 5 dB, errors can sometimes reach 20 dB. These predictions have therefore a very limited value.

Despite certain inaccuracies, the prediction system according to CRPL world maps[7] has been used most of all for a long time. The CCIR system[418, 419] is more complicated, but more accurate.

Prediction systems give for each location, season and time of day:

1. the field value required in the presence of noise for a given type of service (CRPL)

2. the field value equivalent to the noise (CCIR), or
3. the values in dB of the ratio of noise power to thermal noise of an elemental antenna (CCIR).

Apart from regular variations, that can be predicted with more or less accuracy, atmospheric noise varies considerably from day to day, even in the absence of local thunderstorms. In the case of a local thunderstorm, atmospheric noise can attain extremely high values, rendering reception of any kind impossible.

Direction

Atmospheric noise often has a preferred direction which is the one of the centre of the thunderstorm's activity.

7.2.1.4 Cosmic noise

The origin of all cosmic noise is still unknown, but it has been possible to prove that it is caused by some extraterrestrial source, and that the direction of its maximum is fixed in relation to the stars. Its origin is therefore probably linked with the Galaxy.

Its behaviour is the same as that of white noise; the intensity changes slowly with frequency.

Measuring method; units

Only the direct method is used in this case. Measurement is rather difficult, especially when noise is weak. Receivers with very low system noise are required, and the receiving station must be well away from any source of industrial noise. The measured results are evaluated by means of statistical methods.

Cosmic noise is expressed:

1. in μV/m for a given transmission band. However, as with other types of noise, the signal required in the presence of noise is frequently used for decametre waves. Since noise field varies very little, a small margin or no margin at all is taken for fading.

   The following equation can be used for converting from one passband to another:

$$E_n = E_{0n} + 10 \log B \quad \text{dB} \tag{7.8}$$

   where: E_{0n} = noise field in dB related to 1 μV/m for a passband of 1 Hz

   B = passband in Hz

2. in watts per unit surface, or per unit angle
3. in equivalent absolute temperature. This is the temperature of a black body radiating the same power over the same passband at the same

frequency by thermal radiation. Since cosmic noise does not possess the same spectrum as a black body, the equivalent temperature is frequency dependent.

These last two units are most often used for very short waves. It is quite easy to pass from one system of units to the other.

The measurement result depends to a great extent on the directivity of the receiving antenna, because cosmic noise has preferred direction.

Intensity

There are two cases:

Antenna with little directivity

In this case the cosmic noise value is nearly constant. The sum of all measurements—which are well coherent—gives the following mean value of cosmic noise:

$$E_n = -47 + 10 \log B - 1{\cdot}5 \log f \qquad (7.9)$$

(in dB referred to 1 μV/m)

where f = frequency in MHz

B = passband of receiver in Hz.

Antenna with high directivity

(With a beam at half power points of less than 15–20°). A very distinct maximum is observed in a direction whose equatorial coordinates are those of the assumed centre of the Galaxy (R/A = 17 h 30 min; $D = -30°$).

Since the antenna is involved in the diurnal motion, its beam will describe a circle on the stellar sphere. This circle will pass more or less closely to the region of maximum noise, according to the declination of the antenna. Cosmic noise will therefore pass each day through a maximum at the same sidereal time.

Here the value of maximum cosmic noise is the most important factor in the prediction of communications. An approximate value can be established by using the nomogram of Fig. 68. We find on the left hand side the intersection of the latitude curve for the place of reception and the azimuth angle towards which the receiving antenna is turned (counting from the north in a direction to give $\leq 180°$). The intersection of a horizontal line drawn through this point with the curve at the relevant frequency gives the value, of 10 log T_{max} which can be read from the horizontal scale on the right hand bottom side.

This temperature can be converted to power by using equation (7.2). It can also be converted to equivalent noise field by equations similar to (7.5) and (7.6).

7.2.1.5 Specific extraterrestrial noise sources

Apart from cosmic noise, there are other sources of noise in space: the sun, certain stars, and invisible heavenly bodies called radio stars.

Radio astronomy—the study of the radiation of astronomic bodies—is still in its infancy.

Generally speaking, these phenomena do not affect radio transmissions. However, certain solar disturbances can cause rather strong noise between 30 and 300 MHz. Radar operating in this band is affected by this noise.

The equivalent field can attain 1 or 2 μV/m, i.e. of the same order of magnitude as the equivalent field of cosmic noise.

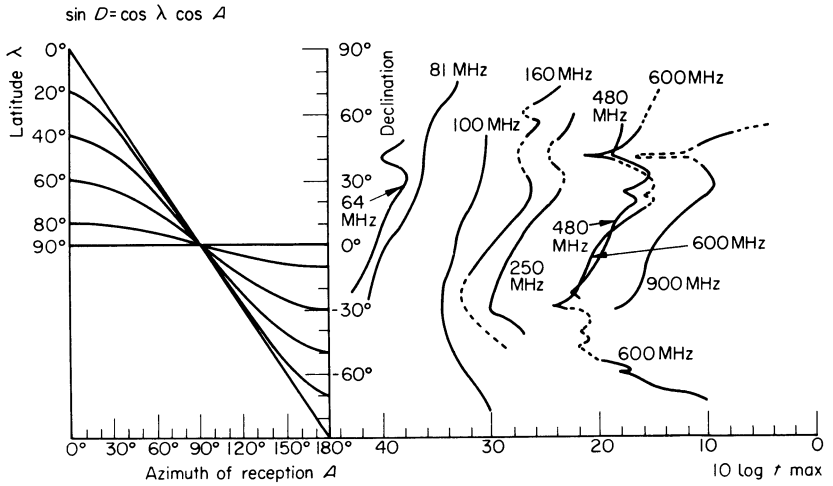

Fig. 68

7.2.1.6 Industrial noise

In contrast with other types of noise, industrial or man made noise is much more a form of shot noise. Definition of its characteristics is very difficult. However, the vertical component of its field is generally stronger than the horizontal one, so that horizontal antennae are less subject to industrial noise. The effective range of this noise is of the following order of magnitude:

Electric motors	200 m
High voltage power lines	1 to several km (especially when it is raining)
Motorcars	500 m
Aircraft	1 km

Radio stations should therefore be installed away from roads and airports at a distance exceeding the figures given above.

7.2.1.7 **Composition and comparison of different types of noise**

Noise emanating from different sources is combined in the receiver and gives a total noise output. Since noise currents possess random phase, their energies (proportional to their squares) are summed. As we have seen in Section 7.1.1.1, the different types of noise will only combine to give a larger figure if their intensities are more or less identical. If not, only the strongest will appear to exist.

This makes it important to know, in each case, the source of the greatest noise. Figure 69 gives a survey of the problem for a band width of 6 kHz (A_3).

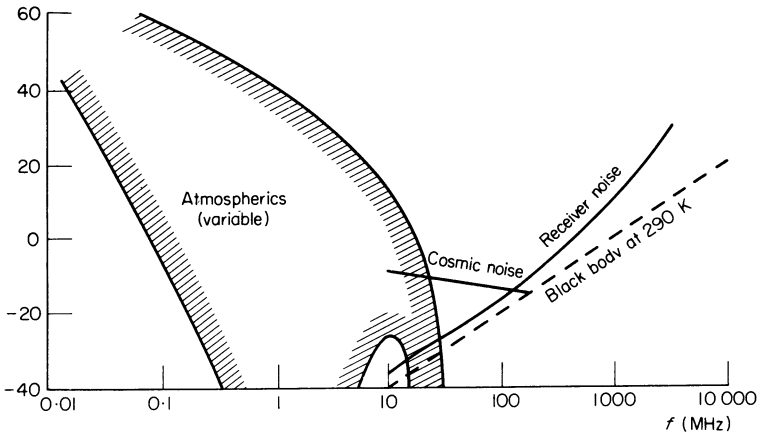

Fig. 69

Among different types of natural noise, atmospheric noise usually prevails up to 20 MHz, followed by cosmic noise up to 100 MHz (which can be stronger at certain times if the antenna is strongly directive). Finally, receiver noise dominates all other noise at very high frequencies.

7.2.1.8 **Calculating total noise**

Practical methods for calculating total noise are described in Chapter 8.

7.2.2 REQUIRED SIGNAL-TO-NOISE RATIO

7.2.2.1 **Service grade and signal-to-noise ratio**

Whether reception is aural or mechanical, it is only possible when the signal can be distinguished from the noise, which obviously requires a sufficiently high signal-to-noise ratio.

More specifically, on increasing the signal-to-noise ratio from zero, we arrive at a threshold value where the signal is just apparent, but not good enough for use. Continuing the increase of the signal-to-noise ratio, the number of reception errors is reduced, at first rapidly, then increasingly slowly, so that eventually a very small error percentage can only be achieved at the cost of a considerable increase in signal level.

Moreover, the required signal-to-noise ratio varies with the type of service. For example, the human ear, thanks to the mechanisms of attention and intelligence, allows us to distinguish signals in the noise which mechanical receivers would be quite unable to distinguish. The latter, in turn, are more or less sensitive to the effect of noise, according to the modulation mode used, the receiving system, and the mechanism of reconstructing the signal.

Similar considerations apply to jamming and interference by transmitters outside the communication network.

Therefore, the required signal-to-noise ratio depends on the required reception quality (service grade), and the type of equipment.

7.2.2.2 **Effect of field fluctuations**

The problem is complicated by the fact that the noise field fluctuates, and that its distribution function varies according to the type of noise. Both signal and inteference source can also be affected by fading—with various distribution functions.

From an operational standpoint, it is requested to have a signal that can be used during a given percentage of the time (time availability), which must be higher when the service must be of better quality. We assume that the distribution functions of noise and signal are known. We must now determine the relation between their r.m.s. values, so that the ratio of their instantaneous values remains higher than the required minimum value for the required part of the time.

This is a problem in probability calculation. Without it being necessary to resolve the problem explicitly, it is obvious that the ratio of the effective signal value to the noise must be greater in the case of fluctuating fields than in that of stable fields. We must therefore set aside a fading margin. This margin must be greater according as the service must be maintained for a longer part of the time.

The required margin will be greater in the case of unstable fields (ionospheric propagation of decametre waves) than when the fields are stable (ground wave or line-of-sight propagation of microwaves). It must be much greater if noise is very variable (waves with a frequency of less than 30 MHz).

7.2.2.3 Methods for calculating the required signal-to-noise ratio

The CRPL method[7]

As we have seen, noise is defined by the signal field required in the presence of noise for a certain type of service. The field value thus determined by CRPL includes a safety margin against fading; there is therefore no need for adding a separate margin.

The reference type of service is double sideband telephony (A3), i.f. receiver pass band 6 kHz, 90 per cent intelligibility for 90 per cent of the time (the standard corresponding to a good telephone conversation).

For determining the required field for another type of service, a correction is applied to the field required for telephony, expressed in dB. This method has the advantage of simplicity.

The CCIR method[416,417,418,419]

CCIR has conceived a more accurate method, which will undoubtedly be the only one used in the future. With this method we determine:

1. the required signal-to-noise ratio for the case that both signal and noise are constant, and for a given service grade.
2. the safety margin against fading in the case of decametre waves.

Instructions for using this method will be found in Chapter 8.

7.2.3.3 Effect of receiving antenna

The gain of the receiving antenna affects the signal-to-noise ratio in a more complex manner than at the transmission end, where the transmitted power is proportional to antenna gain. This is due to the presence of external noise sources.

Signal-to-noise ratio with nearly constant directivity

When varying the gain of the receiving antenna without appreciably modifying its directivity diagram (e.g. a short vertical antenna of adjustable length), the energy of both signal and external noise will vary in accordance with the antenna gain.

On increasing the gain from zero (Fig. 70), as long as the external noise supplied by the antenna is distinctly weaker than the internal noise of the receiver, the total noise will be virtually equal to the latter. On the other hand, the signal will be increased in proportion to the gain. The signal-to-noise ratio is therefore proportional to the gain.

But if the gain has attained a value which is sufficient to make the external noise definitely greater than the internal noise, the latter will no longer play

any part; signal and noise will increase in proportion, and their ratio will be constant.

There must therefore be a limit for an antenna with a given directivity, above which no improvement in the signal-to-noise ratio will be observed when antenna gain is increased. This explains why little attention is paid to the antenna and its matching to the receiver when receiving waves with a frequency of less than 30 MHz.

Discrimination gain

Generally speaking, the gain of directional antennae is not the same for the signal and for atmospheric noise. Indeed, the antenna is obviously orientated in such a direction that the waves arrive in a direction close to a maximum in the directivity diagram. If the noise does not mainly arrive in a direction close to a maximum in the diagram, the gain will be greater for the signal than for the noise.

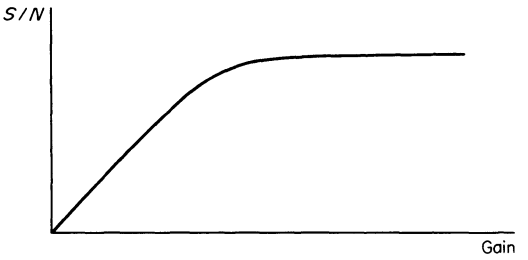

Fig. 70

External noise usually arrives from all directions. Assuming that its intensity does not depend on direction, the discrimination gain can be defined as the gain in signal-to-noise ratio due to the receiving antenna.

Discrimination gain is expressed in dB and is the difference between the gain of the antenna used (calculated as for transmission) and the gain of an isotropic antenna (imaginary antenna with a spherical directivity diagram), situated at the same point and having the same direction of polarization; because of the presence of the ground, the latter depends on the elevation angle Δ of the waves. Discrimination gain can be higher or lower than the gain of the transmitting antenna. The actual discrimination gain is lower than the calculated value during periods of poor propagation conditions[426].

Calculating gain at the receiver

Decametre and longer waves. We must first calculate the various types of noise and see which one is the strongest.

If system noise dominates, the antenna gain is the same as on transmission duty.

If external noise dominates:

1. if the antenna possesses weak directivity (linear or L-antenna), discrimination gain is virtually zero. This means that if a simple antenna produces external noise in the absence of a signal, which is distinctly greater than the receiver noise, reception cannot be improved by improving the antenna
2. if a directional antenna is orientated towards a noise source (especially frequent in tropical regions), discrimination gain is still zero. In this case, the use of a directional antenna is generally of no practical advantage
3. in the case of a strongly directional antenna (rhombic), we must subtract algebraically the gain of the antenna when transmitting expressed in dB the gain in dB of the isotropic antenna with horizontal polarization, situated at the same height H as that of the actual antenna. Finally, it is convenient to subtract 6 dB from the obtained value[426], to take periods of poor reception into account.

Metre and shorter waves. Because of the small value of cosmic noise it is usually possible to take the gain on reception the same as on transmission. However, in the case of propagation by tropospheric scattering, the antennae may undergo an antenna-to-medium coupling loss (Section 2.3.2.2).

7.3 CALCULATING THE MINIMUM REQUIRED FIELD

In order to determine the minimum required field, we must:

1. Calculate the fields equivalent to the various types of noise, and combine them if necessary.
2. Add to the thus calculated noise the signal-to-noise ratio required for the type and grade of service in question, as well as the fading margin which corresponds to the required time availability.
3. Subtract from the result the gain of the receiving antenna.

Practical calculation methods and corresponding numerical data will be found in Chapter 8.

CHAPTER 8

PRACTICAL CALCULATION OF RADIO LINKS

8.1 INTRODUCTION

The theory of the propagation conditions discussed in the previous Chapters must lead to numerical results, which can be put to practical use for the establishment of radio communications. This is the purpose of this chapter.

8.1.1. RELATIVE VALUE OF PROPAGATION CALCULATIONS

These calculations are based on the median values of certain physical quantities (fields, noise, etc.), but the latter sometimes show considerable variations around these median values. For example:

1. atmospheric noise varies considerably from day to day
2. ionospheric characteristics are unforeseeably affected by perturbations
3. it is extremely difficult to give an exact definition of the terrain (conductivity, shape)
4. meterological conditions change all the time.

We should therefore be careful not to attribute an absolute character to the results obtained, which they do not possess. Let us mention in this respect that:

1. predictions give the best chance of achieving a good communication; the probability of this result is high. However, there are cases when communication is simply impossible, although all the predicted conditions are present
2. if the case presents itself for ground wave propagation, and more especially for tropospheric wave propagation, one should always try moving one or both of the communicating stations. A displacement of a few dozen metres can make a very great difference to the quality of the communication, in a manner which cannot be foreseen. This is due to local reflections, which produce standing waves
3. if communication is essential (life saving, military operations, etc.) one should always attempt to establish it, even if theoretically impossible. It is always possible that thanks to a fortunate combination of circumstances, the link can be established. As far as we know at

present, calculation cannot be opposed to need, unless confirmed by a test. However, the fact that a communication operates in an acceptable manner for a few hours or a few days does not guarantee that it will operate continuously

4. it is entirely useless to try imparting in the calculations a higher degree of accuracy than shown in the graphs of this chapter. Fractions of decibels, in particular, are completely useless.

8.1.2 GENERAL CALCULATION METHOD

Communication is only possible when the ratio of the field received to the background noise is in accordance with or exceeds that required by the specific type of communication (telegraphy, telephony, etc.). The factors of the calculation will therefore always be the same:

1. transmitter power
2. transmitting antenna gain; gain (or discrimination gain) of the receiving antenna
3. attenuation due to the path
4. receiver noise
5. atmospheric noise (below 30 MHz); cosmic noise (below 200 MHz); industrial noise (below 500 MHz)
6. type of service.

Only the manner of determining these factors varies with the frequency range.

This chapter contains graphs with the aid of which these determinations can be carried out. The use of these graphs is explained in the following sections.

8.1.3 UNITS

In order to facilitate the calculation of the field received (or of the power received), all values playing a part in the calculation are expressed in logarithmic units (decibels).

In the case of decametric (h.f.) and longer waves:

1. the transmitted power is expressed in dB in relation to 1 kW
2. fields are expressed in dB in relation to 1 μV/m for a power of 1 kW radiated by an elementary vertical dipole at ground level
3. antenna gain is related to the $\lambda/2$ antenna.

In the case of metric (v.h.f.) and shorter waves:

4. transmitted and received powers are expressed in dB in relation to 1 W
5. antenna gain is related to the isotropic antenna. If it is necessary to relate this gain to the $\lambda/2$ antenna, subtract 2 dB.

8.1.4 SOURCES OF DATA

1. Data on atmospheric noise have been taken from CCIR Report 322[419]
2. the field relations for the various types of communication have been derived from CCIR Recommendation 339–1[416]
3. data on the ionosphere wave have been taken:
   for the MUF from NBS Handbook No. 90[18]
   for field strength from NBS Circular 462[7]
4. antenna gains have been derived from Report No. 2 of the Radio Propagation Unit of the U.S. Army, or from calculations made by the author
5. field curves of the ground wave have been taken from CCIR Recommendations 368[214] and 370–1[138].
6. statistical distribution curves of the fields received by line-of-sight communication from CCIR Report 338
7. some data on the propagation of the tropospheric wave by diffraction have been adapted from papers by K. E. Bullington[101] and Dougherty and Maloney[221].
8. data on the propagation of the tropospheric wave by scattering have been taken from a very large number of papers published on this subject, particularly CCIR Report 244–1[139], the research carried out by CNET[166] and work done by the author.

Many other data and calculation methods have been published. We have adopted those that appeared to be the most certain, or the easiest to use. In particular, in accordance with the conclusions of CCIR report 252–1[356], we have preferred the method for calculating the field strength of the ionospheric wave described in NBS Circular 462[7] to the RPU method[20], because the latter, although less empirical and probably more accurate, leads to extremely long calculations, especially for great ranges.

8.2 DECAMETRIC (h.f.) AND LONGER WAVES

8.2.1 FIELD REQUIRED IN THE PRESENCE OF NOISE

We want to determine the minimum field required to ensure a particular service quality in the presence of noise from various origins. The most complex case is that of atmospherics, because of their variability both in space and time.

8.2.1.1 **Mean field of atmospherics**

The seasons shown in Figs 71–96 correspond to the months shown in Table 8.1.

TABLE 8.1

Month	Local season	
	Northern hemisphere	Southern hemisphere
December, January, February	Winter	Summer
March, April, May	Spring	Autumn
June, July, August	Summer	Winter
September, October, November	Autumn	Spring

Select from the above table and the desired time interval (00–04, 04–08, 08–12, 12–16, 16–20, 20–24 hours local time) the figure numbered between 71 and 96 that will be used. Locate on the chart at the place where the receiving station is situated the value of the mean noise factor F_{am} in dB above thermal noise at a frequency of 1 MHz.

Now select on the lower left hand graph of the same figure the curve identified by the same number as the noise parameter gained above. Fix the frequency for your calculation and you can read off the value of F_{am} in-ordinate at the intersection of chosen frequency and the curve selected.

The following footnotes apply to Figs. 71 to 96

F_{am} = median value of hourly values of F_a over a period of time
F_a = equivalent antenna noise factor resulting from the external noise power available from a loss-free antenna

——— atmospheric noise
—·—·— industrial noise
— — — — extraterrestrial noise

σ_{Fam} — standard deviation of F_{am} values
D_u — ratio of first decile (tenth percentile of the distribution; percentile is the distribution of a random variable) to median value of F_{am}
σ_{Du} — standard deviation of D_u values
D_l — ratio of median value of F_{am} to last decile
σ_{Dl} — standard deviation of D_l values
V_{dm} — expected value of median deviation from the average potential (bandwidth 200 Hz)

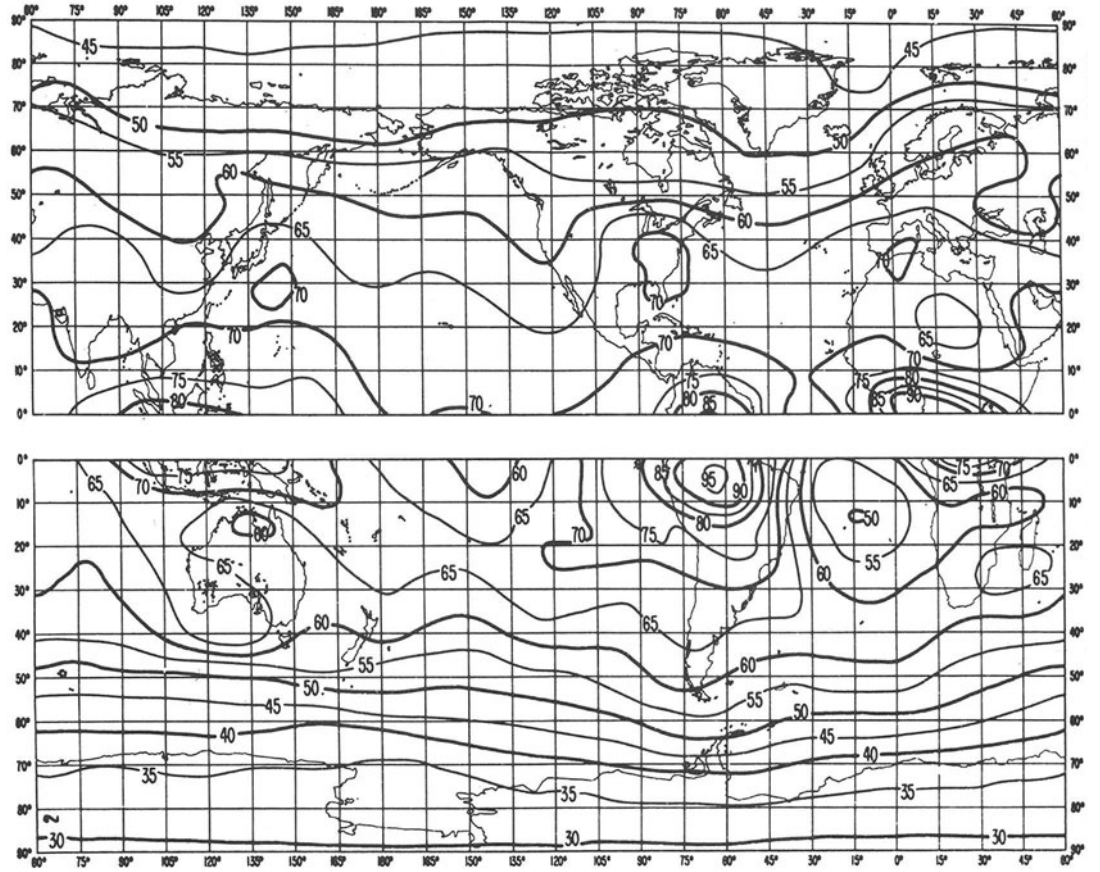

Fig. 71 Winter; between 0000 and 0400 h

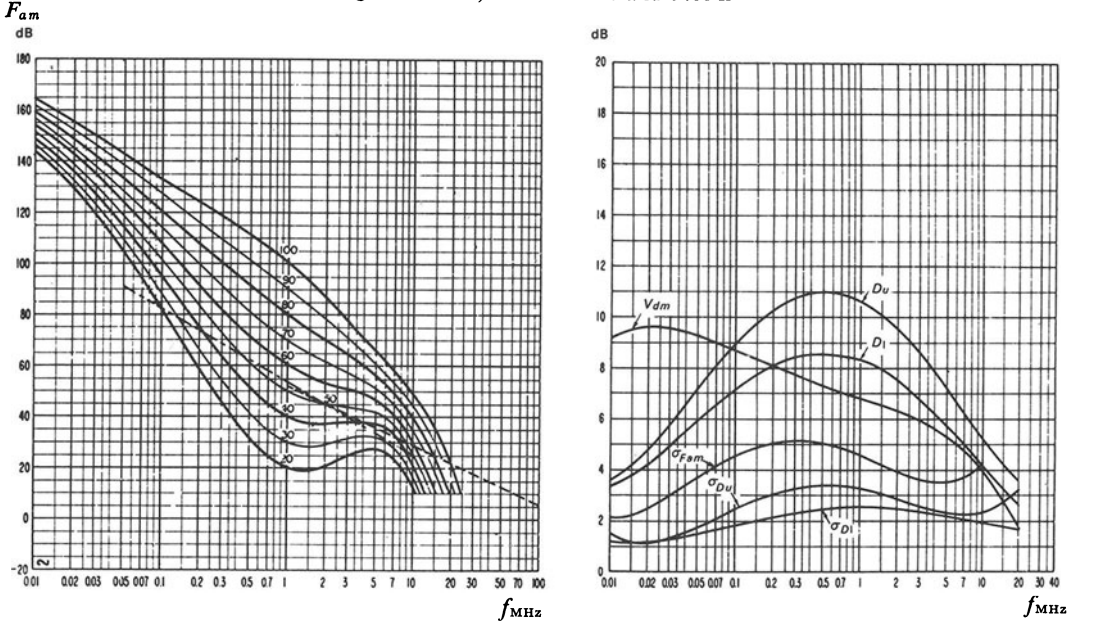

Fig. 72 Winter; between 0000 and 0400 h

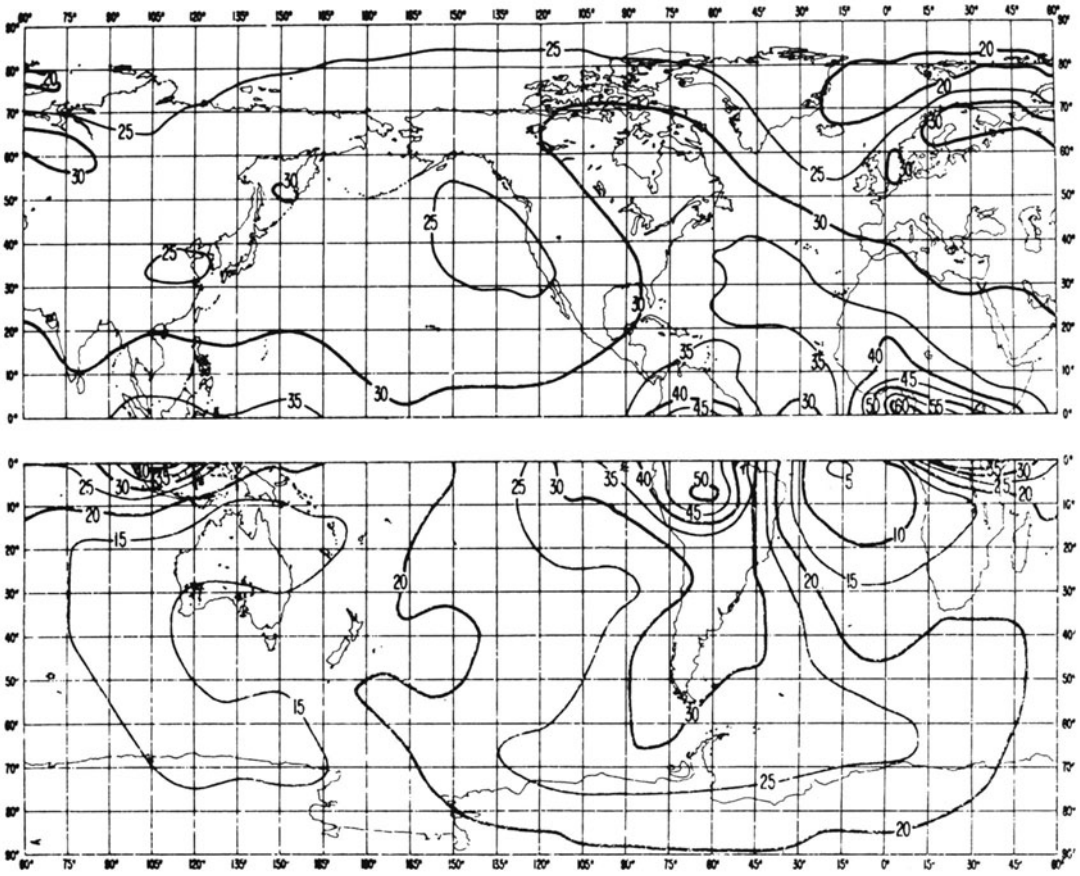

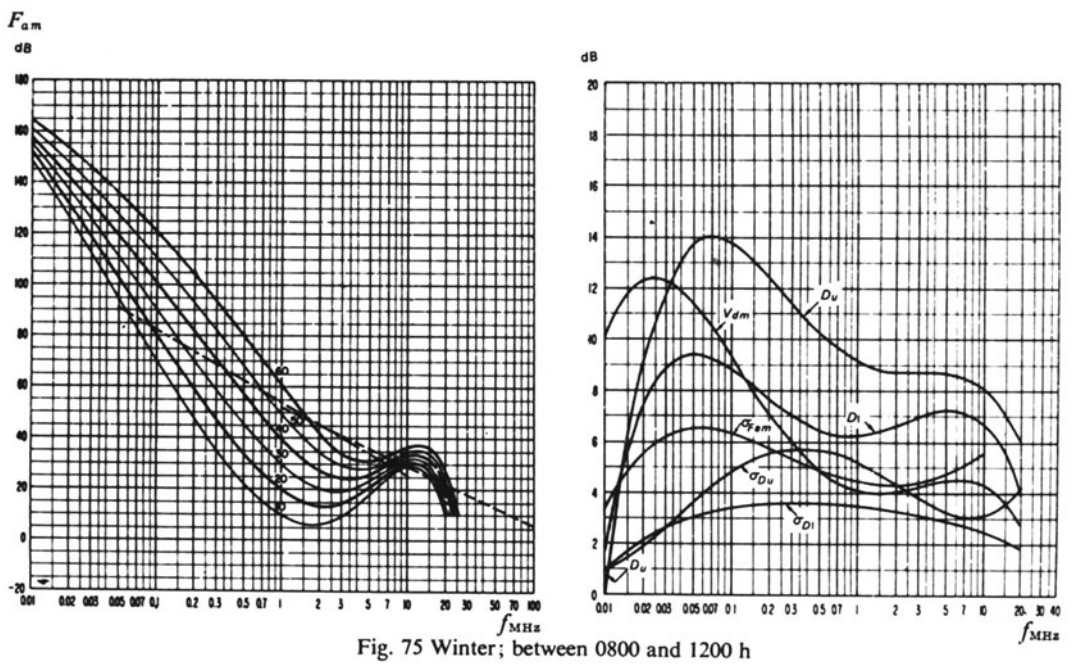

F_{am}

Fig. 75 Winter; between 0800 and 1200 h

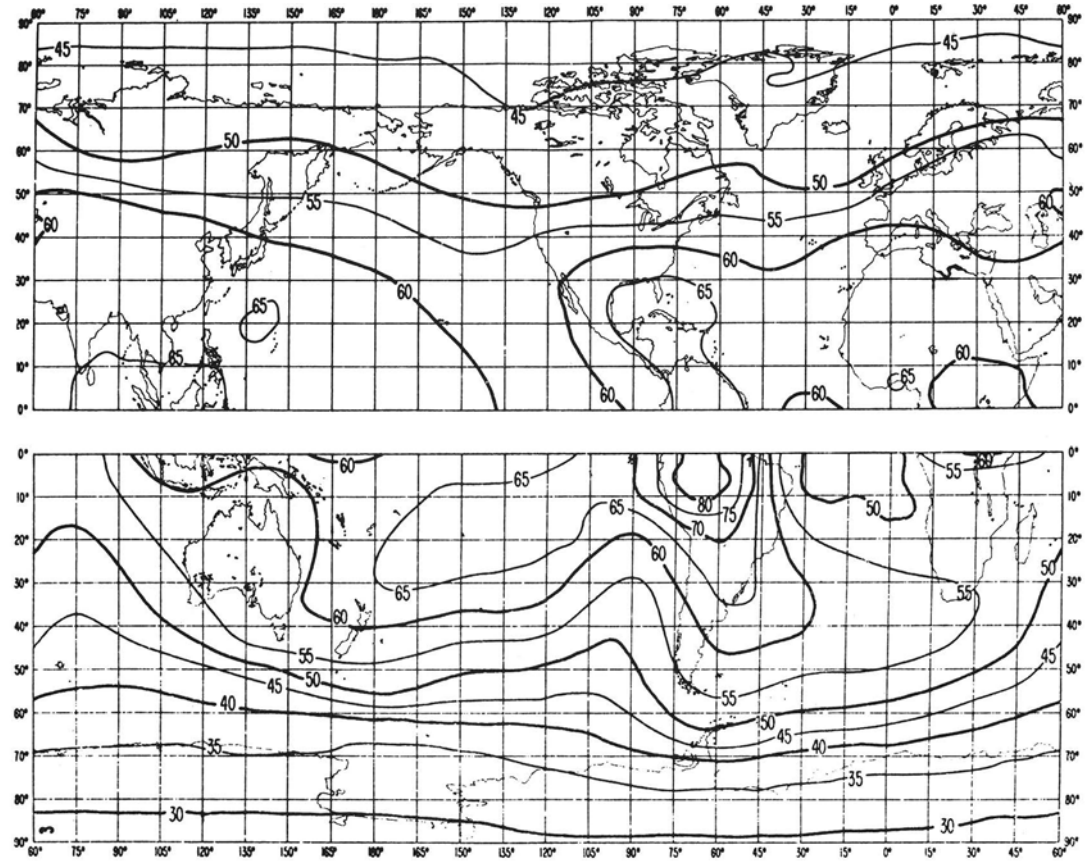

Fig. 73 Winter; between 0400 and 0800 h

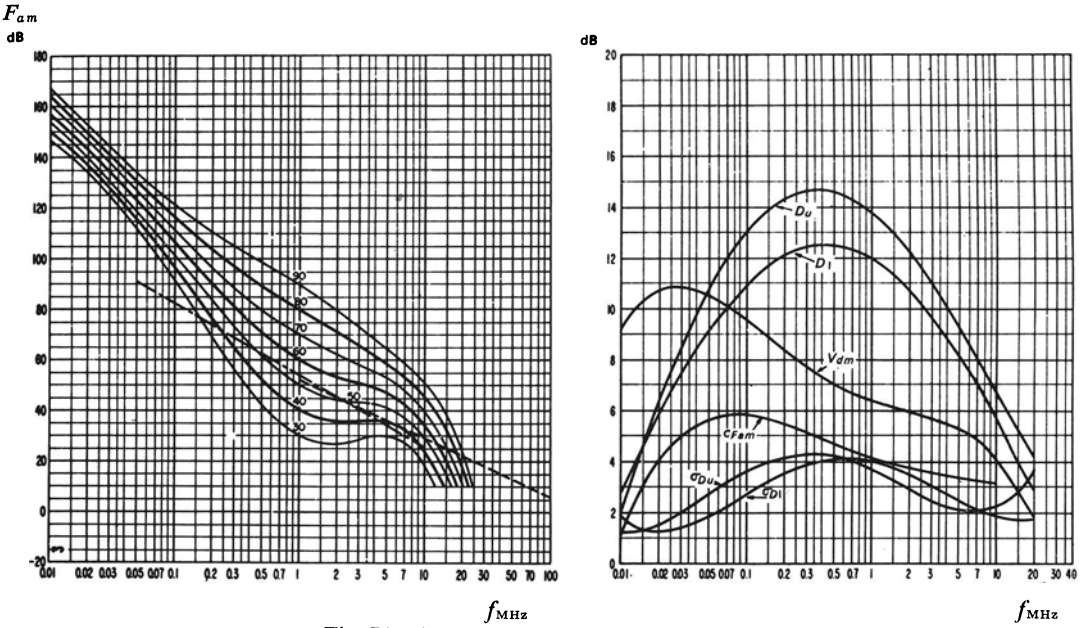

Fig. 74 Winter; between 0400 and 0800 h

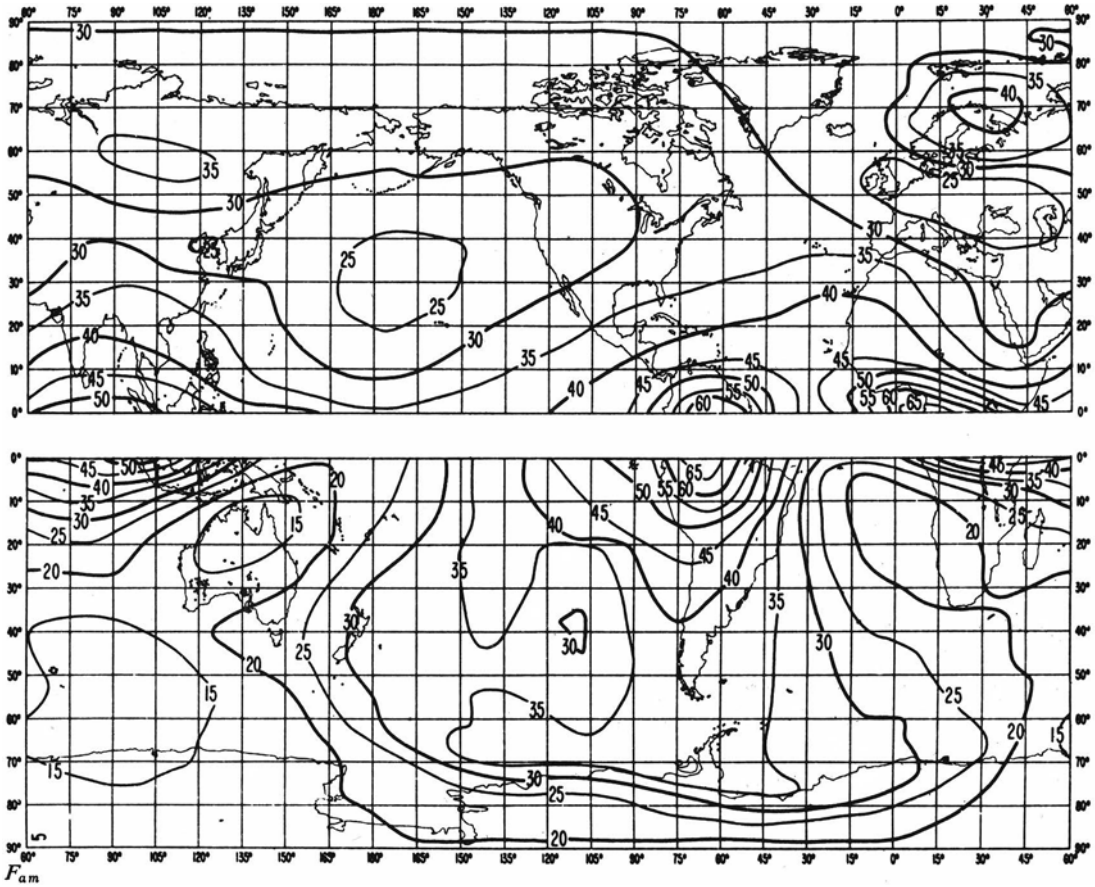

F_{am}

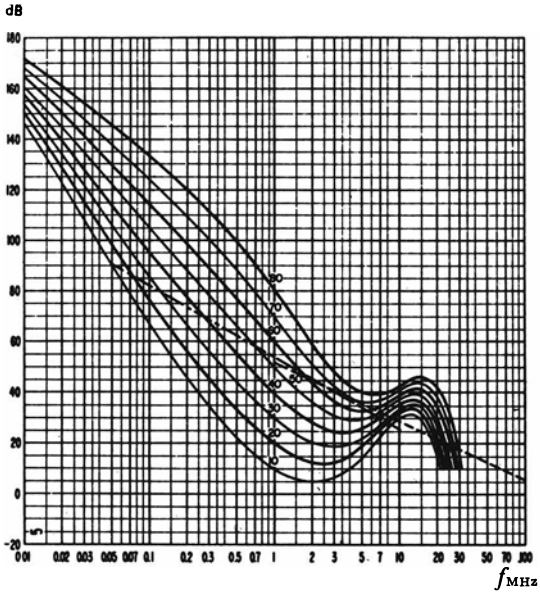

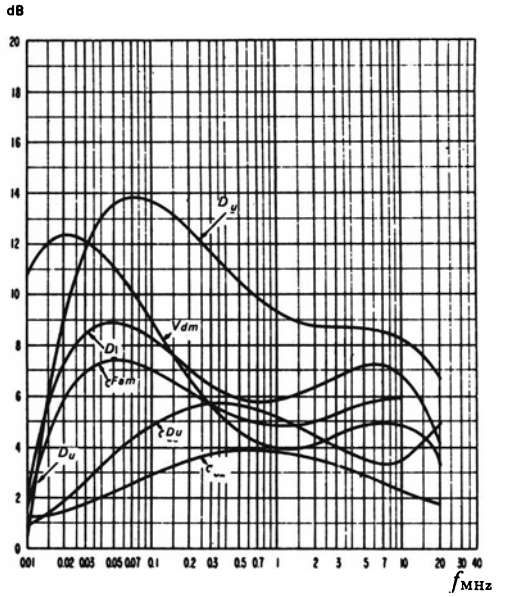

Fig. 76 Winter; between 1200 and 1600 h

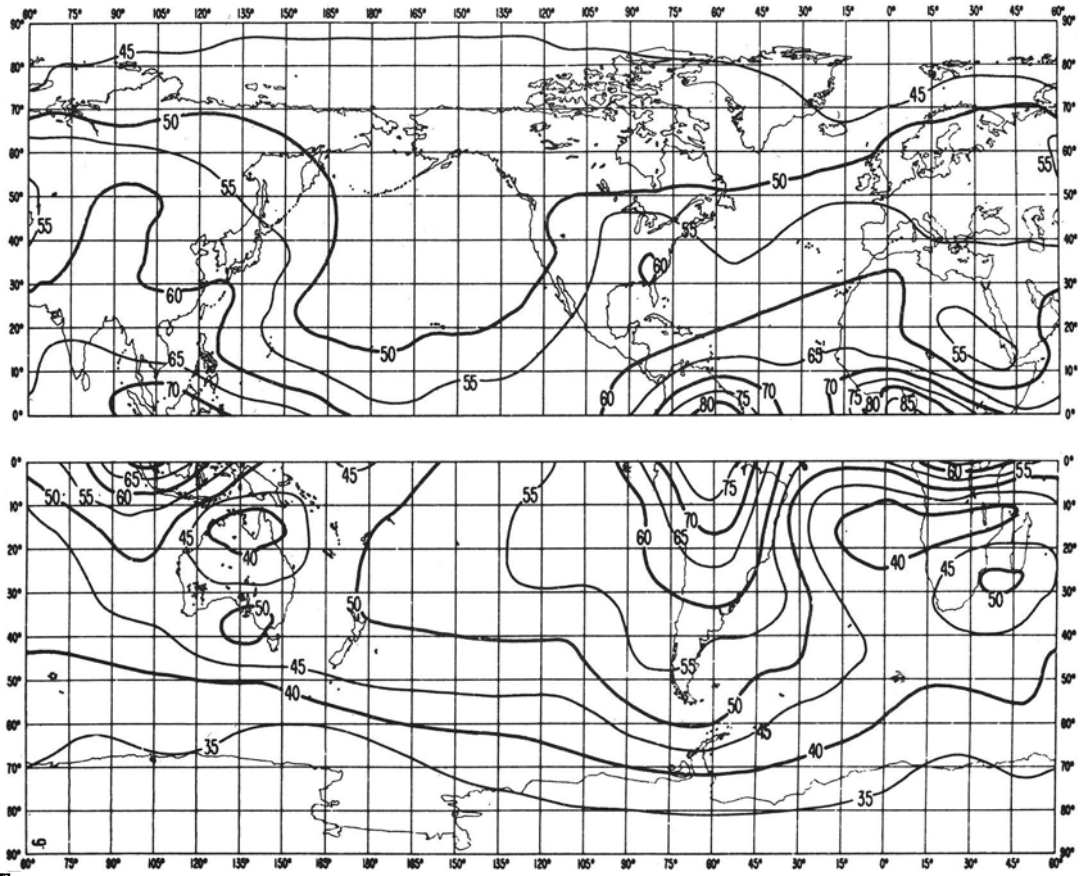

F_{am}
dB

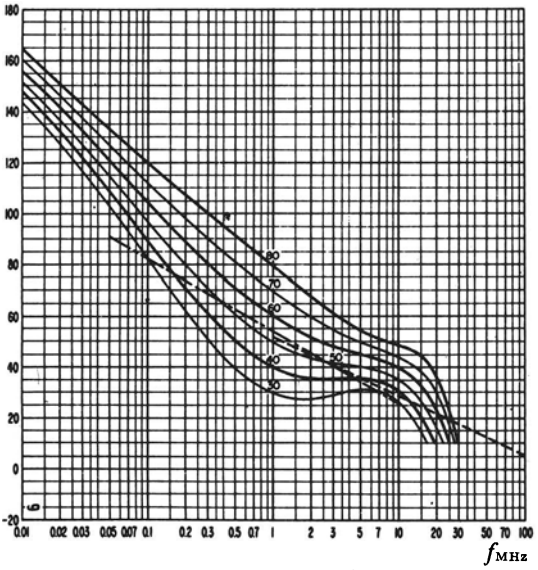

f_{MHz}

dB

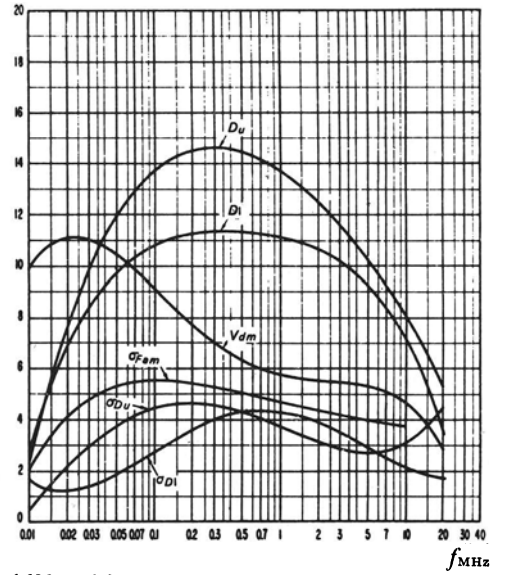

f_{MHz}

Fig. 77 Winter; between 1600 and 2000 h

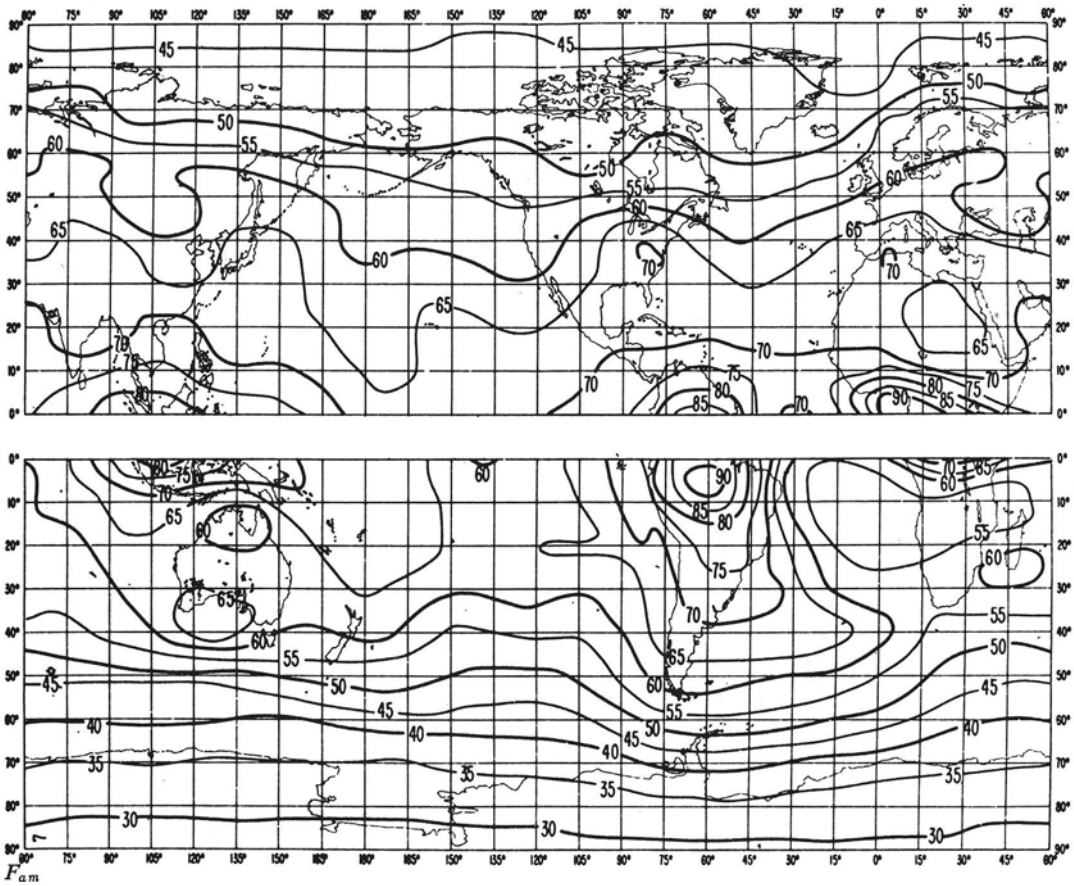

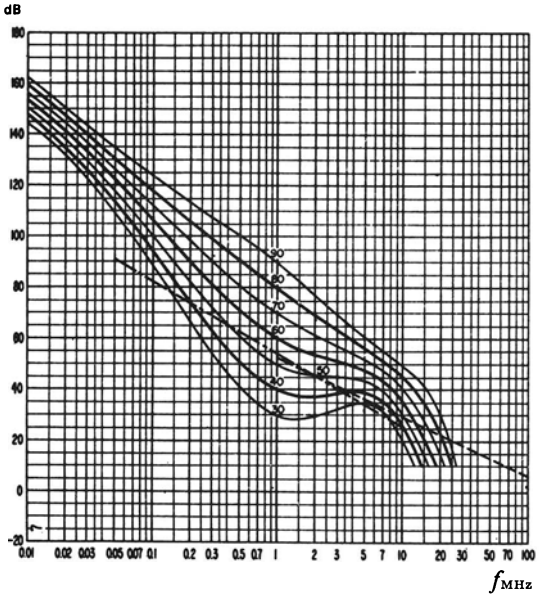

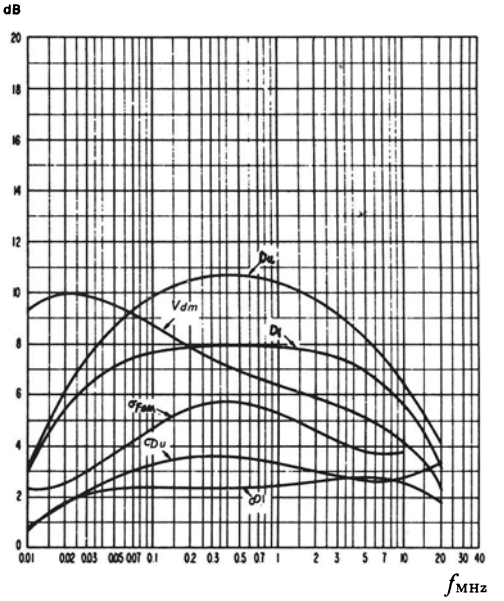

Fig. 78 Winter; between 2000 and 2400 h

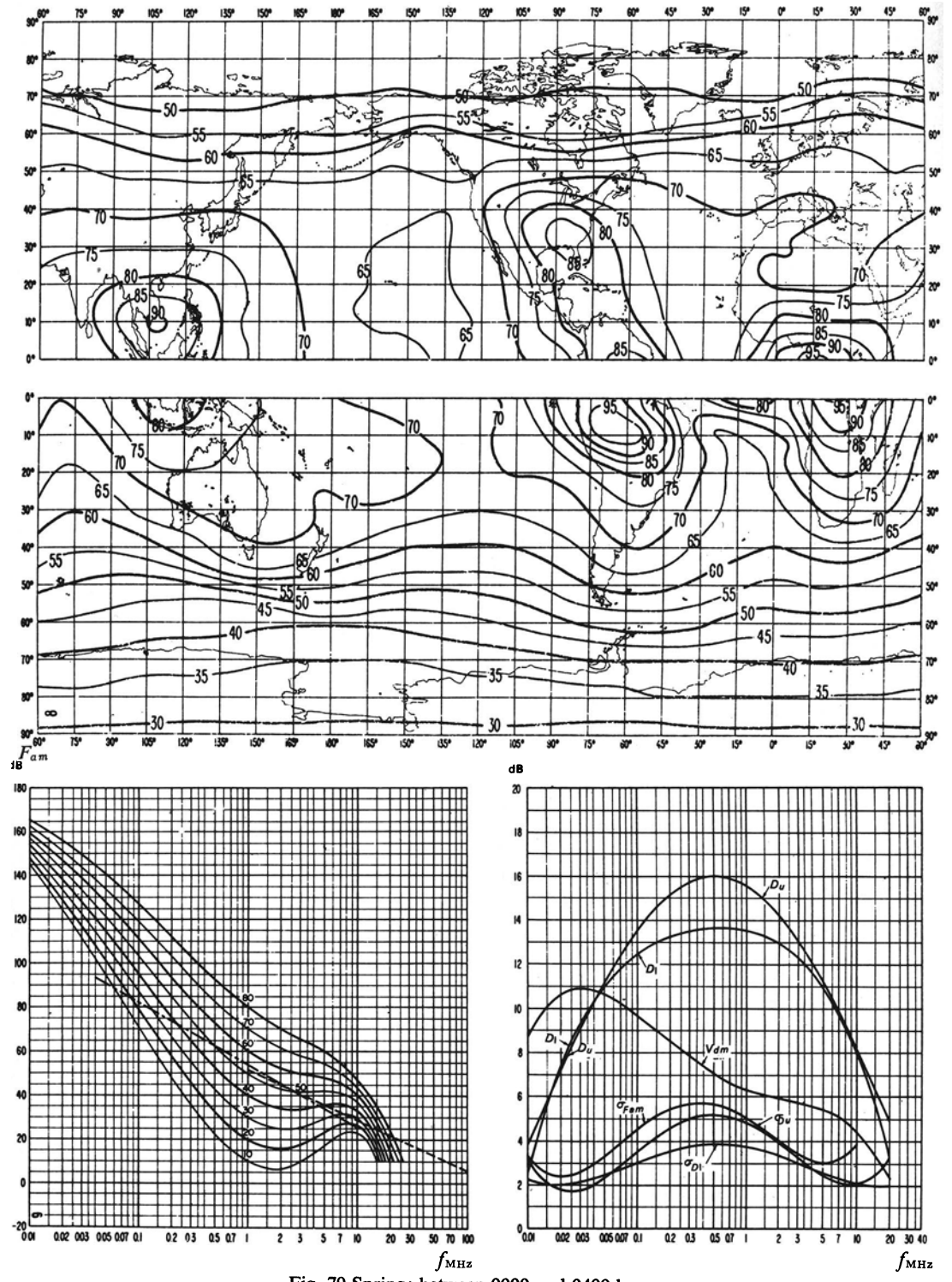

Fig. 79 Spring; between 0000 and 0400 h

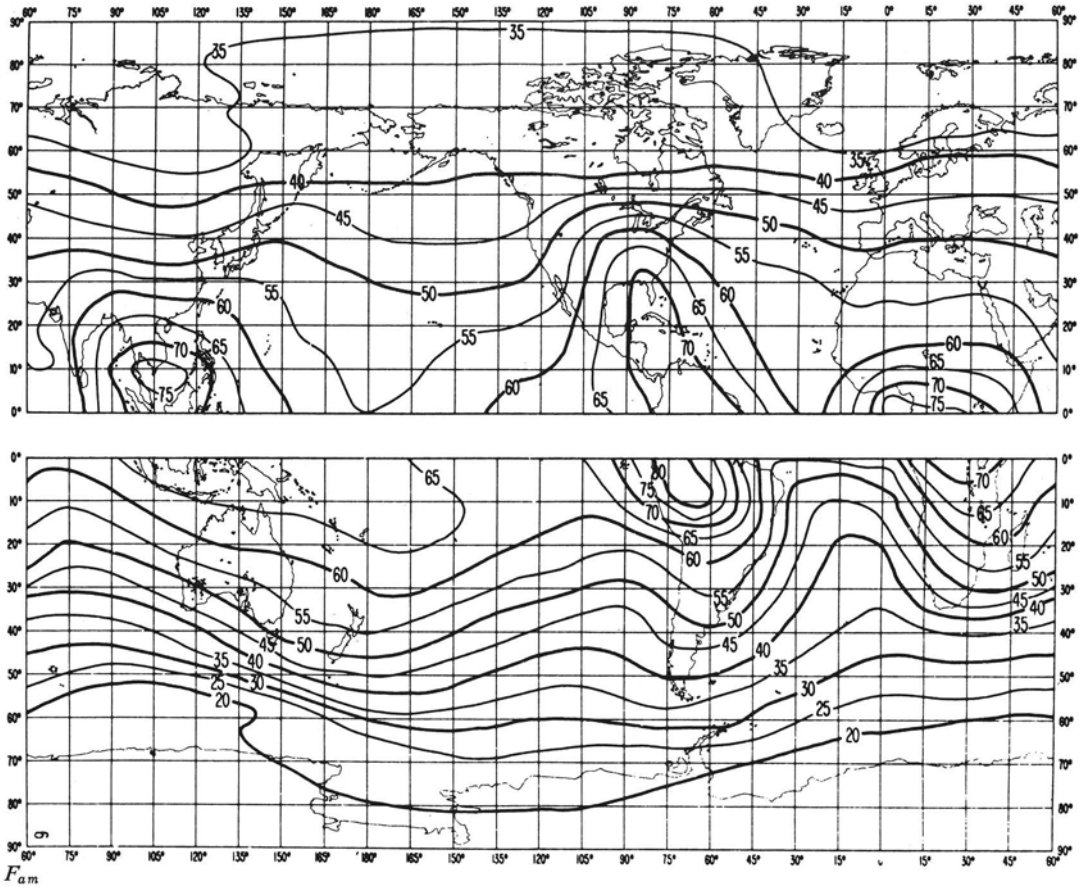

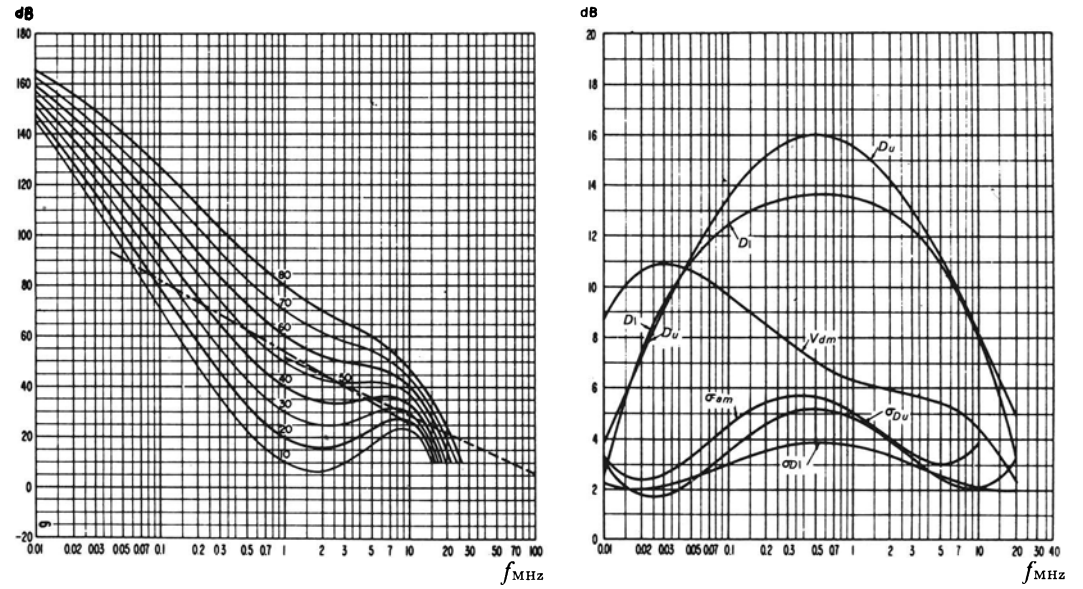

Fig. 80 Spring; between 0400 and 0800 h

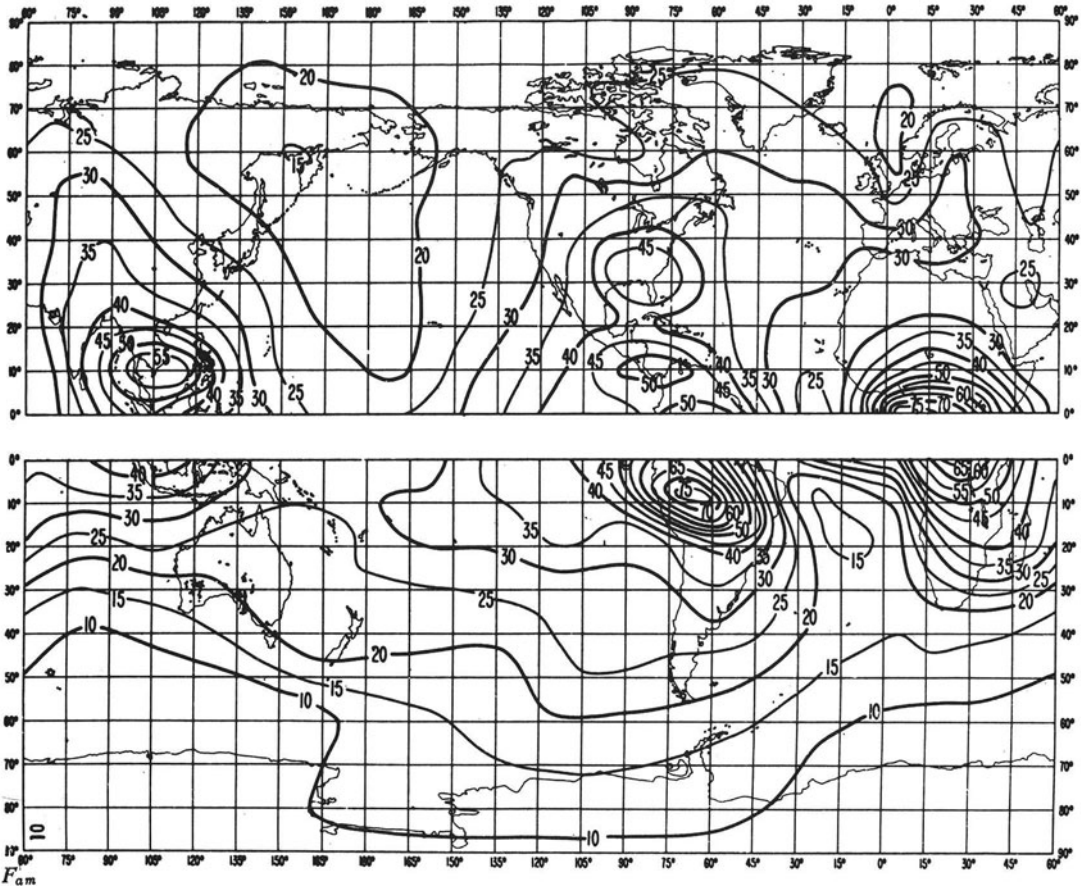

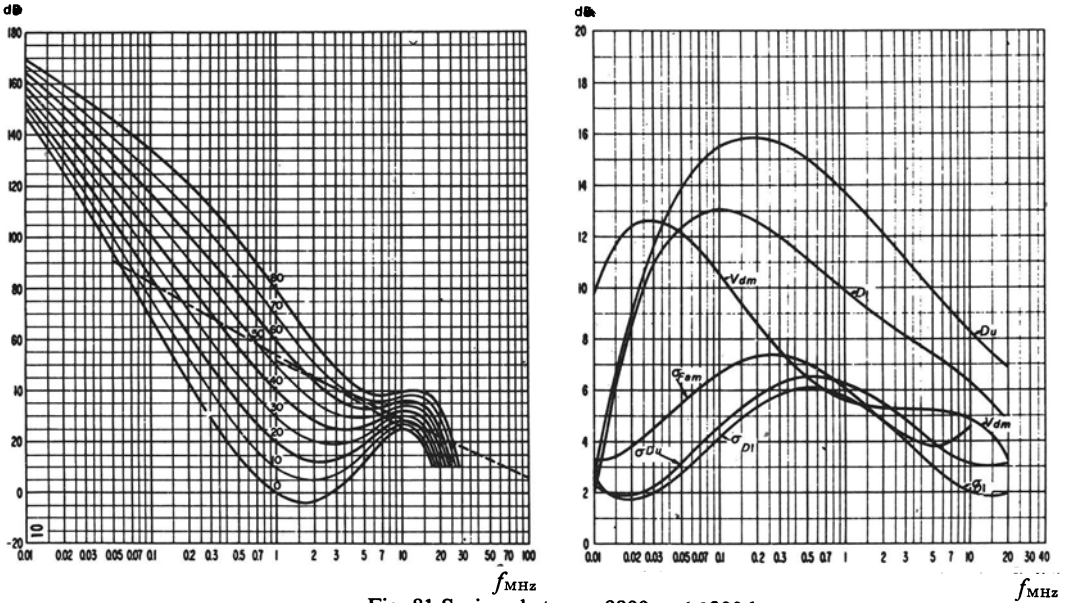

Fig. 81 Spring; between 0800 and 1200 h

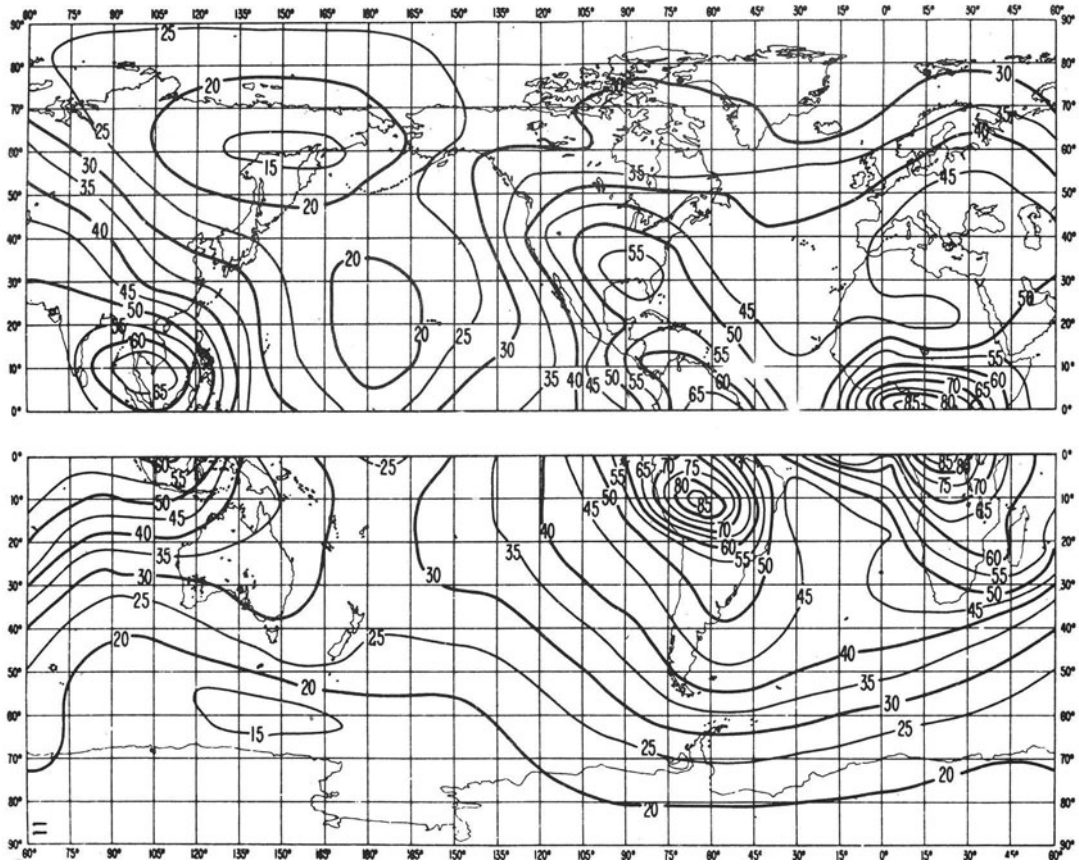

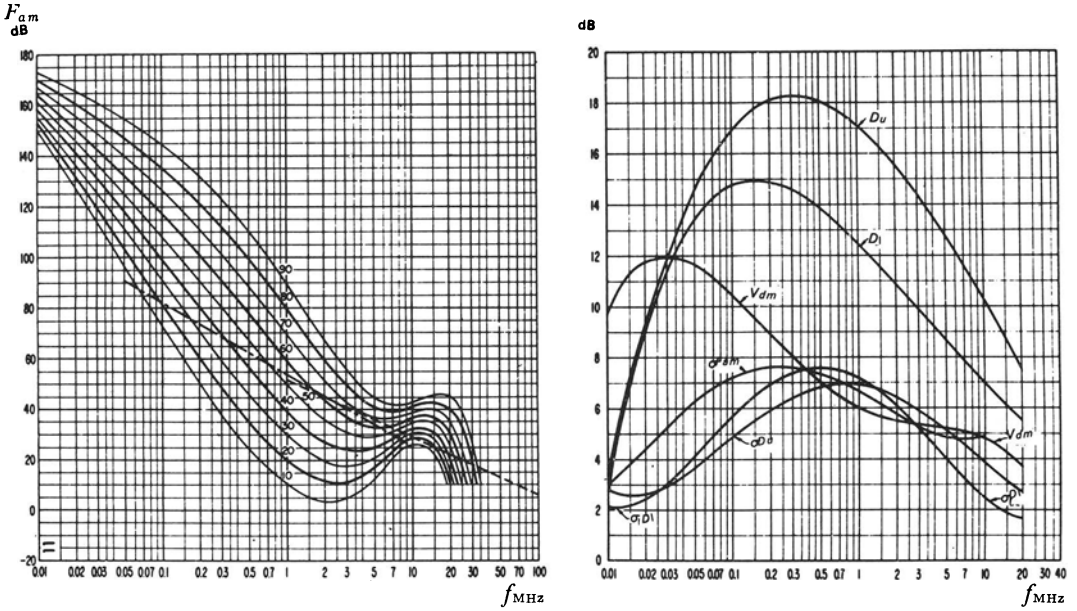

Fig. 82 Spring; between 1200 and 1600 h

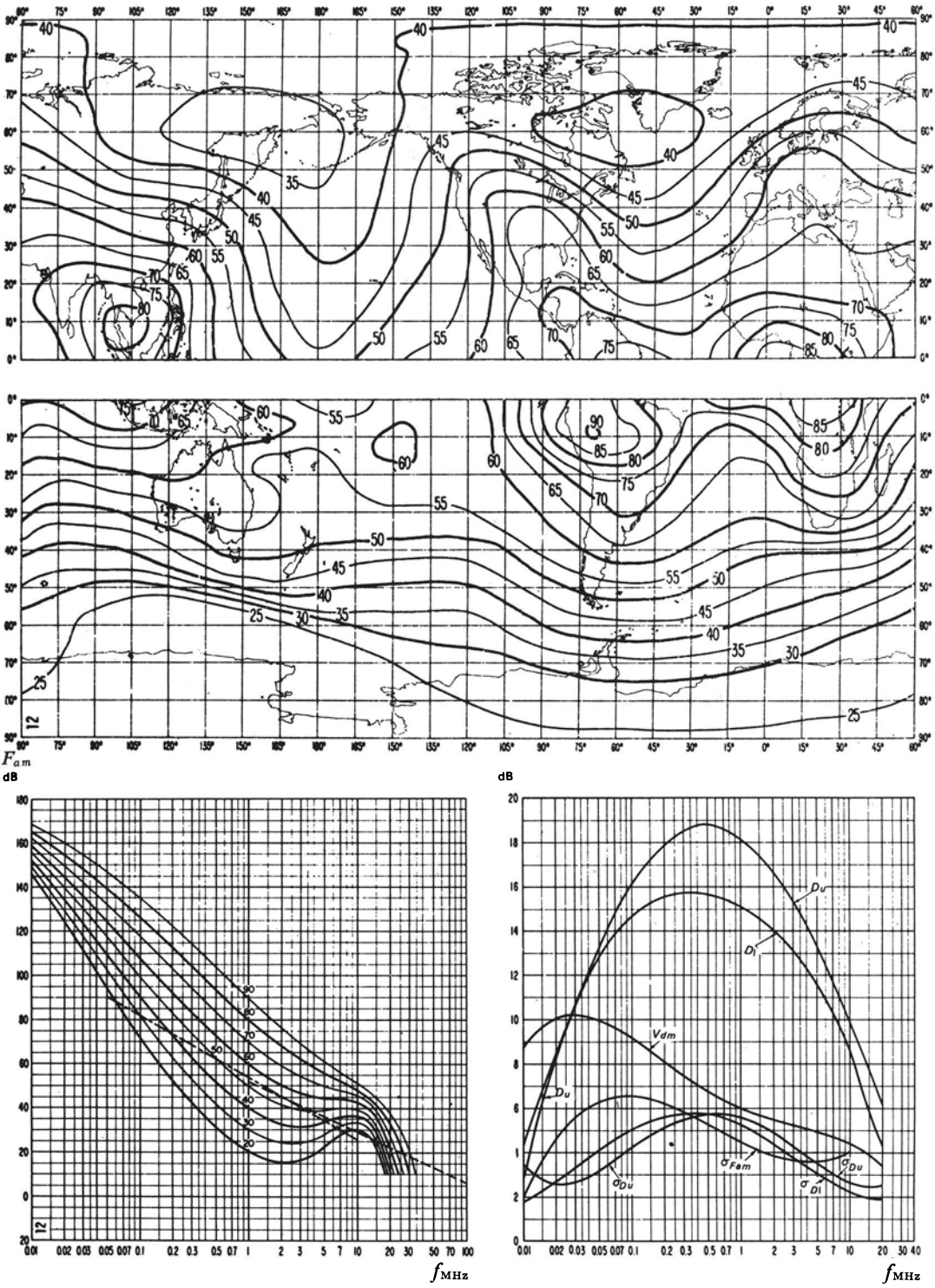

Fig. 83 Spring; between 1600 and 2000 h

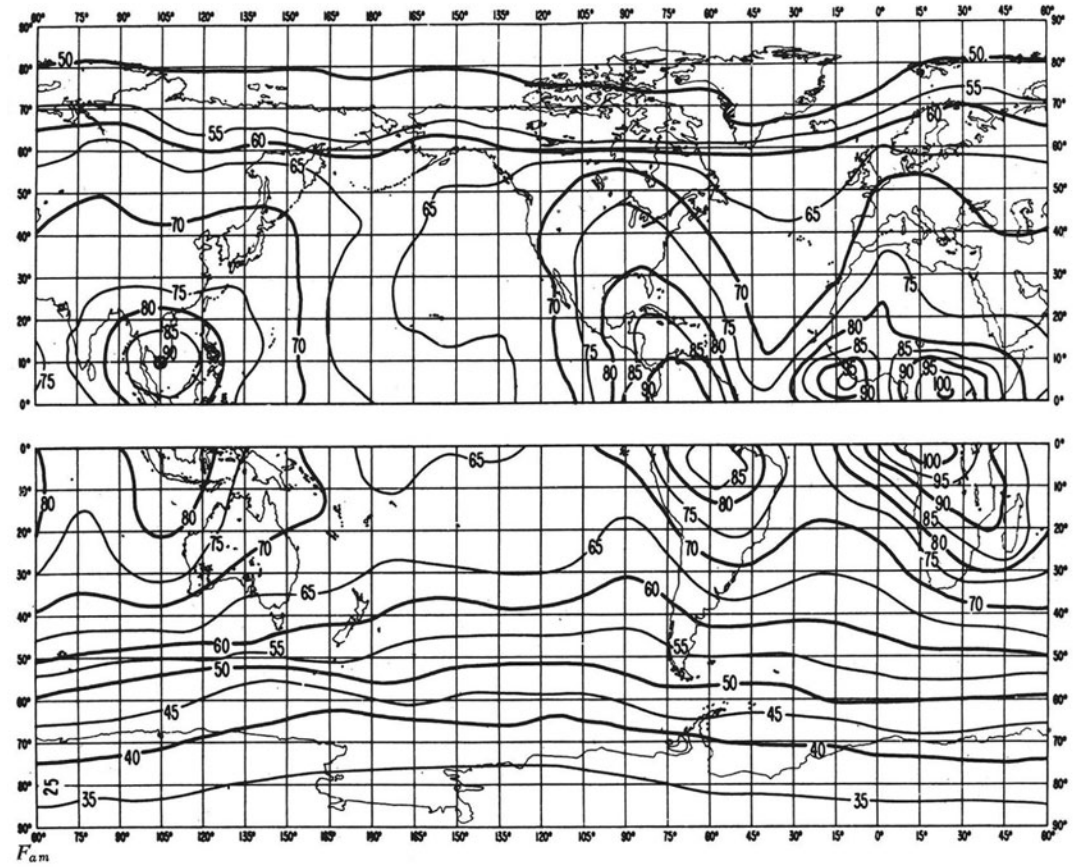

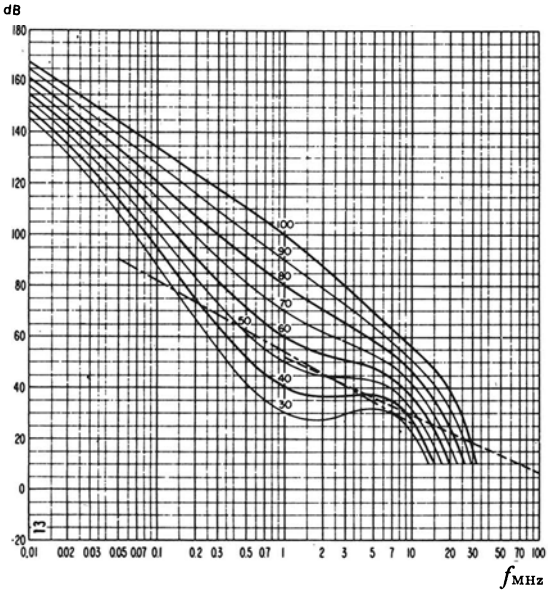

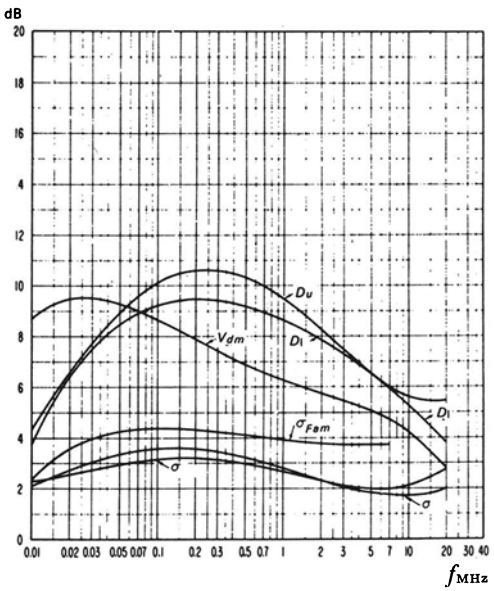

Fig. 84 Spring; between 2000 and 2400 h

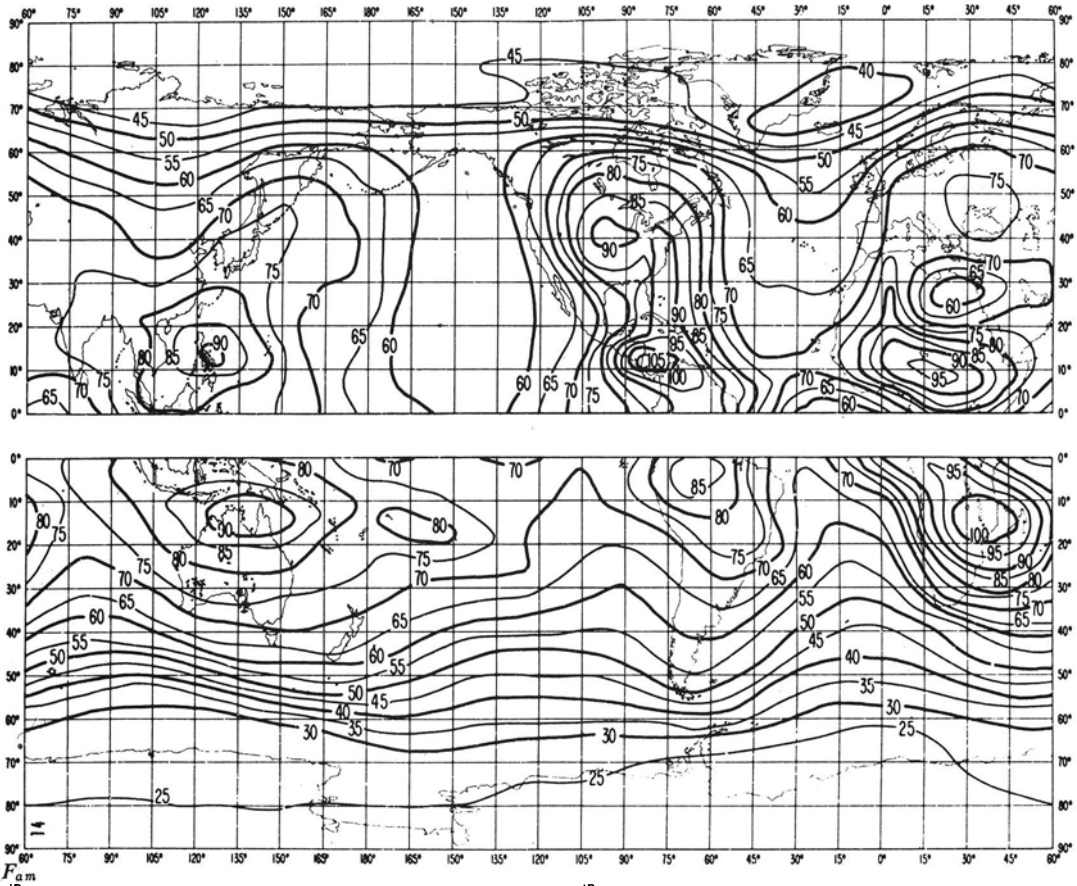

F_{am}

dB

dB

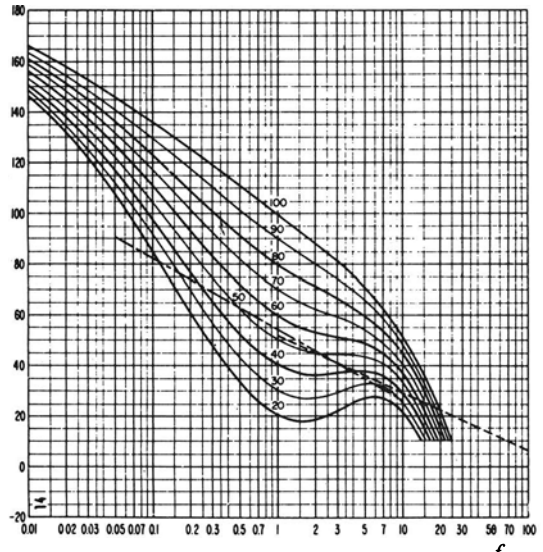

f_{MHz}

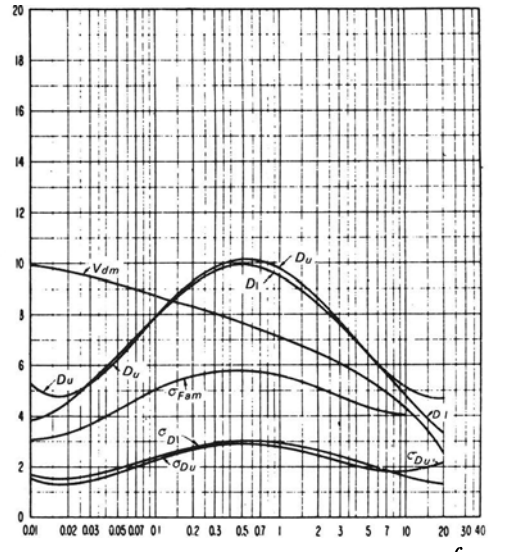

f_{MHz}

Fig. 85 Summer; between 0000 and 0400 h

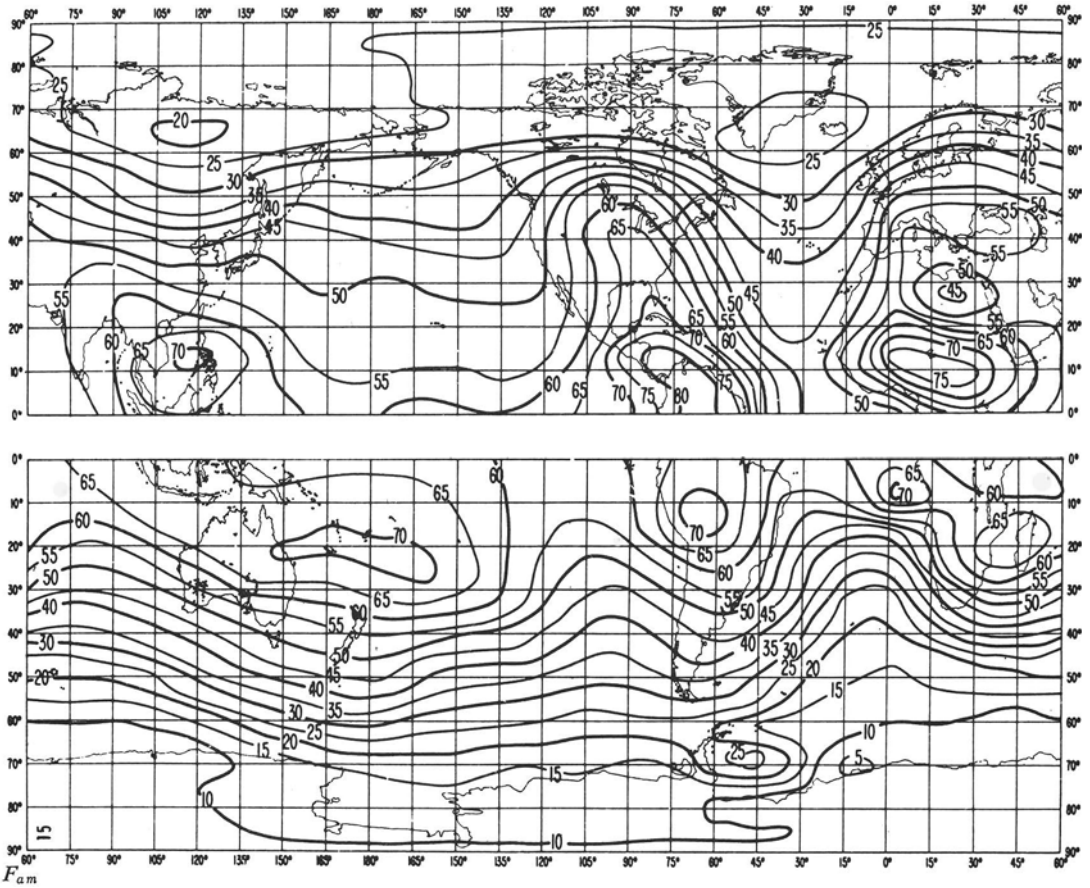

F_{am}

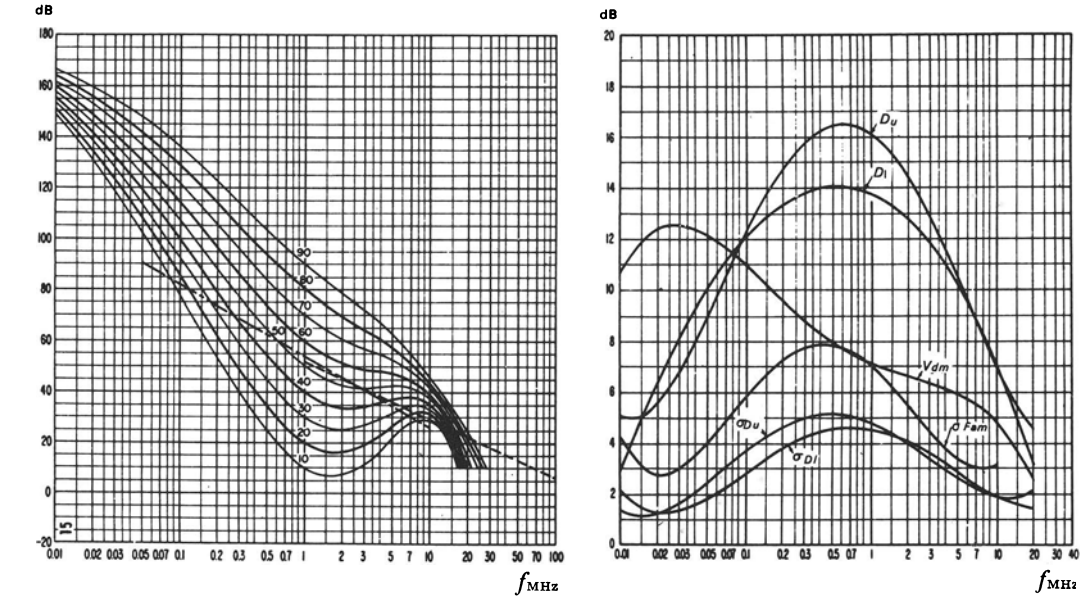

Fig. 86 Summer; between 0400 and 0800 h

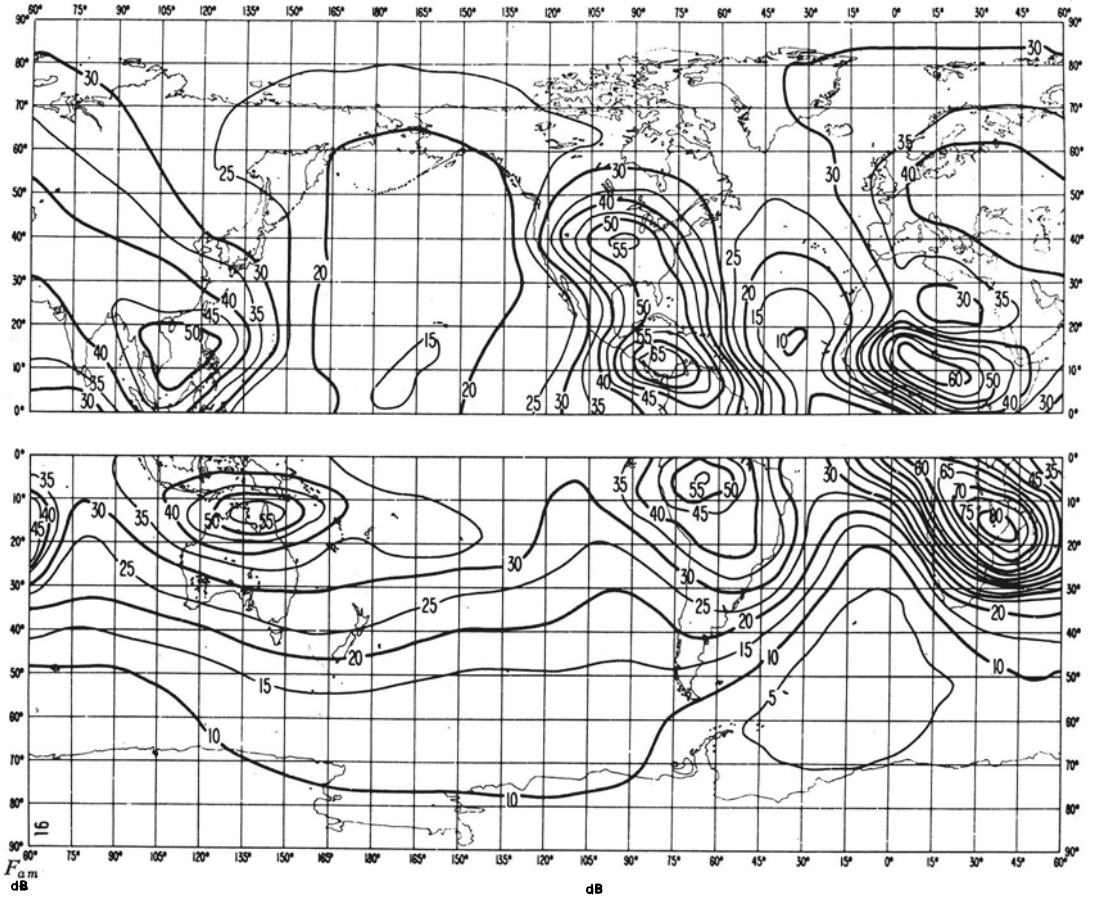

F_{am} dB

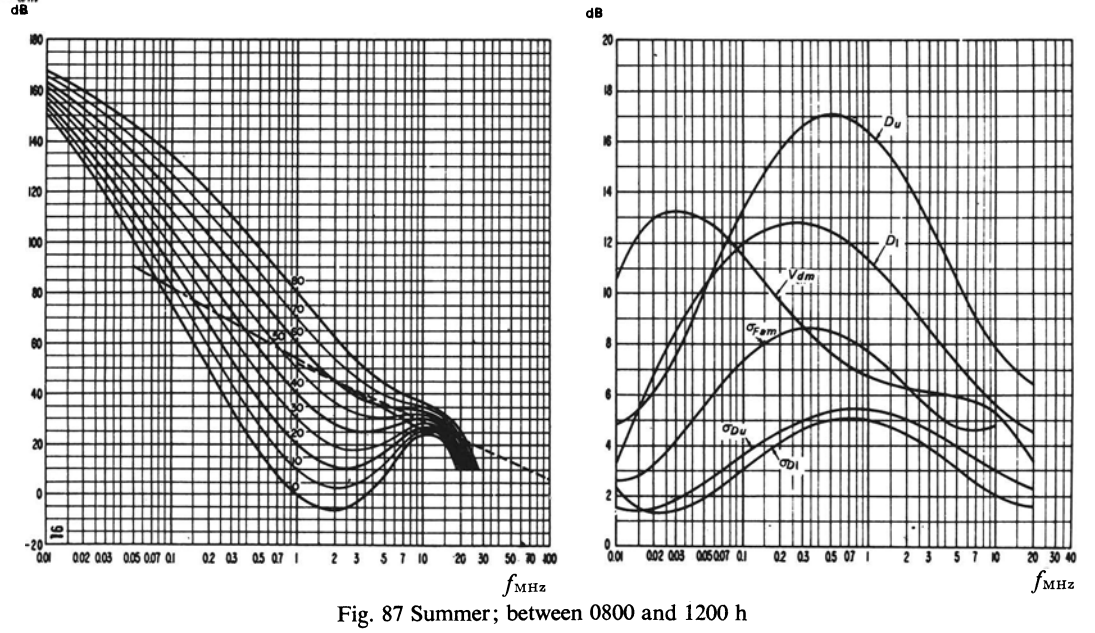

Fig. 87 Summer; between 0800 and 1200 h

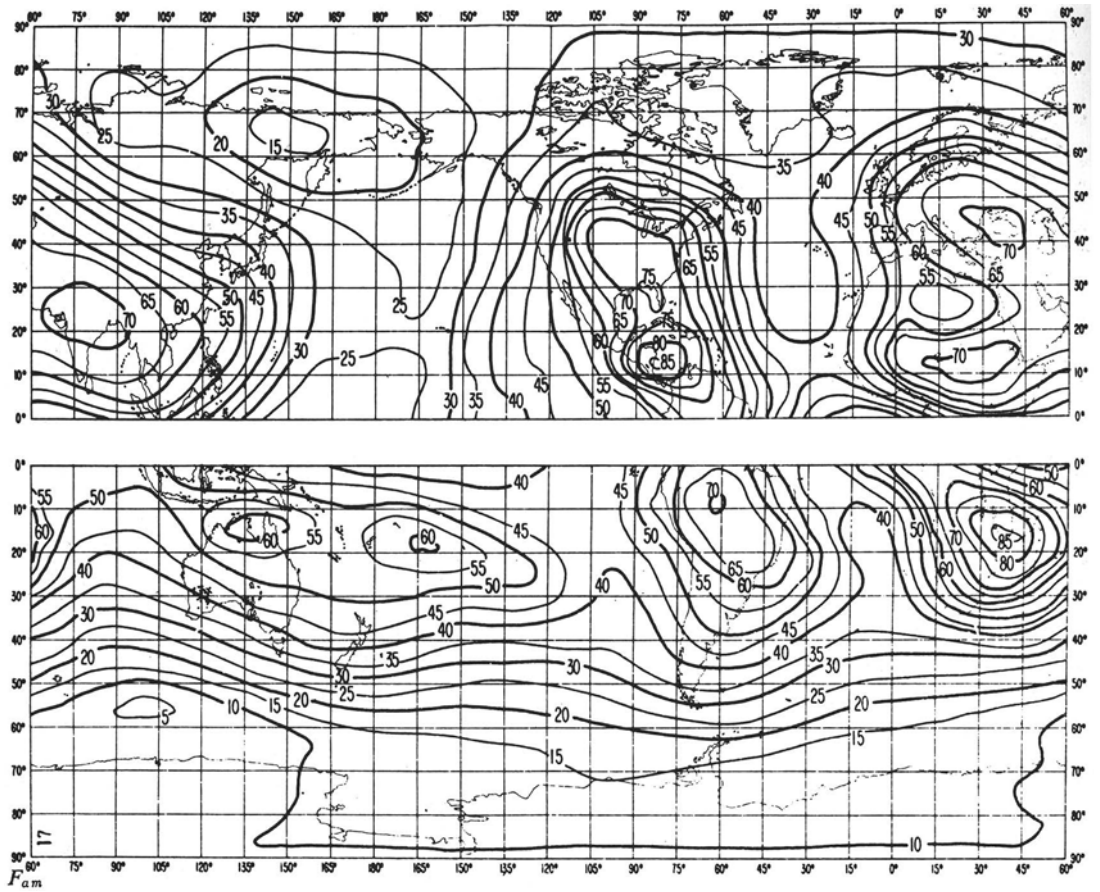

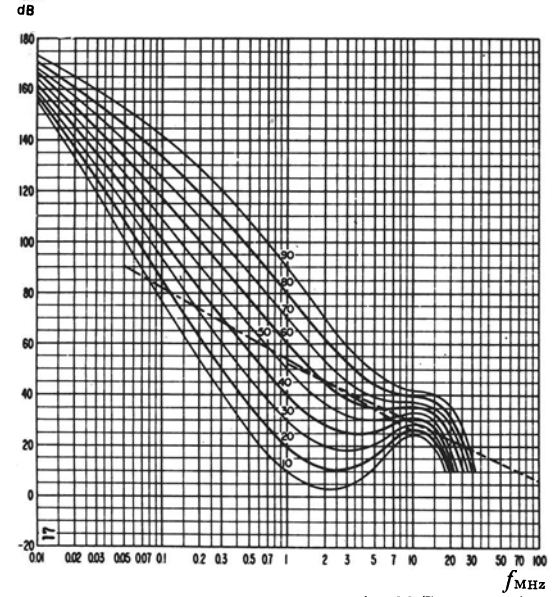

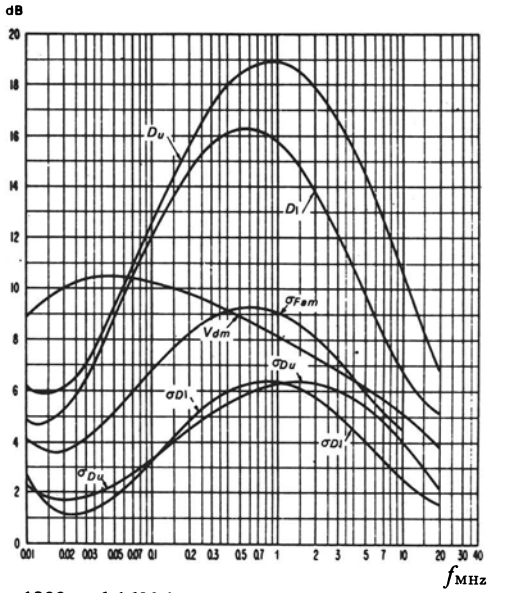

Fig. 88 Summer; between 1200 and 1600 h

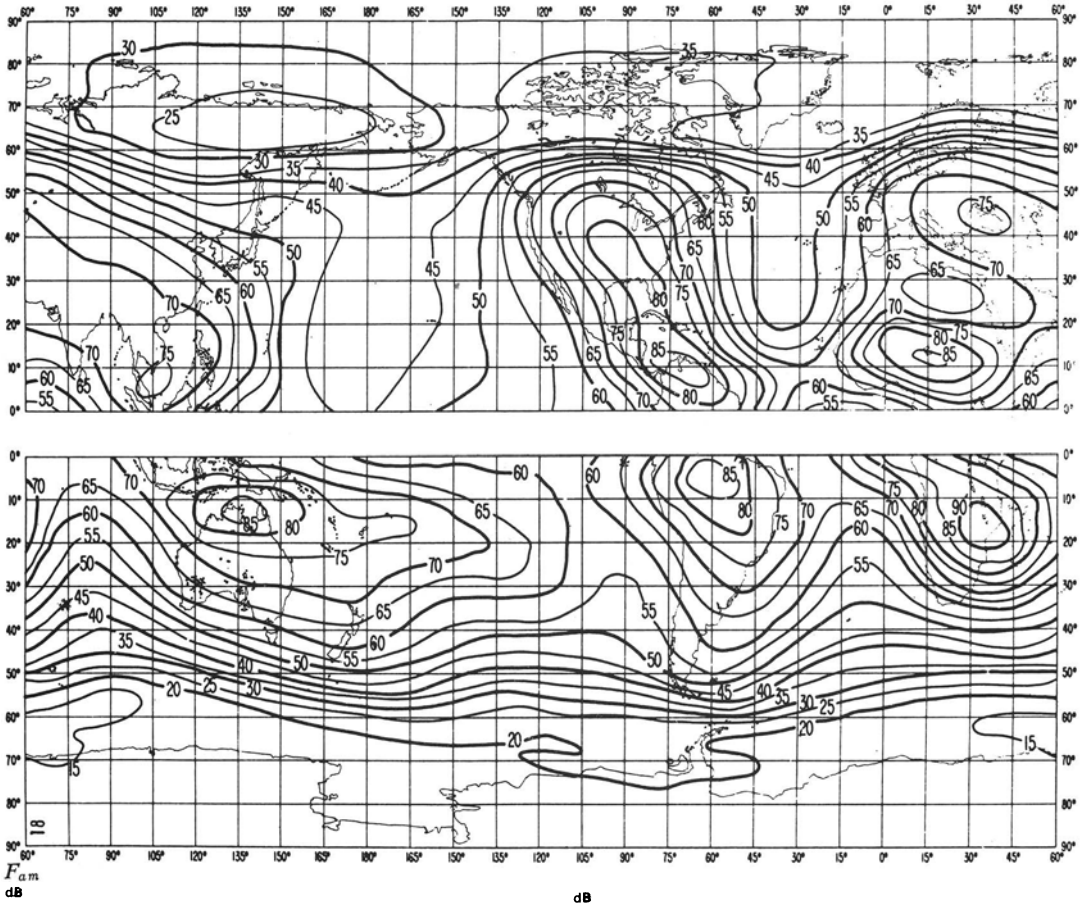

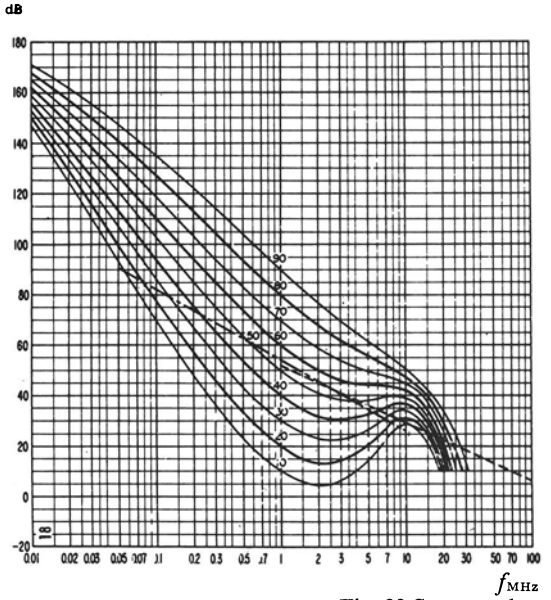

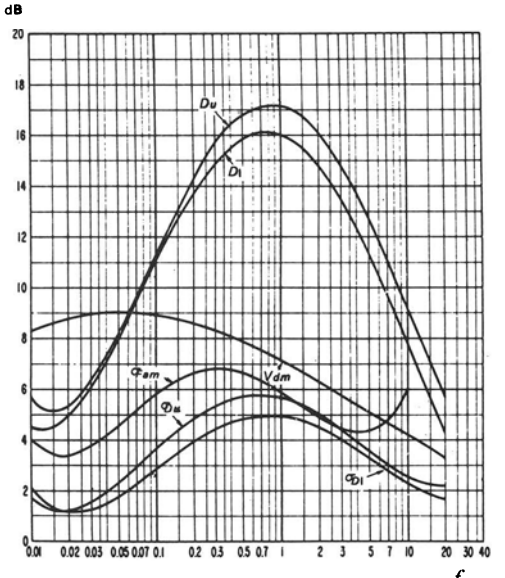

Fig. 89 Summer; between 1600 and 2000 h

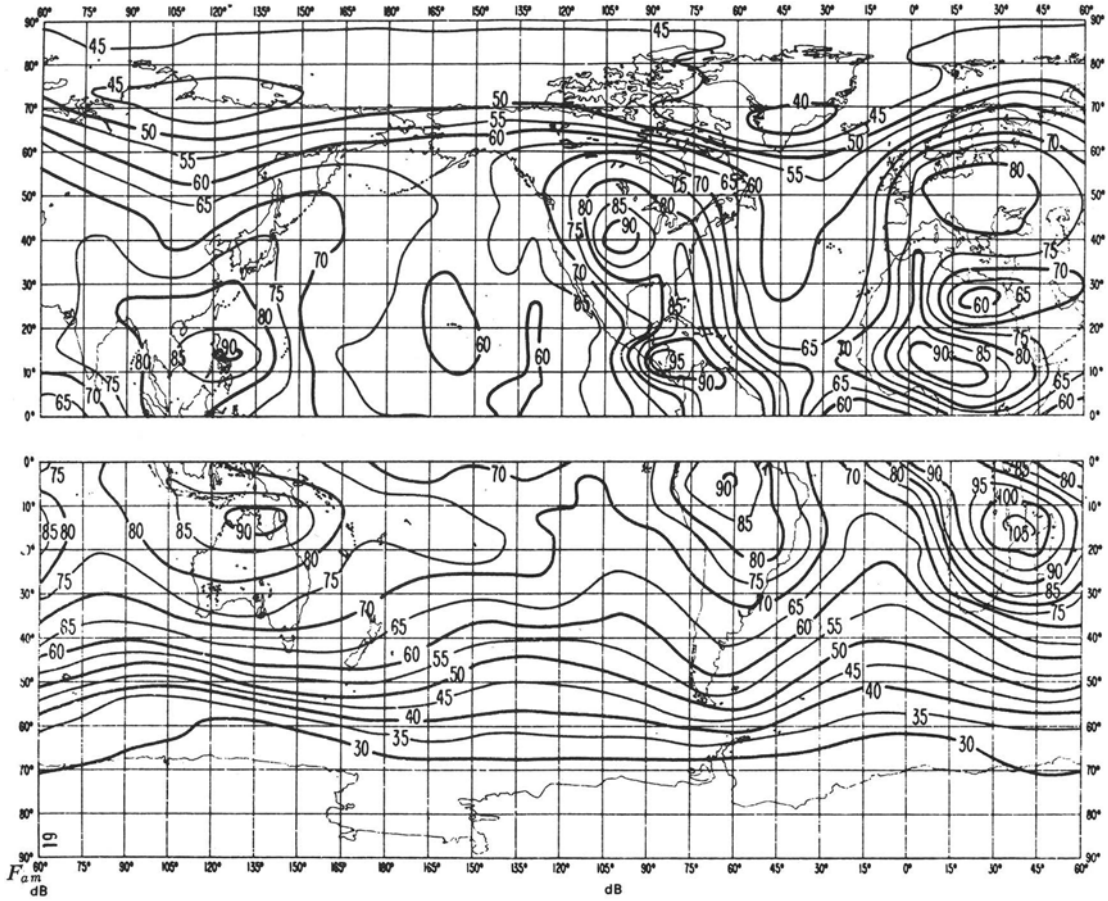

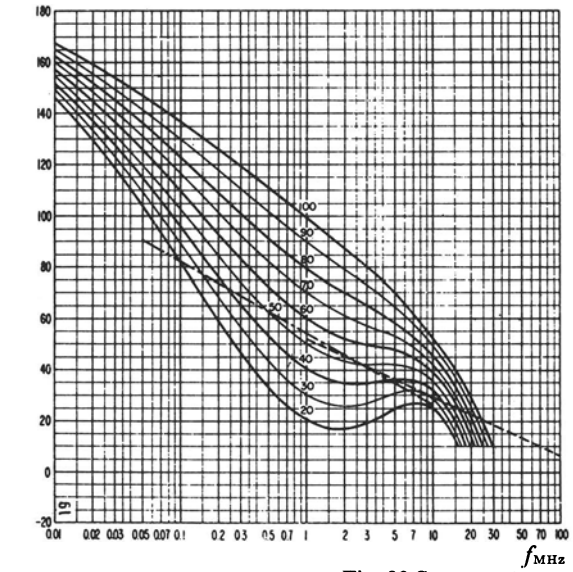

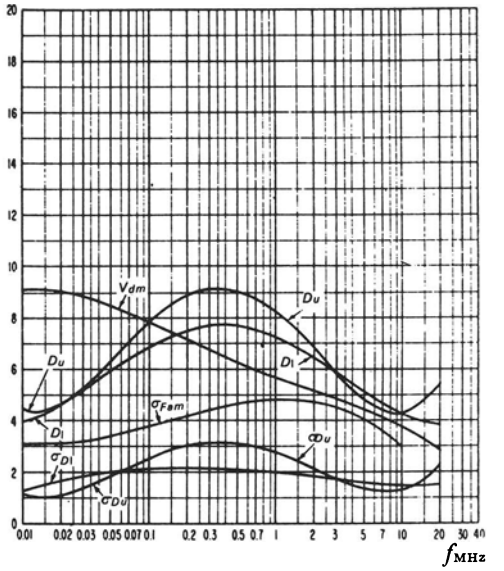

Fig. 90 Summer; between 2000 and 2400 h

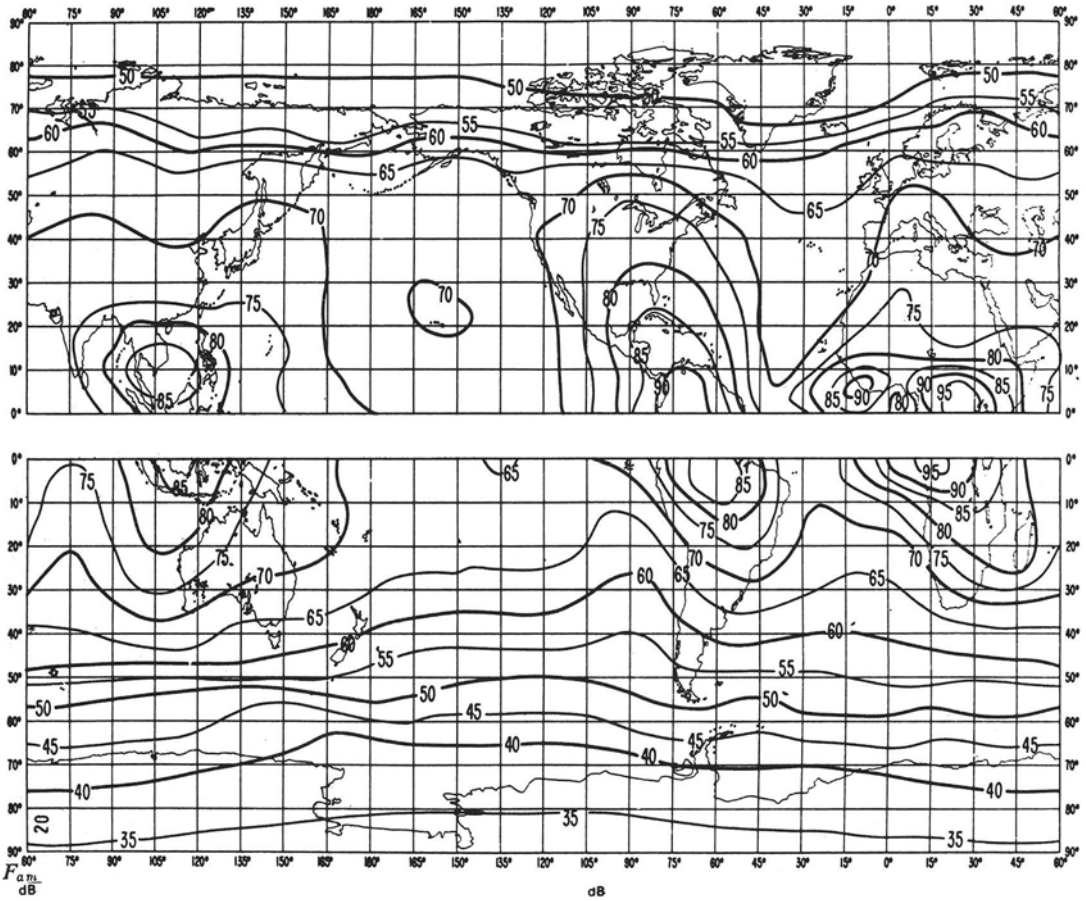

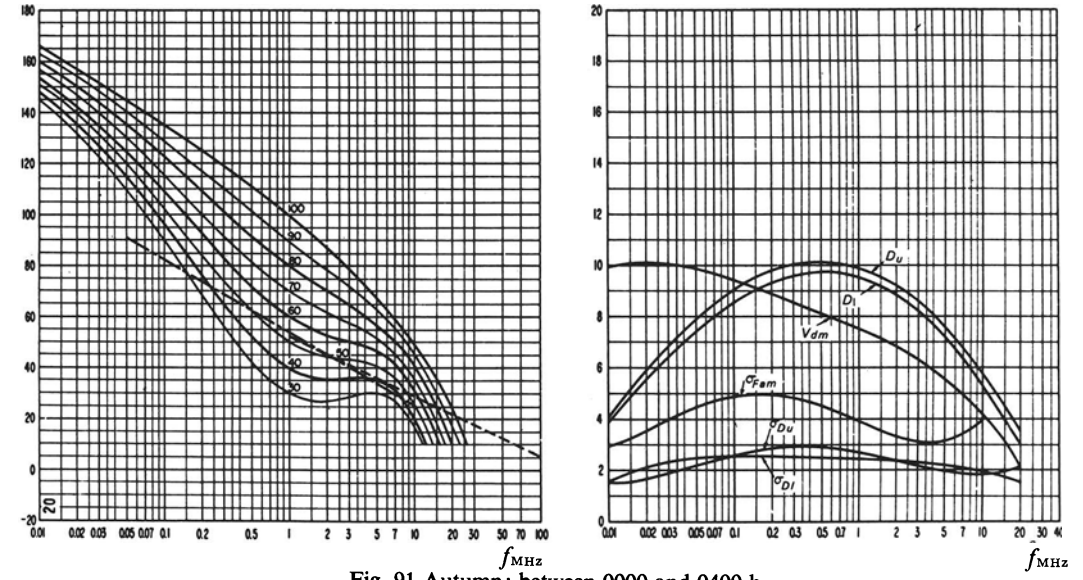

Fig. 91 Autumn; between 0000 and 0400 h

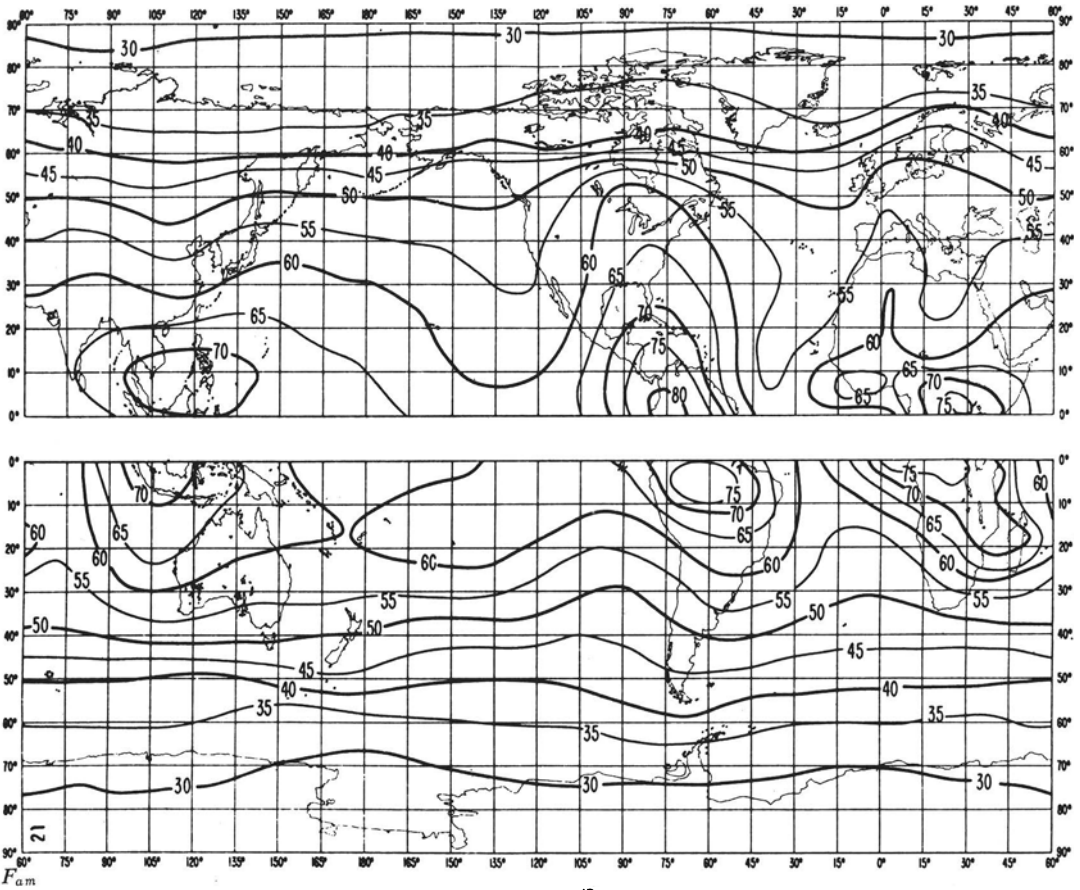

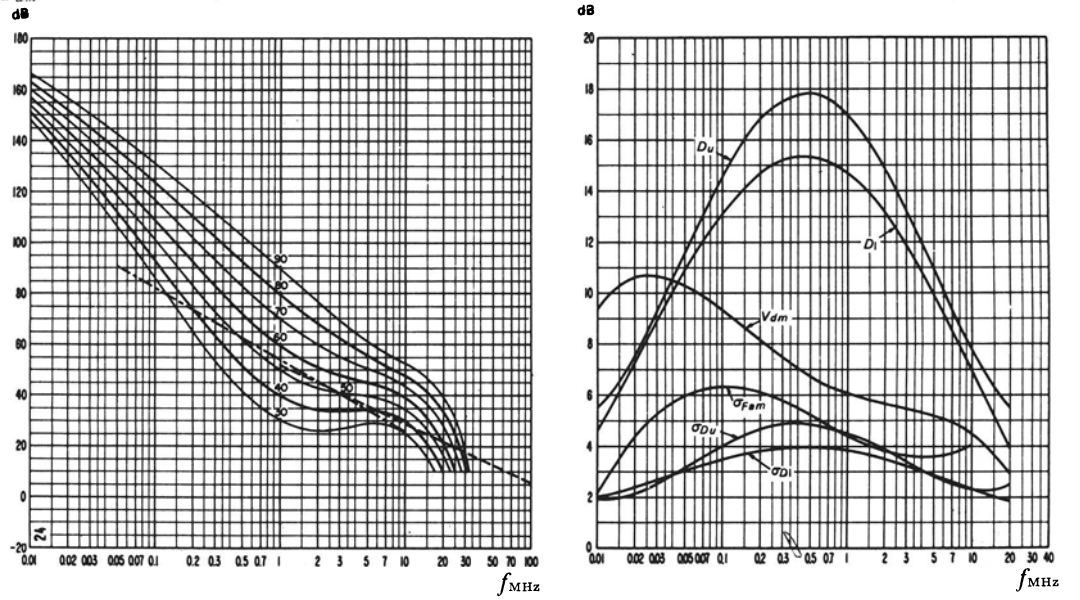

Fig. 92 Autumn; between 0400 and 0800 h

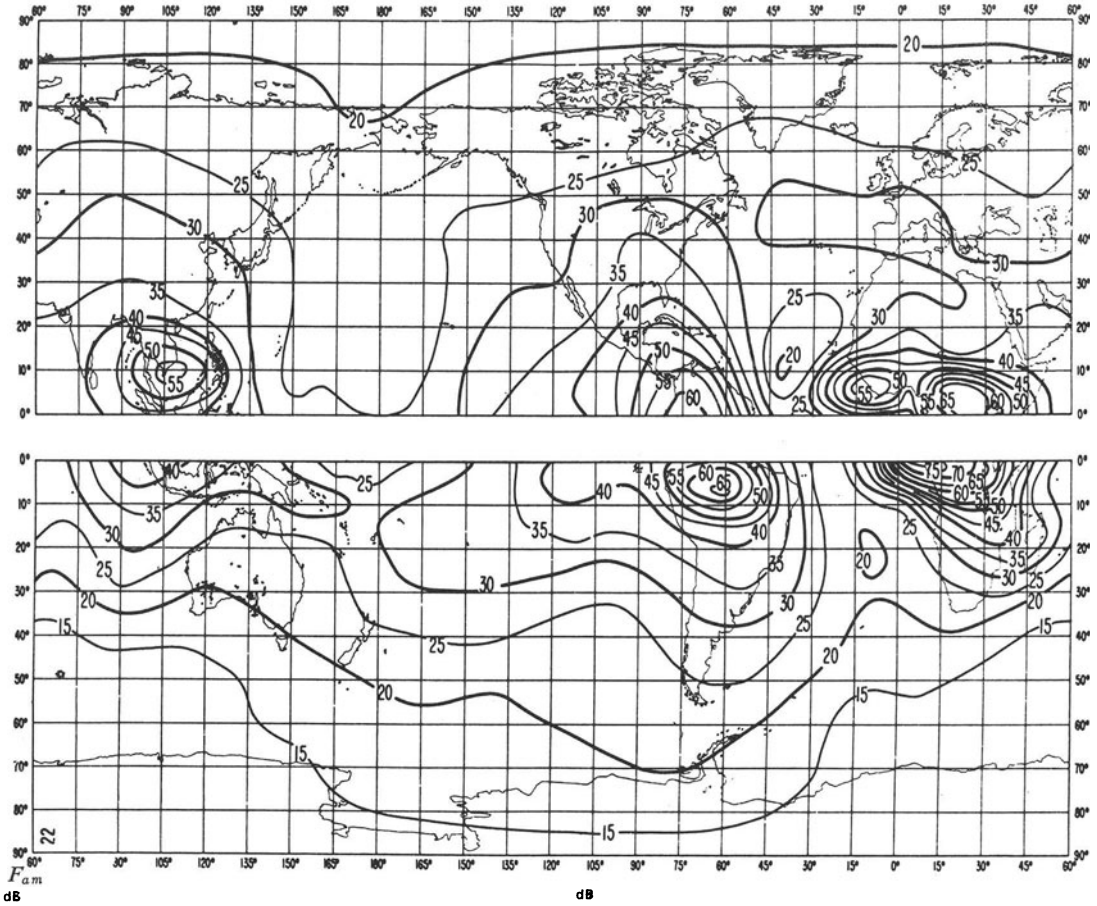

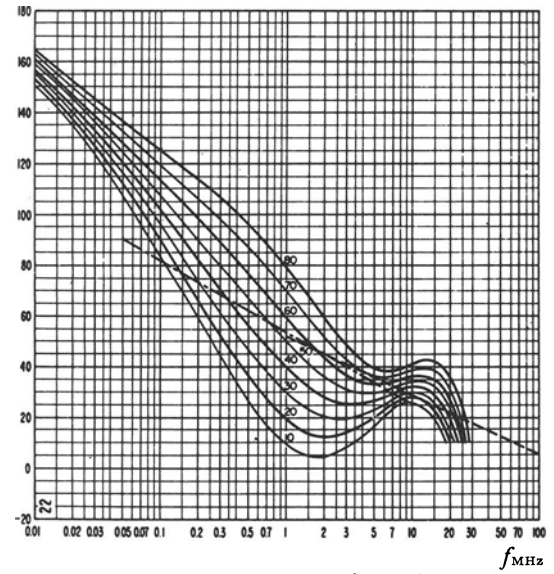

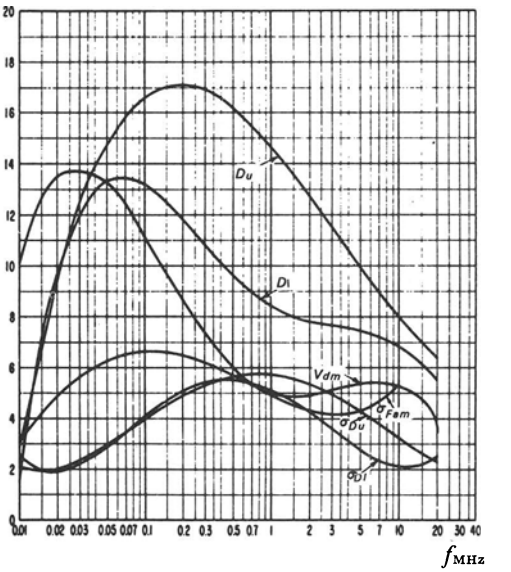

Fig. 93 Autumn; between 0800 and 1200 h

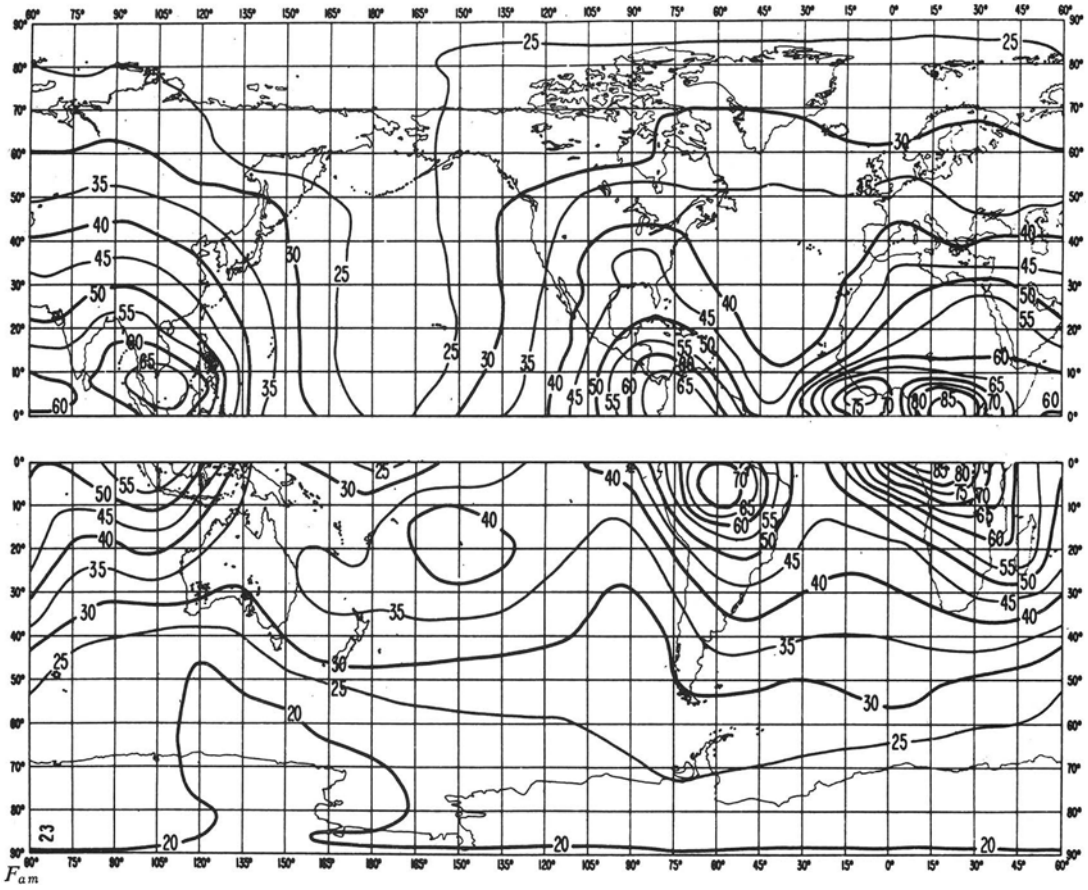

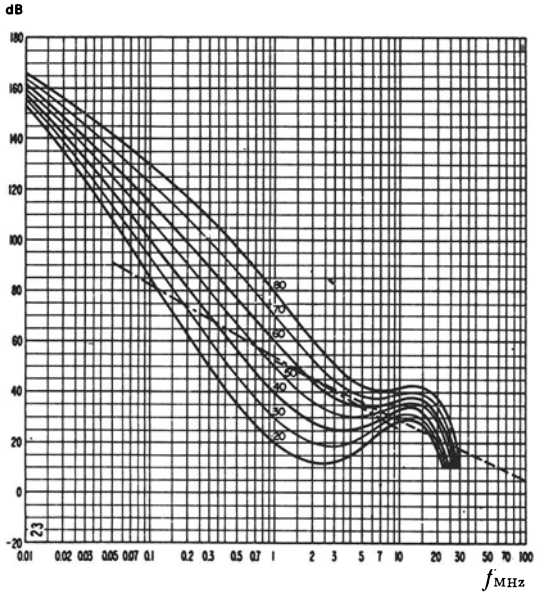

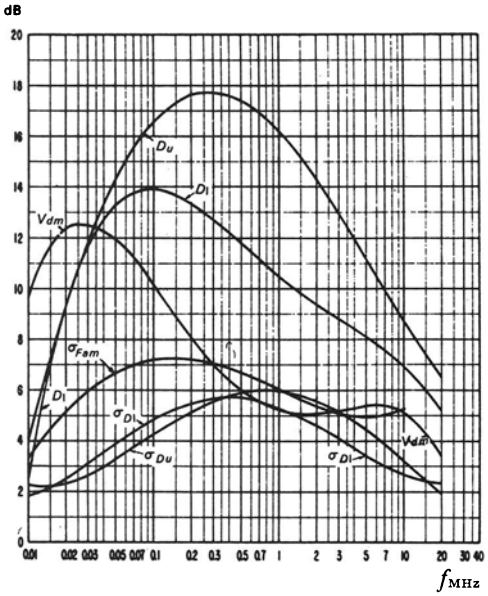

Fig. 94 Autumn; between 1200 and 1600 h

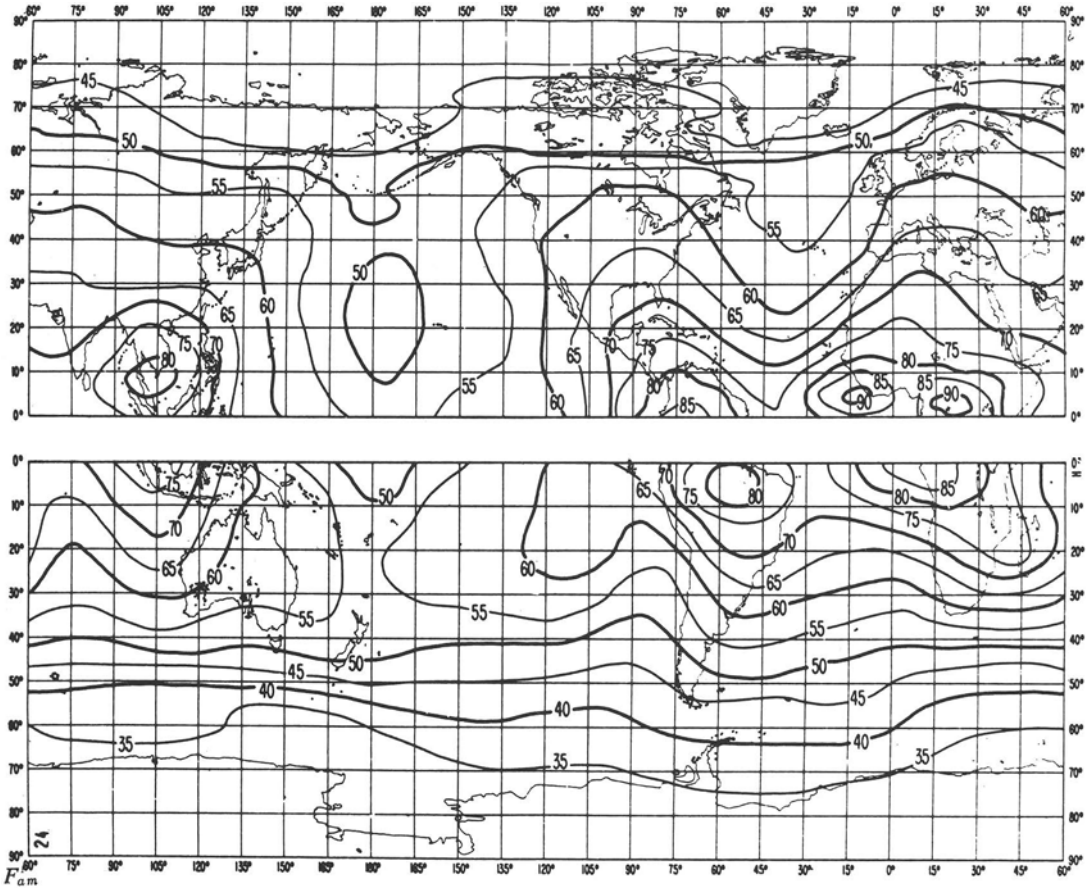

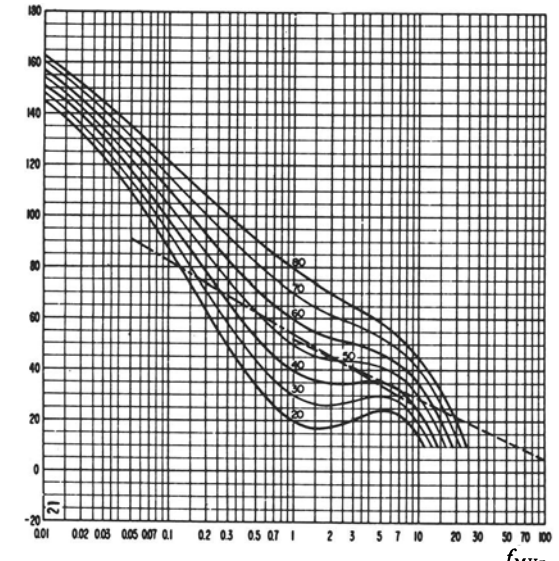

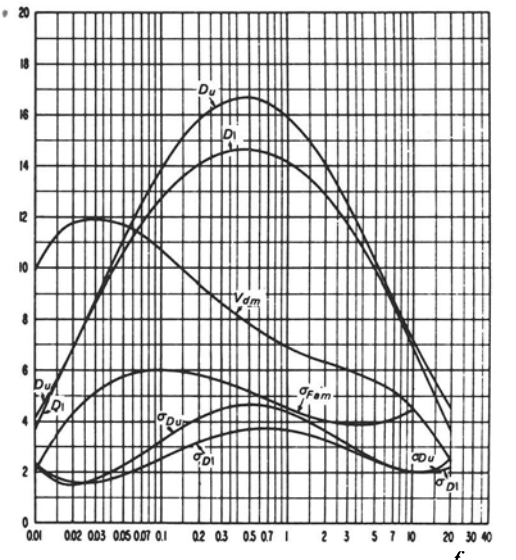

Fig. 95 Autumn; between 1600 and 2000 h

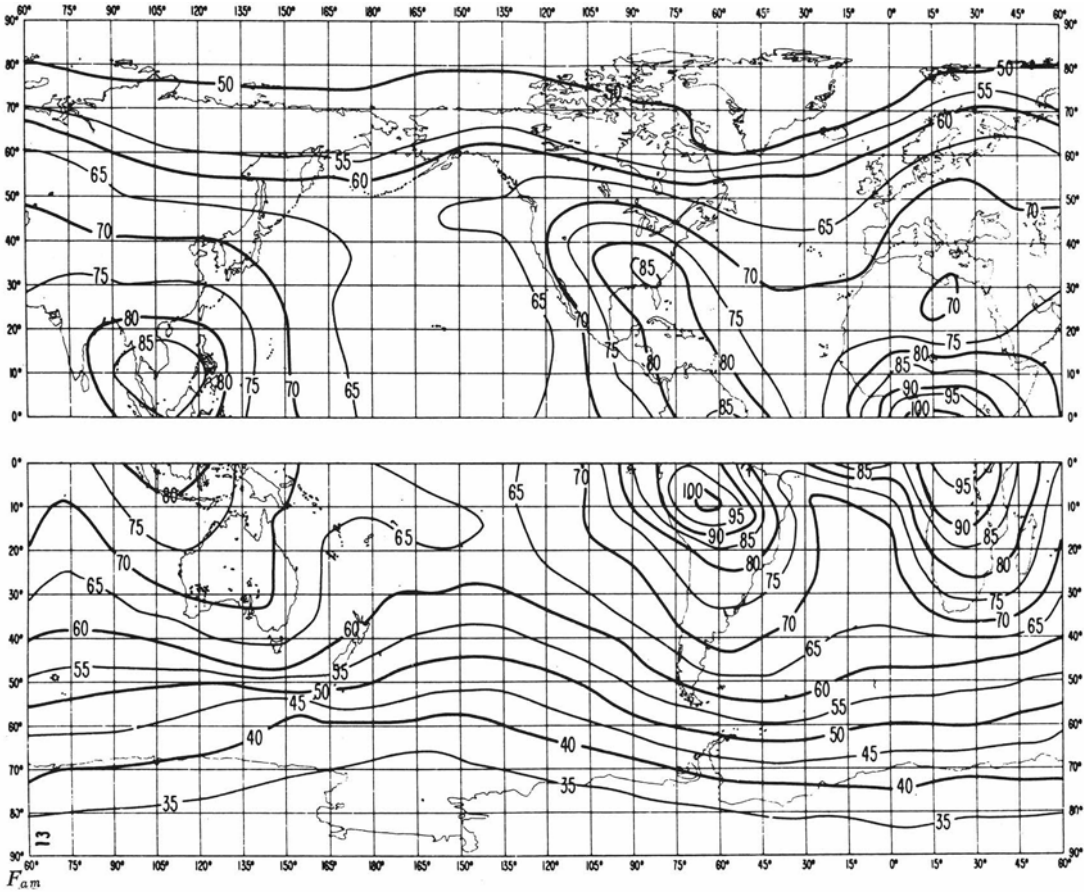

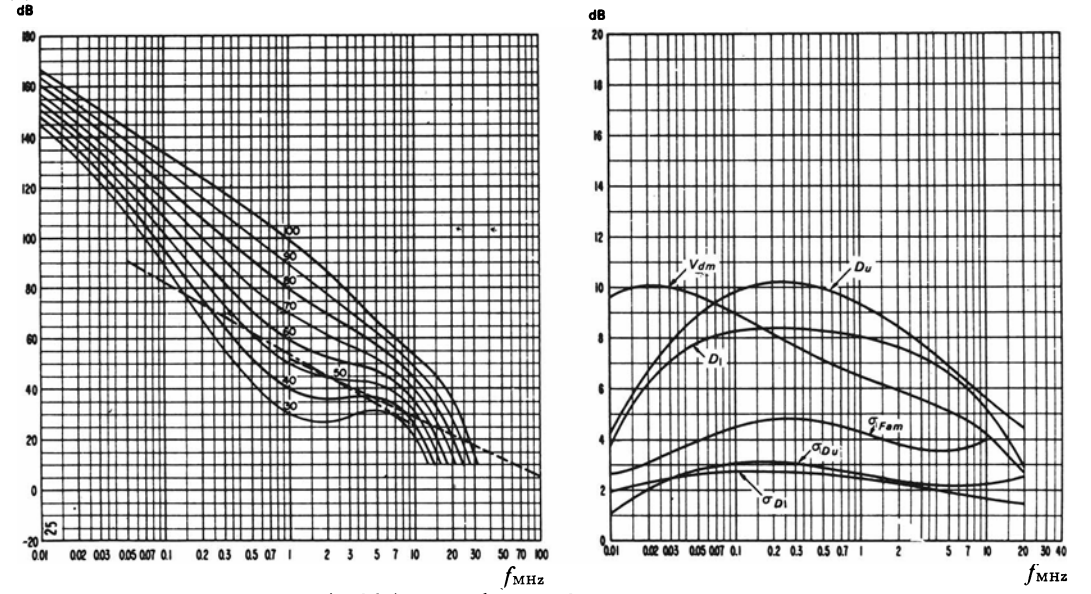

Fig. 96 Autumn; between 2000 and 2400 h

You can convert F_{am} to the median noise field E_n for your frequency by means of the nomogram of Fig. 97. This nomogram shows E_n in dB above 1 μV/m.

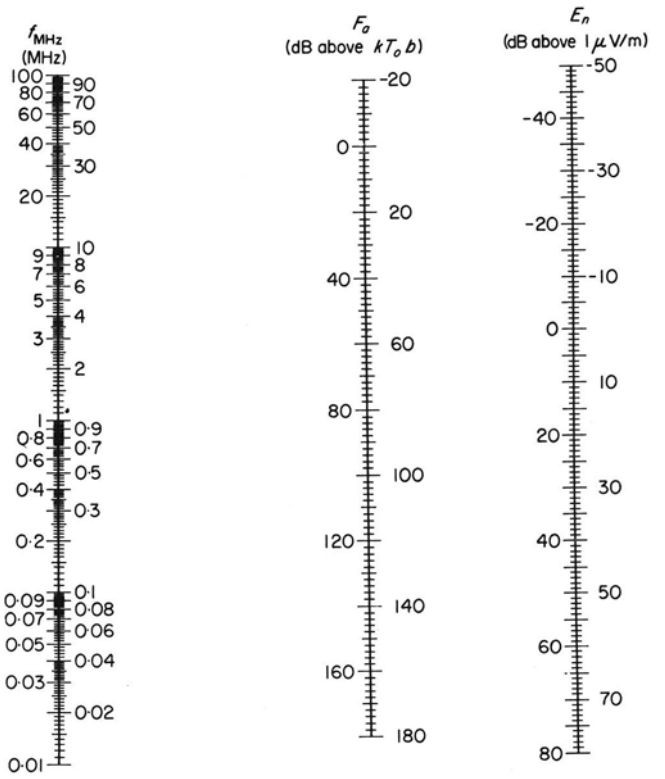

Fig. 97 Nomogram for the conversion of F_a to E_n as a function of frequency

$$E_n = F_a + 20 \log_{10} f_{MHz} - 65.5$$

E_n = quadratic mean of noise field strength for a bandwidth of 1 kHz (in dB above 1 μV/m)

F_a = equivalent antenna noise factor resulting from the external noise power applied to a perfect antenna

8.2.1.2 **Fluctuation margin**

Noise obeys a normal logarithmic distribution; this also applies to the signal median value. In the case of ionospheric waves, the instantaneous signal values vary around the hourly median value in a Rayleigh distribution.

The fluctuation margin is defined here as the change in signal required to maintain the signal-to-noise ratio above a certain value (service grade) for a certain percentage of the time (time availability).

This margin is calculated as follows.

Read value D_u of the maximum deviation of F_{am} for 90 per cent time availability from one of Figs 71–96.

Calculate:

$$\sigma = \frac{(D_u^2 + D_s^2)^{\frac{1}{2}}}{1{\cdot}3}$$

where $D_s = 0$ for the ground wave, and $D_s = 7$ dB for the ionospheric wave (σ = standard deviation of the ratio of the hourly median values of signal to noise).

Find in Fig. 98 (single reception) or Fig. 99 (double diversity reception) the value of σ found above and the complement to unity of the time availability, and read the corresponding fluctuation margin expressed in dB from the ordinate.

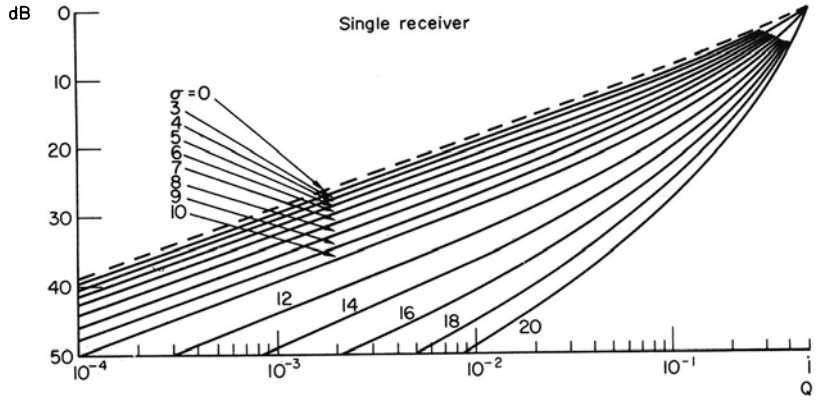

Fig. 98 Convolution of Rayleigh distribution with lognormal distribution

8.2.1.3 **Uncertainty margin**

The above calculated values for F_{am} and the fluctuation margin are both mean values. In view of the unavoidable uncertainty of the data used, only half of the communication circuits realized by means of these data will produce the expected result. If the service probability should exceed 50 per cent, a power margin must be added, which we shall call 'uncertainty margin'.

The calculation is carried out as follows.

Read the value of σ_{DU} from the graph on the lower right hand side of one of the figures 71–96.

Calculate:

$$\sigma_{CU} = (\sigma_{DU}^2 + \sigma_{DS}^2)^{\frac{1}{2}}$$

where $\sigma_{DS} = 0$ for the ground wave, $\sigma_{DS} = 1{\cdot}5$ for the ionospheric wave, and σ_{CU} = standard deviation of the distribution of the ratio of the hourly median values of signal to noise for 90 per cent time availability.

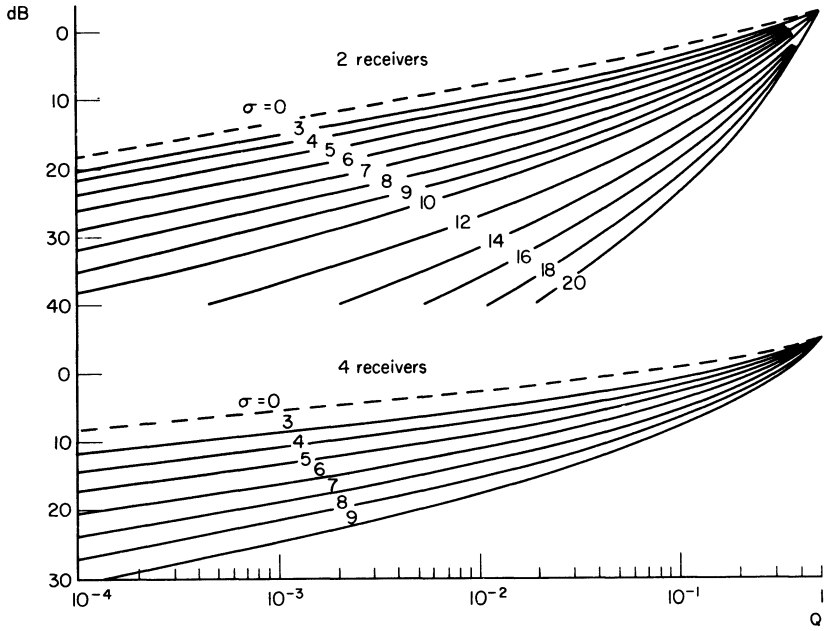

Fig. 99 Fading distribution for diversity reception (switch type)

Note in Fig. 100 the percentage of time availability (as already used above) on the left hand scale, and the value of σ_{CU} on the right hand scale. σ_C is then read from the central scale.

Add the squares of

1. σ_C, calculated above
2. σ_{Fam}, read from the lower right graph of the Figs 71–96
3. σ_P, quadratic average error in the calculation of the power received (2–5 dB)
4. other possible errors.

Calculate:

$$\sigma_T = (\sigma_C^2 + \sigma_{Fam}^2 + \sigma_P^2 + \ldots)^{\frac{1}{2}}$$

Note on the left hand scale of Fig. 100 the value of the required service probability, and on the right hand scale the value of σ_T obtained above. Read the uncertainty margin (in dB) from the central scale.

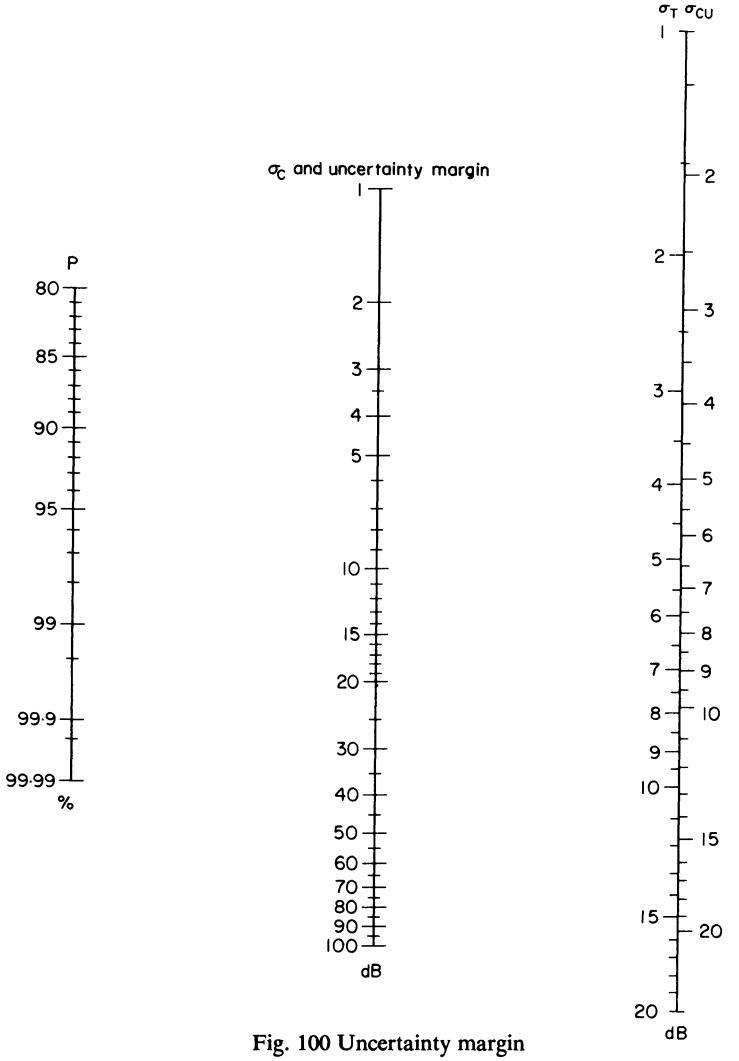

Fig. 100 Uncertainty margin

8.2.1.4 Field required in the presence of atmospherics

Select in Fig. 101 the required signal-to-noise ratio for the type of service under consideration (stable signal and noise).

Add to this ratio.

1. the field E_n
2. the fluctuation margin
3. the uncertainty margin.

The discrimination gain of the receiving antenna, calculated as mentioned in Section 8.2.3.4 must if necessary be deducted from the obtained result. The result will be the required field.

Note. In view of the large values of the probable deviations used in these calculations and the existence of ionospheric disturbances or local thunderstorms, calculations carried out for very high probability percentages have no practical value. The circuits are usually calculated for probability percentages of between 90 and 95 per cent.

Fig. 101 Signal-to-noise ratio required for different types of service (stable signal, stable noise)

Nature of transmission	Carrier-noise ratio or PEP-noise ratio for a band of 1 kHz (dB)
Telegraphy A 1	
8 bauds, poor quality	1
24 bauds	16
120 bauds, recorder	8
50 bauds, teleprinter	10
Telegraphy A 2, modulated carrier wave	
8 bauds, poor quality	−1
24 bauds	10
Telegraphy with shift frequency keying F 1	
120 bauds, recorder	10
50 bauds, teleprinter	6
Fascimile F 4, F.M., transmitted by	20
Script telegraph system	11
Telephony	
Double band, between skilled operators	20
Double band, barely commercial	29
Double band, good commercial link	37
SSB and independent side bands	
1 channel (PEP power)	31
2 channels (PEP power)	33
3 channels (PEP power)	34
4 channels (PEP power)	35

8.2.1.5 **Internal receiver noise**

In the case of modern professional receivers, it hardly ever happens that internal noise exceeds atmospheric noise. This can nevertheless be the case when a very short antenna (vehicle antenna) is being used.

If we have:

$$F \gg F_{am} - G_D - L$$

where F = receiver noise factor

G_D = discrimination gain of receiving antenna

L = loss in the antenna–receiver coupling circuit (usually attenuation due to a poor matching);

replace F_{am} by F when calculating the required field.

If F and F_{am}-G_D-L are of the same order of magnitude, the required field must be calculated successively for these two values, and Fig. 102 is used to obtain the final value.

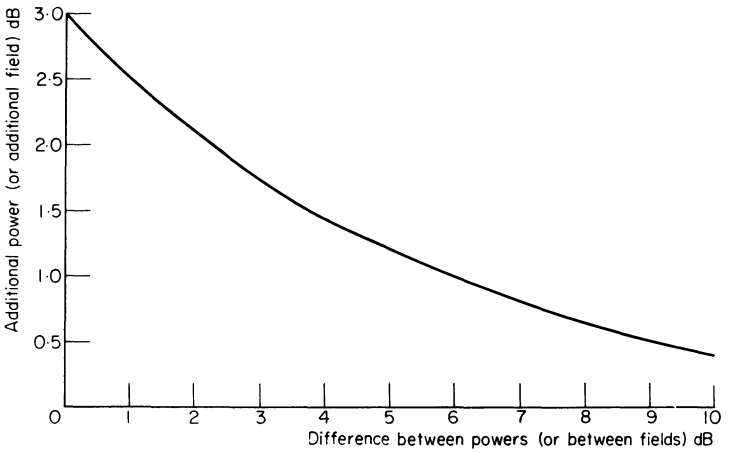

Fig. 102 Quadratic addition chart

How to use this graph: Calculate the difference between the powers in dB. Read from the graph the corresponding additional power and add this value to the greatest power.

8.2.1.6 **Industrial noise**

For medium wave broadcast reception in urban regions, industrial (or man made) noise usually dominates. In this case, the fields required are:

Industrial regions	10–50 mV/m
Residential areas	2–10 mV/m
Small towns	0·5–1 mV/m

8.2.2 GROUND WAVE

The ground wave is the normal propagation mode of hectometric (m.f.) and longer waves over medium ranges, and of decametric (h.f.) and shorter waves over short ranges.

The typical calculation for these waves is as follows:

'An antenna and a transmitter of known power are given; determine the range for one or more frequencies in the spectrum.'

This problem is solved by:

1. determining the required field in dB in relation to 1 μV/m, as explained above.
2. determining the radiated power in dB in relation to 1 kW as a function of transmitter power and antenna gain
3. deducting one from the other and plotting this difference on a propagation graph that gives the field (in dB in relation to 1 μV/m) as a function of the distance for a radiated power of 1 kW. The range is then read from the scale of the distances in this graph.

8.2.2.1 **Radiated power**

Convert the transmitter power into dB (in relation to 1 kW) by using Fig. 103.

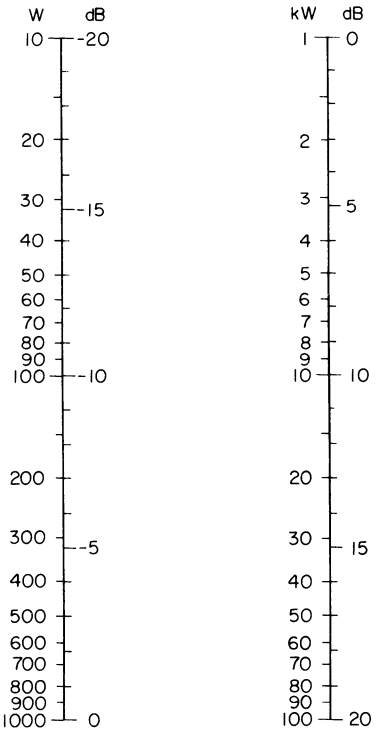

Fig. 103 Conversion of power into decibels (referred to 1 kW)

Read the antenna gain as a function of the type of transmitting antenna and of the frequency from Figs 104 and 105.

Add these two values together, taking the signs into account. This gives the equivalent radiated power in dB in relation to 1 kW.

8.2.2.2 **Range**

(a) Deduct the radiated power from the required field, taking the signs into account.

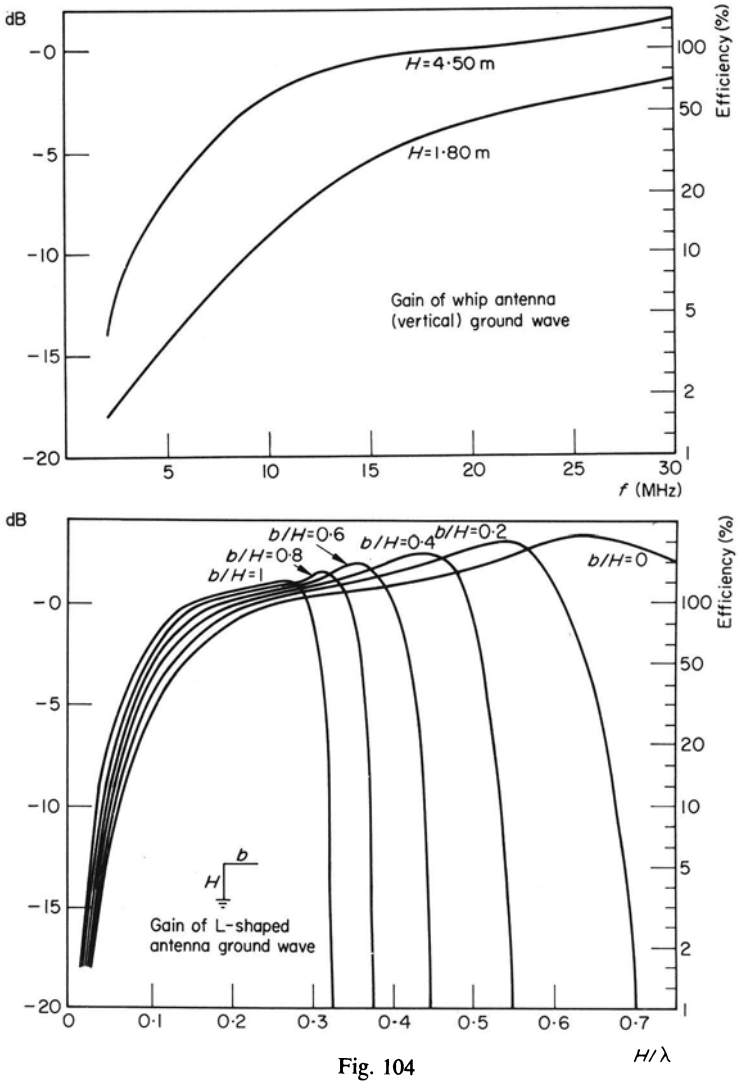

Fig. 104

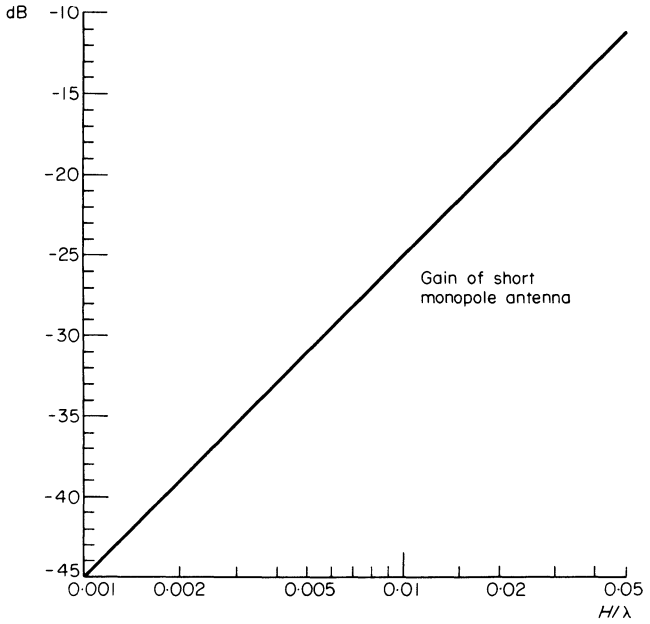

Fig. 105
Note. Calculated for earth of buried wires. Efficiency varies greatly with quality of the earth.

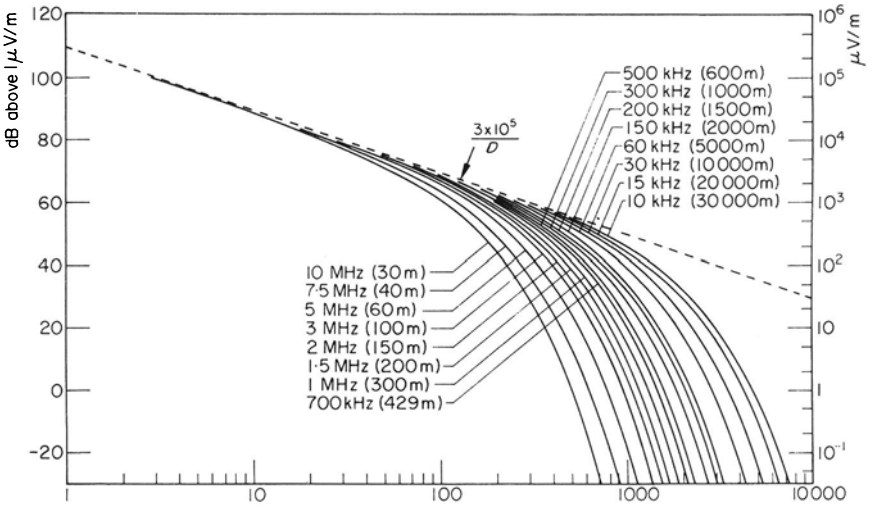

Fig. 106 Ground-wave field over the *sea* for 1 kW radiated power;
$\sigma = 4\ \Omega^{-1}\mathrm{m}^{-1}\ \varepsilon = 80$

(b) Select the relevant graph from the series of figures 106–110.

By 'good ground' we mean arable ground, thick top soil, clay soil, and the lower parts of humid valleys. By 'poor ground' we mean rocky ground, dry sand and desert regions.

(c) Plot the number of dB found in (a) on the selected graph, and read the range by means of the curve that corresponds to the frequency used

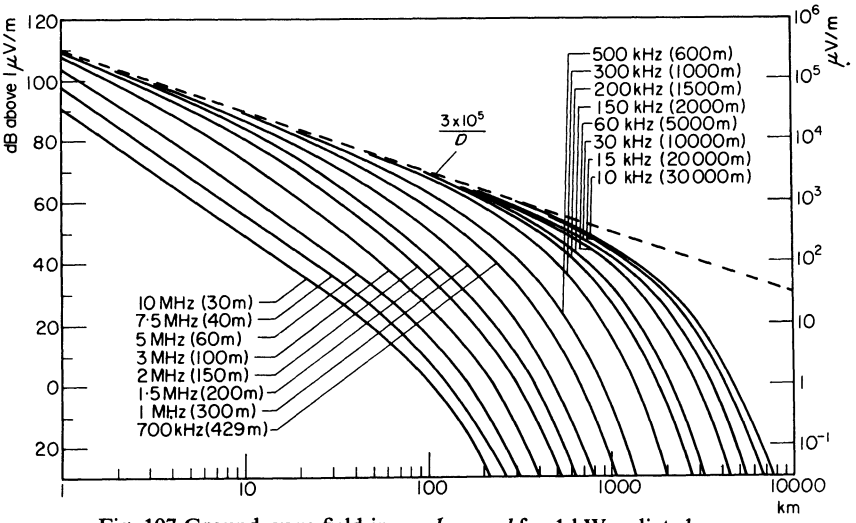

Fig. 107 Ground-wave field in *good ground* for 1 kW radiated power;
$\sigma = 10^{-2}\ \Omega^{-1}\mathrm{m}^{-1}\ \varepsilon = 4$

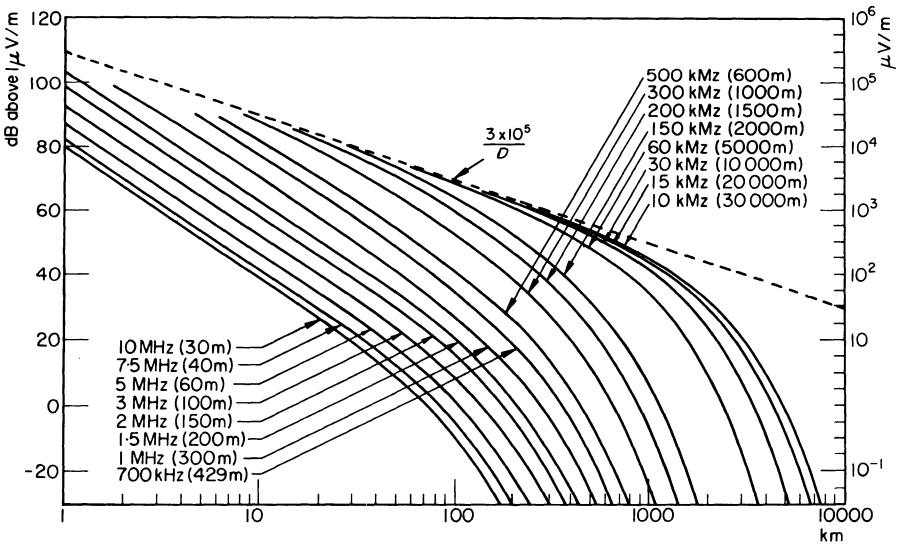

Fig. 108 Ground-wave field in *poor ground* for 1 kW radiated;
$\sigma = 10^{-3}\ \Omega^{-1}\mathrm{m}^{-1}\ \varepsilon = 4$

(d) If the path contains an obstacle of some importance, use the nomogram of Fig. 111 and follow the instructions. Multiply the range obtained in (c) by the coefficient of range reduction read from Fig. 111.

(e) As the field required varies with the period of time under consideration, the preceding operations must be carried out for each period of time during which the radio link is in operation.

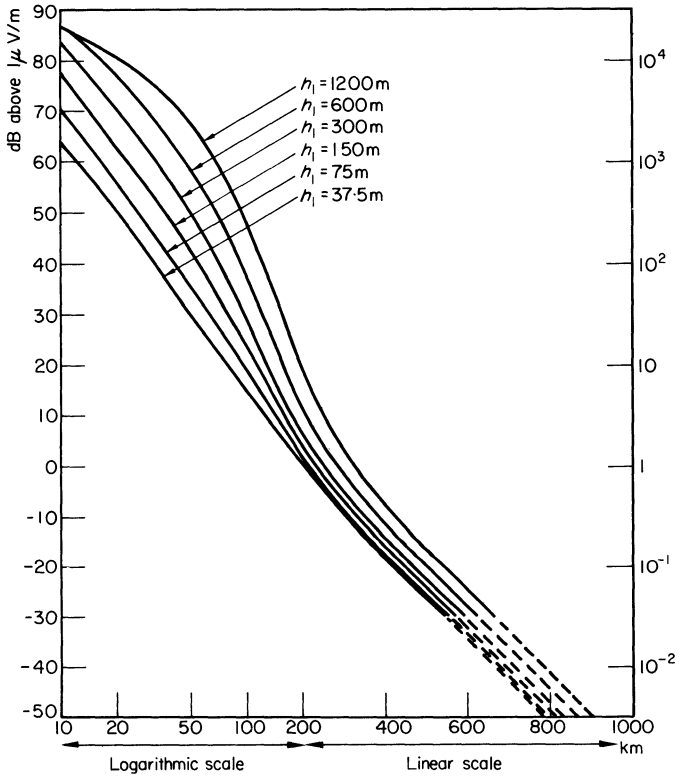

Fig. 109 Median ground-wave field over *land and sea*; frequency 40–250 MHz; h_2 = 10 m; 1 kW radiated power

8.2.3 IONOSPHERIC WAVE (DECAMETRIC WAVE: h.f.)

The ionospheric wave is the normal propagation mode for decametric waves over mean and large ranges.

The problem can be stated as follows:

'A link between two points, a defined antenna and a transmitter of known power are given. We wish to determine the frequencies one should use during different hours of the day.'

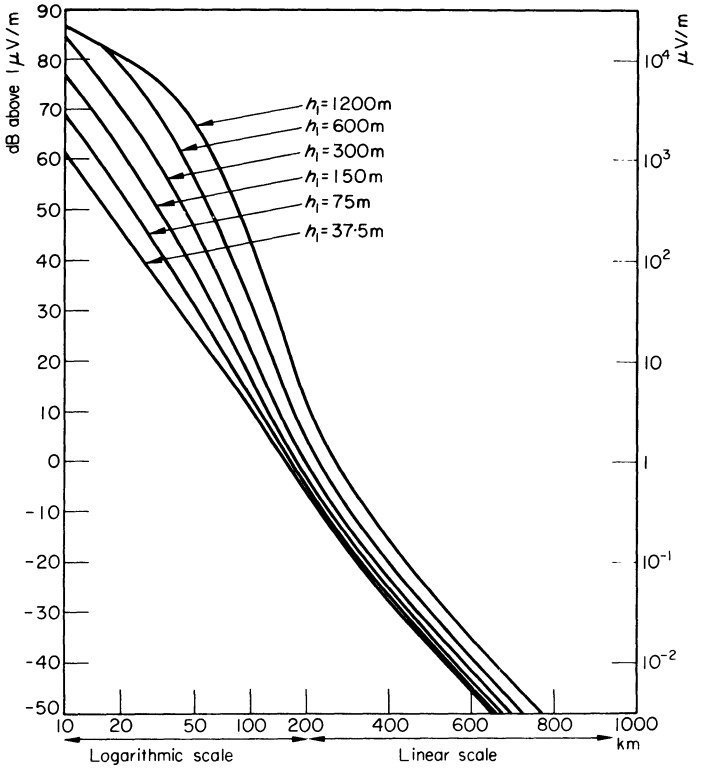

Fig. 110 Median ground-wave field over *land*; frequency 450–1000 MHz; h_2 = 10 m; Δh = 50 m; 1 kW radiated power

The CRPL method of ionospheric prediction is rather complex (see below), but it has the advantage of being usable for any path, anywhere in the world, and only requires the possession of a few simple documents.

Calculation can be considerably simplified when investigating a number of circuits with similar characteristics.

The calculation is divided into the stages shown in Table 8.2.

8.2.3.1 Calculating MUF and FOT

The MUF is the highest possible frequency capable of travelling between two points in the season and at the hour of day under consideration.

The calculations produce the median MUF (50 per cent probability that this value is not exceeded).

The FOT is the highest possible frequency capable of travelling during 90 per cent of time availability. This is usually the more advantageous frequency for use in a radio link.

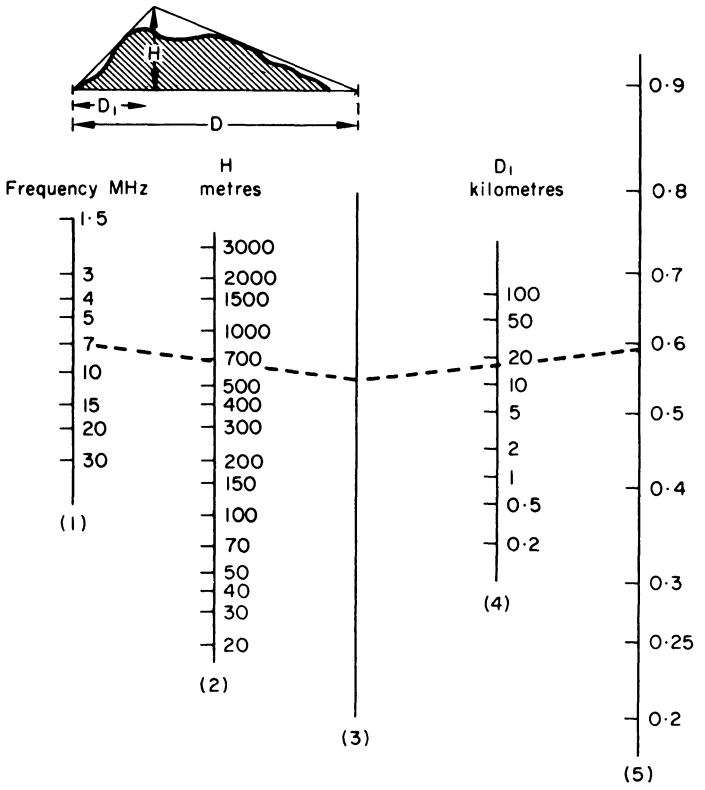

Fig. 111

How to use this nomogram:

1. Draw the triangle equivalent to the obstacle on the profile of the terrain. Determine height H and distance D_1 between the normal to the base from the apex of the triangle and the nearest base corner.
2. Join the frequency (scale 1) to height H (scale 2) and extend the line to scale 3.
3. Join the point of intersection with scale 3 to distance D_1 (scale 4) and extend the line to scale 5.
4. Multiply the carrier wave which would have been obtained without an obstacle by the factor read from scale 5.

TABLE 8.2

Calculated elements	Documents to be used
MUF and FOT	Figs 112–130 CCIR Report 340. CCIR Atlas of Ionospheric Characteristics*
Ionospheric absorption	Figs 114–125 Fig. 129 Figs 131 and 132
Field strength	Figs 133–171
Field required in the presence of noise	see Section 8.2.1 Fig. 172
Conclusions	Results of preceding calculations

* The MUF and FOT can also be calculated by means of documents published by the Radio and Space Research Station, Slough, Bucks. The 'Service National de Prévisions Ionosphériques', Château de la Martinière, Saclay, France, publishes monthly predictions for certain regions and certain paths.

MUF and FOT (ranges of less than 4000 km)

These values are calculated as follows:

(a) Place a sheet of tracing paper over the chart of Fig. 112. Identify and mark the two terminals of the path by means of their geographic coordinates. Trace the equator or the pole and the origin meridian (longitude 0). Trace a second meridian at 360° to the first, so that these two meridians enclose the path to be studied.

(b) Place the tracing on the chart of the corresponding great circles map (Fig. 113).

The continuous curves in these charts represent the great circles on the globe, in the same projection system as that of the preceding charts.

The numbered dash-dot-dash curves represent a scale of distances in thousands of km along these great circles.

Now slide the tracing so that the equator (or the pole) traced in (a) remains on the middle horizontal line (or the centre) of the chart, and the extremities of the path are situated on the same great circle (or between two of these circles).

Determine the centre of the path by means of the dotted curves and mark this on the tracing paper. Use the dotted curves for marking points with a separation of 500 km (these points will be used to calculate absorption). Make a note of the length of the path.

(c) To determine the MUF relating to the F_2-layer (F_2-MUF):

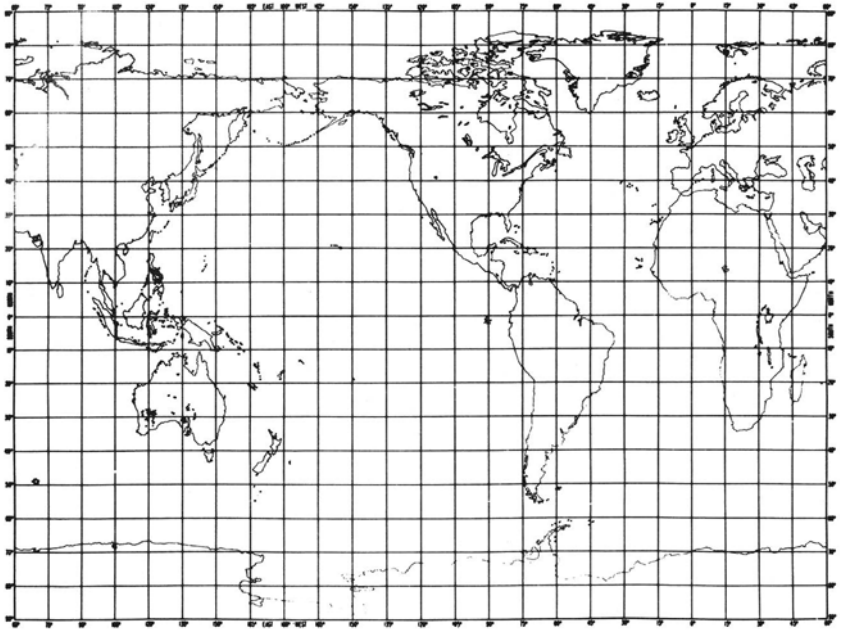

Fig. 112 World map; modified cylindrical projection

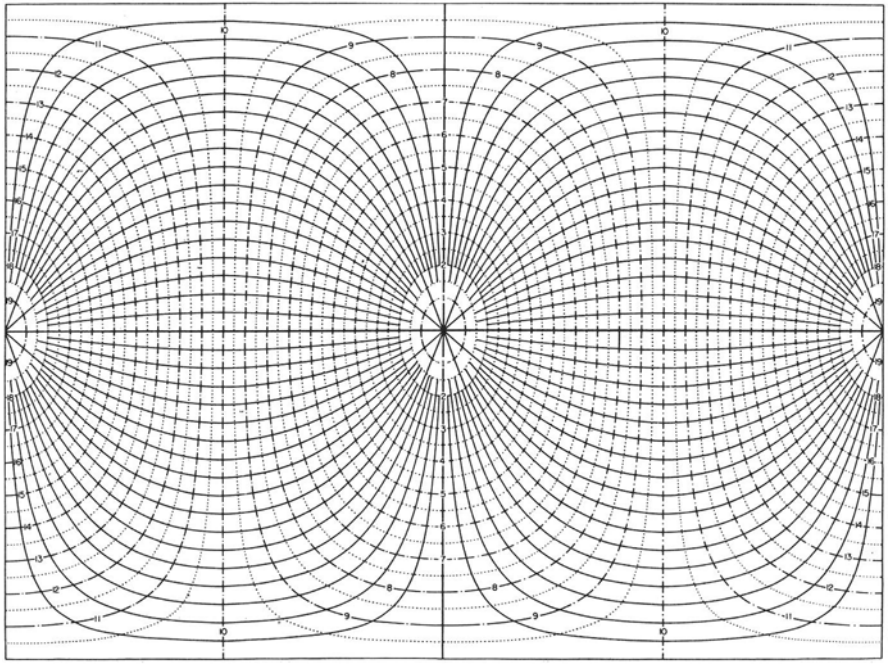

Fig. 113 Great circle chart centred on equator for modified cylindrical projection. (Solid lines represent great circles; numbered dot–dash lines indicate distance in km $\times 10^3$)

1. Place the tracing on the chart '$R_{12} = 0$; EJF (zero) F_2 (MHz)' of the CCIR Report 340 corresponding to the required month and hour, and sliding the sheet of paper so that the equator coincides with the equator of the chart (or the pole with the pole) and the origin meridian with meridian 0 of the chart. Read the MUF-zero-F_2 on the curve that passes through the centre of the path. Make a note of this frequency.
2. Repeat the same process on the chart '$R_{12} = 100$; EJF (zero) F_2 (MHz)' for the same month and hour.
3. Make linear interpolation between the values obtained in (1) and (2), agreeing to the actual value of R_{12}. This gives the zero-MUF.
4. Act in the same manner with the charts 'EJF (4000) F_2 (MHz)'. This gives the 4000-MUF.
   (Examples of ionization charts are given in Figs 126 and 127.)
5. Plot the two obtained values on the nomogram of Fig. 128 (on the left hand and right hand scales respectively) and join them with a transparent ruler. Follow the vertical corresponding to the transmission range to its intersection with the transparent ruler. Follow the oblique line passing through this intersection to one of the margins of the nomogram. Read the frequency at the extremity of the oblique line. This is the MUF of the path for the F_2-layer at the selected month and hour.
6. Repeat operations 1 to 5 for each even hour by using the corresponding charts, and—if necessary—the second origin meridian on the tracing.

(d) To determine the MUF relating to the E- and F_1-layers (E-MUF)

1. Select from Figs 114–125 the chart of zenith angle of the sun that corresponds to the month under consideration.
2. Place the tracing over the selected chart so that the equator coincides with that of the chart and the origin meridian with 00 h. Make a note of the zenith angle that corresponds to the centre of the path.
3. Select this angle on the left hand scale of the nomogram of Fig. 129. Select on the right hand scale of the same nomograph the sunspot number R_{12}. Join the two points by means of a transparent rule and read the value of the E-2000-MUF from the oblique scale of the nomogram (left hand graduations).
4. Select this value on the left hand scale of the nomogram of Fig. 130 and the distance on the right hand scale. By joining these two points by means of a transparent ruler, the E-MUF at 00 h UT can be read from the central scale.
5. Repeat operations 1, 2, 3 and 4 for each even hour by sliding the tracing over the chart so that one of the origin meridians coincides successively with the even hours.

(e) The effective MUF of the path for each even hour is the higher of the F_2-MUF and E-MUF as determined above.

(f) The F_2-MUF can be converted to F_2-FOT by using the conversion scale of Fig. 128.

The E-FOT is the same as the E-MUF.

The effective FOT of the path is the larger one of these two FOT values.

Note 1. When proceeding to calculate the field strength, and when the range is greater than 400 km, the process can be simplified by calculating the E-MUF by the method described in (b) in the next section.

Note 2. It is usually unnecessary to calculate the E-MUF for ranges exceeding 2000 km because propagation at these ranges is almost exclusively by the F_2-layer.

MUF and FOT (ranges exceeding 4000 km)

(a) Follow the method described in (a) in the previous section, but trace—if necessary—three origin meridians (at separations of 360°), so that each terminal point of the path will be enclosed by two origin meridians.

(b) Follow the method described in (b) in the previous section, but instead of marking the centre of the path, mark two control points, each situated at 2000 km from the corresponding terminal point.

(c) Determine the F_2-MUF for each hour at each control point, following the instructions of (c) in the previous section.

(d) For each hour, the MUF of the path is the lower MUF that corresponds to the two control points.

(e) Determine the FOT by using the conversion scale of Fig. 128.

8.2.3.2 **Calculating ionospheric absorption**

The absorption coefficient, which is required for calculating the field strength, is the product of three factors:

1. coefficient K, depending on the zenith angle of the sun
2. coefficient J, covering the effect of the season
3. coefficient Q, covering the degree of solar activity.

Coefficient K varies along the path. In practice, we use a form of average, represented by $\bar{K}$, which varies with the hour. The product $KQ = I$ is called 'absorption index'.

The required absorption coefficients are:
for ranges of less than 3200 km:

$$A = JQ\bar{K} = J\bar{I}$$

for ranges greater than 3 200 km:

$$Ad = JQ\bar{K}d = J\bar{I}d$$

where d = length of path.

Calculating $\bar{I}$ or $\bar{K}d$

This is done by means of the tracing of the path we already used for calculating the MUF, and Figs 114–125, 129, 131 and 132.

This tracing contains:

1. the path of the great circle, graduated in distances of 500 km
2. the equator and the origin meridian of the hours (or several origin meridians, at separations of 24 h)
3. the value of I or K at each point of the path at a certain hour is found by first placing the tracing on the chart of Figs 114–125 that corresponds to the month under consideration, so that the equator as well as the origin meridian coincide with the meridian corresponding to the time (UT) for which the absorption has to be calculated. The zenith angle of the sun can be read at the point considered.

The next step is to enter the zenith angle on the left hand scale of Fig. 129 and the sunspot number R_{12} on the right hand scale. I is then read from the right hand graduation of the oblique central scale. Selecting the sunspot number $R_{12} = 0$ on the right hand scale, one reads K from the same graduation of the same scale.

We now only have to calculate the mean values $\bar{I}$ or $\bar{K}d$.

Ranges smaller than 3 200 km; determination of $\bar{I}$

If the whole path lies in the zone where the zenith angle is greater than 105°, we obviously have $\bar{I} = 0$.

If the zenith angle is smaller than 105° at the two terminal points of the path, the value of I at the centre is taken as $\bar{I}$.

If one of the terminal points is in a zone where the zenith angle is smaller than 105° and the other point in a zone where it is greater:

1. Determine length d' of the path situated in the zone where the zenith angle is smaller than 105°.
2. Calculate value of I at the centre of d', name it I_0.
3. Use the formula:

$$\bar{I} = I_0 \frac{d'}{d}$$

Carry out this calculation for each hour UT.

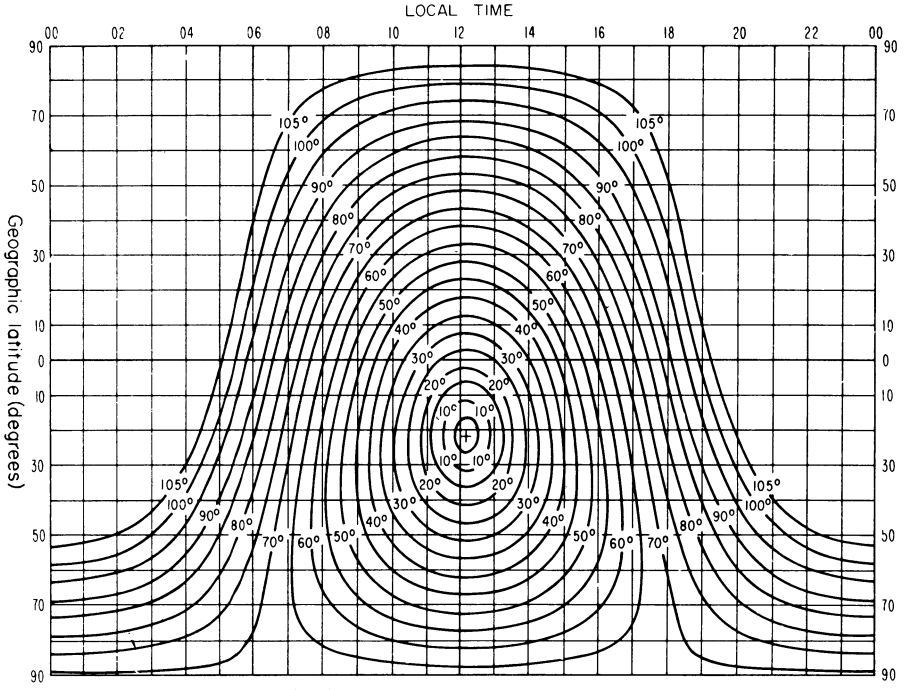

Fig. 114 Zenith angle of the sun; January

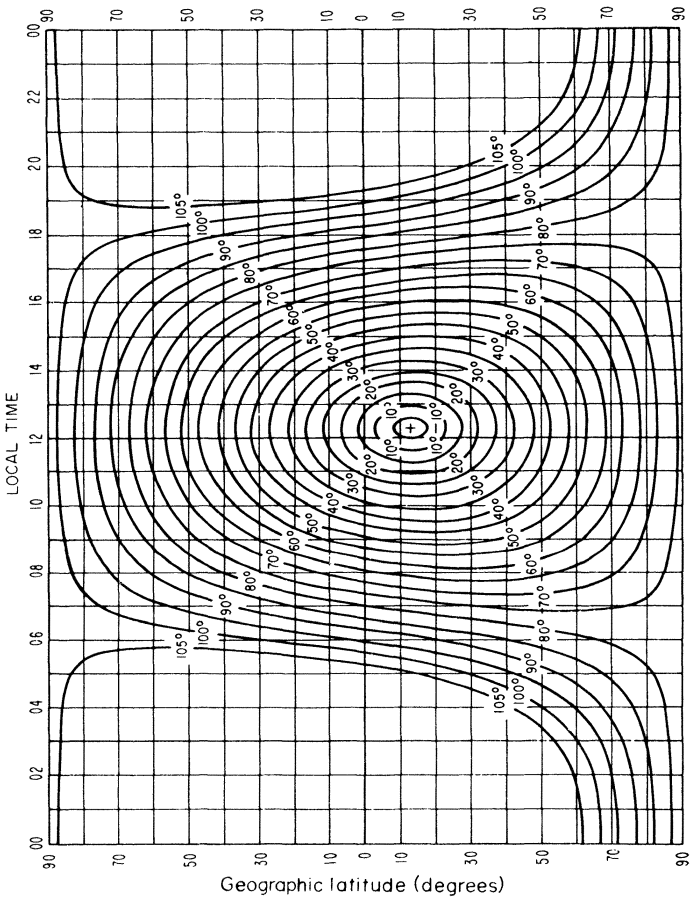

Fig. 115 Zenith angle of the sun; February

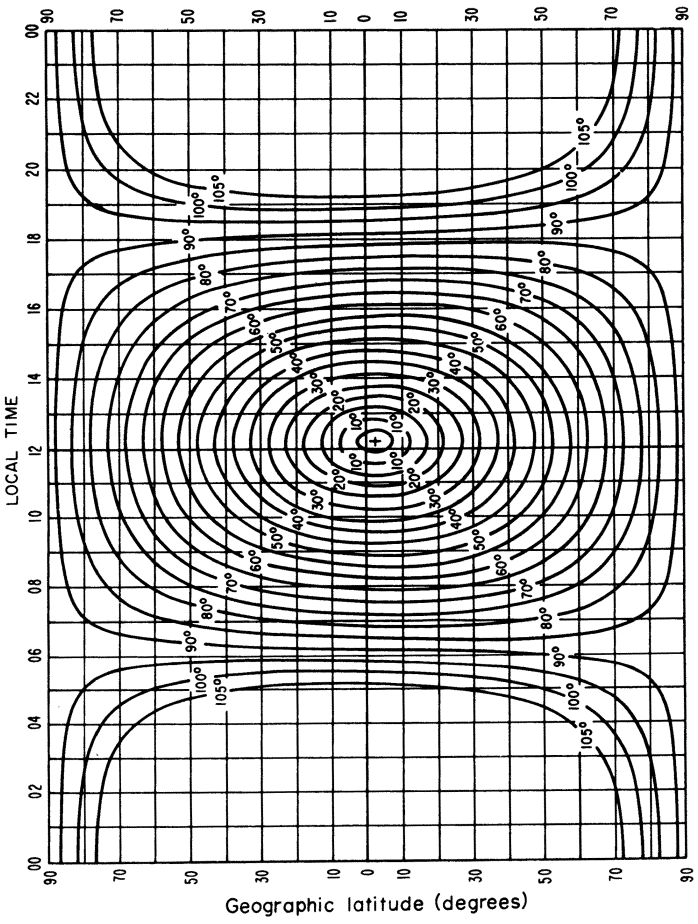

Fig. 116 Zenith angle of the sun; March

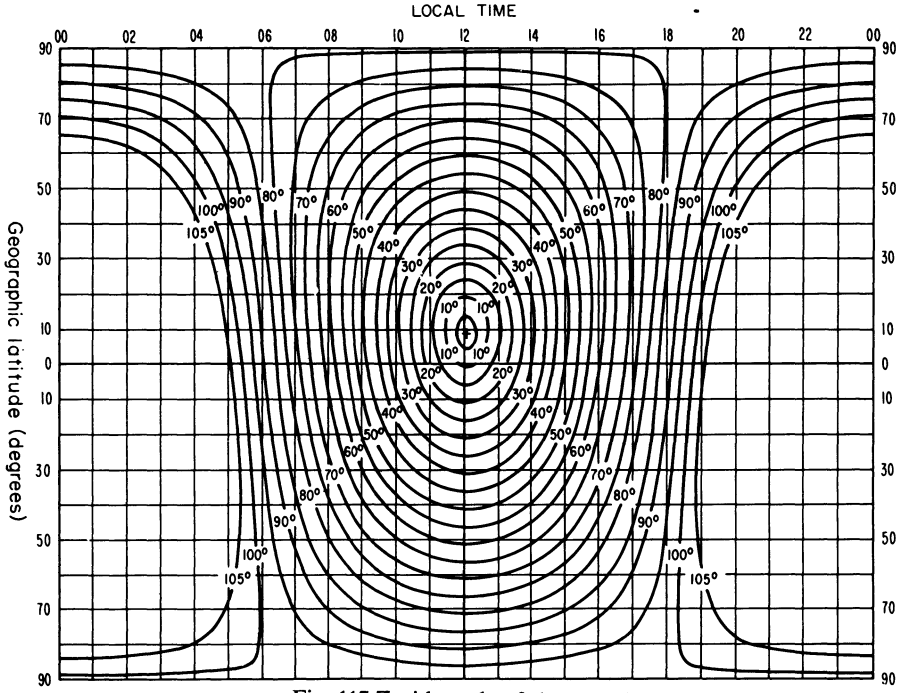

Fig. 117 Zenith angle of the sun; April

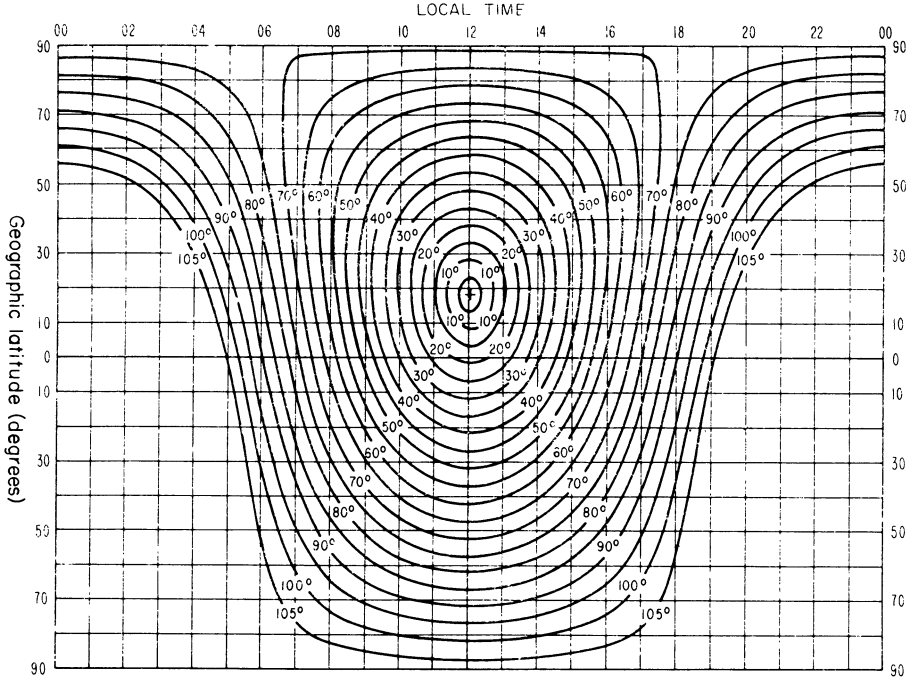

Fig. 118 Zenith angle of the sun; May

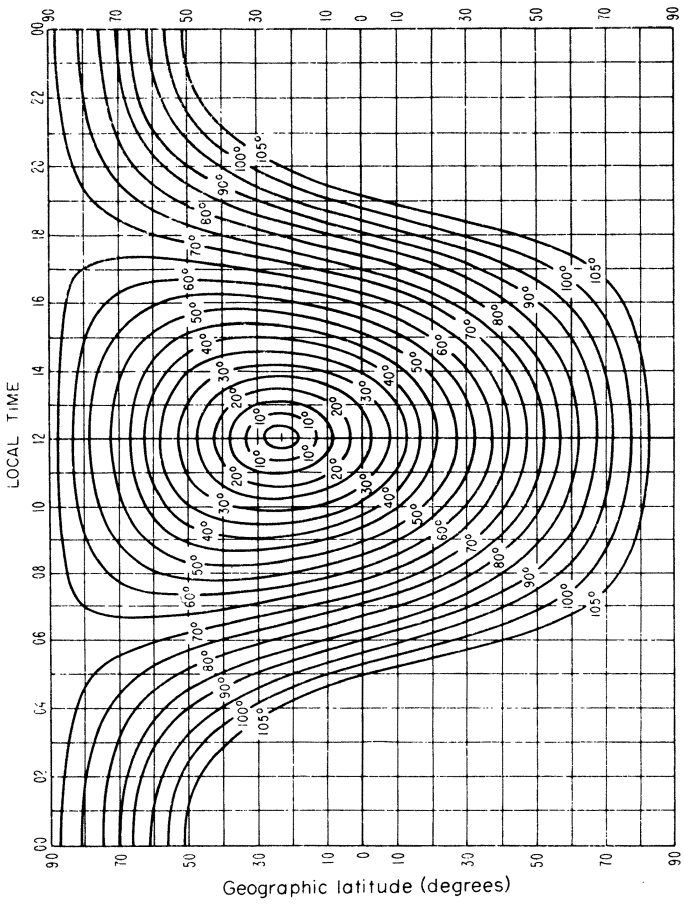

Fig. 119 Zenith angle of the sun; June

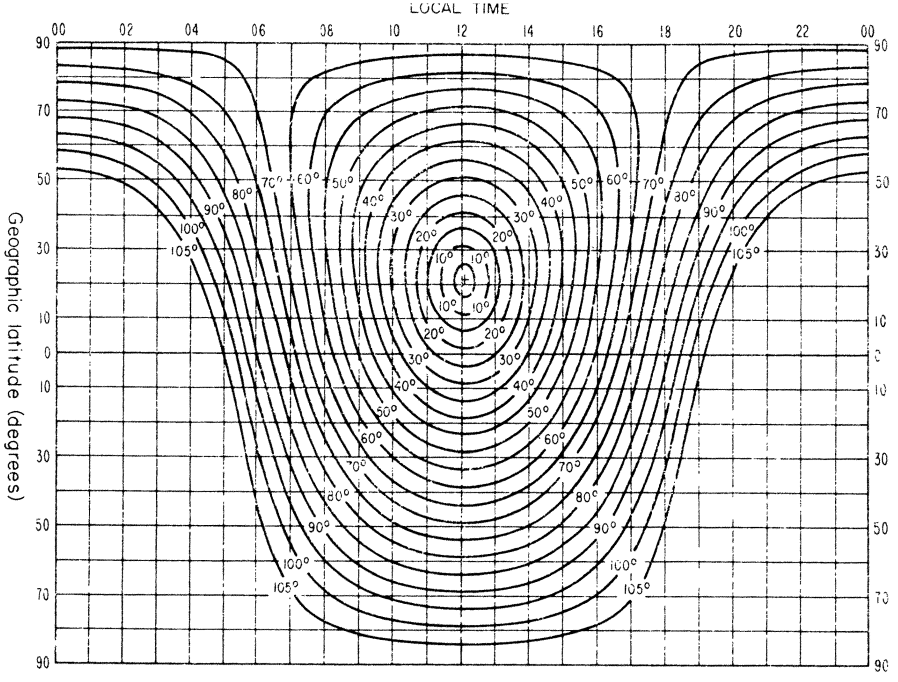

Fig. 120 Zenith angle of the sun; July

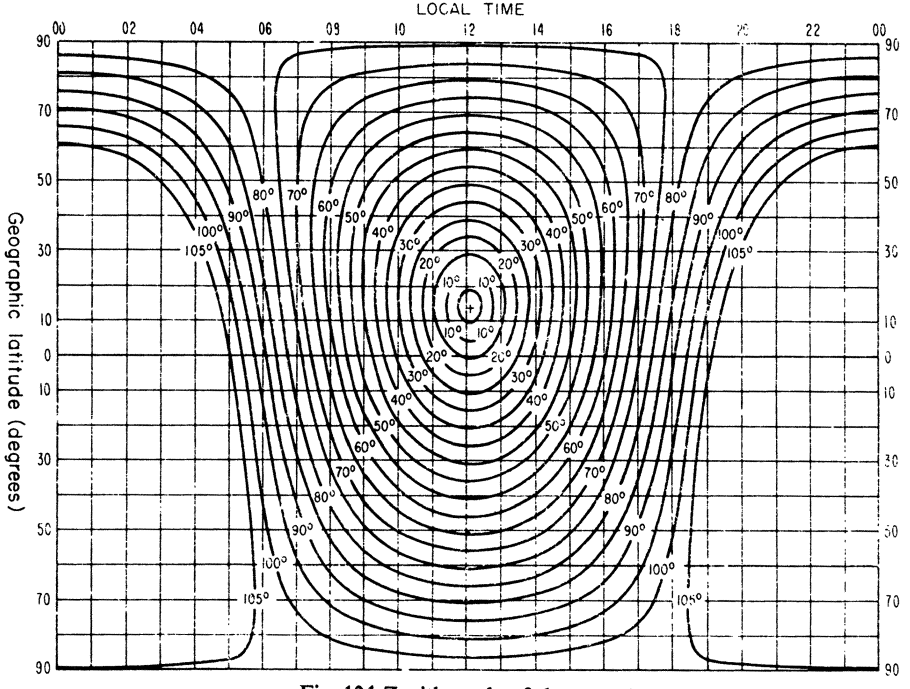

Fig. 12.1 Zenith angle of the sun; August

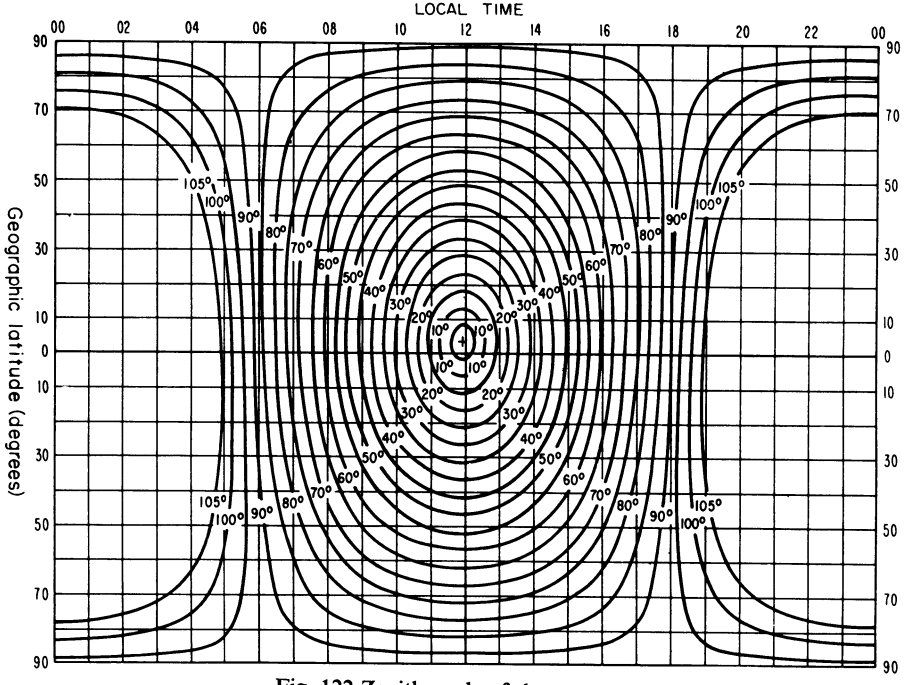

Fig. 122 Zenith angle of the sun; September

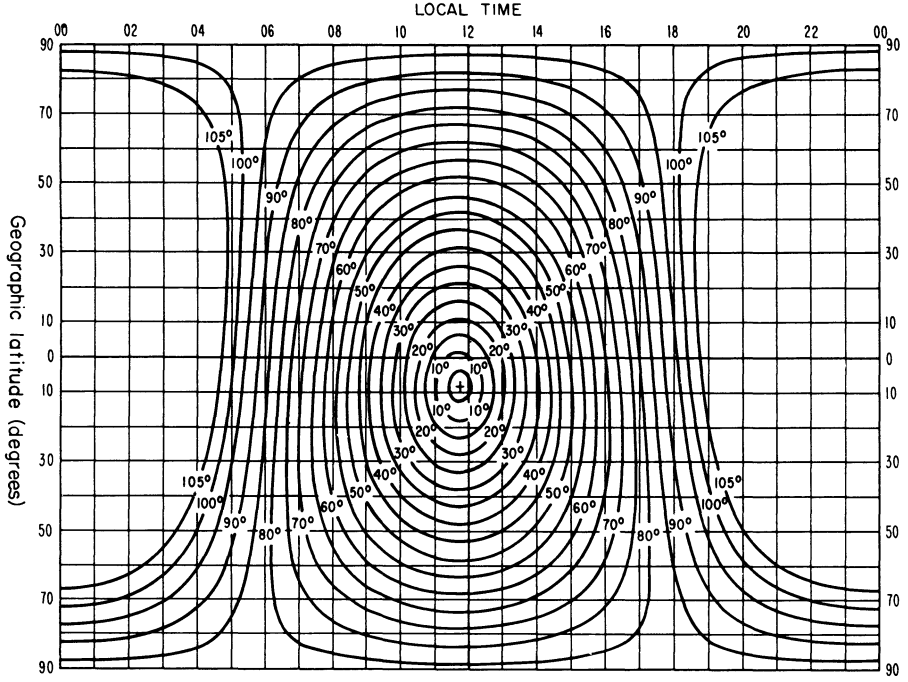

Fig. 123 Zenith angle of the sun; October

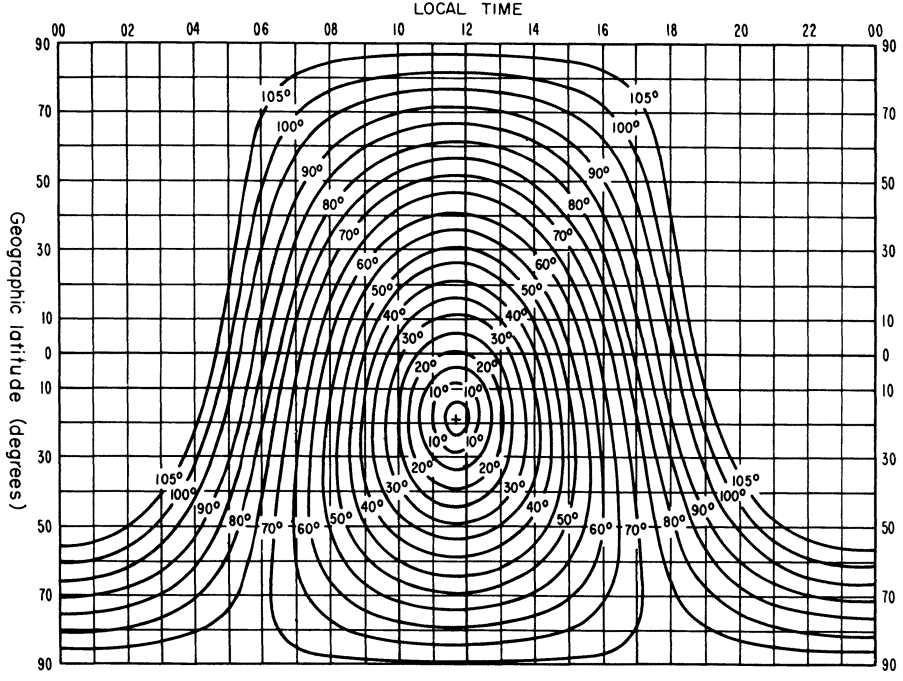

Fig. 124 Zenith angle of the sun; November

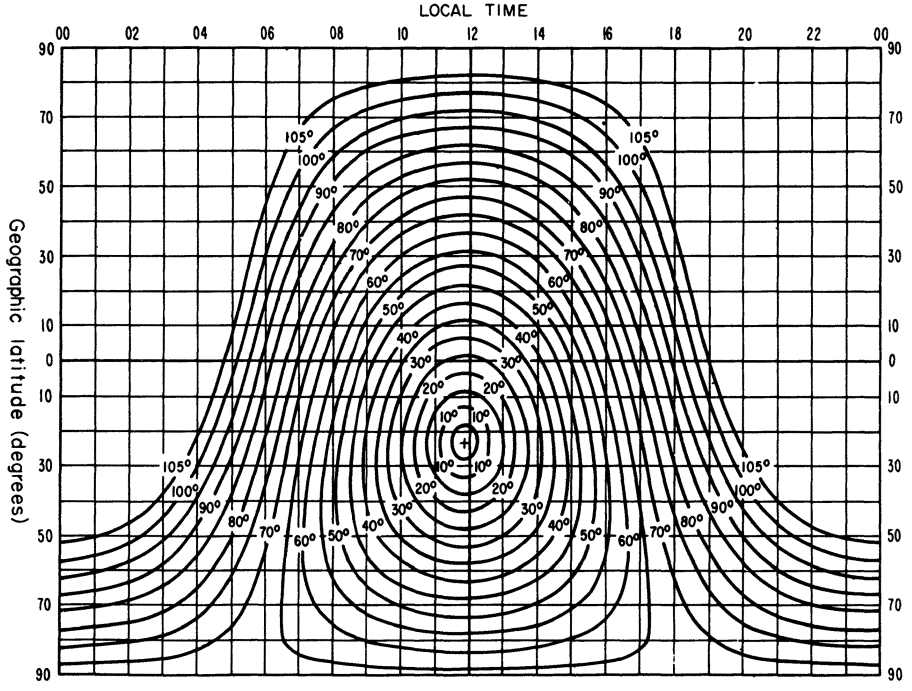

Fig. 125 Zenith angle of the sun; December

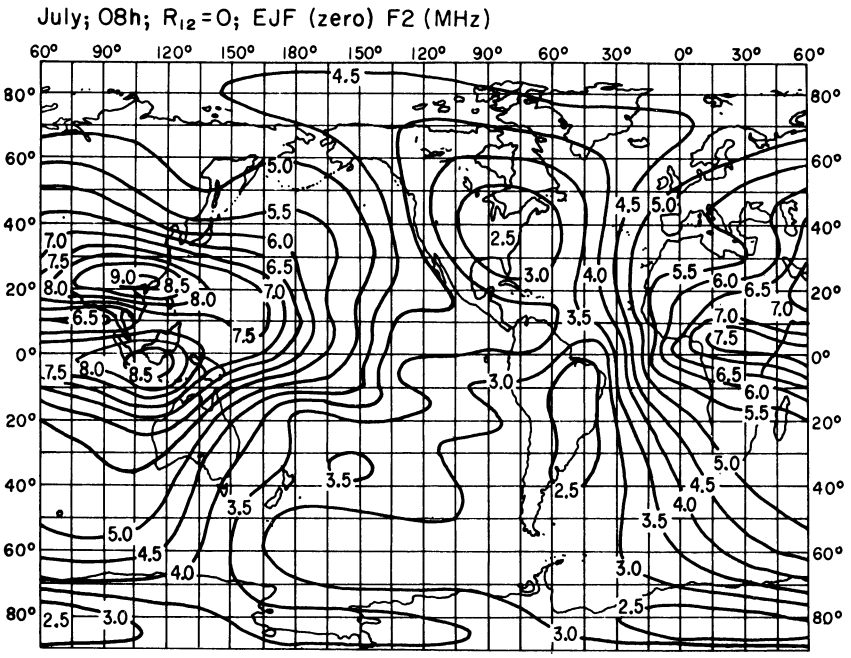

Fig. 126

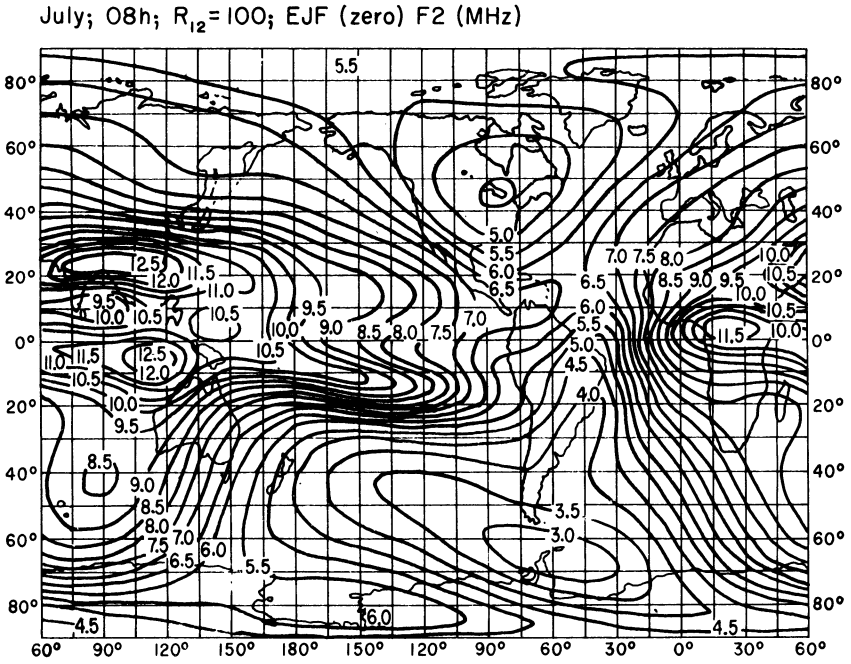

Fig. 127

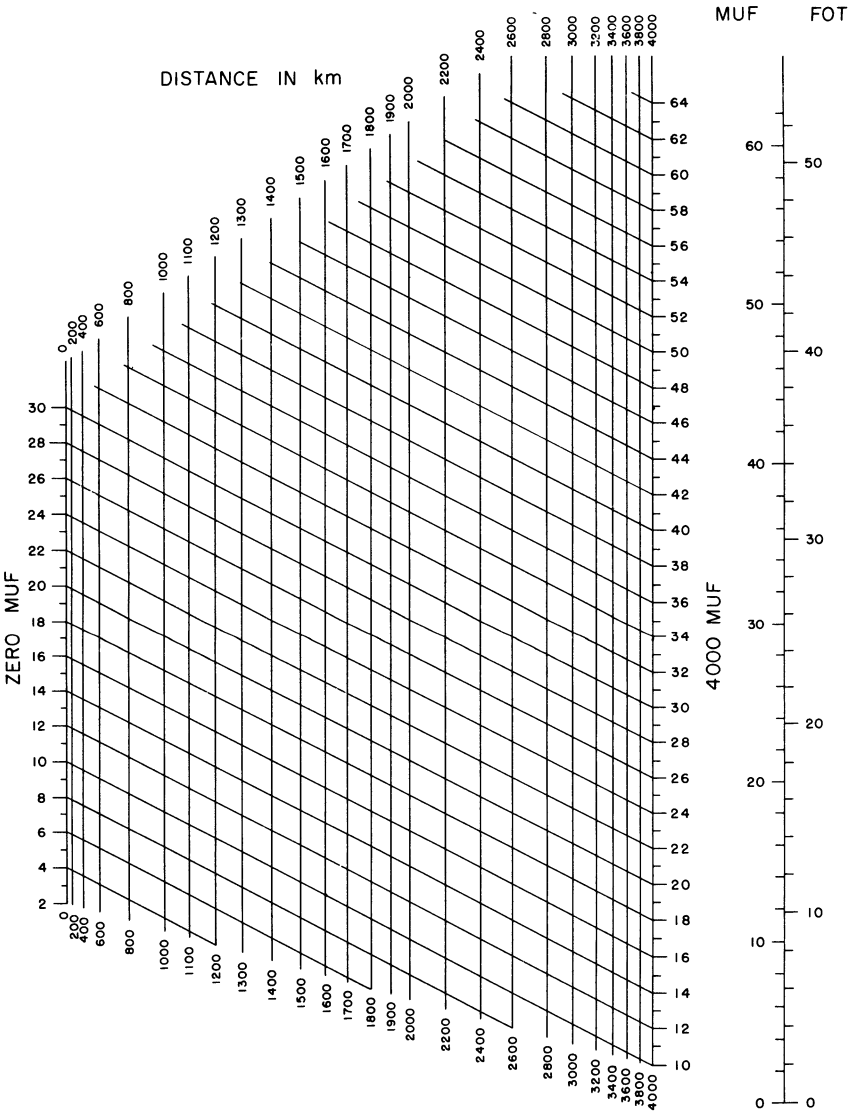

Fig. 128 Nomogram for transforming F_2-zero-MUF and F_2–4000-MUF to equivalent maximum usable frequencies at intermediate transmission distances; conversion scale for obtaining optimum working frequency (FOT)

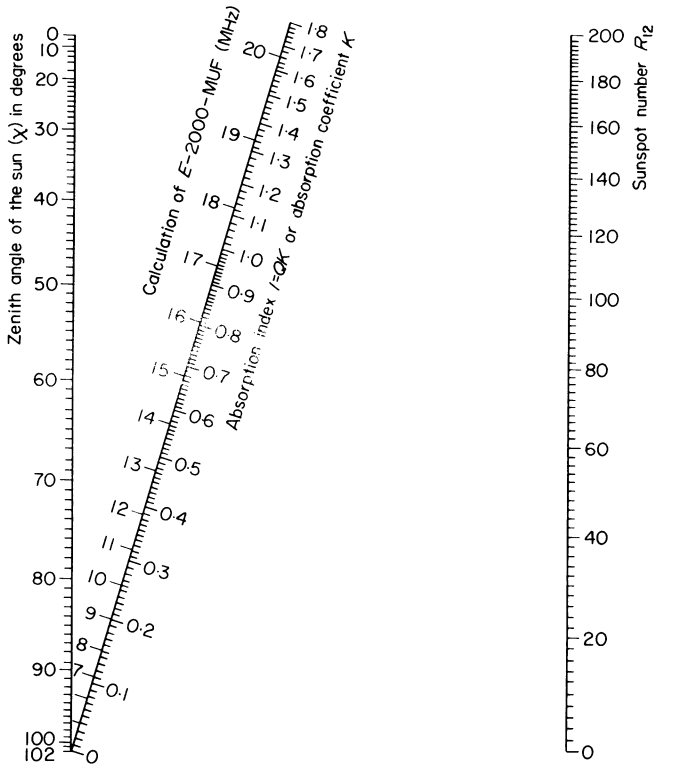

Month	Both stations in the same hemisphere		One station in each hemisphere
	Northern	Southern	
Jan.–Feb.	1.3	1.0	1.15
Mar.–Apr.	1.15	1.15	1.15
May–June	1.0	1.3	1.15
July–Aug.	1.0	1.3	1.15
Sept.–Oct.	1.15	1.15	1.15
Nov.–Dec.	1.3	1.0	1.15

Fig. 129 Calculation of *E*–2000–MUF and absorption index.
Seasonal adjustment factor J

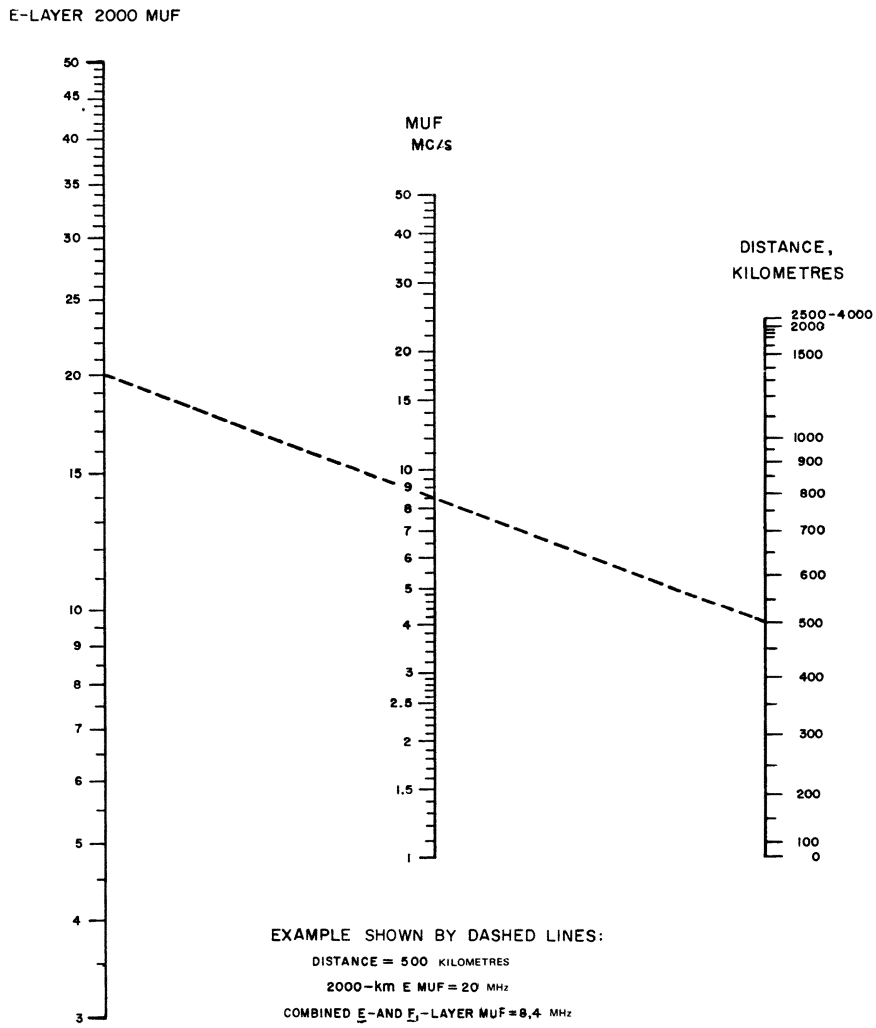

Fig. 130 Nomogram for transforming *E*-layer 2000-MUF to equivalent maximum usable frequencies and optimum working frequencies. The F_1-layer is approximately accounted for at distances between 2000 and 4000 km.

Ranges exceeding 3 200 *km; determination of* $\bar{K}d$

Determine as described above the values K_1 and K_2 of K at the two terminal points of the path.

Determine length d' for that part of the path where the zenith angle is smaller than 105°.

Enter on the nomogram of Fig. 131 the values of $(K_1 + K_2)$and d' and read $\bar{K}d$ from the left hand scale.

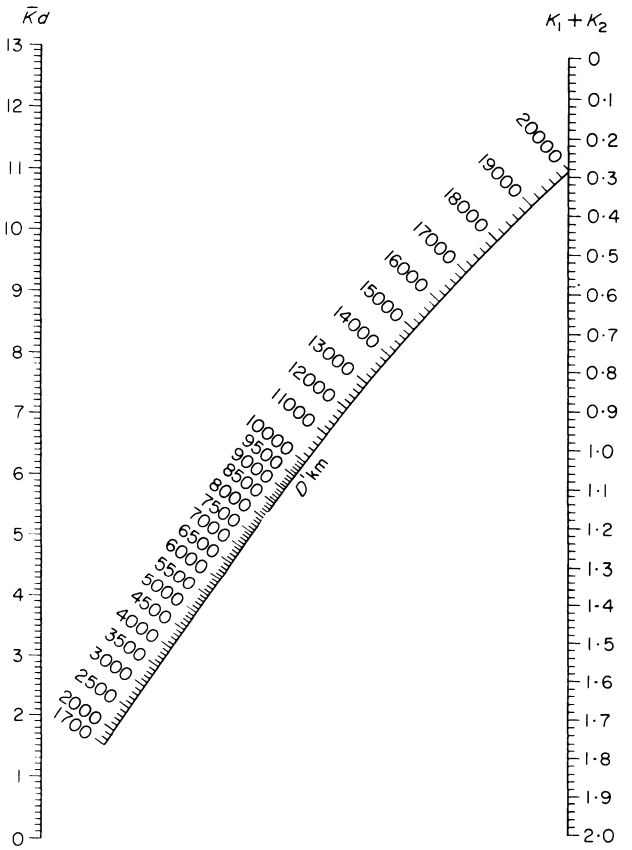

Fig. 131 Calculation of $\bar{K}d$ for ranges up to 20 000 km

Carry out this calculation for each hour UT.

Note. If the length of the path is approximately 20 000 km, it must be divided into two parts. Calculate $\bar{K}d$ for each part and add the results.

Auroral absorption

If the path traverses one of the auroral zones, the waves are subjected to very strong and very variable absorption. A rough estimate of this absorption can be made by means of Fig. 132, by placing the tracing on this figure in the manner described above. The correction which should be added to $\bar{I}$ or to $\bar{I}d$ is made as follows:

For ranges smaller than 3 200 km, read the values of K for points 500 km apart from the curves of the figure and establish the mean value $\bar{K}$. Multiply this result by:

$$Q = 1 + 0{\cdot}0037\, R_{12}$$

where R_{12} = sunspot number. This gives us I.

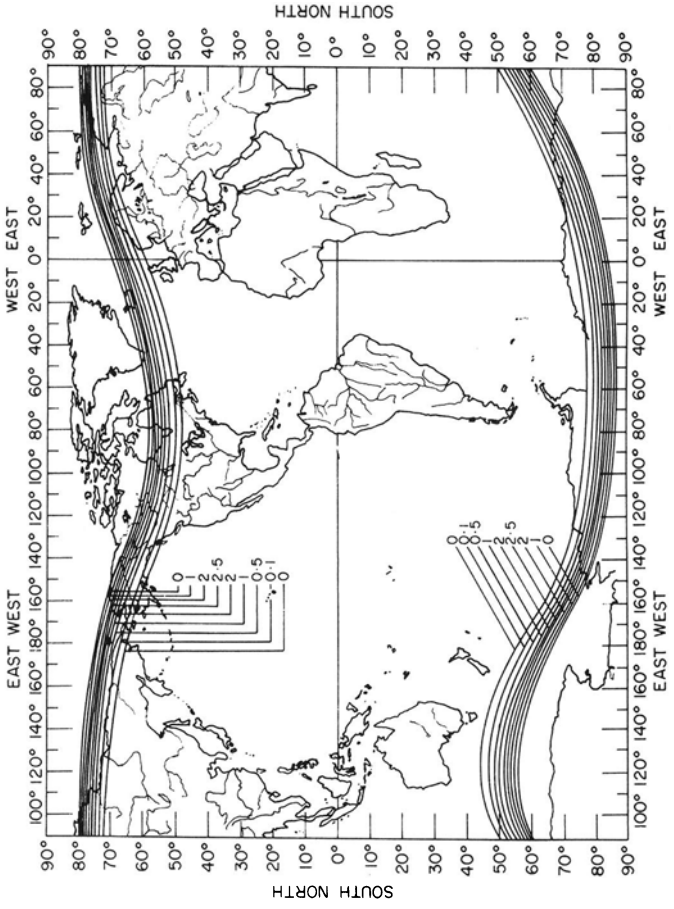

Fig. 132 Absorption in auroral regions

For ranges greater than 3 200 km, determine the distance along the arc of the great circle between the curves of the figure, multiply each distance by the mean value of K on the two curves that enclose it, and sum the products obtained. This gives $\bar{K}d$.

Add the result to the value of either $\bar{I}$ or $\bar{K}d$ obtained by means of the normal method.

Calculating J and A

J is given in the table of Fig. 129. We have:

$$A = J\bar{I} \text{ (for distances smaller than 3 200 km)}$$

$$Ad = JQ\bar{K}d \text{ (for distances greater than 3 200 km)}$$

who:

$$Q = 1 + 0{\cdot}0037\,R_{12}$$

8.2.3.3 Received field strength

The calculation method described below applies to frequencies defined in advance. See Section 8.2.3.5 below for the selection of these frequencies.

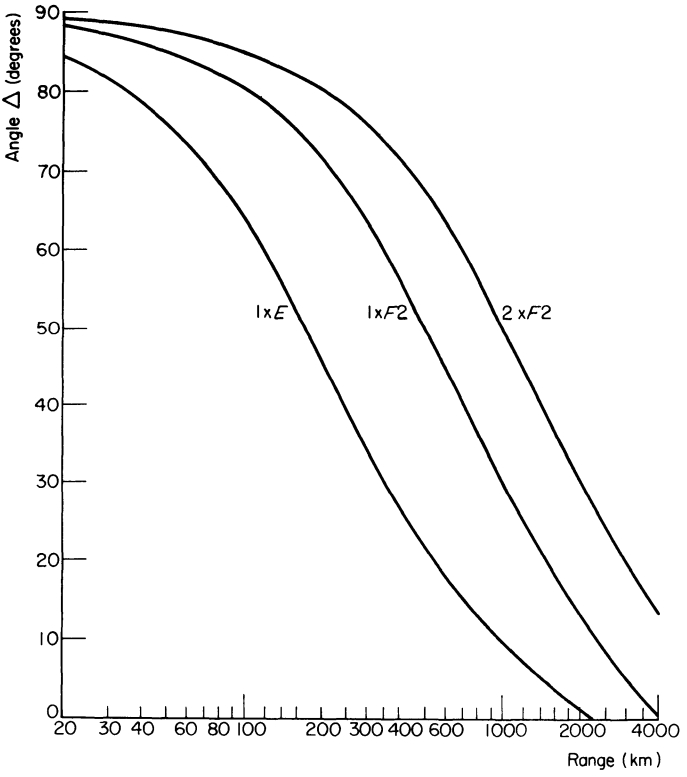

Fig. 133 Ionospheric wave; departure or arrival angle against range

Calculation of the field received only makes sense for frequencies below the MUF, because higher frequencies are not propagated.

The field received depends on:

1. the power of the transmitter
2. the gain of the antenna in the direction of propagation, therefore on the elevation angle. The latter in turn depends on the reflecting layer used and on the number of reflections from the ionosphere and the ground
3. absorption during travel.

Ranges of less than 400 km

Possible modes and corresponding elevation angles

The only important modes for small ranges are 1X*E* and 1X*F*. Mode 1X*E* is always possible if the frequency to be used is lower than the *E*-MUF for the range under consideration. Mode 1X*F* is only possible if the frequency

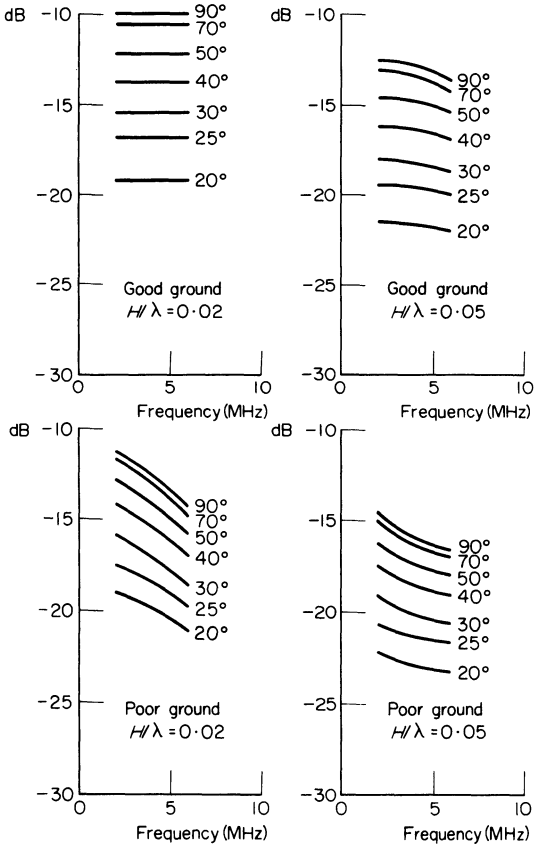

Fig. 134 Ionospheric wave; gain of horizontal $\lambda/2$ antenna

is both lower than the F_2-MUF and higher than the occultation frequency of the E-layer.

We therefore apply the following method:

(a) Determine from Fig. 133 the elevation angle for modes 1XE and 1XF.

(b) Read from curve 1XE the distance corresponding to the elevation angle for 1XF. Calculate the corresponding E-MUF by means of Fig. 130. This is the occultation frequency of the E-layer.

(c) Compare the frequency under investigation to the E-MUF, the F_2-MUF and the occultation frequency of the E-layer. This tells us which mode or modes are possible.

(d) Make a note of the corresponding elevation angle or angles.

Calculating field strength

(a) Convert the power of the source into dB related to 1 kW by means of Fig. 103.

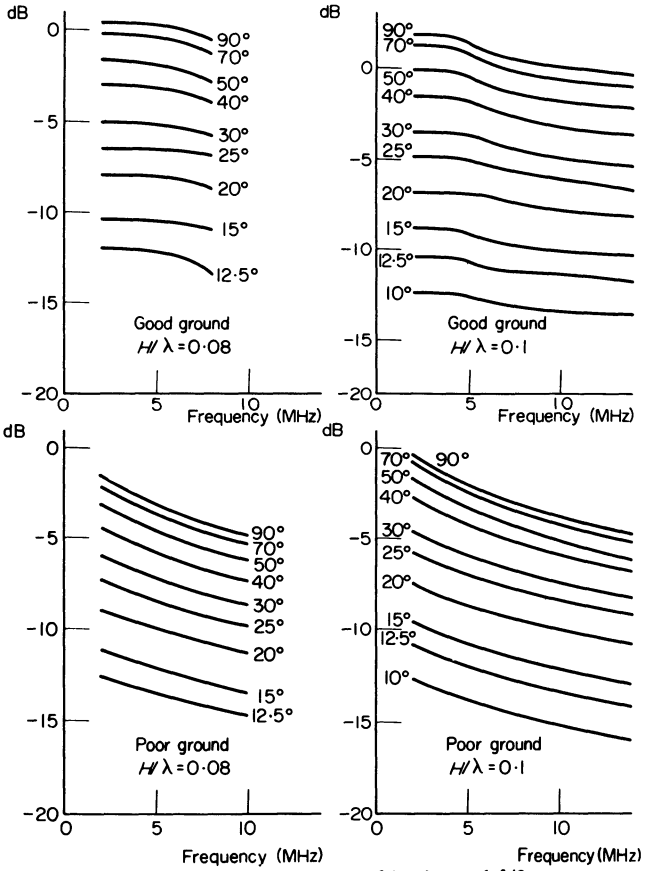

Fig. 135 Ionospheric wave; gain of horizontal $\lambda/2$ antenna

(b) Determine the gain of the antenna for the frequency under investigation for that elevation angle (calculated above) which gives the greatest gain. This is done by means of Figs 134–160. Adding this gain to the power expressed in dB gives the 'apparent power'.

(c) We now use the nomogram of Fig. 161 and enter on the left hand scale the apparent power as calculated above.

(d) Enter on the right hand scale the absorption coefficient A obtained in Section 8.2.3.2.

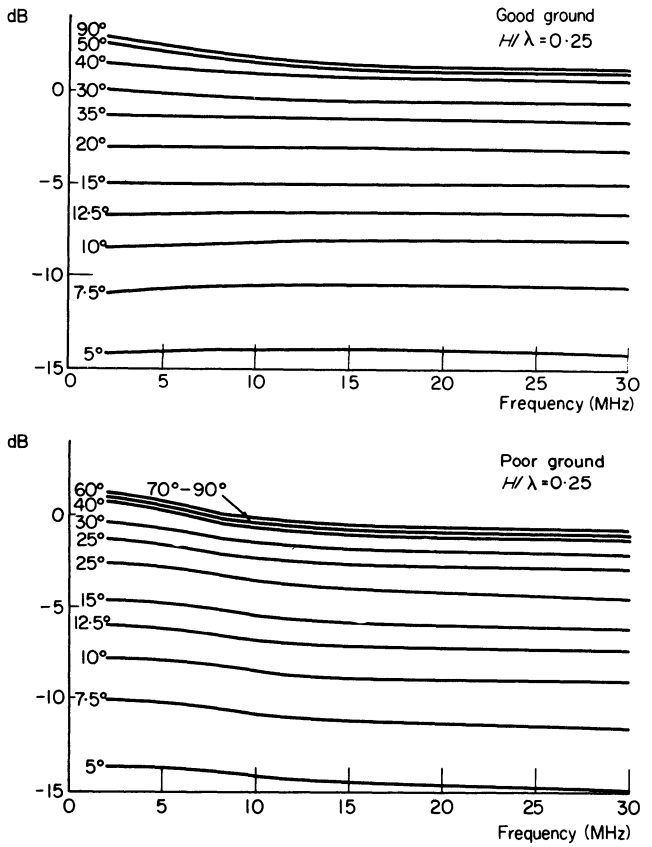

Fig. 136 Ionospheric wave; gain of horizontal $\lambda/2$ antenna

(e) Join these two points by means of a transparent ruler. Follow the vertical corresponding to the frequency to its intersection with the transparent ruler. Follow the oblique line passing through this intersection to one of the margins and read the field value in dB above 1μ V/m.

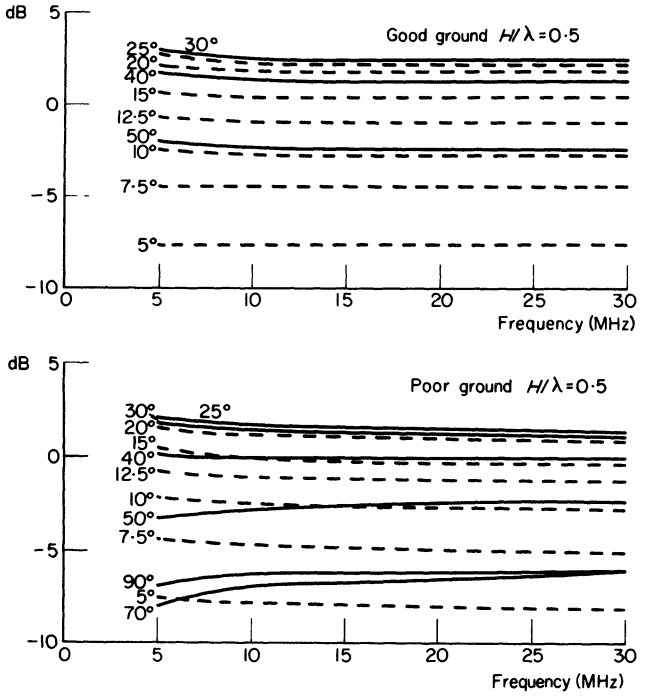

Fig. 137 Ionospheric wave; gain of horizontal $\lambda/2$ antenna

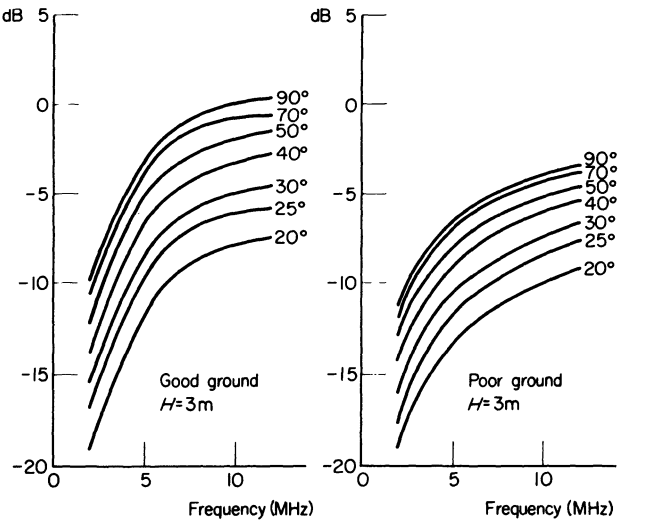

Fig. 138 Ionospheric wave; gain of horizontal $\lambda/2$ antenna

Ranges between 400 and 3 200 km

Possible modes and elevation angles

The most important modes are 1X*E*, 1X*F* and 2X*F*.

Mode 1X*E* is possible when the frequency is lower than the *E*-MUF.

Mode 1X*F* is possible when the frequency lies between the occultation frequency of 1X*F* by the *E*-layer and the F_2-MUF.

Mode 2X*F* is possible when the frequency lies between the occultation frequency of 2X*F* by the *E*-layer and the F_2-MUF for half the range.

It is essential to determine all possible modes and the corresponding elevation angles. This is done as follows:

(a) Follow the method described in Section 8.2.3.1(c) for determining the F_2-MUF for half the range ($2 \times F_2$-MUF).

(b) Select the graphs (in Figs 162–169) that correspond to the distance (or enclose it). Take the curve that corresponds to the absorption coefficient

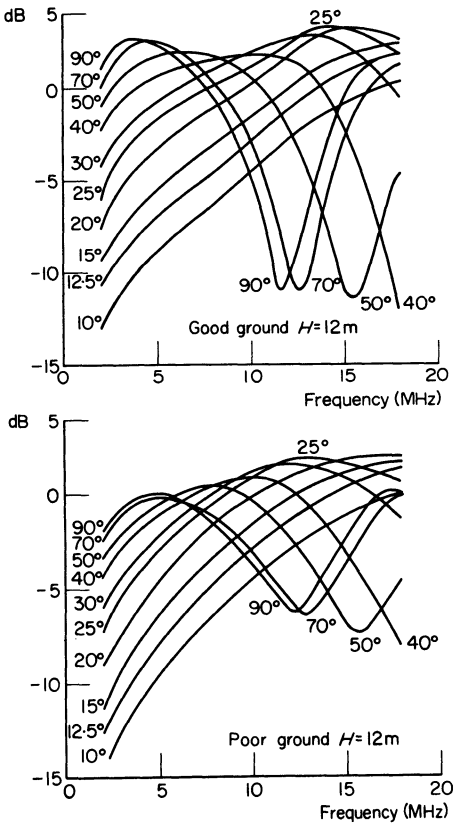

Fig. 139 Ionospheric wave; gain of horizontal $\lambda/2$ antenna

A and to the seasonal coefficient J as determined in Section 8.2.3.2. The intersections of these curves produce:

1. E-MUF (which needs therefore not to be calculated by the more complex method described in Section 8.2.3.1(d).
2. Occultation frequency of 1XF by the E-layer.
3. Occultation frequency of 2XF by the E-layer.

(If the range lies between these two graphs, the above data must be interpolated.)

(c) We now know which modes are possible for the particular frequency, and the corresponding elevation angles can be read from Fig. 133.

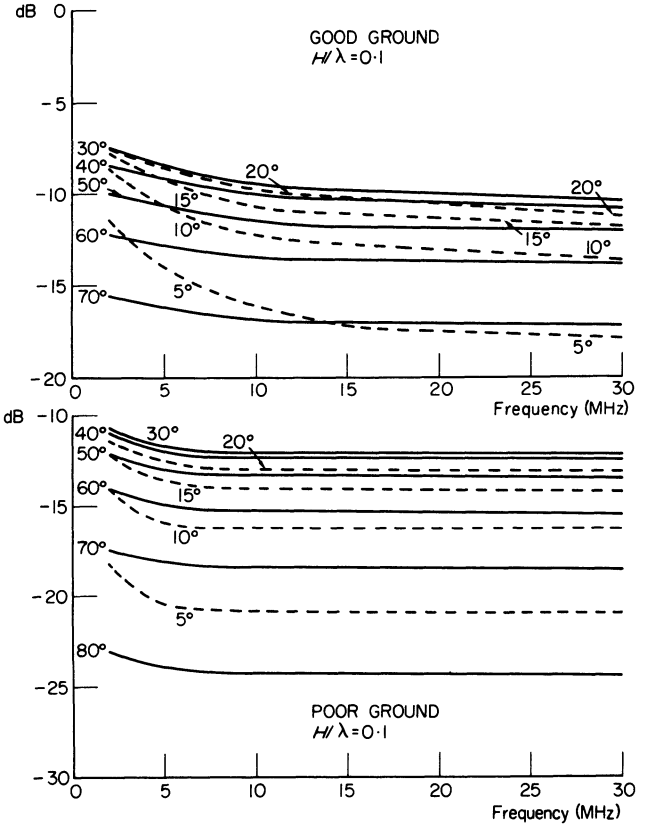

Fig. 140 Ionospheric wave; gain of vertical antenna on land

Calculating field strength

(a) Convert the power of the transmitter into dB related to 1 kW by using Fig. 103.

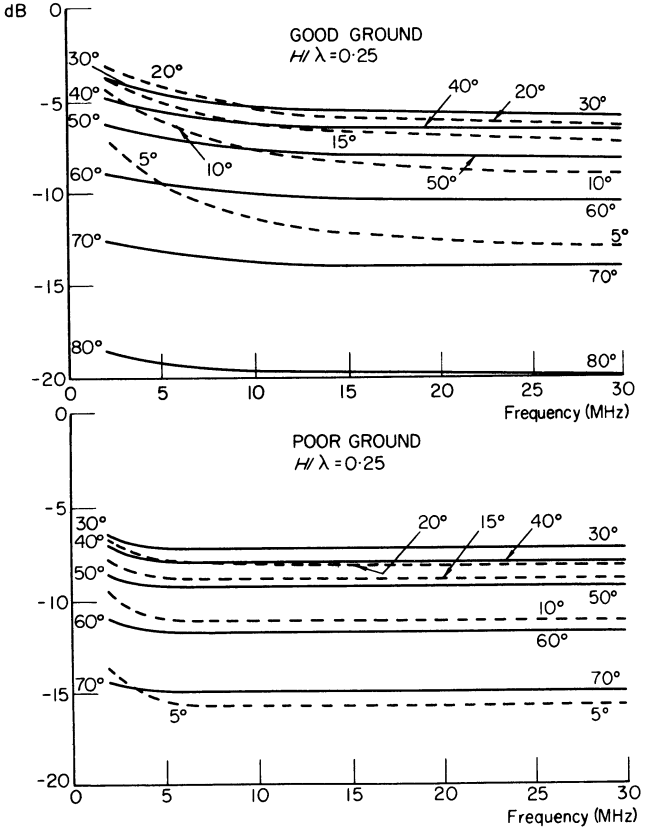

Fig. 141 Ionospheric wave; gain of vertical antenna on land

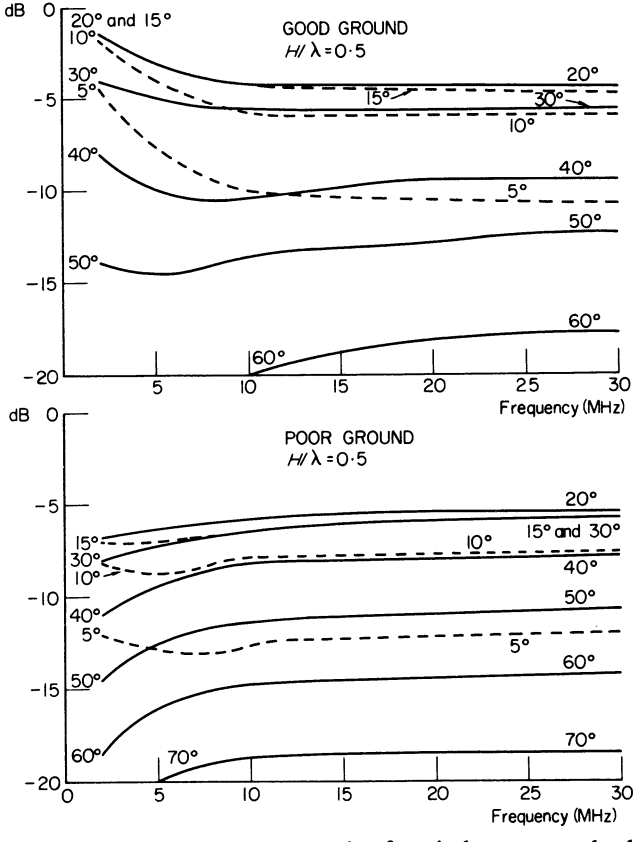

Fig. 142 Ionospheric wave; gain of vertical antenna on land

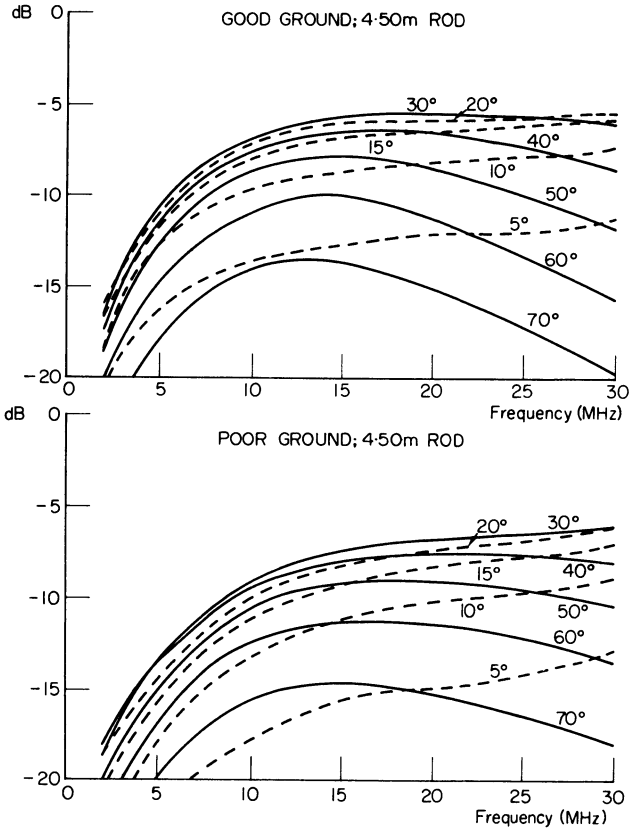

Fig. 143 Ionospheric wave; gain of vertical antenna on land

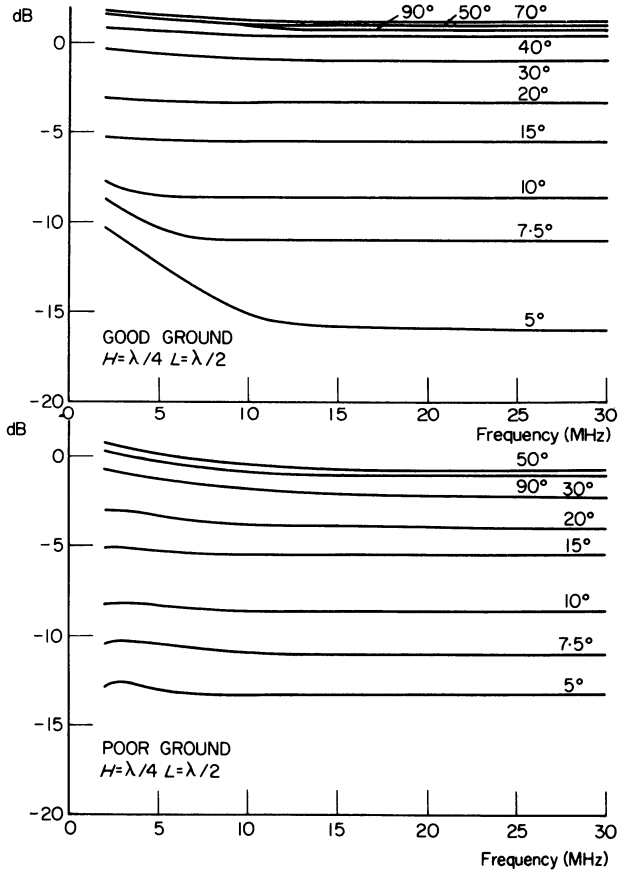

Fig. 144 Ionospheric wave; gain of L-antenna on land

(b) Determine the antenna gain by means of Figs 134–160 for the elevation angle corresponding to one of the modes that have been found possible, as well as for the frequency under consideration. Add this gain to the result of the previous operation.

(c) Determine the field strength for a radiated power of 1 kW on the graph corresponding to the mode under consideration, and add this value to that of the previous operation. This gives us the field value in dB above $1\mu V/m$ for the mode envisaged.

(d) Follow the same method for the other possible modes and take the highest value as the field strength.

Ranges greater than 3 200 km

A great number of modes are possible at such ranges, including reflection or scattering by strongly ionized nuclei, which are sometimes outside the plane of the great circle through the transmitter and the receiver. The CRPL method does not claim to identify them; it is a purely empirical method.

Elevation angle of waves

The elevation angle is continuously variable, in general between 7 and 15°, but often between 0 and 30°. Several modes coexist frequently—each with a different angle. The transmitting antenna must therefore not possess too high vertical directivity.

Calculating field strength

(a) Convert the power of the transmitter into dB related to 1 kW, using Fig. 103.

(b) Now use Figs 134–160 to determine the gain of the antenna used for that particular frequency and for elevational angles of 5, 10, 15, 25 and 30°.

(c) Convert these gains into power by means of Fig. 103.

(d) Take the arithmatic mean of these powers.

(e) Convert this mean into antenna gain by means of Fig. 103. This gives us the equivalent antenna gain for great ranges. Add to this gain the value of the power in dB, and we have the apparent radiated power.

(f) Calculate the field for 1 kW radiated, using Fig. 170 or Fig. 171, according to the value of *Ad*.

(g) Select the value of *Ad* obtained above on the right hand scale.

(h) Select the range on the left hand scale.

(i) Join these two points by means of a transparent ruler. Follow the vertical that corresponds to the frequency to its intersection with the transparent ruler.

(j) Read the field strength for 1 kW radiated in dB above $1\mu V/m$ on the oblique line that passes through this intersection.

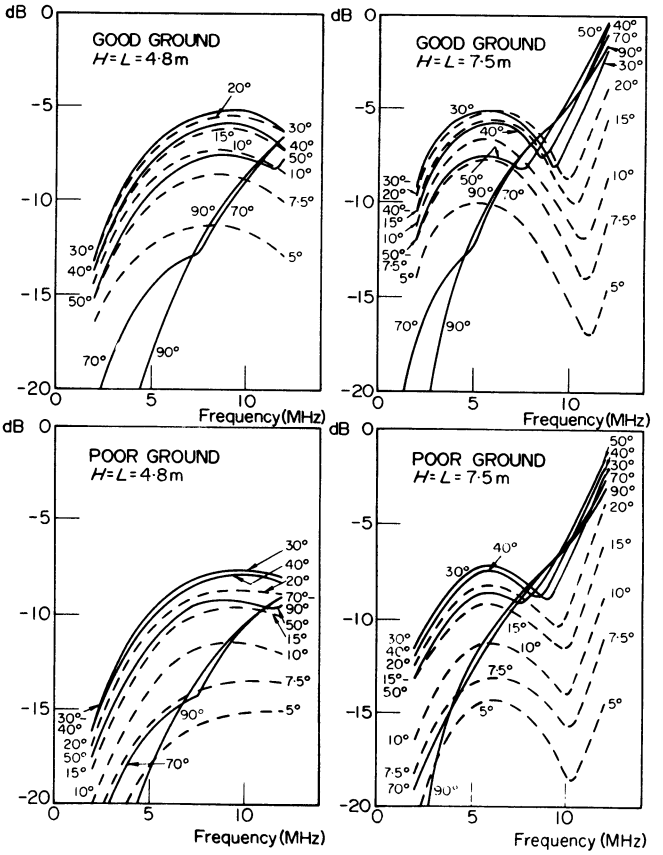

Fig. 145 Ionospheric wave; gain of L-antenna on land

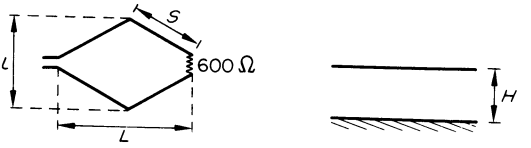

Type	*S*	*L*	*l*	*H*
A	112·5	215	77	19·5
B	105	197	72	18
C	94·5	177·5	65	17
D	87	160·5	66·5	16·5
E	81	146·5	68·5	16
F	73·5	130	68	15·5
G	67·5	117	67·5	15

Fig. 146 Dimensions of rhombic antennae; form of antenna, A, B, C, . . .

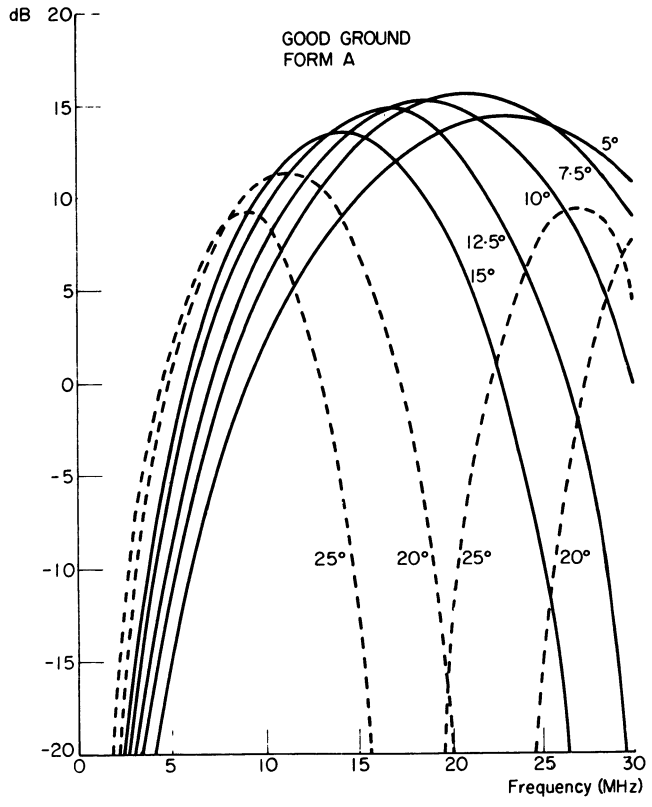

Fig. 147 Ionospheric wave; gain of rhombic antennae

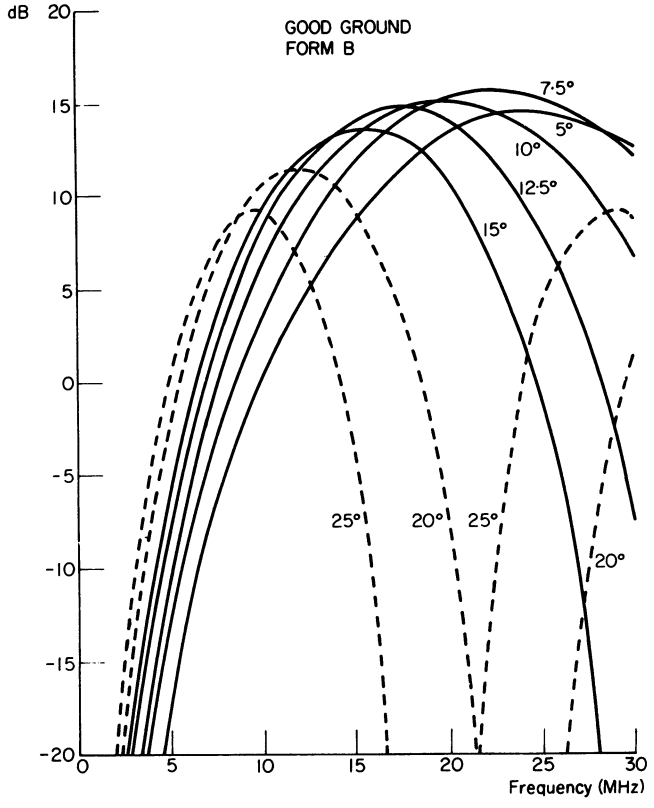

Fig. 148 Ionospheric wave; gain of rhombic antennae

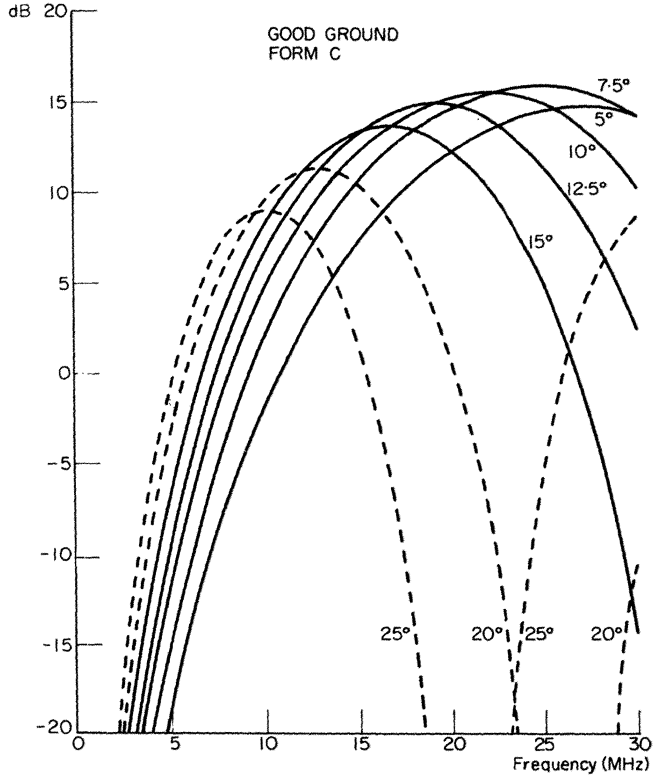

Fig. 149 Ionospheric wave; gain of rhombic antennae

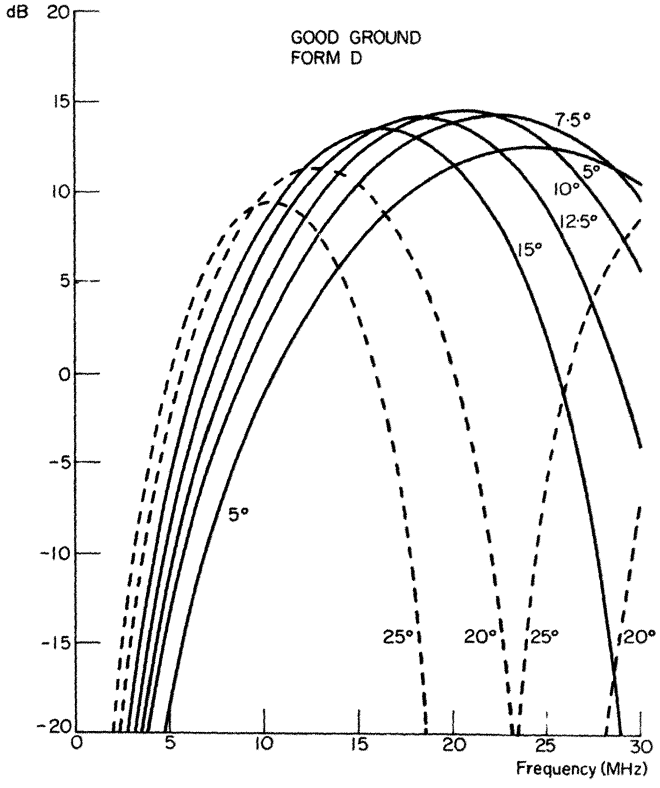

Fig. 150 Ionospheric wave; gain of rhombic antennae

(k) Add this value to the apparent radiated power and we have the field strength received, in dB above $1\mu V/m$.

8.2.3.4 **Discrimination gain**

Discrimination gain is zero for antennae with little directivity (rectilinear or *L*-shaped), or when the antenna is directed towards a strong source of noise (see Figs 71–96).

In all other cases, discrimination gain equals the algebraic sum of the antenna gain (Figs 134–160) and the gain of the isotropic antenna at the same height, but with the opposite sign (Fig. 172). (The resultant gain is usually not achieved during periods of poor propagation. This fact may lead to the subtraction of 6 dB from high gains).

The discrimination gain must be deducted from the required field (Section 8.2.1.4).

8.2.3.5 **Conclusions**

The results of the above calculations now allow us to determine the frequencies that must be used for a given communication.

For a frequency to be useful at a given hour, it must at that hour be lower than the MUF, and the field received at this frequency at that hour must be greater than the required field at the same frequency and at the same hour.

There are two possibilities:

The frequencies are already known

This is the case when they have been allocated by some authority. In this case:

(a) We start by eliminating, for each hour, all frequencies higher than the MUF.

(b) We calculate for each of the other frequencies the field received and the field required at each hour. All frequencies for which the field received is lower than the required field are removed.

(c) All remaining frequencies, at each hour, can be used. The highest of them is always the most favourable if lower than or equal to the FOT.

How to determine possible frequencies

This case occurs for example when making a request for frequencies from the allocating authority. In this case:

(a) We trace the curve of the MUF and the FOT as a function of the hour, which gives the upper limit.

(b) We determine the LUF (Lowest Usable Frequency) for each hour and trace the curve.

(c) The interval between the curves of the FOT (or to the limit, of MUF) and of the LUF is the usable frequency band for that particular link, at any time.

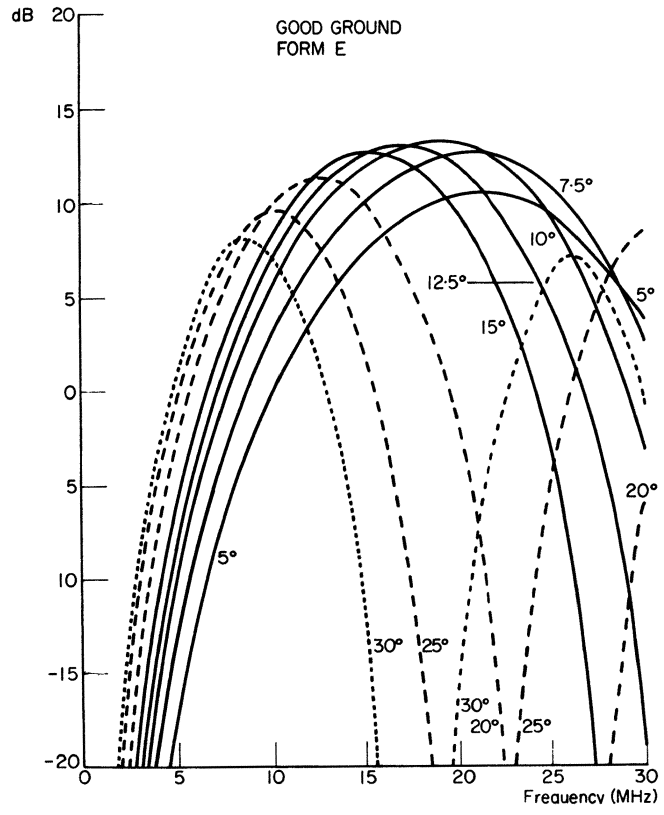

Fig. 151 Ionospheric wave; gain of rhombic antennae

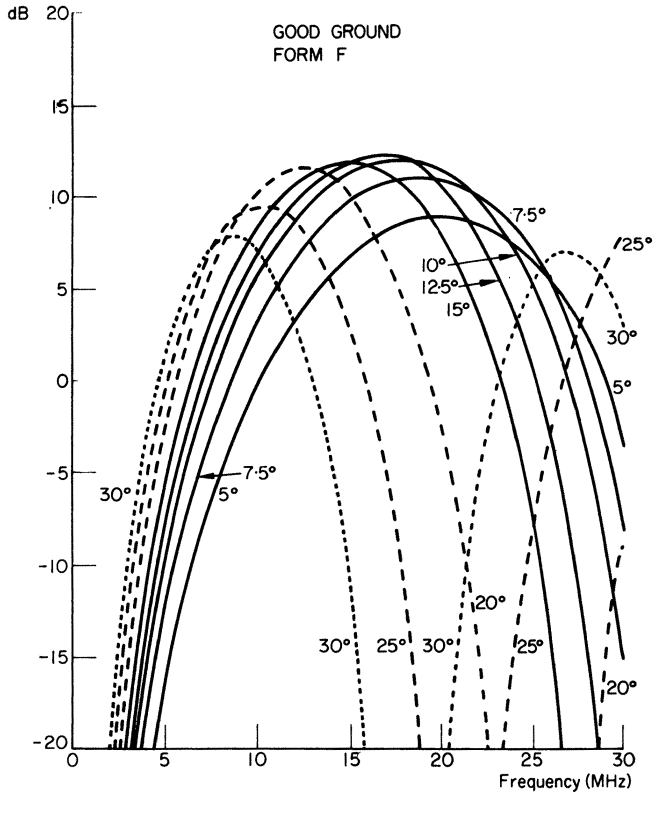

Fig. 152 Ionospheric wave; gain of rhombic antennae

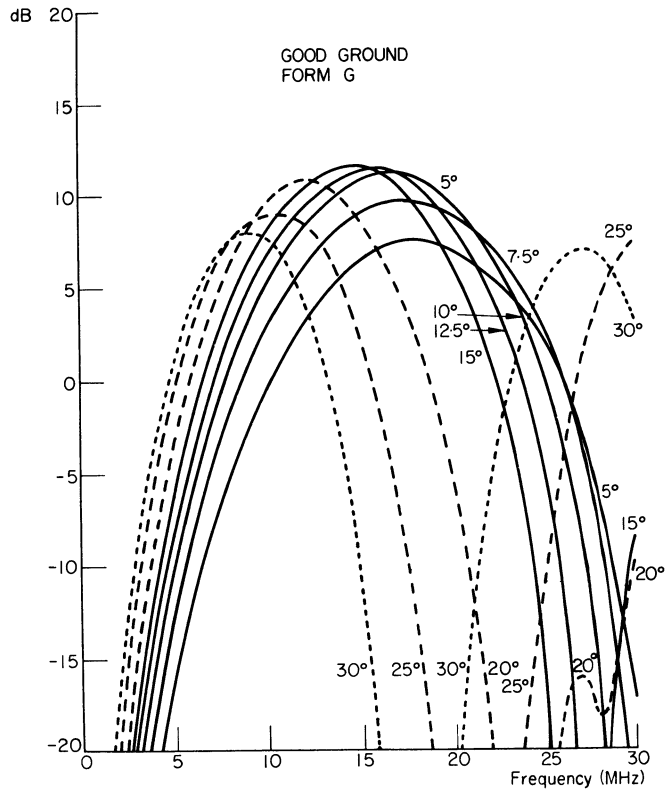

Fig. 153 Ionospheric wave; gain of rhombic antennae

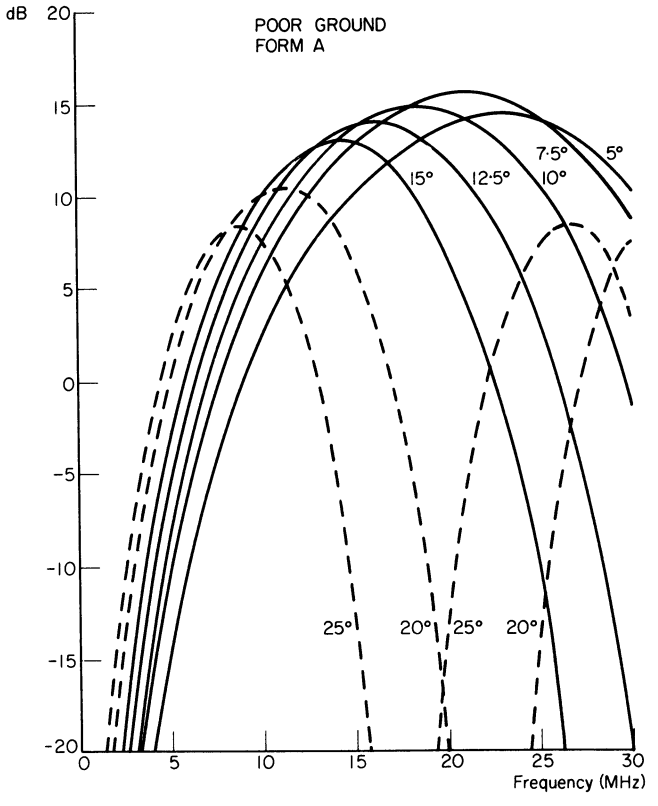

Fig. 154 Ionospheric wave; gain of rhombic antennae

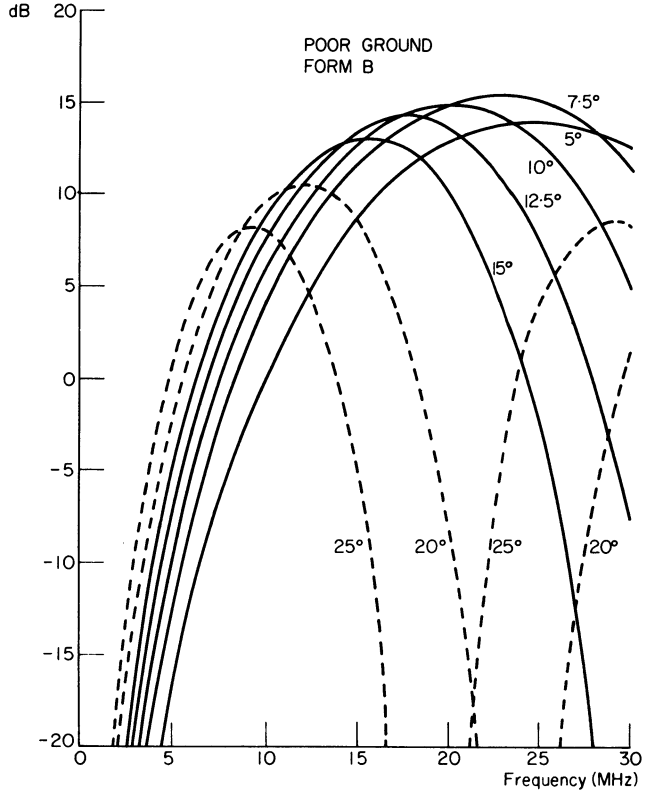

Fig. 155 Ionospheric wave; gain of rhombic antennae

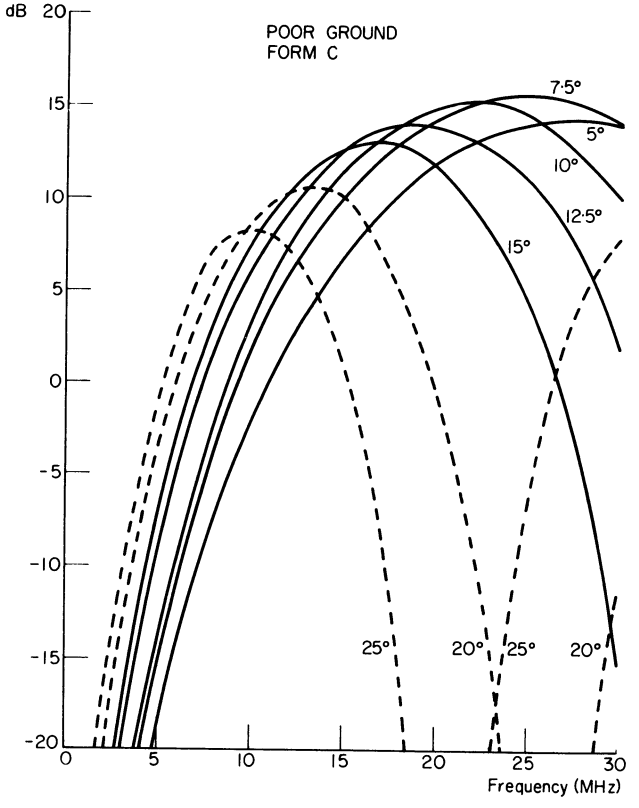

Fig. 156 Ionospheric wave; gain of rhombic antennae

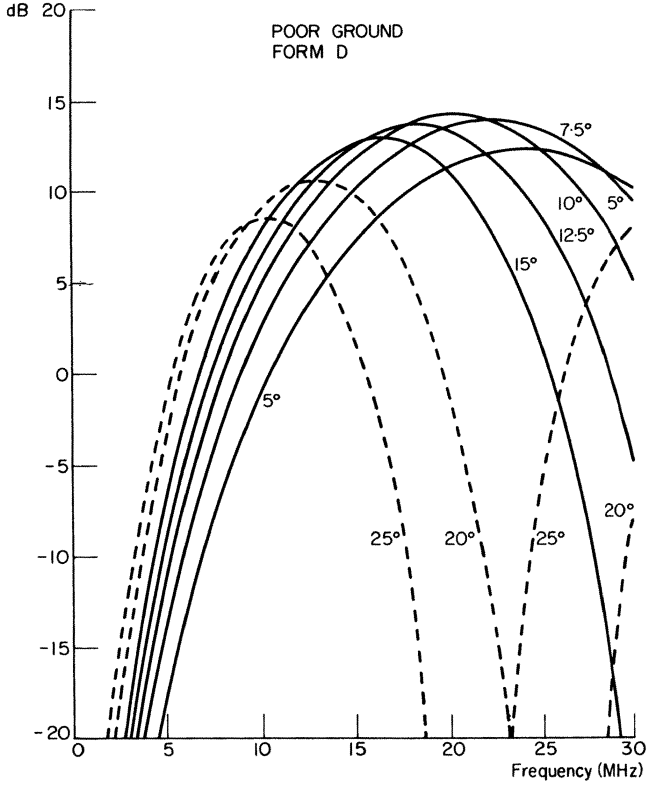

Fig. 157 Ionospheric wave; gain of rhombic antennae

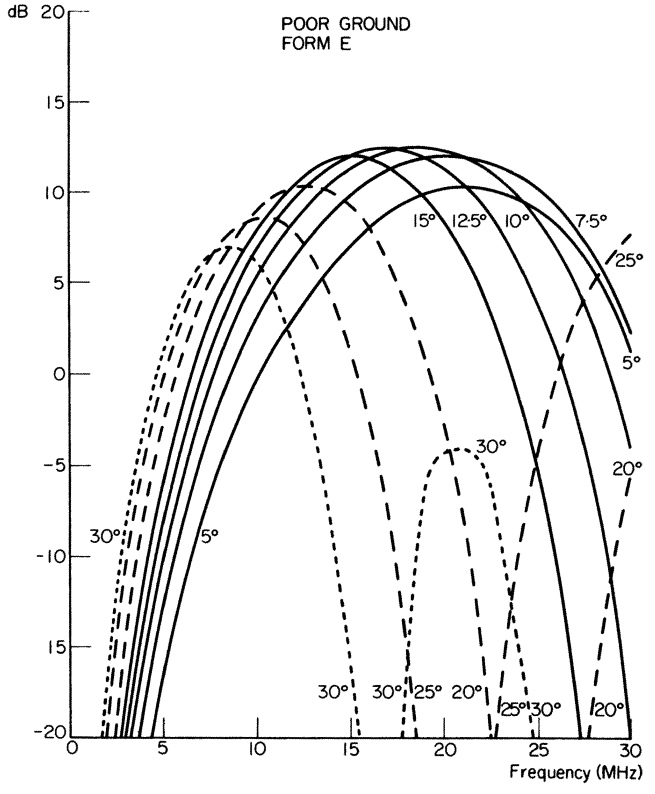

Fig. 158 Ionospheric wave; gain of rhombic antennae

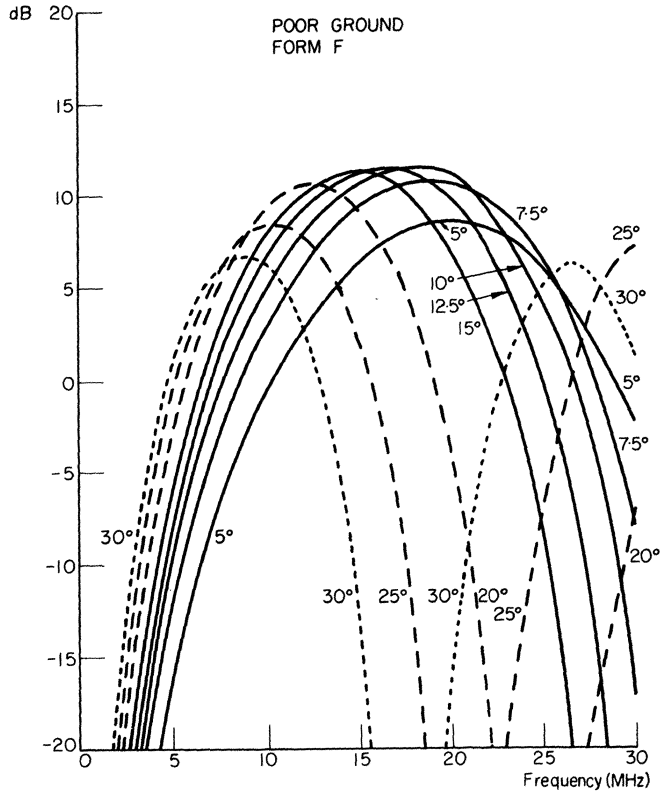

Fig. 159 Ionospheric wave; gain of rhombic antennae

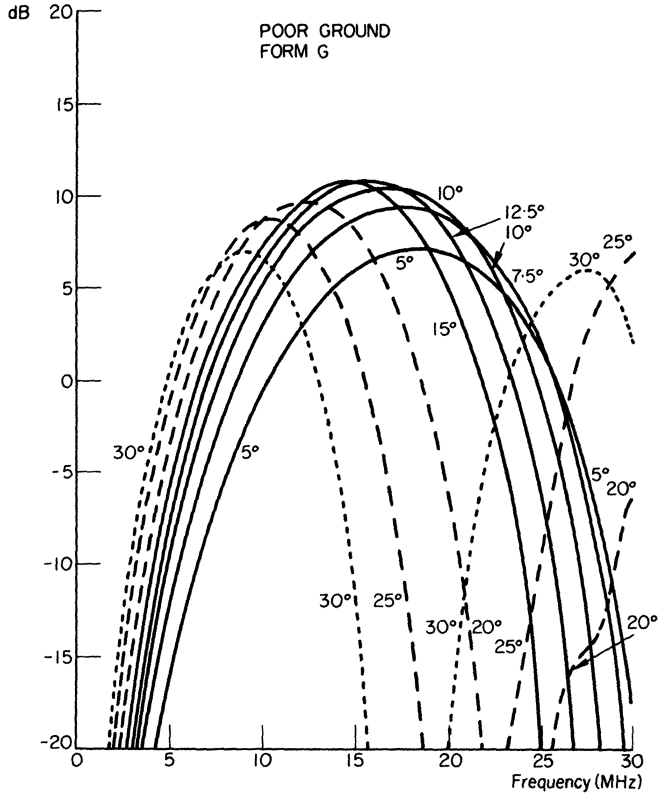

Fig. 160 Ionospheric wave; gain of rhombic antennae

The simplest method for calculating the LUF is to calculate the field received (Section 8.2.3.3) and the required field (Section 8.2.1.1) for three different frequencies, e.g. the FOT, half the FOT and one quarter of the FOT. We then plot for each hour the curves of the field received and the required field as a function of frequency. The point of intersection of these curves indicates the LUF for that particular hour.

Note 1. The LUF does not imply a sudden transition, as does the MUF. It has therefore only an approximate value.

Note 2. When making a request for frequencies, the above calculations must be made for January and June, which represent the extreme propagation conditions.

8.2.3.6 CCIR Computer program

CCIR Report 252–2[368] proposes a much more sophisticated method for the computation of both the MUF and the field-strength.

The important features of this method are as follows.

1. Ray tracing versus true height of the ionized layers is used. The relevant model of ionosphere includes two parabolic layers:

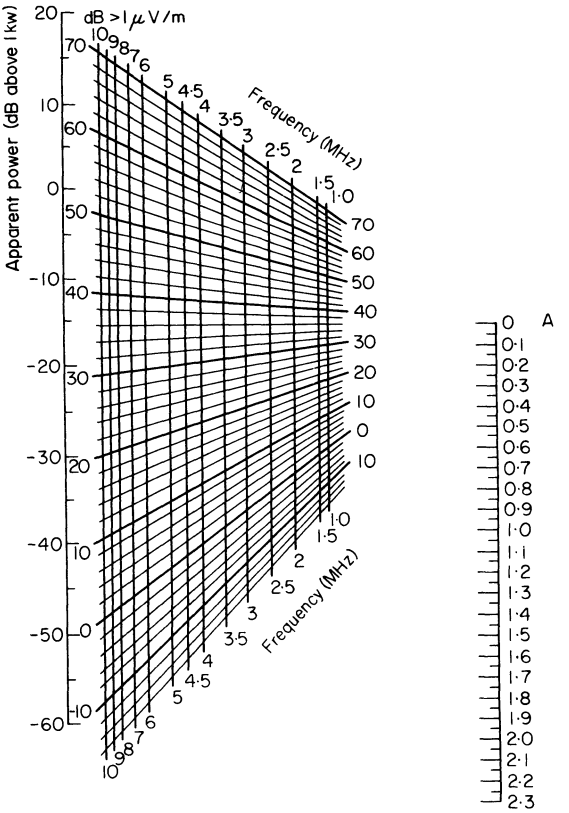

Fig. 161 Field strength of ionospheric wave for ranges of less than 400 km

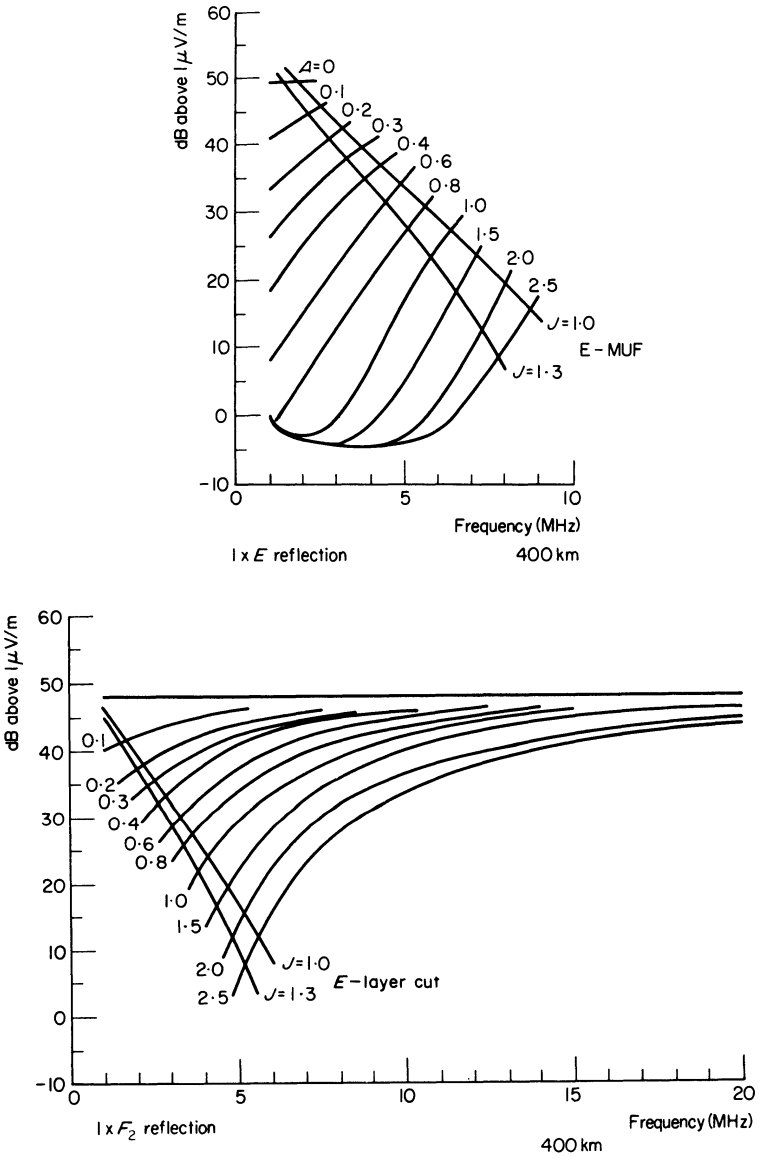

Fig. 162 Field strength of ionospheric wave for 1 kW radiated power

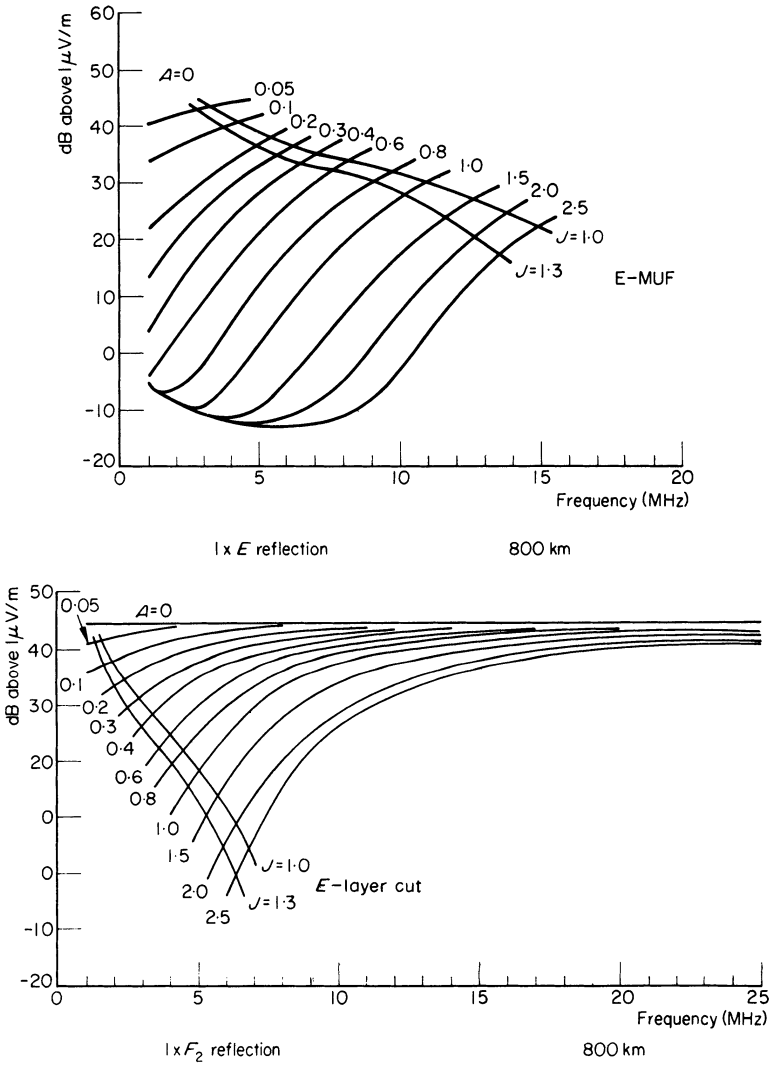

Fig. 163 Field strength of ionospheric wave for 1 kW radiated power

(i) E–layer, with a maximum of ionization at an altitude of 110 km, and with a semi-thickness of 20 km. The critical frequency f_0E is deduced from experimental world maps.

(ii) F_2–layer, the value and altitude of ionization maximum of which are deduced from CCIR Report 340[367]. Semi-thickness of this layer is deduced from an unpublished Report by LEFTIN.

2. Study of various modes for the same circuit. Up to 9 modes (the most probable ones) are studied. Probability of existence and field intensity are calculated for each of the selected modes.

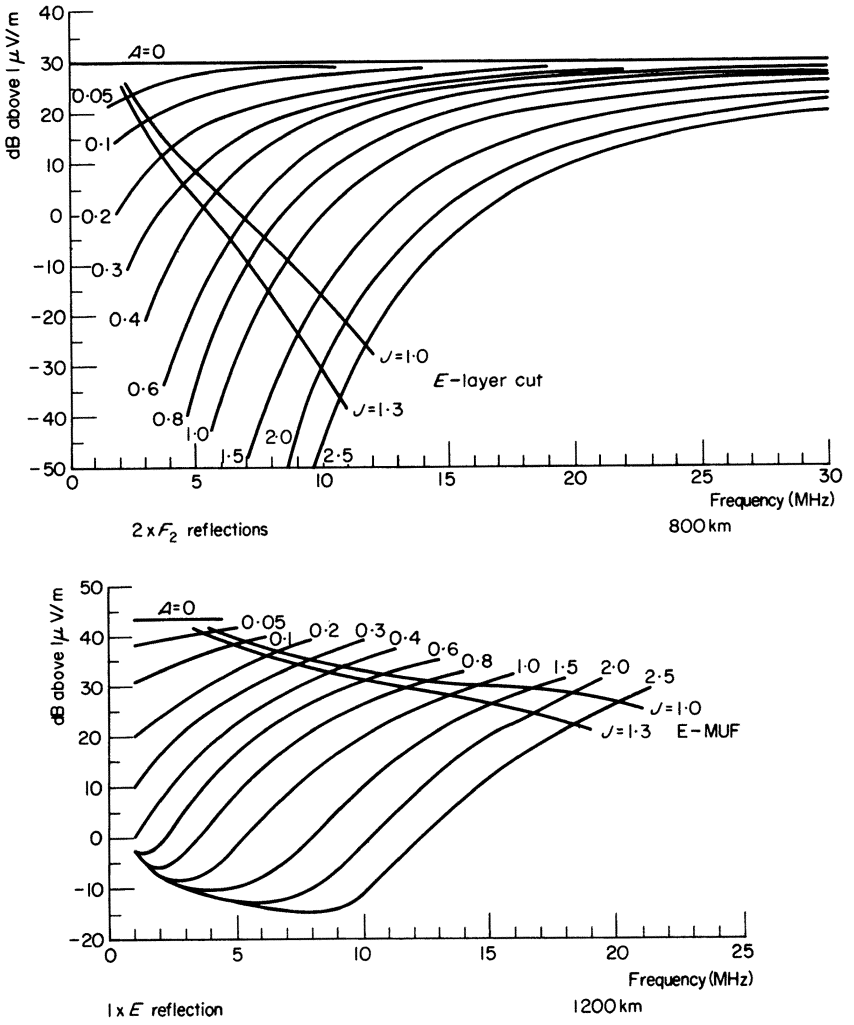

Fig. 164 Field strength of ionospheric wave for 1 kW radiated power

For E–Modes, and for frequencies at or below the E–MUF, the probability assumed is 99 per cent. For F_2–modes, the calculation of the probability is based on a χ^2 distribution, assuming a linear relation between F_2–MUF and χ^2.

An empirical formula is used to calculate the total ionospheric loss, while the ground reflection loss is calculated by the conventional theory. An 'Excess System Loss', deduced from empirical tables, is added to take into

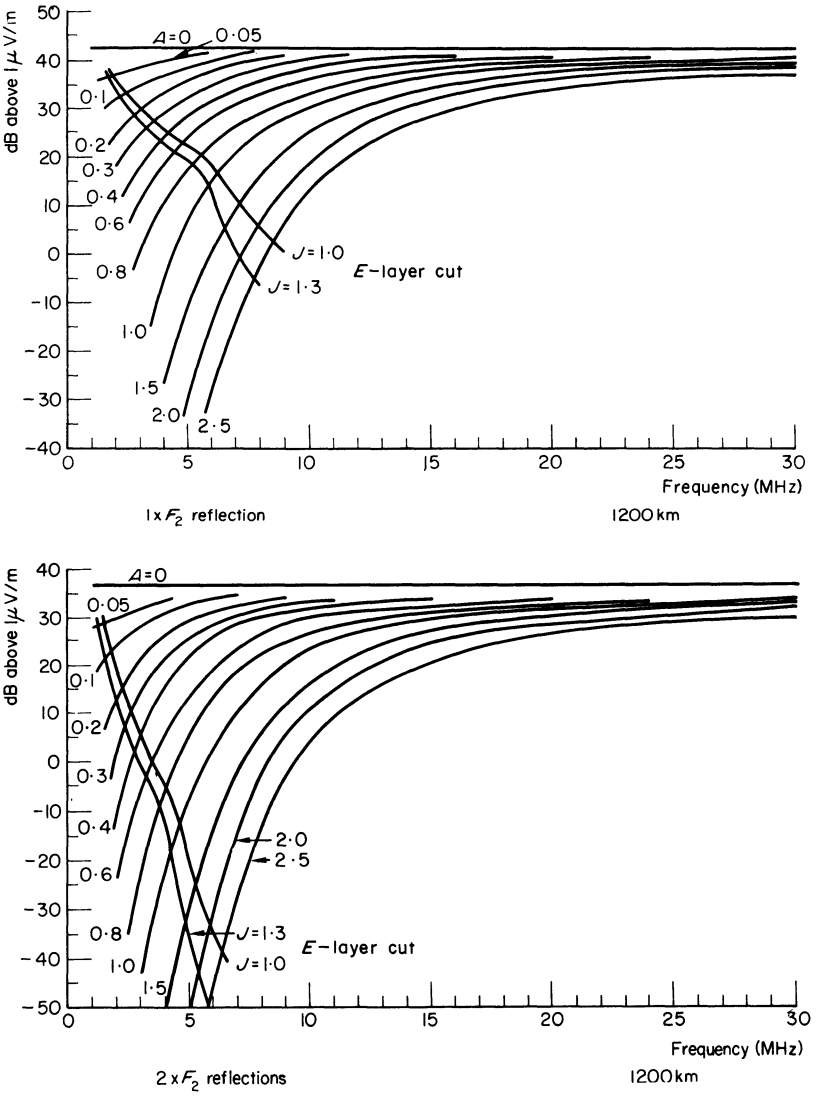

Fig. 165 Field strength of ionospheric wave for 1 kW radiated power

account the factors not covered by the previously mentioned calculations.

3. The final listing gives, for every UT-hour:

(i) The MUF (50 per cent of the days), the most probable mode for this frequency, and for the referred mode, the angle of departure, the propagation delay, virtual height of reflection, propagation loss between isotropic antennas, field intensity in dB above 1 microvolt per metre, signal power at the terminals of the receiving antenna, and probability that a specified signal level will be equalled or exceeded.

(ii) For any specified frequency, the same data as supplied for the MUF, plus the probability that the most probable mode as listed will exist.

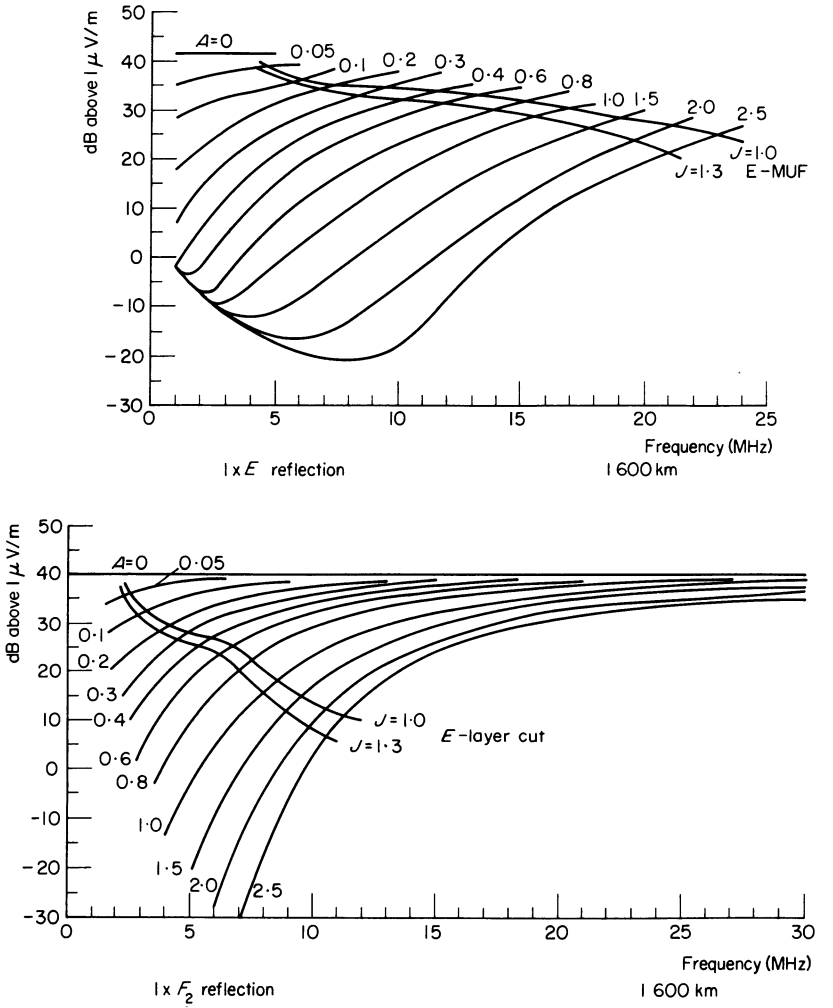

Fig. 166 Field strength of ionospheric wave for 1 kW radiated power

4. Due to the number of parameters involved and of modes investigated, as well as to the use of complex interpolation and cut-and-try procedures, the method can only be used with a computer program. The relevant program can be supplied by CCIR.

8.3 METRE AND SHORTER WAVES

Metre waves and waves with shorter wavelengths are used:

1. for coverage of a zone (TV, radio, communication between a fixed station and mobile stations, or between a number of mobile stations), or

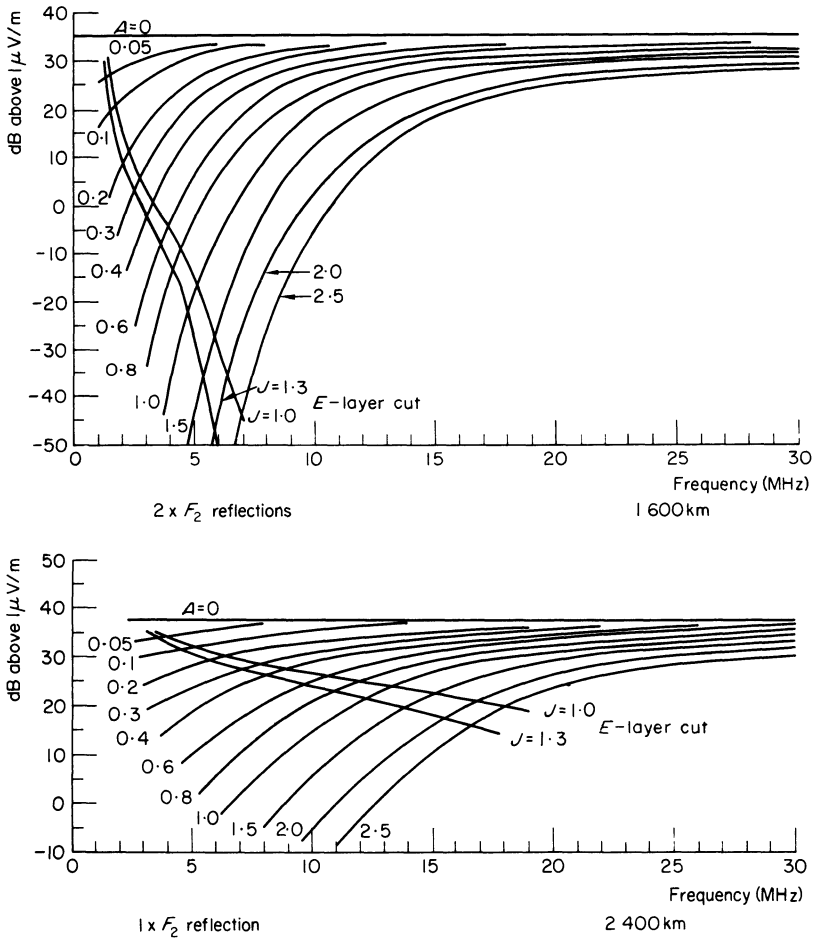

Fig. 167 Field strength of ionospheric wave for 1 kW radiated power

2. for point-to-point links, making use of:
   (a) line-of-sight propagation
   (b) diffraction
   (c) scattering.

8.3.1 COVERAGE OF A ZONE

The simplest procedure is to calculate the range of the ground wave, using the method described in Section 8.2.3 for decametre and longer waves. The antenna gain is usually given by the manufacturer of the antenna. The omnidirectional antenna (vertical $\lambda/4$) has practically zero gain. Antennae mounted on vehicles usually possess a negative gain, that must be measured after the antenna has been installed on a certain vehicle. Figures 109 and 110 contain the propagation graphs to be used. The figures shown on the curves of these graphs are the heights h_1 of the highest antenna, while the

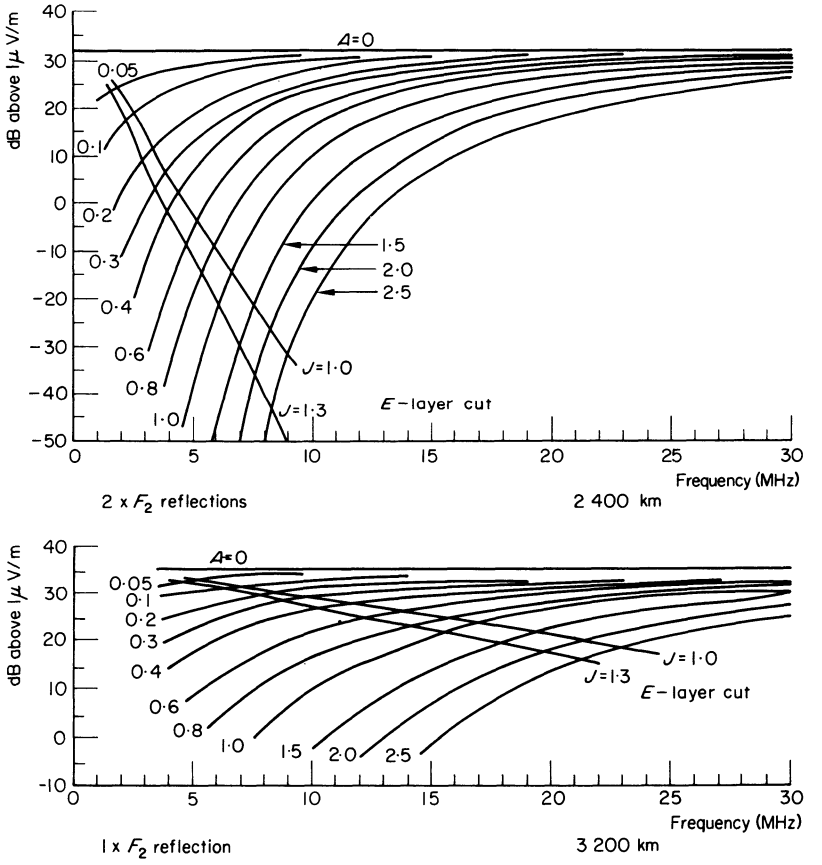

Fig. 168 Field strength of ionospheric wave at 1 kW radiated power

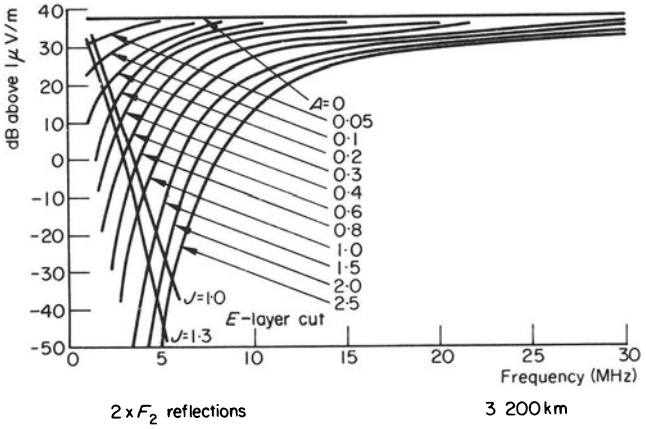

Fig. 169 Field strength of ionospheric wave for 1 kW radiated power

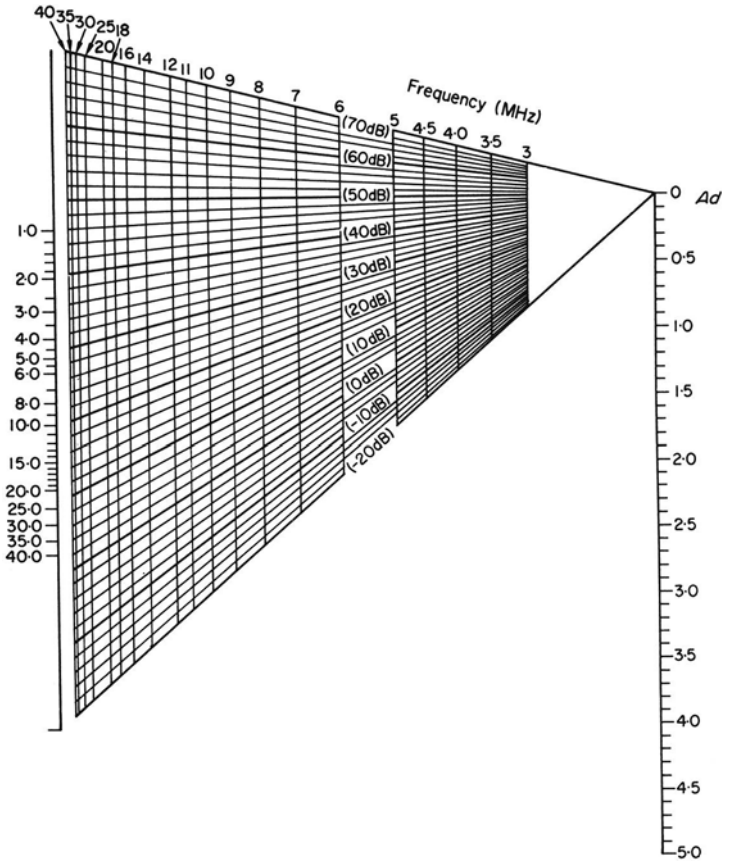

Fig. 170 Field strength of ionospheric wave for ranges greater than 3200 km and for 1 kW radiated power (small values of *Ad*)

other is assumed to be situated at a height h_2 of 10 m. This makes it possible to determine the range of a radio station, or a base station for communication with vehicles.

In view of the considerable effect of natural and artificial obstacles, especially those situated in the proximity of the antennae, all ranges calculated are only averages. The actually achieved range between two given stations may differ considerably from this value. If a computer is available, more accurate results can be obtained by the method described in Reference 231.

8.3.2 POINT-TO-POINT LINKS

The problem can be stated as follows:

'Two geographic points and a frequency in one of the authorized bands are given. We wish to determine the power of the transmitter and the gain of the antennae required for the realization of the link.'

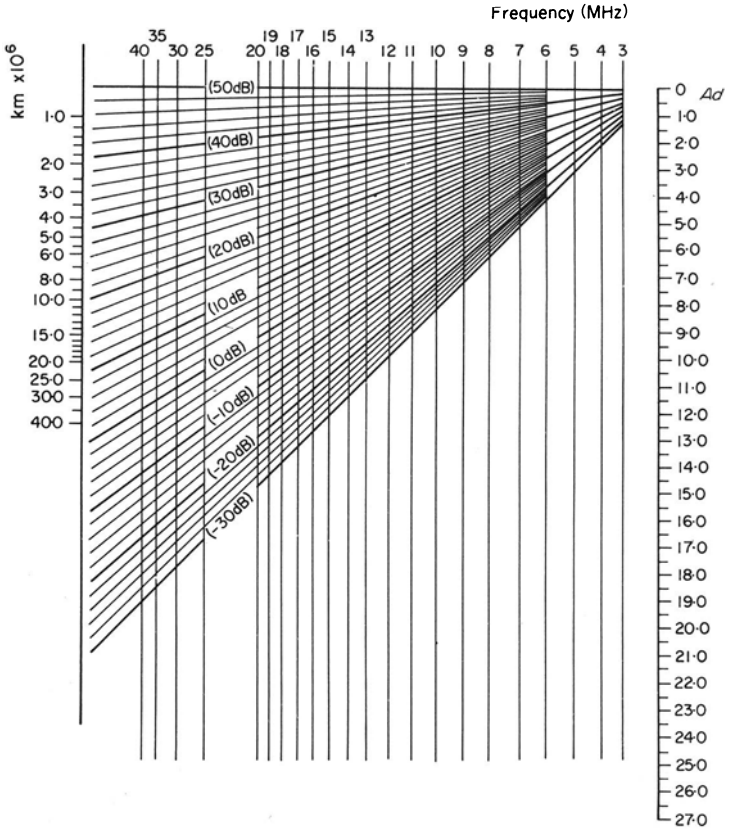

Fig. 171 Field strength of ionospheric wave for ranges greater than 3200 km and for 1 kW radiated power (large values of Ad)

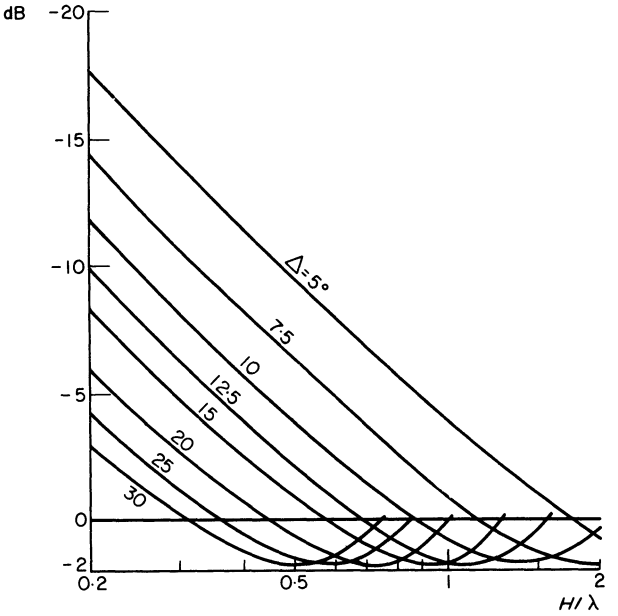

Fig. 172 Calculation of discrimination gain (gain of isotropic antenna with horizontal polarization); H = antenna height

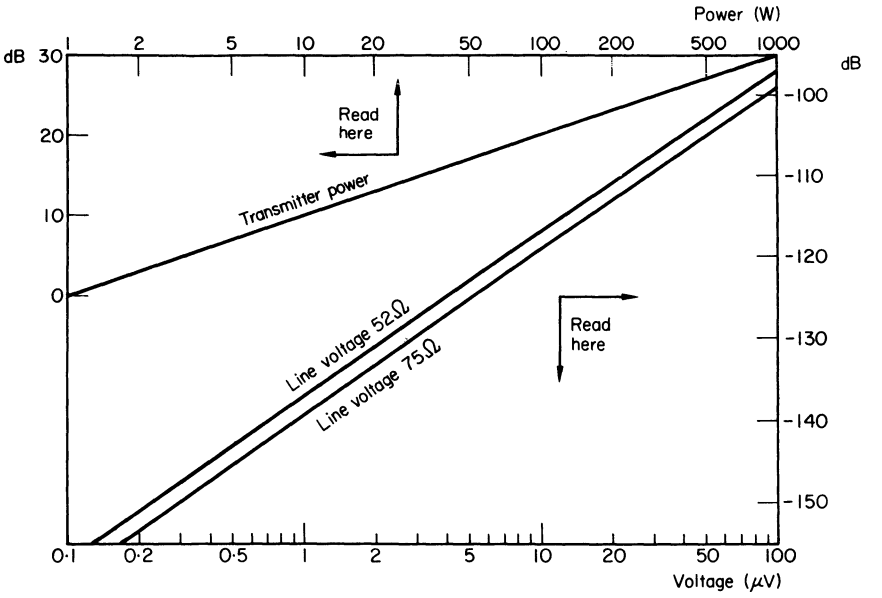

Fig. 173 Conversion of power and voltage into decibels above 1 watt

8.3.2.1 Terrain profiles

When we want to calculate a link, we must first know the profile of the terrain between the two stations. This profile can be studied by means of maps, but its verification by topographic survey or photogrammetry is often mandatory. The maps or photogrammetric data give the altitude of the various points of the terrain in relation to sea level, but we must take into account the earth's curvature, and atmospheric refraction.

Two methods can be used; these are detailed below.

Curved ground method

The profile is plotted on a sheet of tracing paper, placed on one of the diagrams of Figs 174 and 175, which take into account the earth's curvature as well as normal atmospheric refraction. The wave path (radio ray) can then be represented by a straight line.

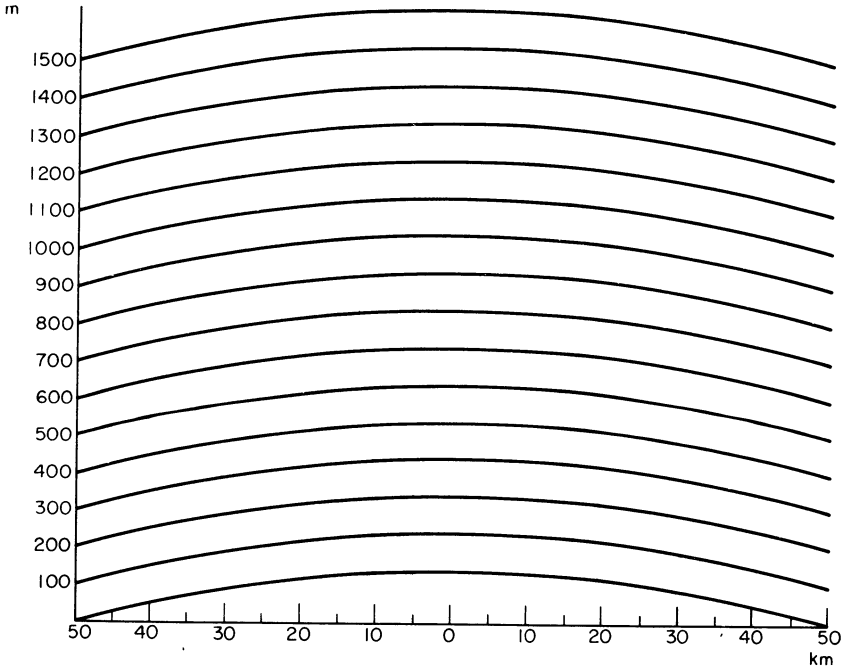

Fig. 174 Curved ground method; diagram for terrain profile $K = 4/3$

Flat ground method

The profile is plotted on a sheet of transparent millimetre paper, using the scales of Figs 176–178:

Vertical scale 1 : 20 000; horizontal scale 1 : 1 000 000.

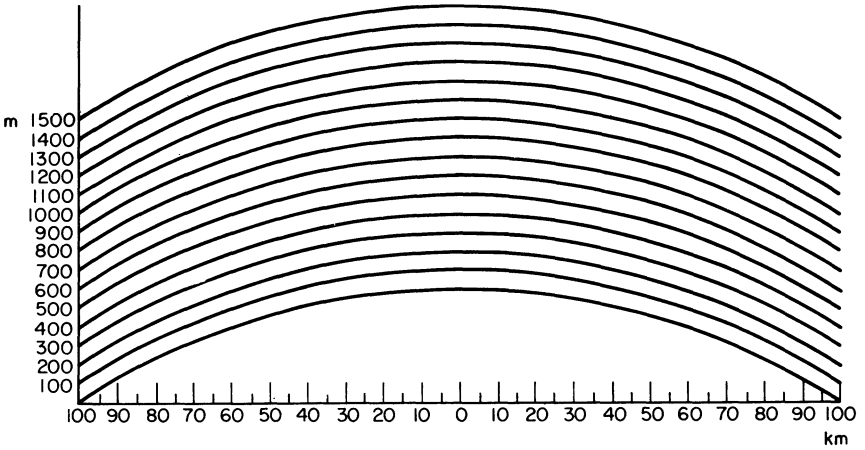

Fig. 175 Curved ground method; diagram for terrain profile $K = 4/3$

The path of the radio ray for normal refraction ($K = 4/3$) is given by the curve marked '$d \times 0$' of Fig. 176. The profile is then placed on this figure, so that the vertical lines of the profile are parallel to the vertical line in the centre of the figure, and shifted until its two terminal points are situated on the curve '$d \times 0$'. This curve, which represents the path of the radio ray, is then traced. Figures 177 and 178 allow one to trace in the same manner the radio rays for $K = 1$ and $K = 0{\cdot}8$ respectively.

Note. If the terrain is either very steep or almost flat, coincidence with the $d \times 0$ curve will not be possible. In this case we must:

(a) trace a straight line between the terminal points of the path on the first profile;

(b) establish a second profile by vertical plotting of the positive or negative altitudes of the terrain in relation to the previously drawn straight line, and trace the rays on this second profile.

8.3.2.2 **Line-of-sight propagation**

First Fresnel zone

Line-of-sight propagation does not only imply the absence of obstacles on the path of the ray between the stations. It is also necessary that the first Fresnel zone is at least partly free. The specifications issued by telephone companies or administrations, usually indicate which fraction of the first Fresnel zone must be free for a given value of K. The following method should be used to make certain that these conditions are satisfied: first trace the radio ray; then trace below this ray the first Fresnel zone. This is done as follows:

(a) Determine the radius of the zone in the centre of the path by means of Fig. 179.

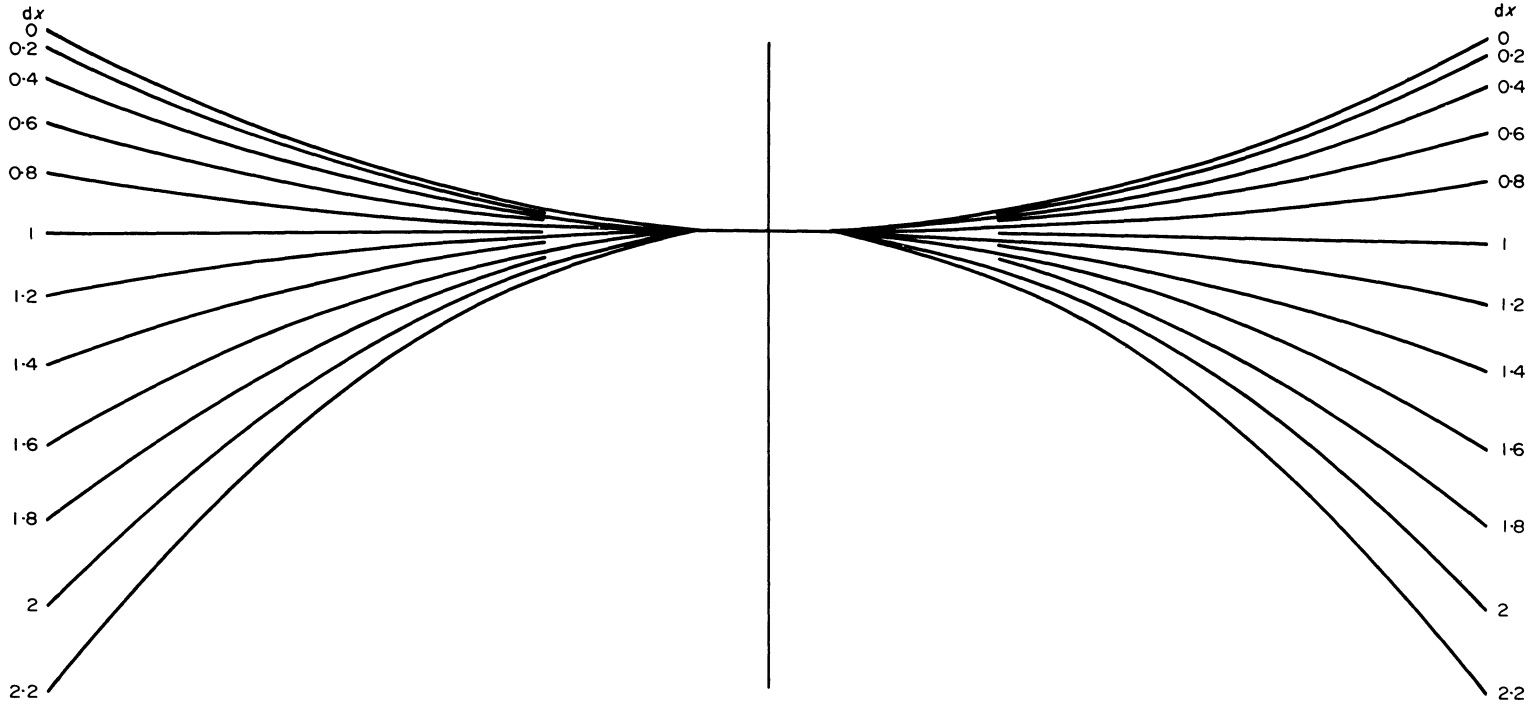

Fig. 176 Flat ground method; diagram for terrain profile; $K = 4/3$ (50%)
vertical scale 1:20000; horizontal scale 1:1000000

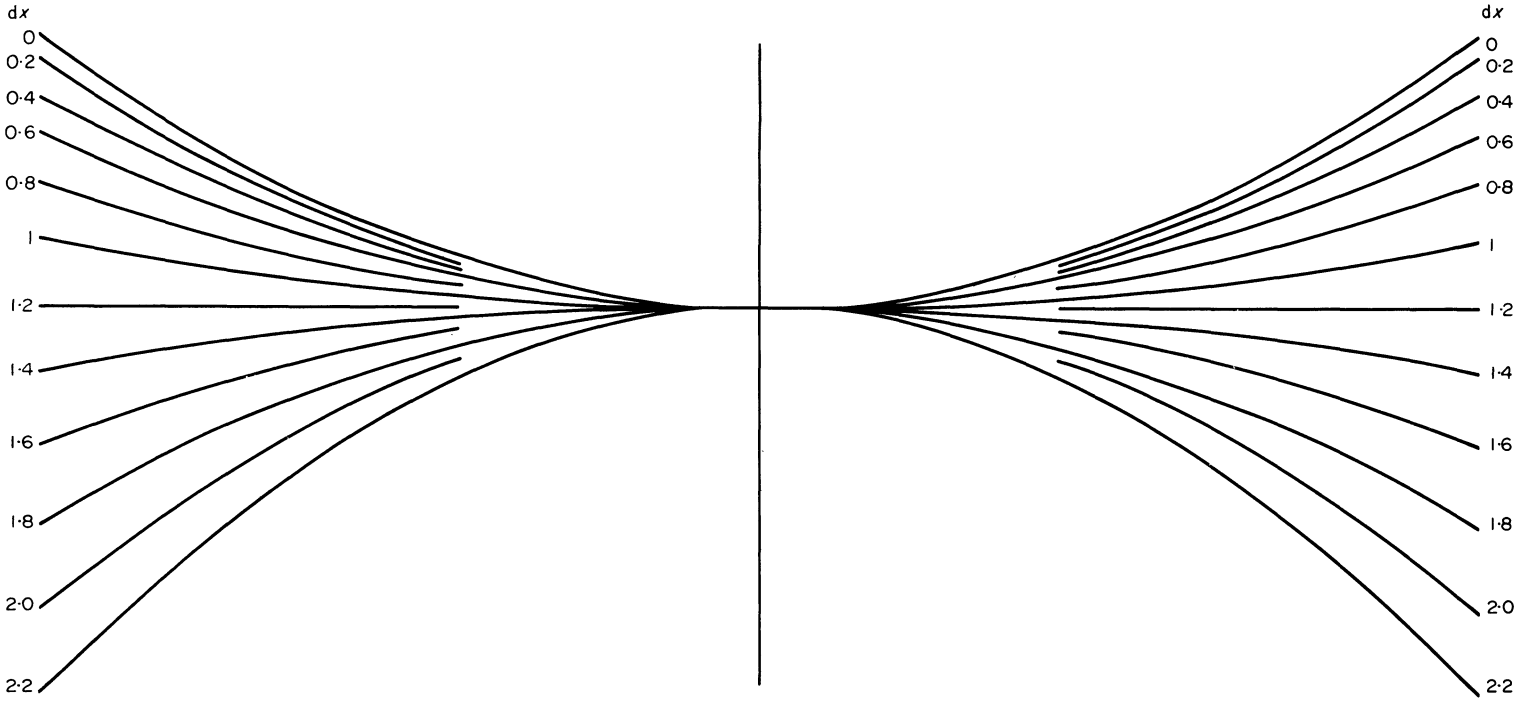

Fig. 177 Flat ground method; $K = 1$ (99%) diagram of the Earth's profile;
vertical scale 1:20000; horizontal scale 1:1000000

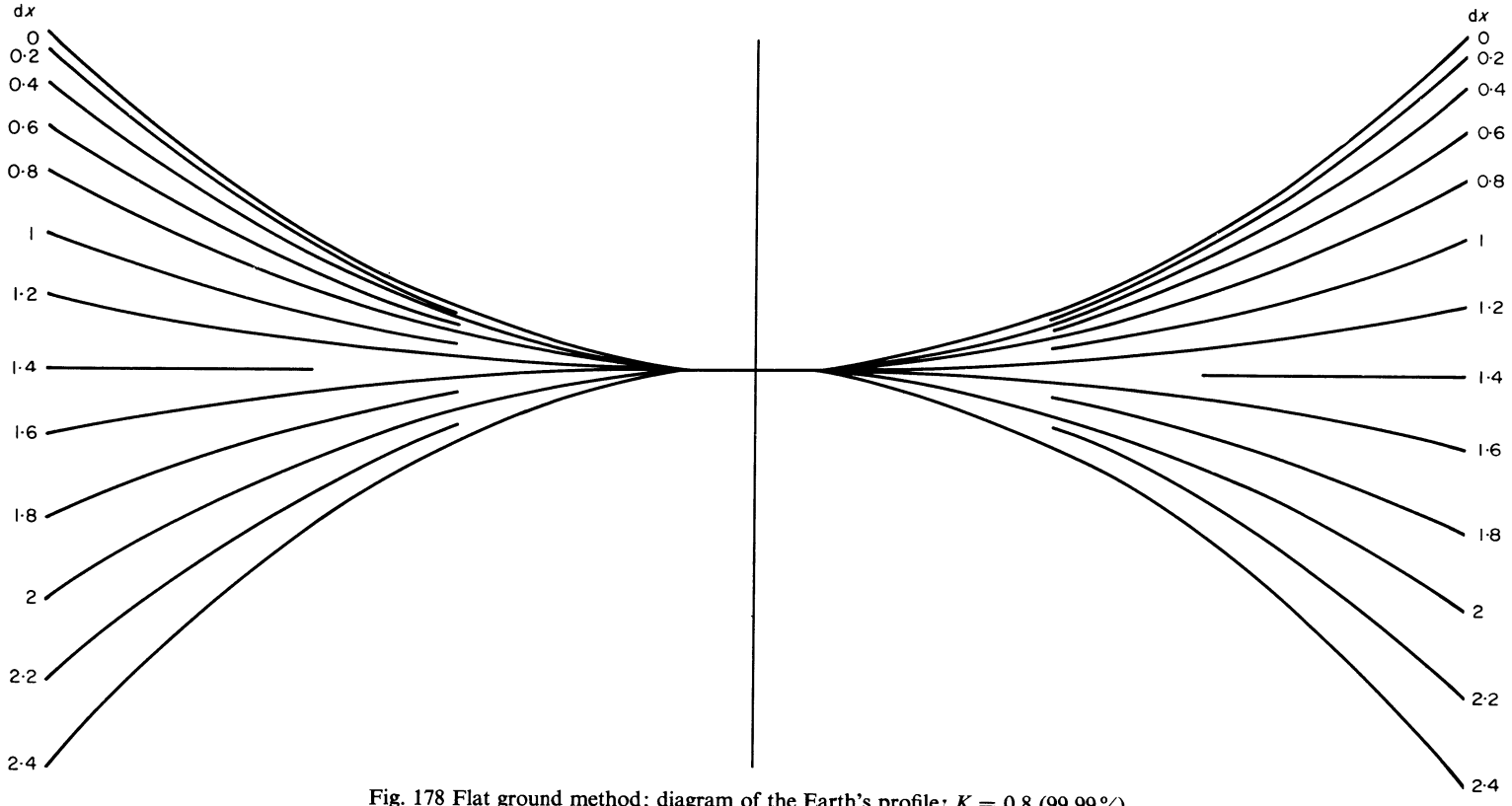

Fig. 178 Flat ground method; diagram of the Earth's profile; $K = 0.8$ (99.99%)
Vertical scale 1:20000; horizontal scale 1:1000000

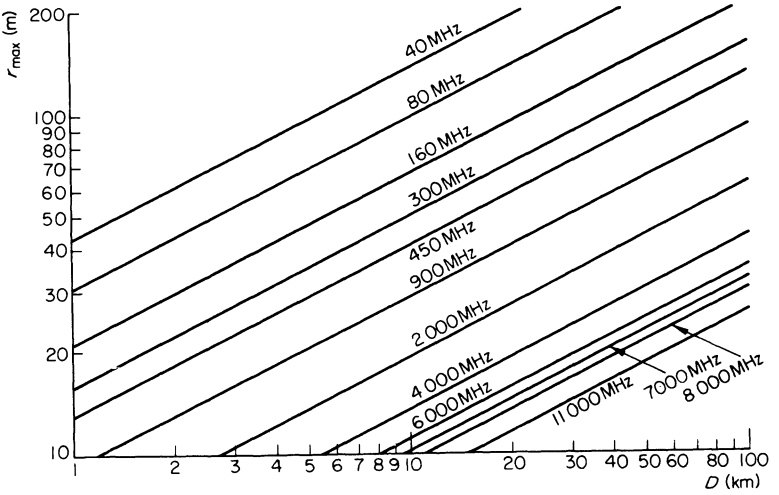

Fig. 179 Radius of first Fresnel zone at centre of path

(b) Deduce the radius of the zone at a few points on the path, using Fig. 180.

(c) Use Fig. 181 in the proximity of the antennae.

(d) Join the thus obtained points and check the position of the ground and the obstacles in relation to the zone.

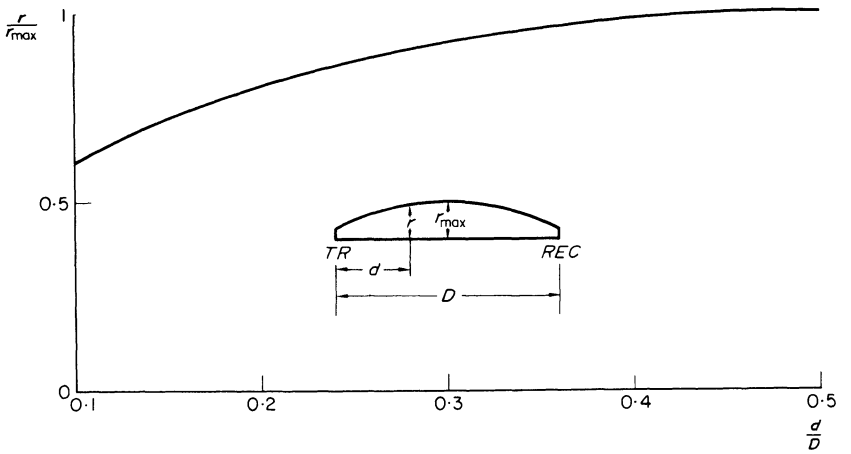

Fig. 180 Ratio of radius of first Fresnel zone to radius at centre of path

Calculating the required power and antenna gain

(a) The required power at the input of the receiver in dB in relation to 1 W is determined as follows:

1. If the threshold value of the receiver sensitivity in microvolts is known, convert this voltage into power by means of Fig. 173 (lower and right hand scales. Use the curve for 52 Ω or the curve for 75 Ω according to the input impedance of the receiver).
2. If the sensitivity of the receiver is not known, calculate the required power in dB in relation to 1 W by means of the following formula:

$$P_R = -194 + 10 \log B + F$$

where: B = passband at 3 dB points of the i.f. amplifier (in Hz)

F = noise factor of the receiver (in dB).

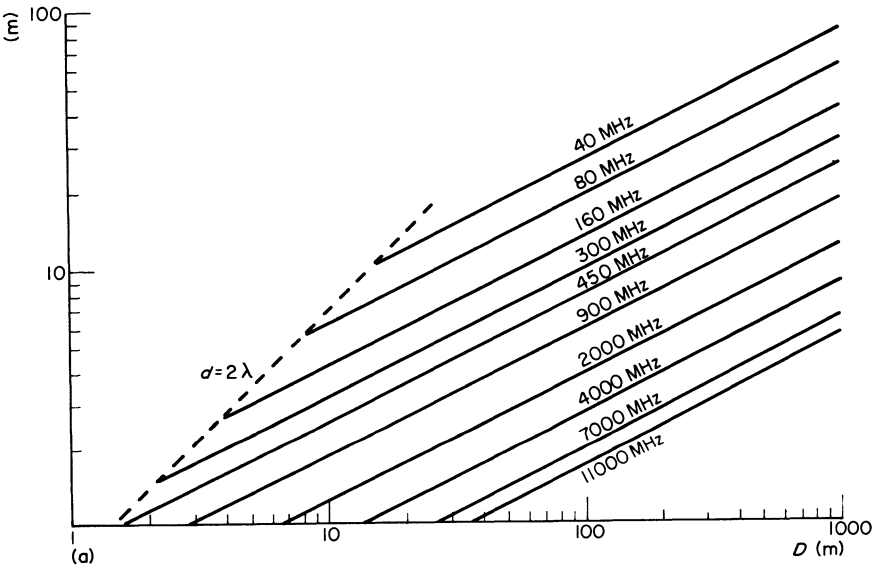

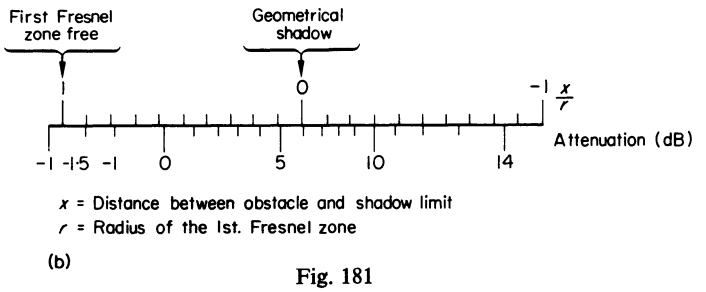

x = Distance between obstacle and shadow limit

r = Radius of the 1st. Fresnel zone

(b)

Fig. 181

(a) Radius of first Fresnel zone in the proximity of the antennae
(b) Effect of an obstacle in the zone

This formula gives the power corresponding to the threshold of f.m. receivers, or to a signal-to-noise ratio of 10 dB for a.m. receivers.

(b) Determine the attenuation in free space between isotropic antennae as a function of distance and frequency, using Fig. 183 (or Fig. 184 in the case of a passive reflector).

(c) Calculate the loss in the antenna feeders and filters, using the data provided by the manufacturer.

(d) Determine the fading margin.

Figure 185 gives the fading margin directly as a function of the percentage of the total time, for the following conditions: temperate climate, uneven terrain, frequency 4 GHz. If the conditions differ from these, CCIR recommend that this figure should be used 'with care'. However, it would seem that the results for 6 GHz do not differ much from those for 4 GHz.

In other cases, we must first of all know the percentage x of the total time during which fading is produced. This value may be known from experience, if other radio beams are being used under similar conditions.

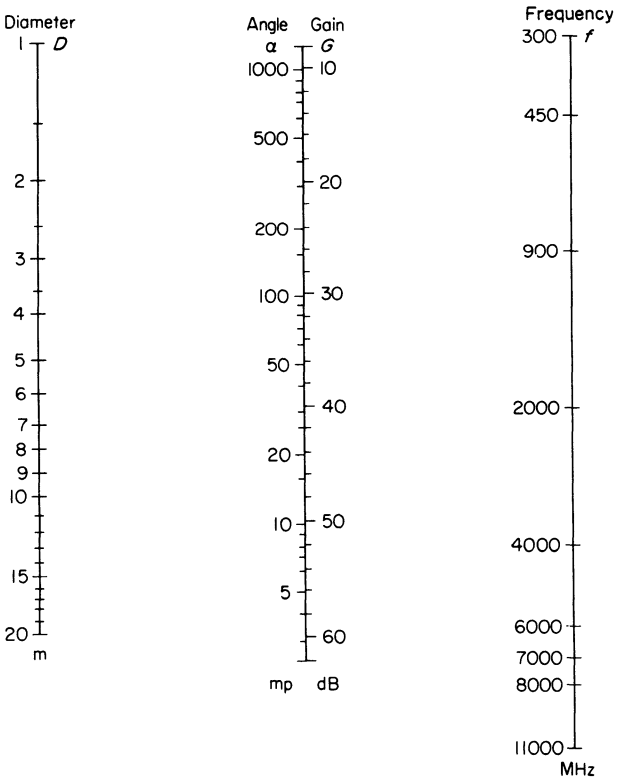

Fig. 182 Gain and beam angle of parabolic antennae

Fig. 183 Attenuation between isotropic antennae in free space

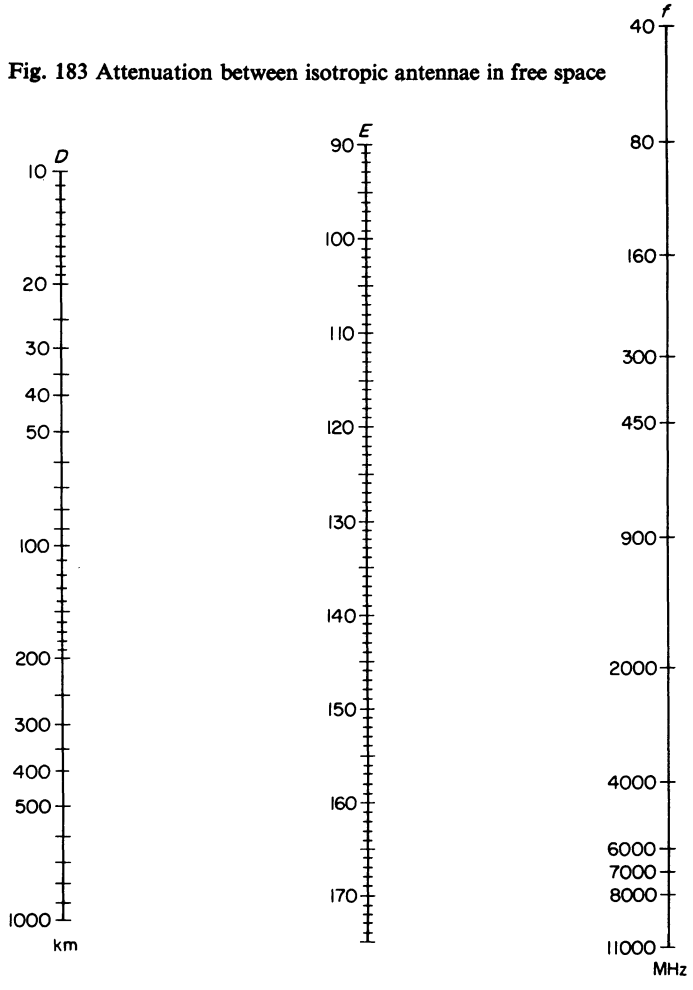

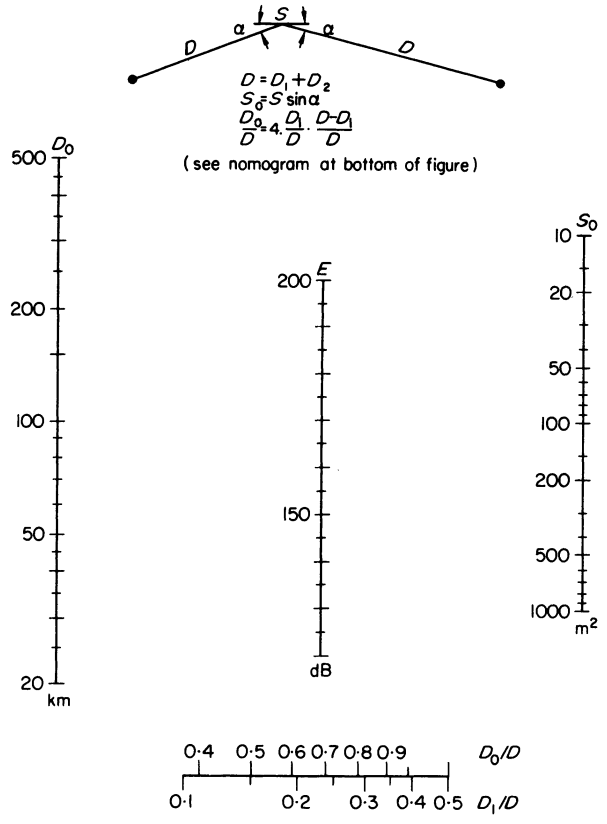

Fig. 184 Attenuation between isotropic antennae with passive reflector

If no experimental data are available, 25 per cent is generally taken as the first estimate for preliminary calculations. The value of the signal which is exceeded a fraction Q of the time will then be that corresponding to the value $Q_1 = 100\ Q/x$, read off from the signal distribution curves for the type of fading in question.

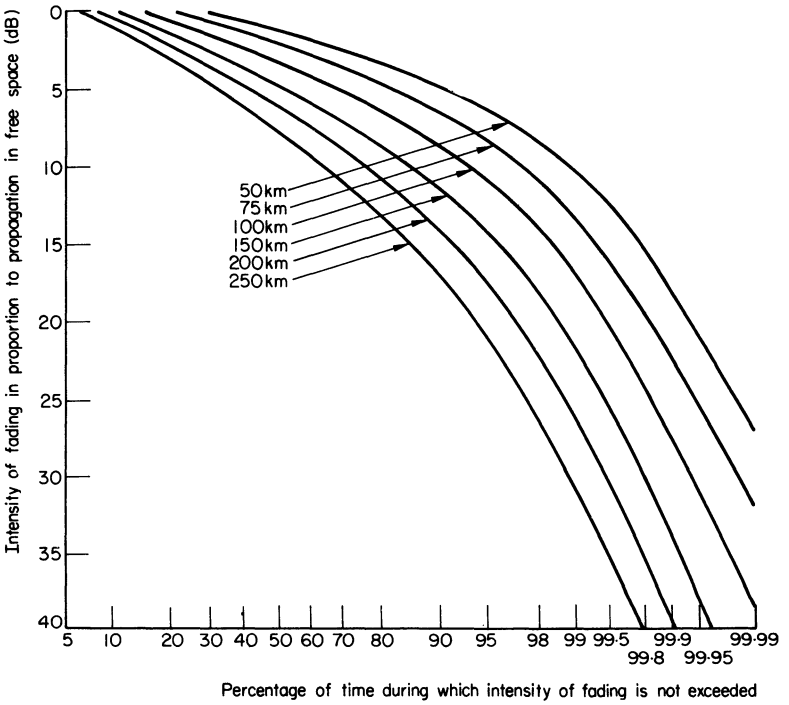

Fig. 185 Fading distribution for temperate climate (4 GHz)

After Q_1 has been determined, make use of this value in the graph of Fig. 196:

1. For single reception over uneven ground, use the curve:
   'Rayleigh receiver.'
2. For double diversity reception or instantaneous passage on a reserve circuit over uneven ground, use the curve:
   'Diversity by commutation—2 Rayleigh receivers.'
3. For single reception with reflection from a very flat plain, or from the sea, use the curve:
   '1 receiver—2 components.'
4. For double-diversity reflection or instantaneous passage on a reserve circuit, with reflection from a very flat plain or from the sea, use the curve:
   'Diversity by commutation—2 receivers, 2 components.'

(e) Add the results obtained in a, b, c and d, not forgetting the signs. The result is the sum

$$P_E + 2G$$

where: P_E = transmitted power in dB in relation to 1 W. Figure 173 (left hand and top scales) permits us to convert the dB into power.

G = antenna gains (assumed to be equal for both transmitter and receiver) in dB. Antenna gain is usually indicated by the manufacturer. If parabolic antennae are used, their gain can be determined by means of Fig. 182.

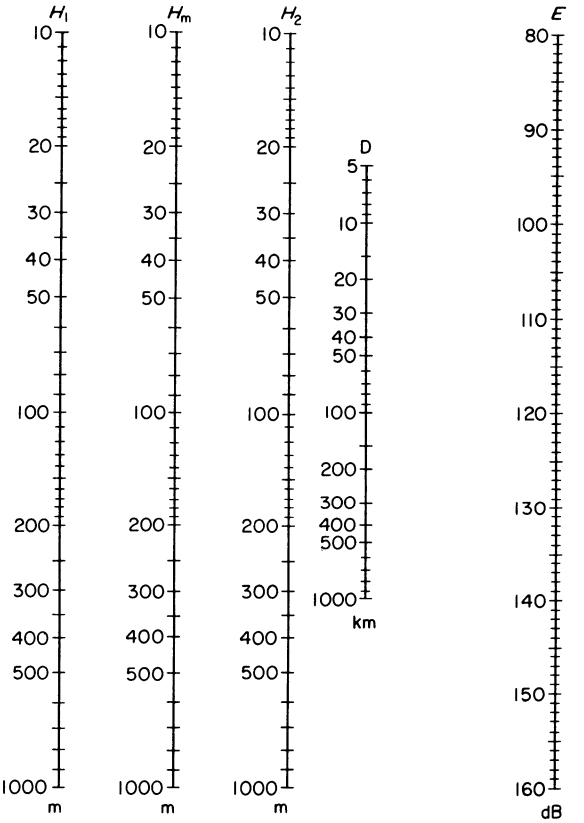

Fig. 186 Attenuation between isotropic antennae on flat ground. Only valid if the result is higher than that obtained from Fig. 183.
How to use this nomogram.
Enter the relevant scales with the antenna heights H_1 and H_2.
Read $H_m = (H_1 H_2)^{\frac{1}{2}}$ on the corresponding scale.
Join H_m to D, and read E on the right-hand scale

Once we know which transmitters and antennae can be used for the link, it is easy to select the best solution by trying out various combinations of transmitters and antennae.

8.3.2.3 **Propagation by diffraction**

Curved earth method

(a) Determine the required input power to the receiver in the manner described in (a) in the previous section.

(b) To calculate the attenuation between isotropic antennae as a function of distance, frequency and antennae heights, we can:

1. Either add the results of Figs 186 and 187 (provided the heights of the antennae do not exceed the maximum height shown in Fig. 187)

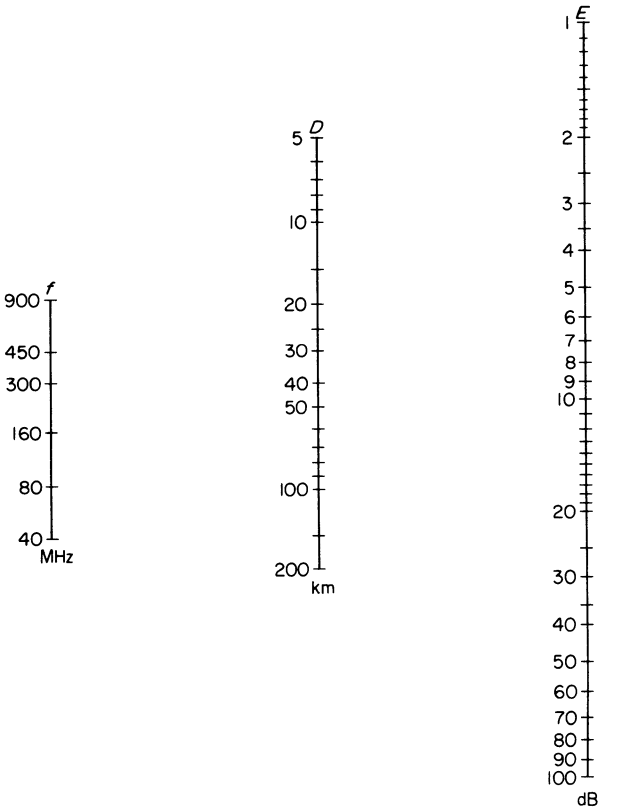

Fig. 187 Attenuation between isotropic antennae due to terrestrial curvature. To be used in conjunction with Fig. 186. Only valid if the antenna height does not exceed:
135 m at 40 MHz; 80 m at 80 MHz; 50 m at 160 MHz, 33 m at 300 MHz; 25 m at 450 MHz; 15 m at 900 MHz

2. or add the results of Figs 183 and 188. If the first method is applicable, it gives more accurate results.

(c) An obstacle is considered as isolated if it constitutes the common horizon of the two stations (see Fig. 32 of Chapter 4). It is considered as thin if the radius of curvature R at its summit satisfies the inequality

$$R < \lambda/64\,\theta^3$$

(where θ is in radians, and R and λ are expressed in the same units).

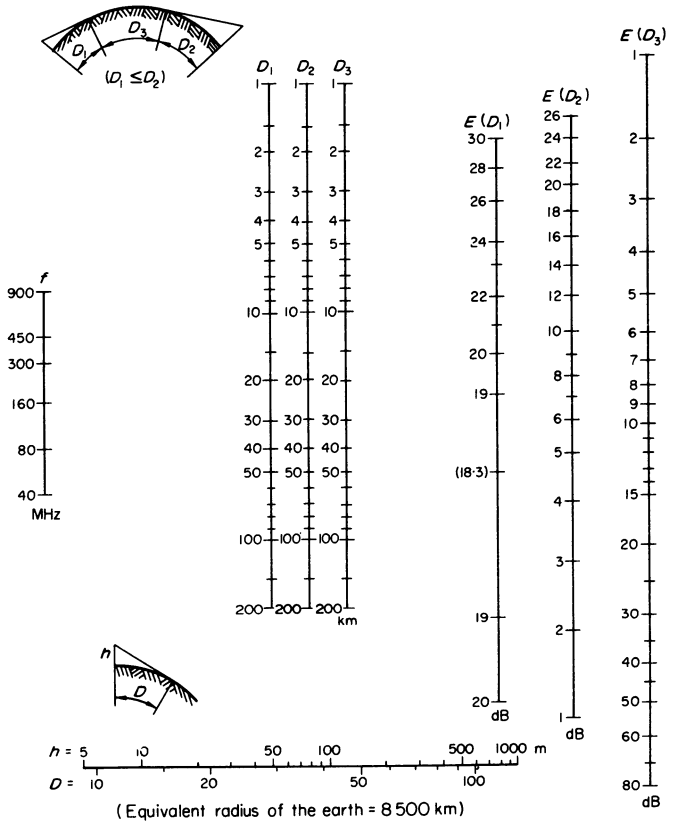

Fig. 188 Attenuation between isotropic antennae related to attenuation in free space. To be used in conjunction with Fig. 183.

For an isolated thin ('knife-edge') obstacle, calculate the loss due to the obstacle with the aid of Fig. 189. If the obstacle is high and thin enough to ensure that the first Fresnel zone is free on both sides between the stations and the obstacle, this loss is added to the loss in free space given by Fig. 183, increased by 6 dB. If this is not the case, the loss determined by Fig. 189 is added to that calculated by Fig. 186.

For several knife-edge obstacles (see Fig. 191), first of all, calculate as described above the loss produced by the obstacle which gives the strongest one (A in the figure), than that produced by obstacle B above the line AS_2 (distance D_1', height h'), and so on.

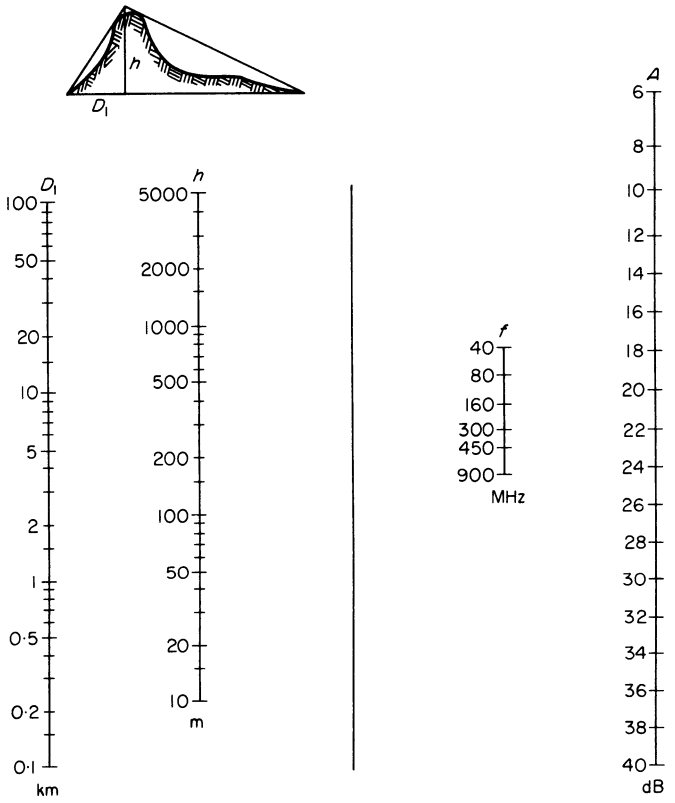

Fig. 189 Attenuation caused by isolated obstacles

Instructions for use:

1. Plot the terrain profile by means of the graphs of Figs 174 and 175. Plot the enclosing triangle and read off D_1 and h.
2. Use these values to define a point on the central ungraduated scale.
3. Determine the attenuation by means of this point and the frequency.

For a rounded obstacle, use Fig. 190. Calculate the values of ν and ρ from the formulae given in this figure, then note these values in the graph and read the loss. Add to the free-space loss, Fig. 183.

(d) Calculate the loss in the antenna feeders.

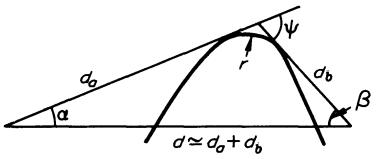

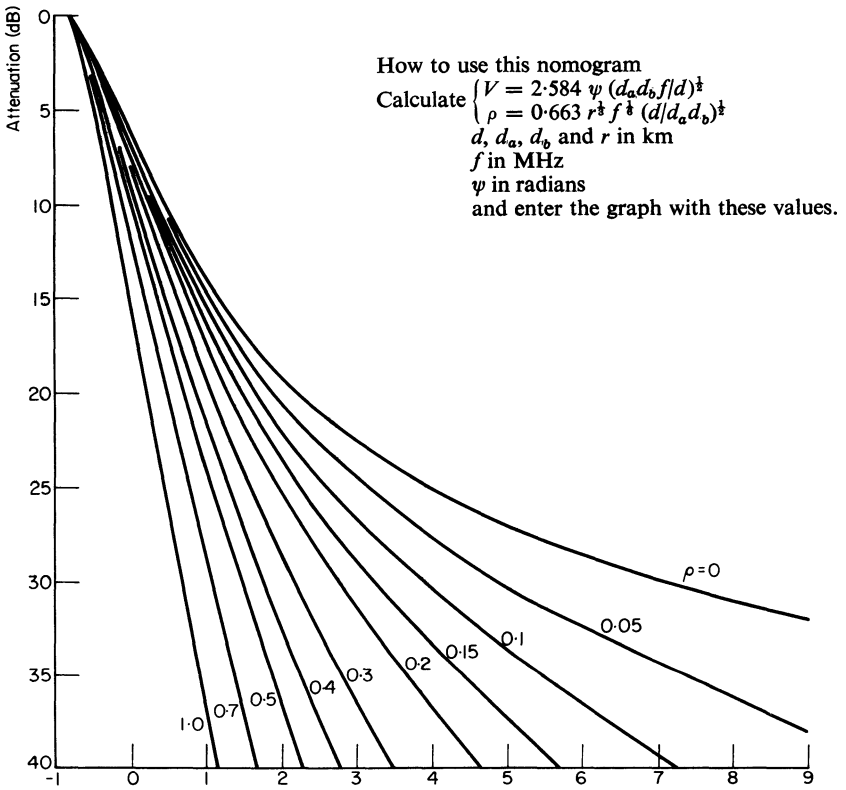

Fig. 190 Effect of a round obstacle

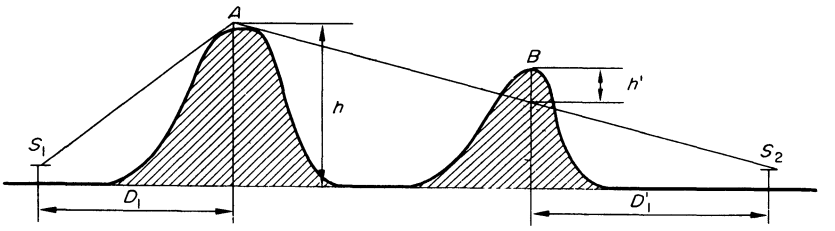

Fig. 191

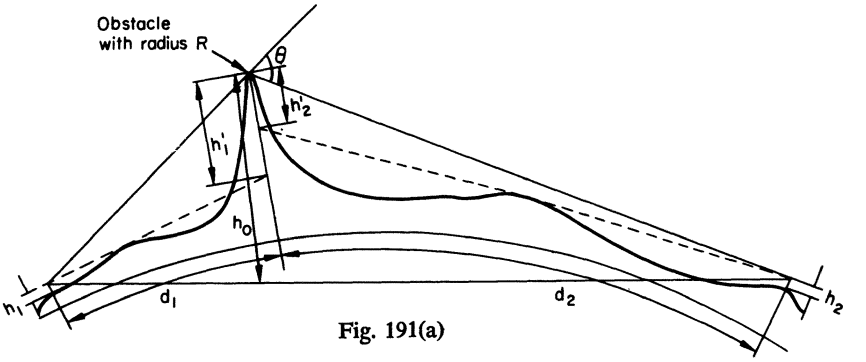

Fig. 191(a)

(e) Determine the fading margin. It is usual to take the following values for single reception:

10 dB for an availability of 90 per cent
20 dB for an availability of 99 per cent
30 dB for an availability of 99·9 per cent
40 dB for an availability of 99·99 per cent.

These values may be halved in the case of double diversity reception.

(f) Add the results obtained from (a), (b), (c), (d) and (e). The final result is the sum:

$$P_E + 2G$$

This is dealt with as described in section on calculating required power and antenna gain, part (e).

Flat ground method

The advantage of this method lies in the fact that it takes the curvature of the terrain into account. It is the most convenient method for terrains of complex shape, without having particularly high obstacles.

(a) Determine the required input power of the receiver.

(b) Trace the profile of the terrain as described in the flat ground method in Section 8.3.2.1. Place this profile successively on Figs 176, 177 and 178. Vertical lines of the profile must remain parallel to the central vertical line of the figure. Slide the tracing until the highest points and the terminal points of the profile are situated on the same curve. Read the multiplication coefficient (dx) from the curves on the three figures.

(c) Calculate the hourly median of attenuation between isotropic antennae for the availability percentages corresponding to the three figures. This is done as follows:

1. Determine the attentuation on flat ground by means of Fig. 186.
2. Multiply the path length by the coefficient obtained in (b), and use this distance to determine the additional attenuation by means of Fig. 187.
3. Add the results of Figs 186 and 187.

We now have three values of the hourly mean of attenuation, which roughly correspond to availabilities of 50, 99 and 99·99 per cent.

(d) To calculate the attenuation for the required availability:

1. Calculate the standard deviation of the time medians by means of the following formula:

$$\sigma = \frac{A(99\%) - A(50\%)}{2{\cdot}3}$$

or

$$\sigma = \frac{A(99{\cdot}99\%) - A(50\%)}{3{\cdot}7}$$

Take the greatest of the values found.

2. Select the value of σ and the required availability in either Fig. 98 (single reception) or Fig. 99 (diversity reception) and read the corresponding fading margin (taking rapid signal fluctuations into account).
3. Add this margin to the value of attenuation during 50 per cent of the time, A(50 per cent), as calculated in (c). The result is the attenuation we wanted to determine.

(e) Calculate the losses in the antenna feeders.

(f) Add the results obtained in (a), (d) and (e). The result is interpreted as in (e) in the previous section.

'Knife edge' obstacles

When a sharp obstacle is present in the path, the attenuation of the propagation may be weak. (This phenomenon has been improperly called 'obstacle gain').

These calculations are only valid if the terrain between the obstacle and the stations is not very rough.

Attenuation is calculated as follows:

(a) Calculate the value:

$$v_0 = h_0\left[\frac{2}{\lambda}\left(\frac{1}{d_1}+\frac{1}{d_2}\right)\right]^{\frac{1}{2}}$$

(b) Trace the exact profile of the terrain on either Fig. 174 or Fig. 175. From each antenna, draw the tangent to the profile and determine graphically the distances and heights indicated in Fig. 191(a).

(c) The additional attenuation in relation to free space (to be added to the result of Fig. 183) will then be given by the formula:

$$A = 1 + 20\log v_0 - 20\log\sin\left|\frac{2\pi h_1 h_1'}{\lambda d_2}\right| - 20\log\sin\left|\frac{2\pi h_2 h_2'}{\lambda d_1}\right|$$

If the following two conditions:

$$\left.\begin{aligned} h_1 &= \frac{2n+1}{4}\frac{\lambda d_2}{h'_1} \\ h_2 &= \frac{2n'+1}{4}\frac{\lambda d_1}{h'_2} \end{aligned}\right\} n, n' = 0, 1, 2 \ldots$$

can be realized simultaneously, the attenuation will be as small as possible, and be reduced to:

$$A = 1 + 20 \log v_0 \text{ dB}$$

8.3.2.4 **Propagation by scattering**

(a) Determine, as in (a) in 'calculating the required power and antenna gain' in Section 8.3.2.2, the required input power to the receiver.

(b) Determine, using Fig. 183. the attenuation between isotropic

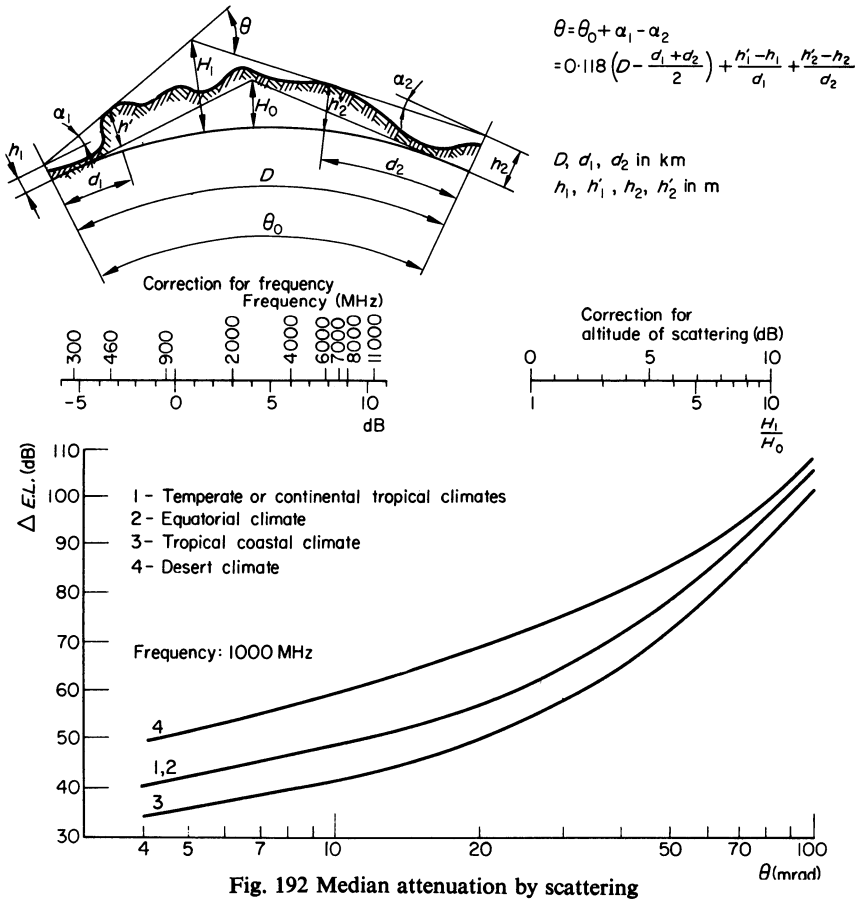

Fig. 192 Median attenuation by scattering

antennae in free space, which corresponds to the total distance between the actual antennae.

(c) To calculate the median attenuation by scattering:

1. Trace the profile of the terrain and the radio rays travelling from the two antennae to their respective horizons, by one of the two methods

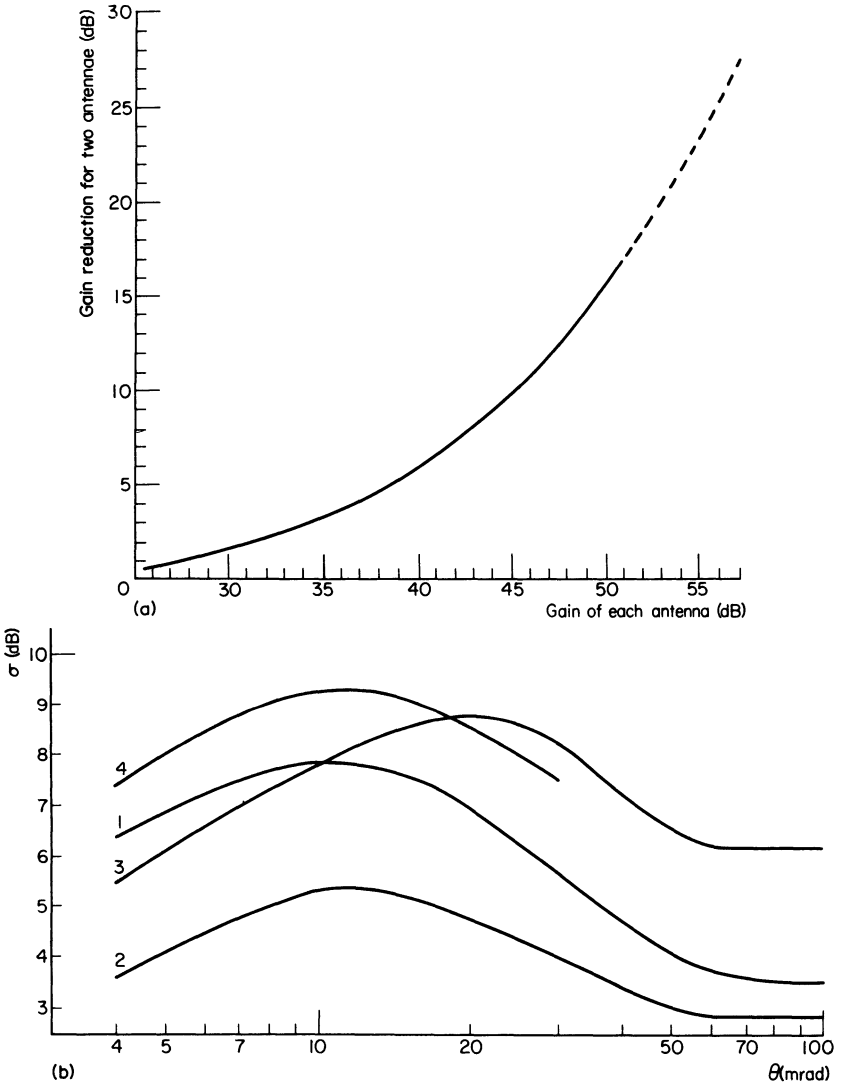

Fig. 193

(a) Antenna-to-medium coupling loss.

(b) Standard deviation of the scattered field (meaning of the curve numbers as per Fig. 192)

described in Section 8.3.2.1. Accurately determine the heights of the antennae, as well as the altitudes and distances to the antennae from the points where the radio rays meet the horizon.

2. Calculate scattering angle θ, using the formula of Fig. 192.
3. Determine the median scattering attenuation at 1 000 MHz as a function of this angle and of the climate, by means of the curves in the lower part of Fig. 192.

(d) If the frequency is not 1 000 MHz, add the frequency correction shown on the nomogram at the middle left hand side of the same figure.

(e) If the terrain is rough, add the altitude correction in the following manner:

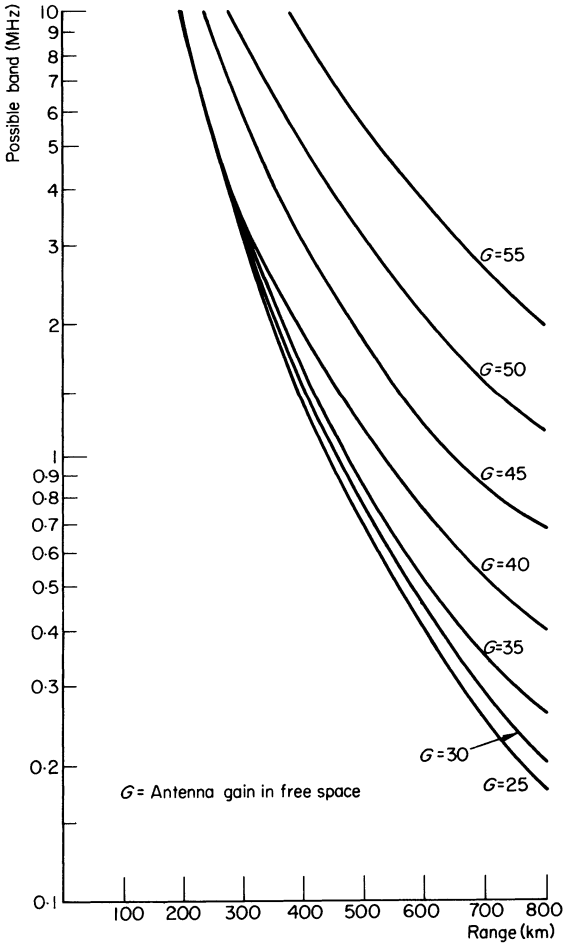

Fig. 194 Frequency band that can be used in tropospheric scattering

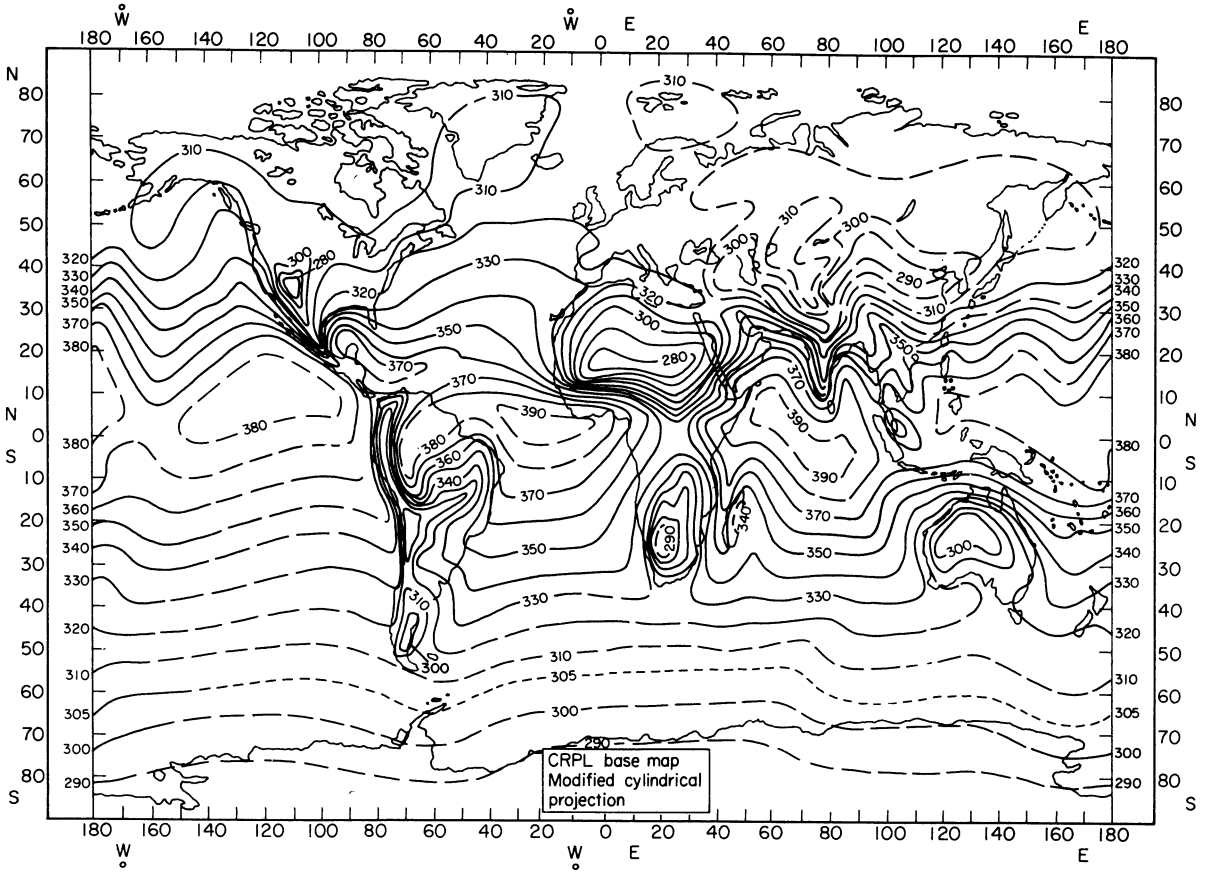

Fig. 195 Minimum monthly median of the index at the ground

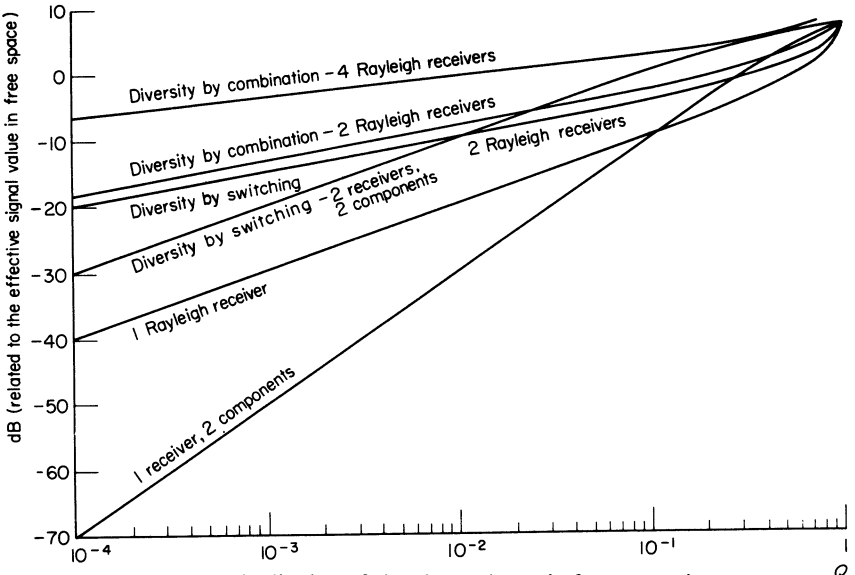

Fig. 196 Distribution of signal-to-noise ratio for one section

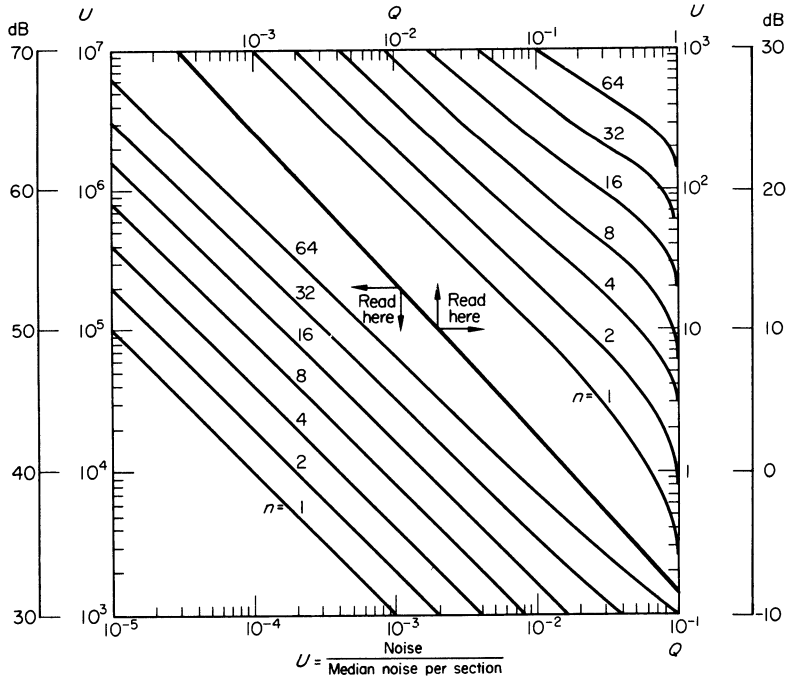

Fig. 197 Statistical noise distribution for 2^n sections; line of sight; Rayleigh fading; simple reception

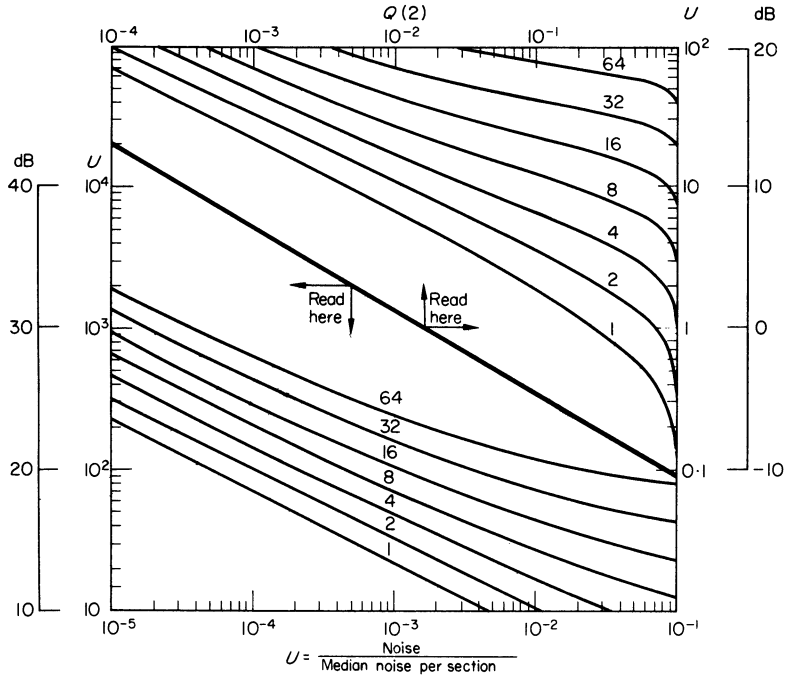

Fig. 198 Statistical noise distribution for 2^n sections; line of sight; Rayleigh fading, double reception; diversity with quadratic combinator

$$U = \frac{\text{noise}}{\text{median noise per section}}$$

1. Determine by means of the nomogram in the lower part of Fig. 188, the altitude H_0 where scattering would take place if the ground were spherical.
2. Determine on the profile the height H_1 where scattering actually takes place.
3. Calculate the ratio H_1/H_0 and read the corresponding correction from the middle right hand nomogram of Fig. 192.

(f) Calculate the losses in the antenna feeders and—if necessary—add the losses in duplex filters or circulators.

(g) Calculate the attenuation margin as follows:

1. Read from the lower graph of Fig. 193 the standard deviation of the hourly medians of scattering attenuations as a function of the angle of scattering and the climate.
2. Read from either Fig. 98 (single reception) or Fig. 99 (diversity reception) the required fading margin.

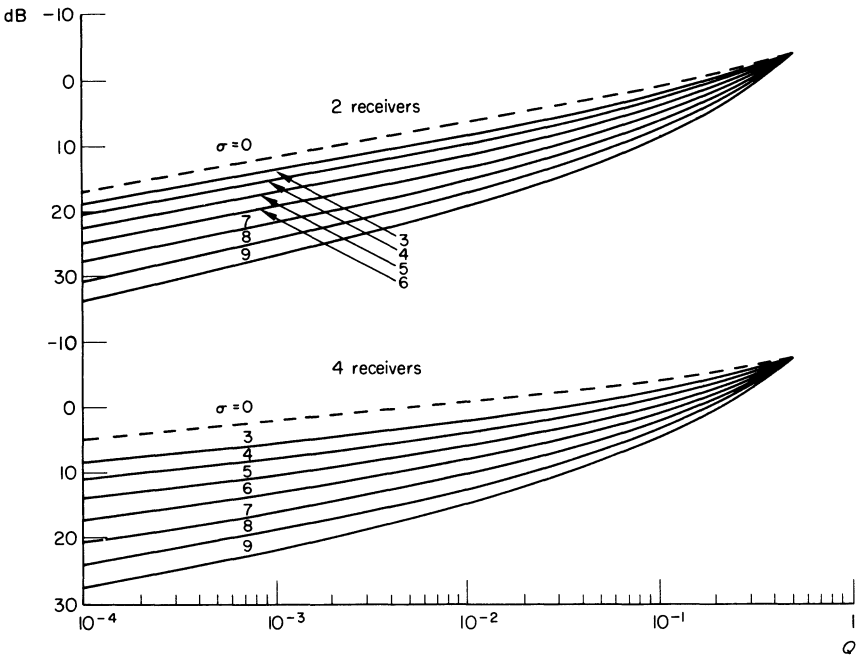

Fig. 199 Distribution of signal-to-noise ratio with quadratic combinator

(h) Add the results from (a), (b), (c), (d), (e), (f) and (g), taking the signs into account. The result is the sum:

$$P_E - 2G - R$$

where: P_E = transmitter power in dB in relation to 1 W. Figure 176 (left hand and top scales) converts dB into power

G = antenna gain (supposed equal at both ends)

R = reduction in antenna gain, given as a function of G in the upper graph of Fig. 193.

The antenna gain is usually indicated by the manufacturer. If parabolic antennae are used, their gain can be determined by means of Fig. 182.

Once we know the various types of transmitter and antenna that can be used for the link, it is easy to choose the most suitable one by trying out different combinations of transmitters and antennae.

(i) Figure 194 gives a tentative estimate of the usable frequency band of a circuit by tropospheric scattering as a function of antenna gain and distance.

APPENDICES

BASIC CONCEPTS OF MATHEMATICAL PHYSICS

APPENDIX 1 UNITS

A.1.1 MKSA (or GIORGI) SYSTEM

Units of the rationalized MKSA system are used in this book. They have the advantage of linking the units of mechanics with the electromagnetic units by adoption of the ampere as the fourth fundamental unit.

This system is relatively recent (1950), so that many theoretical studies of recent years have been described either in one of the systems using CGS units, or in the mixed fundamental system.

Equations expressed in these systems only differ from those expressed in the MKSA system by numerical coefficients.

Table A.1 shows the main units of the MKSA system used in this book.

TABLE A.1
Units of the MKSA (or Giorgi) system

Quantity	Symbol	Unit	Symbol	Relation to CGS units	
				electro-static	electro-magnetic
Length	d, D, l, h, etc.	metre	m	10^2	10^2
Mass	m	kilogramme	kg	10^3	10^3
Time	t	second	s	1	1
Work, energy	w or W	joule	J	10^7	10^7
Power	P	watt	W	10^7	10^7
Electric current	i or I	ampere	A	3×10^9	10^{-1}
Potential difference	v or V	volt	V	$1/3 \times 10^2$	10^8
Resistance or impedance	r, R or Z	ohm	Ω	$1/9 \times 10^{11}$	10^9
Conductance	G	siemen	S	9×10^{11}	10^{-9}
Conductivity	σ	siemen per metre	S/m	9×10^9	10^{-11}
Electric field	E or E	volt per metre	V/m	$1/3 \times 10^4$	10^6
Magnetic field	H or H	ampere turns per metre	At/m	$12\pi \times 10^7$	$4\pi \times 10^{-3}$
Dielectric constant	ε	farad per metre	F/m	$36\pi \times 10^9$	$4\pi \times 10^{-11}$
Magnetic permeability	μ	henry per metre	H/m	$10^{-13}/36\pi$	$10^7/4\pi$

In the MKSA system:

The speed of light (c) is 3×10^8 m/s.

The dielectric constant ε of a medium is usually expressed by

$$\varepsilon = \varepsilon_0 \varepsilon_r$$

where ε_0 = dielectric constant of free space = $10^{-9}/36\pi$ F/m

and ε_r = relative dielectric constant (referred to a vacuum) of the medium in question.

Similarly, the magnetic permeability μ of a medium is expressed by

$$\mu = \mu_0 \mu_r$$

where μ_0 = magnetic permeability in a vacuum = $4\pi \times 10^{-7}$ H/m

and μ_r = relative magnetic permeability (referred to a vacuum) of the medium in question.

Furthermore we have

$$\varepsilon_0 \mu_0 = \frac{1}{9 \times 10^{16}} = \frac{1}{c^2} \quad (c = \text{speed of light in vacuo})$$

A.1.2 LOGARITHMIC UNITS

The quantities to be considered in propagation theory are subject to very large variations; they are usually expressed in decibels, referred to an arbitrary reference level.

Powers are expressed in decibels referred to one kilowatt (watt).

We have:

$$P \text{ decibels} = 10 \log_{10} P \text{ kilowatt (watt)}$$

Electric fields are expressed in decibels referred to 1 microvolt per metre. We have:

$$E \text{ decibels} = 20 \log_{10} E \text{ microvolt per metre}$$

APPENDIX 2 PROPERTIES OF ELECTROMAGNETIC FIELDS

A.2.1 ELECTROMAGNETIC FIELDS

The presence of electromagnetic waves is shown by the simultaneous presence of two fields; each field can be represented by a vector (quantity possessing both magnitude and direction) whose value is proportional to the strength of the field and whose direction and sense are those of the field. These two fields are called the electric and the magnetic field; they are but two aspects of the same phenomenon, i.e. the electromagnetic field, which is capable of imparting part of its energy to a receiving antenna in the form of high frequency electrical energy.

The effect of the field on an antenna (wire or loop) can be calculated by using either the electric or the magnetic field; the result will obviously be the same in both cases. However, in the case of open antennae it is easier to start from the electric field, because the necessary calculations are then remarkably simple. Similarly, the effect of the field on a closed antenna (loop, ferrite) is best calculated by starting from the magnetic field.

A.2.2 UNITS OF STRENGTH

CCIR Report 227 (Section 6)[415] recommends the presentation of the value of the electromagnetic field:

1. for all frequencies by the value of the electric field in volts per metre, or a convenient submultiple.
2. or for frequencies exceeding 1 000 MHz by the value of the energy (in watts) crossing a surface of 1 m^2, perpendicular to the direction of propagation.

However, the value of the electromagnetic field is sometimes defined by the power passing through a given solid angle. The latter may be expressed either in spherical angle (steradians), in circular degrees (angle at the centre of a cone with an opening of one degree), or in square degrees (angle at the centre of a quadrangular pyramid with an opening of one degree in each direction).

A.2.3 POLARIZATION

Apart from its strength, an electromagnetic field is defined by the direction of the electric field, i.e. the direction of polarization, or simply polarization. When this direction does not vary, we speak of plane polarization. When this direction rotates continuously, we call it circular or elliptical polarization, depending on whether or not the field remains constant during rotation.

APPENDIX 3 MAXWELL'S EQUATIONS

The elctromagnetic force obeys Maxwell's equations at any point in space, irrespective of bodies present.

One can find the derivation of the referred equations for quasi-stationary conditions (slowly varying currents and voltages) in all books on electricity, starting from Ampère's theorem (work of a magnetic mass when describing a closed loop round a current) and Faraday's law (the induced electromagnetic force in any circuit is proportional to the rate of change of the flux linked with the circuit). Maxwell and many other authors who have written on this subject have shown that these laws are always valid, irrespective of the frequency of the current, provided the displacement current in the dielectrics is taken into account[4].

In the study of electromagnetic wave propagation, there are neither electric charges nor magnetic masses. Furthermore, the magnetic permeability of the media in which propagation takes place is very close to that of free space ($\mu_r = 1$, $\mu = \mu_0$).

Adopting the following symbols:

$\boldsymbol{D}$ = vector representing the electric displacement

$\boldsymbol{E}$ = vector representing the electric field

$\boldsymbol{H}$ = vector representing the magnetic field

$\boldsymbol{i}$ = vector representing the current of conduction

σ = conductivity of the medium

ε_r = its relative dielectric constant

we can write Maxwell's equations as:

$$\left.\begin{aligned} \nabla \times \boldsymbol{E} &= -\mu_0 \frac{\partial \boldsymbol{H}}{\partial t} \\ \nabla \times \boldsymbol{H} &= \boldsymbol{i} + \frac{\partial \boldsymbol{D}}{\partial t} \\ \text{(or if } \varepsilon_r \text{ is independent of time)} \quad \nabla \times \boldsymbol{H} &= \sigma \boldsymbol{E} + \varepsilon_0 \varepsilon_r \frac{\partial \boldsymbol{E}}{\partial t} \\ \nabla . \boldsymbol{E} &= \nabla . \boldsymbol{H} = 0 \end{aligned}\right\} \qquad \text{(A.1)}$$

to which we should add the equations of continuity of the tangential field components at the interface between two media:

$$\left.\begin{aligned} (\boldsymbol{E}_T)_1 &= (\boldsymbol{E}_T)_2 \\ (\boldsymbol{H}_T)_1 &= (\boldsymbol{H}_T)_2 \end{aligned}\right\} \qquad \text{(A.2)}$$

It can also be shown that the electric energy stored per unit volume in a space with an electric field E equals:

$$\frac{\varepsilon_0 \varepsilon_r}{2} E^2 = \varepsilon_0 \varepsilon_r E^2_{\text{r.m.s.}} \tag{A.3}$$

and that the magnetic energy stored per unit volume in a space with a magnetic field H equals:

$$\frac{\mu_0}{2} H^2 = \mu_0 H^2_{\text{r.m.s.}} \tag{A.3a}$$

Finally, the energy passing through a surface S equals the flux through this surface from Poynting's vector:

$$\mathrm{d}\boldsymbol{W} = \boldsymbol{E} \times \boldsymbol{H} \tag{A.3b}$$

APPENDIX 4 RETARDED POTENTIALS

Maxwell's equations as written above are localized equations, relating the electric and magnetic fields at adjacent points. In order to relate these fields to their causes, i.e. to the movement of electric charges in the transmitting antenna, we use Lorentz's retarded potentials.

The transmitting antenna is usually situated in air, so that we can write in good approximation:

$$\varepsilon_r = 1 \qquad \sigma = 0$$

We first define the function:

$$\Psi(r) = \Psi = \mathrm{e}^{-\mathrm{j}\omega r/c} \tag{A.4}$$

where r = distance from transmitter. The modulus of this function varies as $1/r$ and its phase rotates as that of a wave propagated along a ray r at the speed of light c.

The retarded potentials are now defined by means of Kirchoff's equations:

$$\left.\begin{aligned} V &= \frac{1}{4\pi\varepsilon_0}\iiint \rho\Psi \,\mathrm{d}v \\ \boldsymbol{A} &= \frac{1}{4\pi}\iiint \boldsymbol{i}\Psi \,\mathrm{d}v \end{aligned}\right\} \tag{A.5}$$

where ρ = electric charge density, i = current density, and $\mathrm{d}v$ = volume element, the integral being extended to such a volume as to contain all charges and currents.

The fields can be derived from these potentials by means of the equations:

$$\left.\begin{aligned} \boldsymbol{E} &= -\nabla V - \mu_0 \frac{\partial \boldsymbol{A}}{\partial t} \\ \boldsymbol{H} &= \nabla \times \boldsymbol{A} \end{aligned}\right\} \tag{A.6}$$

The proof of these relations will be found in books on electrical theory and general radioelectricity[4]. It is shown that the fields calculated by means of these equations satisfy Maxwell's equations.

APPENDIX 5 HERTZIAN VECTOR

To determine the electromagnetic field at a certain point, we must know the six components of $\boldsymbol{E}$ and $\boldsymbol{H}$, which means the solving of six equations. However, these calculations can sometimes be considerably simplified by using the hertzian vector $\boldsymbol{\Pi}$, which is defined by three equations:

$$\left.\begin{aligned} &\frac{\partial \boldsymbol{\Pi}}{\partial t} = \boldsymbol{A} \\ &\nabla . \boldsymbol{\Pi} = -\varepsilon_0 \varepsilon_r V \\ &\nabla^2 \boldsymbol{\Pi} - \frac{\varepsilon_r}{c^2} \frac{\partial^2 \boldsymbol{\Pi}}{\partial t^2} = 0 \end{aligned}\right\} \tag{A.7}$$

Equations A.6 then show that:

$$\left.\begin{aligned} &\boldsymbol{E} = \frac{1}{\varepsilon_0 \varepsilon_r} \nabla \times (\nabla \times \boldsymbol{\Pi}) \\ &\boldsymbol{H} = \nabla \times \frac{\partial \boldsymbol{\Pi}}{\partial t} \end{aligned}\right\} \tag{A.8}$$

Once we know the value of $\boldsymbol{\Pi}$, we can calculate both the electric and the magnetic fields.

If the direction of the hertzian vector is also known—and this is very often the case in propagation problems—the calculation of the fields is reduced to calculating the modulus of this vector. The number of equations has thus been reduced from six to one.

On the other hand, since the radio vector does not possess an immediate physical significance, any calculations based on its use will have an abstract character.

We see from equations (A.8) that the fields are not modified by adding to vector $\boldsymbol{\Pi}$ a vector with zero curl, i.e. the gradient of an arbitrary scalar function. This observation has been put to good use by Bremmer[5].

The radio vector defined above can be easily calculated when starting from a source consisting of a system of electrical doublets (open antenna). Antipotentials can be obtained by permutating the magnetic and electric quantities, and hence the magnetic hertzian vector, which is easier to calculate when the source is a system of magnetic dipoles (closed antenna)[10].

APPENDIX 6 STATISTICAL DISTRIBUTIONS

One of the most important causes of the variation in characteristic propagation values is the effect of the sun in all its manifestations (time of day, annual cycle, solar activity—a cycle of approximately 11 years). This is a systematic action which can be predicted; its effects should be isolated from those due to unpredictable causes. A discussion of the calculation methods used for this purpose—which are anyway rather arbitrary—would go beyond the scope of this book.

These systematic variations are the subject of more or less long range predictions, which generally refer to the median value of the quantities considered.

Around these predicted values, the field strength varies in an unpredictable manner: a phenomenon commonly called fading. It is to be hoped that in the near future improved prediction methods (e.g. by the inclusion of new factors) will make it possible to remove some of the variations now considered unpredictable to the category of predictable variations.

However, it is not likely that even improved predictions will permit us to forecast the exact properties of fields received at a certain instant and a certain place. There are so many parameters on which the various values depend that their local or instantaneous value does not seem to obey any formula. We therefore have to deal with random variables which depend on space (distribution of the field of a transmitter) and on time (fluctuations in the field received). Here we shall only consider fluctuations in time, which constitute a random process.

It is easy to determine the percentage of time during which a variable exceeds a given value from observations made, and to plot the relevant curve. By exchanging the axes of this curve, we can calculate the value exceeded during a given percentage of the time—the distribution function. In order to provide a good quality of communication, we take as field value the value exceeded during a very large percentage of the time, e.g. 90 or 99 per cent. On the other hand, to evaluate the chances of interference or unwanted listening, the value exceeded during a very small percentage of the time, e.g. 10 to 1 per cent should be taken; this value will nevertheless be far greater than the previous one. A value which is attained or exceeded during 50 per cent of the time is called a median value. One also makes use of the average value, which is the average of values observed at close intervals.

For the theoretical study of phenomena, the observed distribution

function is conveniently replaced by another function, which corresponds as closely as possible to a known type of law, which has been analysed mathematically.

The laws most widely used in the study of wave propagation are detailed below.

A.6.1 RAYLEIGH'S LAW

Lord Rayleigh[401] has calculated the distribution function of the vector—the sum of a large number of vectors with arbitrary phases and comparable amplitudes. We have:

$$P(x) = e^{(-x^2/\langle x^2 \rangle)} \tag{A.9}$$

where $P(x)$ = probability that the sum of the vectors exceeds x (in the present case, $P(x)$ represents the fraction of time during which the sum of the vectors exceeds x)

$\langle x^2 \rangle$ = average value of the square of the sum of the vectors.

This law depends on only one parameter, $\langle x^2 \rangle$, which is twice the square of the r.m.s. value of the variable. The law is only valid when this value remains constant. However, should the r.m.s. value vary slowly in time, one could still apply Rayleigh's law to the ensemble of the values of the variable during a time interval which is short enough to prevent the effective value from varying to any appreciable extent during this interval. This is why Rayleigh's law is commonly used to describe variations in the field received around its median time value, though the latter may vary from one hour to the next. Using the reduced variable:

$$t = \frac{x^2}{\langle x^2 \rangle} = \frac{x^2}{2x^2_{\text{r.m.s.}}}$$

we can write Rayleigh's law as:

$$P(t) = e^{-t} \tag{A.10}$$

We therefore have for small values of t (e.g. $t < 0{\cdot}1$) in good approximation:

$$P(t) \approx 1 - t$$

Table A.2 gives the value of t and the value in decibels of the same variable for a few specific probability values.

TABLE A.2

$P(t)$ (percentage)	0·1	1	10	50	90	99	99·9
$t = x^2/2x^2_{\text{eff}}$	6·9	4·6	2·3	0·693	0·105	0·01	0·001
t (decibels)	8·4	6·6	3·6	−1·6	−9·8	−20	−30

The reader will observe that in this distribution, the median value is 1·6 dB less than the mean value of the square of the variable. In practical applications, the distribution is often referred to its median value. This is achieved by adding 1·6 to the t values in decibels. Recent investigations[411, 413] have shown that the distribution of the resultant remains very close to a Rayleigh distribution, even if the number of component vectors is rather small, e.g. 4 or 5. However, this is not true for the case of only two vectors; the distribution then strongly deviates from Rayleigh's law (see also Rice's law below).

A.6.2 INVERSE RAYLEIGH'S LAW

When receiving an f.m. wave, as long as the signal level remains above the threshold of the receiver the noise level at the output will be inversely proportional to the power of the signal received. If the signal power obeys Rayleigh's law, the noise will obey a law whose distribution function is defined by:

$$P(N) = P(N < N_1) = e^{(-N_0/N_1)} \tag{A.11}$$

where N_0 = sound level without fading.

Pearson called this the inverse Rayleigh's law[428].

For small time percentages, the asymptotic law applies:

$$Q(N) = P(N > N_1) \approx \frac{N_0}{N_1} \tag{A.12}$$

The average noise value—in the sense of probability calculation—is therefore infinite. However, the noise power in a physical system is always finite. If N_{max} represents this limit—determined by the characteristics of the receiving system—it has been shown[424, 428, 432] that in this case, assuming $N_{max} \gg N_0$

$$\langle N \rangle = N_0\left(0{\cdot}423 + 2{\cdot}3 \log \frac{N_{max}}{N_0}\right) \tag{A.13}$$

Pearson[428] admits that the value of N_0 in this equation must be increased by 3 to 7 dB. The probable cause is a reduction of the median signal value in the presence of fading.

A.6.3 LAPLACE–GAUSSIAN LAW

This law is by far the most used in probability statistics and has been the subject of many papers.

It has been shown[12] that the sum of a large number of random variables that are centred on the same value tend to be distributed according to the Laplace-Gaussian law when the number of these variables increases indefinitely, provided that certain mathematical conditions are met—this is usually the case for physical variables (theorem of Liapounoff, or of the

central limit). Gaussian distribution will therefore very often be encountered in physics when phenomena resulting from a great number of random causes are described.

It depends on two parameters:

1. The average value of the variable $\langle x \rangle$, which—for this law—is moreover the same as the median value.
2. The standard deviation σ; its square $\sigma^2 = \langle (x - \langle x \rangle)^2 \rangle$ is called 'variance'.

The normalized deviation is defined by:

$$t = \frac{x - \langle x \rangle}{\sigma}$$

The probability density, i.e. the probability that the variable in question will be between t and $(t + dt)$ is then:

$$p(t)\,dt = \frac{1}{(2\pi)^{\frac{1}{2}}} e^{(-t^2/2)}\,dt$$

and the distribution function:

$$P(x) = \Pi(t) = \frac{1}{(2\pi)^{\frac{1}{2}}} \int_{-\infty}^{t} e^{(-t^2/2)}\,dt \qquad \text{(A.14)}$$

Very complete tables of functions $\Pi(t)$ and $p(t)$ are available. Table A.3 gives a few specific values of $\Pi(t)$:

TABLE A.3

$\Pi(t)$ (percentage)	0·01	0·1	1	10	50	90	99	99·9	99·99
t	−3·7	−3·1	−2·3	−1·3	0	+1·3	+2·3	+3·1	+3·7

Experience has shown that field strengths (expressed in dB) in general obey the Laplace-Gaussian law, as far as propagation is concerned. Such a distribution is called a normal logarithmic distribution.

A.6.4 RICE'S LAWS

We shall group under this term the distribution laws of the sum of a sinusoidal variable (the signal) and one or several random variables (noise or signals).

Laws of this type have first been proposed by Rice[404] and elaborated by other authors[411, 413].

They allow in particular the study of the signal-to-noise ratio with various modulation systems, as well as the study of a signal which is propagated simultaneously along a normal path and along a certain number of other paths, through which it is much weaker.

However, the results obtained are rather complex because of the great number of parameters involved. We shall limit ourselves to mentioning the existence of these types of law.

A.6.5 RESULTANT OF TWO RAYS

In the case of communication by line of sight with sea reflection, direct and reflected rays have approximately the same amplitude; their phase difference is however variable and presents a uniform distribution. The power received is then:

$$W = 4\sin^2\frac{\Delta\varphi}{2}$$

where $\Delta\varphi$ = phase difference.

If Q is the fraction of time during which the signal level is below a given level W, we have:

$$W = 4\sin^2\left(\frac{\pi}{2}Q\right) \tag{A.15}$$

and for small time intervals:

$$W \approx \pi^2 Q^2 \approx 10\,Q^2$$

A.6.6 ALTERNATION OF TWO LAWS

Pearson[428] has represented the distribution of signal level in a section of a radio link, operating in line of sight by the random succession of a Rayleigh distribution and a normal logarithmic distribution with $\sigma = 3$. The result obviously depends on the fraction of the time during which Rayleigh distribution takes place. Pearson has published the corresponding distribution curves.

A.6.7 COMPOSITION OF SOME PROBABILITY LAWS

The study of wave propagation frequently prompts one to compose probability laws. The principle of compounded probabilities may be described as follows:

If event C assumes the realization of two events A and B, its probability is the product of the probability of A and the probability of B occurring in the knowledge that A has occurred.

Let us consider a few important cases[431].

A.6.7.1

To remedy fast and strong variations in signals received, the strongest of the signals received by several antennae or at several frequencies is chosen (diversity reception with selection combining).

(a) Let us assume that the fast variations in the signals obey Rayleigh's

law (see above) and that there is no correlation whatsoever between the signals at the various receivers.

The probability that the signal at one of the receivers has an amplitude of less than x (using the reduced variable t) is:

$$Q(t) = 1 - P(t) = 1 - e^{-t}$$

If there are n identical receivers, the probability that the signals received by all these receivers have an amplitude of less than x (in virtue of the principle of compounded probabilities) will be:

$$Q_{(n)}(t) = (1 - e^{-t})^n$$

The probability that the chosen signal (the best signal received) has an amplitude of more than x will therefore be:

$$P_{(n)}(t) = 1 - (1 - e^{-t})^n = 1 - (1 - e^{(-x^2/2x^2_{\text{r.m.s.}})})^n \qquad \text{(A.16)}$$

Signal improvement is of particular importance in the case of weak signals. We have in this case:

$$P_{(n)}(t) \simeq 1 - t^n$$

(b) In the case of two rays, a similar reasoning produces:

$$W = 4 \sin^2 \left(\frac{\pi}{2} Q^{1/n} \right) \qquad \text{(A.17)}$$

or for small time intervals:

$$W \approx 10 Q^{2/n}$$

The advantage of diversity reception is considerable when Q is small.

A.6.7.2

A still better result is obtained by appropriately combining the signals from the various receivers (diversity reception by maximal-ratio combining). Brennan[412] has shown that if the signal obeys Rayleigh's law, and if the transmission is frequency modulated, the best combination is obtained when:

$$S + N = \sum_1^n a_i (s_i + n_i)$$

where:

$$a_i = \left(\frac{\langle s_i^2 \rangle}{\langle n_i^2 \rangle} \right)^{\frac{1}{2}}$$

S and B are the signal and noise values at the output of the combining device. s_i and n_i are the signal and noise values at the output of the receiver. $\langle s_i^2 \rangle$ and $\langle n_i^2 \rangle$ are the values of signal and noise levels measured over the time interval which corresponds to the time response of the combining device (of the order of milliseconds).

Assuming that this optimum combination is realized at each instant, the following relation can be shown to exist between the instantaneous levels:

$$\frac{\langle S^2\rangle}{\langle N^2\rangle} = \sum_1^n \frac{\langle s_i^2\rangle}{\langle n_i^2\rangle} \tag{A.18}$$

Putting

$$\frac{\langle S^2\rangle}{\langle N^2\rangle} = F^2 \quad \text{and} \quad \frac{\langle s_i^2\rangle}{\langle n_i^2\rangle} = f_i^2$$

we now assume that $\langle F^2\rangle$ and $\langle f_i^2\rangle$ are their average values during a large time interval.

The instantaneous values of s_i and n_i obey Rayleigh's law. Because of the analytical form of this law, this also applies to their quotient.

Putting

$$\frac{f_i^2}{\langle f_i^2\rangle} = t_i \quad \text{and} \quad \frac{F^2}{\langle F^2\rangle} = t$$

equation (A.18) becomes, observing that the average values of the two terms of this equation are equal:

$$t = \sum_1^n t_i \tag{A.19}$$

On the other hand, the probability that the signal-to-noise ratio at the output of the receiver i will have a reduced value of less than t_i is:

$$Q(t_i) = 1 - e^{-t_i}$$

The probability that this value will lie between t_i and $(t_i + dt_i)$ is therefore:

$$q(t_i) = e^{-t_i}$$

The probability that the resulting signal will have a reduced value of less that t is therefore:

$$\int_{\cdot\cdot\cdot}^{n\,\text{times}} \int \exp\left(-\sum_1^n t_i\right) \prod_1^n dt_i$$

the integral being expanded in virtue of equation (A.19) to the range defined by:

$$\sum_1^n t_i \leq t$$

Carrying out this calculation we find:

(a) for two receivers:

$$P_{(2)}(t) = P_{(t)}(1+t) \tag{A.20}$$

which can be reduced for small values of t to:

$$P_{(2)}(t) \simeq 1 - \frac{t^2}{2}$$

(b) for four receivers:

$$P_{(4)}(t) = P(t)\left(1+t+\frac{t^2}{2}+\frac{t^3}{6}\right) \qquad \text{(A.21)}$$

or for small values of t:

$$P_{(4)}(t) \simeq 1-\frac{t^4}{24}$$

A.6.7.3

An often occurring case is that the monthly median values of the signal are known and that we want to know its distribution in time by starting from these values.

The distribution of the median values (or average values, which are identical in this case) expressed in dB of the signal around its monthly median, is a Gaussian distribution, whose standard deviation we know in another connection.

The distribution of the instantaneous values around the median value is a Rayleigh distribution.

If $p_G(x)$ represents the probability (calculated according to the Gaussian distribution by using the given monthly median value and the given standard deviation) for the median signal value to lie between x and $(x+\mathrm{d}x)$ dB, and if $P_R(x)$ represents the probability (calculated according to Rayleigh's law or diversity reception distribution laws) for the instantaneous signal value to exceed x dB, the probability that the signal exceeds x dB is:

$$P(x) = \int_{-\infty}^{+\infty} P_R(x_1)p_G(x_2)\,\mathrm{d}x_2 \qquad \text{(A.22)}$$

with $x_1+x_2 = x$.

A more practical form of this equation for numerical calculation when $P(x)$ is large, is:

$$P(x) = 1-\int_{-\infty}^{+\infty}[1-P_R(x_1)]p_G(x_2)\,\mathrm{d}x_2$$

The integral can be calculated by a method of numerical approximations[1, 424, 431].

A.6.7.4

In the case of a radio beam in line of sight, the noise levels of successive sections must be summed to obtain the total noise at the output of the circuit. Curtis[42] has studied the resulting distribution by starting from a distribution he found by experiment. It would seem more logical to carry out the calculation by assuming that fading obeys Rayleigh's law[432].

Let us put:

$$U = \frac{N}{N_0} \tag{A.23}$$

where N_0 = noise level without fading (or a higher level if one admits Pearson's theory mentioned in Section A.6.2).

(a) With single reception we have in accordance with Section A.6.2:

$$P(N) = e^{-1/U} \tag{A.24}$$

and therefore:

$$dP(N) = \frac{e^{-1/U}}{U^2}\,dU$$

If U_1 and U_2 represent the values of parameter U for two successive sections, we can write the law of distribution of the noise level at the output of the second section as:

$$P_{(2)}(N) = \int_0^U P(U_1).\,dP(U_2) \tag{A.25}$$

where $U = U_1 + U_2$ (adding the noise levels).

Similarly:

$$P_{(2^n)}(N) = \int_0^U P_{(2^{(n-1)})}(U_1)\,dP_{(2^{(n-1)})}(U_2) \tag{A.26}$$

These equations enable us to calculate by numerical integration the noise level at the output of a radio beam with 2^n equal sections.

For small time intervals, corresponding to high noise levels, we find the following asymptotic equation:

$$1 - P_{(n)}(N) = Q_{(n)}(N) \approx \frac{n}{U}$$

In the case of unequal sections, this asymptotic equation still applies if we take the arithmetic average of the lengths of the sections instead of the length of the equivalent section[431].

(b) In the case of diversity reception, similar calculations must be carried out, but substituting for equation (A.24) an equation found by substituting (A.23) in one of the equations (A.16), (A.20) or, exceptionally, (A.21).

The following asymptotic equation applies to maximal ratio combining for two receivers:

$$1 - P_{(n)}(N) = Q_{(n)}(N) \approx \frac{n}{2U^2}$$

and for reception by means of selection combining of two receivers:

$$1 - P_{(n)}(N) = Q_{(n)}(N) \approx \frac{n}{U^2}$$

A.6.7.5

The distribution of the hourly means of the noise level at the output of a radio beam which functions by means of tropospheric scattering, can be calculated in a similar manner as described in the two preceding paragraphs, but the Rayleigh distribution (or distributions derived from it) must be replaced by normal logarithmic distributions whose standard deviation depend on the length of the section[159].

(a) Sheffield[425] has described a very practical method—based on the use of nomograms—for calculating the parameters of the normal logarithmic distribution, which is closest to the resultant distribution.

(b) Jacobson[414] has proposed a more precise solution, which takes into account the third moment of the distribution, and which can be applied to all experimentally determined distributions. Calculation is necessarily more complicated. This method has been officially adopted by CCIR and formed the basis of the studies of CNET[167].

A.6.8 REPRESENTATION OF PROBABILITY LAWS

CCIR Recommendation 311[137] advises the use of specially ruled paper for the presentation of the observed probability curves, such as putting the field strength in dB along the Y-axis and the probabilities along the X-axis, the normal logarithmic distribution is a straight line. This method of presentation is highly practical for studying the true distribution. Figures 98–99 and 196–199 show detailed graphs of the more important distributions discussed in this section. However, the scales used differ for practical reasons from those recommended by CCIR.

APPENDIX 7 FOURIER TRANSFORMS

In their most usual form, Fourier transforms allow the calculation of the spectrum $G(\omega)$ of a current or of a variable potential $f(t)$. Conversely, they permit the calculation of the function $f(t)$ of either the current or the potential by starting from its spectrum $G(\omega)$ by means of the following reciprocal equation:

$$\left.\begin{aligned} G(\omega) &= \int_{-\infty}^{-\infty} f(t) \,.\, e^{-j\omega t} \,.\, dt \\ f(t) &= \frac{1}{2\pi} \int_{-\infty}^{+\infty} G(\omega) \,.\, e^{j\omega t} \,.\, d\omega \end{aligned}\right\} \qquad (A.27)$$

In the particular case of $f(t) = 0$ for $t < 0$ we can also use the analogous forms:

$$\left.\begin{aligned} G(\omega) &= \int_{0}^{\infty} f(t) \,.\, \cos \omega t \,.\, dt \\ f(t) &= \frac{2}{\pi} \int_{0}^{\infty} G(\omega) \,.\, \cos \omega t \,.\, d\omega \end{aligned}\right\} \qquad (A.28)$$

for an even function, and

$$\left.\begin{aligned} G(\omega) &= \int_{0}^{\infty} f(t) \,.\, \sin \omega t \,.\, dt \\ f(t) &= \frac{2}{\pi} \int_{0}^{\infty} G(\omega) \,.\, \sin \omega t \,.\, d\omega \end{aligned}\right\} \qquad (A.29)$$

for an odd function.

Fourier transforms supply the rigorous solution of the problem of shape modification of a signal traversing a dispersive medium such as the ionosphere. However, although very complete tables have been published, it is relatively seldom that the calculations can be carried out by analytical methods. Generally speaking, the transforms—and more specifically the inverse transforms—must be calculated numerically, so that the generality and apparent simplicity of this method becomes illusory.

Fourier transforms are used in the theory of tropospheric scattering to establish the relations between the correlation coefficient as a function of the distance ρ, $C(\rho)$ and the distribution of the dimensions of atmospheric irregularities. The latter distribution is called the spectrum $S(K)$, with $K = 1/l$.

The following equations are used[108]

$$\left.\begin{aligned} C(\rho) &= \int_0^{\infty} S(K)\cos K\rho \, \mathrm{d}K \\ S(K) &= \frac{2}{\pi}\int_0^{\infty} C(\rho)\cos K\rho \, \mathrm{d}\rho \end{aligned}\right\} \tag{A.30}$$

The transforms can also be expanded to functions with more than one variable. Still in the theory of tropospheric scattering, these transforms are used to transform the functions of a vector in a three dimensional space. The transform equations, expressed in a form similar to the previous one, are then[123]

$$\left.\begin{aligned} C(\rho) &= \iint\int_{-\infty}^{+\infty} S(K)\, \mathrm{e}^{-\mathrm{j}\boldsymbol{K}\boldsymbol{\rho}\cdot} \mathrm{d}^3K \\ S(\boldsymbol{K}) &= \frac{1}{8\pi^3}\iint\int_{-\infty}^{+\infty} C(\rho)\, \mathrm{e}^{\mathrm{j}\boldsymbol{K}\boldsymbol{\rho}\cdot} \mathrm{d}^3\rho \end{aligned}\right\} \tag{A.31}$$

where d^3K and d^3p represent the elementary volume in the space of vector $\boldsymbol{K}$ and vector $\boldsymbol{\rho}$ respectively.

We can also move the numerical coefficient ($1/2\pi$, $2/\pi$ or $1/8\pi^3$) from one equation to another in the above pairs of equations. This is how they are used by some authors[123, 132] and in equations (2.16) and (2.17).

APPENDIX 8 FRESNEL ZONES

A.8.1 GENERAL

By virtue of Huygens' principle of superposition, if we consider a closed surface surrounding a light source, the illumination at a point outside this surface will be the same as when each point of this surface has been replaced by a light source of the same intensity for the illumination at this point.

This principle can be applied to radio waves, provided only obstacles are considered that are sufficiently large in relation to the wavelength, and provided that the field is calculated at points that are sufficiently distant from the obstacles[208]. These conditions are assumed to prevail in the following discussion.

Let D be the distance between transmitter and receiver. The first Fresnel zone is defined as the ellipsoid of revolution about the axis joining the transmitter and the receiver (Fig. 200) in such a manner that the sum of the distances of a random point P on the surface of the ellipsoid to the transmitter and the receiver equals $D+\lambda/2$. The equation of this ellipsoid is therefore:

$$SP+PE = D+\frac{\lambda}{2}$$

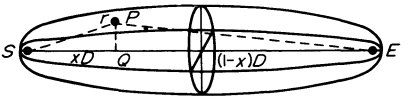

Fig. 200

A second Fresnel zone is similarly defined by the equation:

$$SP+PE = D+\frac{2\lambda}{2}$$

and so on.

A.8.2 DIMENSIONS OF THE FIRST FRESNEL ZONE

Let r be the radius of the first Fresnel zone at a point Q situated at a distance xD from the transmitter.

Distance D is always of the order of several kilometres in practical wave propagation problems. On the other hand, Fresnel zones are only useful in the case of line-of-sight propagation—only used for wavelengths of less than 10 m. Finally, we have seen in Section A.8.1 that the Huygens–Fresnel theory is only valid starting a few wavelengths from the transmitter.

An elementary calculation gives under these circumstances:

$$r = (\lambda D)^{\frac{1}{2}}[x(1-x)]^{\frac{1}{2}} \qquad \text{(A.32)}$$

Radius r attains its maximum value in the centre of the path, i.e. when $x = 0{\cdot}5$. We then have:

$$r_{max} = \frac{(\lambda D)^{\frac{1}{2}}}{2} \qquad \text{(A.33)}$$

The radius varies rather slowly when assuming a more distant position from the centre of the distance covered. When $x = 0{\cdot}1$, r is still $0{\cdot}6\ r_{max}$. Except in very special cases, it is therefore sufficient in practice to calculate r_{max} and to approximate the ellipsoid by a cylinder.

In the proximity of antennae (but at a distance of more than 2λ from the antennae) we have:

$$r = (d\lambda)^{\frac{1}{2}} \qquad \text{(A.34)}$$

where d = distance xD at the centre of the antenna.

A.8.3 DIFFRACTION BY SCREENS

The presence of a screen in the path of radio waves between transmitter and receiver modifies the field received. However, this modification becomes noticeable only when the transmitter is situated in, or in the immediate neighbourhood of the geometric shadow.

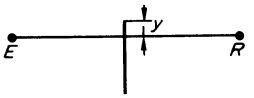

Fig. 201

The simplest case is that of a thin screen with rectilinear and indefinite edges, which forms an opaque 'half plane'. In propagation studies, terrain irregularities are often compared to this type of screen. This rather

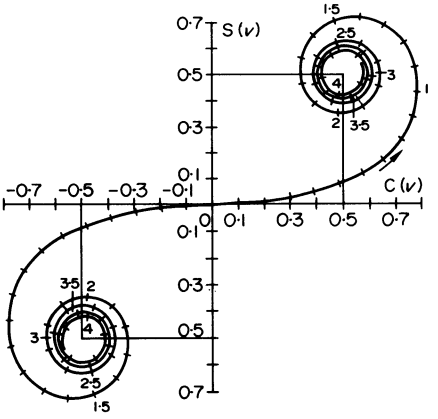

Fig. 202

inaccurate hypothesis nevertheless sufficiently approaches reality, and greatly facilitates calculations.

In Fig. 201 y represents the distance from the screen edge to the axis between transmitter and receiver, and is deemed to be positive in the direction towards free space, while r represents the radius of the first Fresnel zone at the place of the screen. We put $v = 2^{\frac{1}{2}}y/r$. It is easy to calculate the field received by using Cornu's spiral (Fig. 202). All that is necessary is to join on the spiral, point I ($-0{\cdot}5$, $-0{\cdot}5$) to reference point y, and to measure distance l between these two points.

Attenuation in relation to free space is therefore given by

$$A = l\frac{2^{\frac{1}{2}}}{2}$$

Examining this figure, we observe that this attenuation varies particularly rapidly when v varies from $-1{\cdot}3$ to $+1{\cdot}3$, i.e. when y/r varies from $-0{\cdot}92$ to $+0{\cdot}92$; this corresponds very closely to the limits of the first Fresnel zone. For this reason we always try to clear this zone when calculating a line-of-sight radio communication.

APPENDIX 9 DOPPLER EFFECT

In the case of a transmitter and a receiver situated at a short distance from each other, and in the presence of a reflector at a distance d from the transceiving station, when the transmitter emits a wave represented by

$$E_1 = E_0 e^{j\omega t}$$

the receiver will receive

$$E_2 = kE_0 e^{j\omega[t-(2d/c)]}$$

If the reflector is moving at a radial velocity V_r in relation to the fixed station, we have:

$$d = d_0 + V_r t$$

Hence

$$E_2 = kE_0 e^{j\omega[t(1-(2Vr/c)-(2d_0/c))]}$$

The effect for the fixed station will be as though vibration ω had become $\omega\ (1-2V_r/c)$. The relative angular frequency variation observed by this station is therefore:

$$\frac{\Delta\omega}{\omega} = \frac{\Delta f}{f} = -\frac{2V_r}{c} \qquad \text{(A.35)}$$

This variation of the frequency is called the Doppler effect. It is used for the very exact measurement of the radial velocity of a reflector.

In the same way, if the reflector moves in a medium with a refractive index n, we have

$$\frac{\Delta\omega}{\omega} = \frac{\Delta f}{f} = -\frac{2nV_r}{c} \qquad \text{(A.36)}$$

Finally, similar but more complex equations exist for the case that transmitter and receiver are not contiguous.

APPENDIX 10 CALCULATION OF THE SIGNAL-TO-NOISE RATIO FOR f.m.

Radio links using metre and shorter waves are often used for f.m. transmission of a multiplex telephony communication. Although this is not strictly a question of propagation, it may be useful to describe a method for noise calculation in a telephony channel using this type of link, as well as its statistical distribution in time.

We must first determine the relation between transmission attenuation and noise in a telephony channel. We then use the statistical distribution of the attenuation to obtain the statistical noise distribution.

A.10.1 BEHAVIOUR OF f.m. RECEIVERS

Figure 203 is a sketch of the variation of the signal-to-noise ratio ε in a telephony channel as a function of the carrier-to-noise ratio ρ at the receiver input.

When ρ is lower than a certain threshold value (of approximately 10 dB), the signal will be negligible or weak; this also applies to the signal-to-noise ratio. On the other hand, above a certain value of ρ, the signal-to-noise ratio acquires a constant value, due to residual receiver noise (saturation).

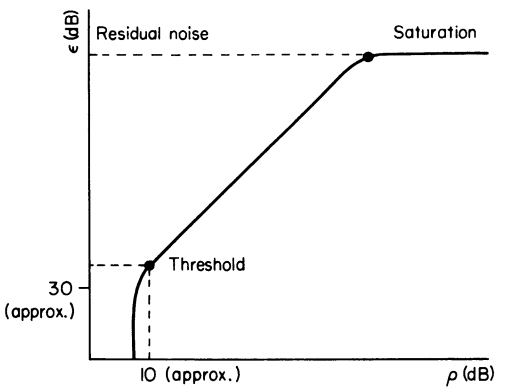

Fig. 203

Above the threshold value, the signal will maintain a constant value. Between the threshold value and saturation, ε and ρ are mutually proportional. Radio links generally operate in this latter zone. We have (with ρ and ε in dB):

$$\varepsilon = 20\log\Delta f - 20\log f_m + 10\log B + \rho - 38 \qquad \text{(A.37)}$$

where Δf = peak frequency deviation (Hz)

f_m = mean frequency of the telephone channel under consideration, at the output of the transmitting multiplexer (Hz)

B = bandwidth at 3 dB points in the i.f. amplifier (Hz).

All specifications of radio links are related to the highest frequency channel f_m, for which ε has the smallest value.

The psophometric noise in this channel, expressed in dB in relation to 1 pW, is given by the equation:

$$N = 87{\cdot}5 - \varepsilon - E \qquad \text{(A.38)}$$

where E = pre-emphasis of the channel in dB (usually $E = 4$ dB).

On the other hand, for a system where all components are at ambient temperature (this is the case in ground links; the case of spatial links is more complex), we have

$$\rho = P_T + 2G - \Delta G - A - A_C + 204 - 10\log B - F \qquad \text{(A.39)}$$

where P_T = transmitted power in dB in relation to 1 W

G = gain of each antenna in dB

ΔG = reduction in gain by tropospheric scattering

A = propagation attenuation in dB

A_C = attenuation in cables and filters, in dB

F = receiver noise factor in dB.

A.10.2 RELATION BETWEEN ATTENUATION AND THERMAL NOISE IN A SECTION

When combining the three above equations, we have between threshold and saturation:

$$N = -V - (2G - \Delta G) + (A + A_C) \quad \text{dBm Op} \qquad \text{(A.40)}$$

where $V = 168{\cdot}5 + 20 \log \Delta f - 20 \log f_m + P_T - F + E$.

V is called the system value. It is usually given by the manufacturer. Its order of magnitude is 130–150 dB for line-of-sight systems, and can attain 180 dB for systems operating by tropospheric scattering.

The sum of the other two terms represents the total attenuation between the transmitter output and the receiver input. This gives a very simple relation between attenuation and thermal noise in a section of a radio link, between the threshold value of the receiver and its saturation.

A.10.3 STATISTICAL DISTRIBUTION OF THERMAL NOISE

A.10.3.1 **One section, line of sight**

The statistical distribution of A has been studied in Chapter 8 (Section 8.3.2.2). The appropriate values can simply be substituted in equation (A.40).

A.10.3.2 Several sections, line of sight, land reflection

(a) Calculate the median attenuation of each section (Section 8.3.2.2)

(b) Calculate the corresponding noise by means of equation (A.40) and convert this value into pW.

(c) Add all median noise values of the various sections (N_0) in pW.

(d) Determine fraction x of the total time during which fading occurs (usually $x = 0{\cdot}25$) and divide the given percentage Q_1 by this fraction.

1. If the result is higher than 50 per cent, there is no additional attenuation.
2. If the result is lower than 50 per cent, it represents fraction $Q = Q_1/x$ of the fading time.

(e) Determine fraction y of the section where fading occurs simultaneously (y varies between 0·25 and 0·5; the greatest values correspond to homogeneous meteorological conditions along the path, and to north–south paths). If n_1 is the number of sections, we have therefore $n = yn_1$ sections with simultaneous fading.

(f) Enter the values of n and Q in Fig 197 (or by way of exception in the case of double-diversity reception in Fig. 198) and read the corresponding multiplier U. We then have a line noise of

$$N = N_0[(1 - y)n_1 + U] \text{ pW}$$

A.10.3.3 One section; diffraction or scattering

(a) Calculate the median attenuation and the standard deviation as indicated in Sections 8.3.2.3 and 8.3.2.4.

(b) Deduce the median noise from the median attenuation by means of equation (A.40).

(c) Enter the value of σ and the required fraction of time:

1. for single reception in Fig. 98
2. for diversity reception with maximal-ratio combining in Fig. 199 in order to determine the increase in noise.

(d) Add this increment to the median noise.

A.10.3.4 Several sections; diffraction or scattering

(a) Calculate the noise distribution in each section (Section A.10.3.3).

(b) For larger percentages of time ($Q \geqslant 0{\cdot}8$) add the noises corresponding to the same percentage.

(c) For small time percentages ($Q < 0{\cdot}1$) add the percentages corresponding to the same noise.

(d) Join the curves obtained in an arbitrary fashion.

A.10.4 FIXED NOISE

To the variable thermal noise calculated in Section A.10.2, we should add other sources of noise:

(a) Thermal noise and intermodulation noise of modulator and demodulator, in stations using demodulation.

(b) Thermal noise of the transmitter and residual noise from the saturated receiver.

(c) Intermodulation noise from both transmitter and receiver.

The values of these types of noise are indicated by the manufacturers.

A.10.5 NOISE AVERAGES

Some CCIR recommendations refer to the noise average during one hour. This average can be calculated as follows:

(a) Plot the statistical noise distribution on a sheet of double logarithmic paper (see for example Figs 197 and 198).

(b) Calculate the noise average between $Q = 1$ and $Q = 10^{-1}$ by means of the formula:

$$N_{-1} = 0{\cdot}2[N(0{\cdot}9)+N(0{\cdot}7)+N(0{\cdot}5)+N(0{\cdot}3)]+0{\cdot}1\,N(0{\cdot}15)$$

(c) Calculate in the same manner the median between $Q = 10^{-1}$ and $Q = 10^{2}$ by means of the formula:

$$N_{-2} = 0{\cdot}02[N(0{\cdot}09)+N(0{\cdot}07)+N(0{\cdot}05)+N(0{\cdot}03)]+0{\cdot}01\,N(0{\cdot}015)$$

(d) Continue to the maximum noise considered, which may be, according to the type of installation:

1. the noise of a receiver without carrier wave (which gives a distinctly exaggerated result)
2. the noise at the moment of 'squelch' (this result gives a better idea of the value of the circuit, provided the percentage of interruption by the squelch does not compromise the required time availability).

A.10.6 RELIABILITY

The circuit is interrupted when in any section the receiver (or all receivers if there are more than one) receive a carrier wave below the threshold value, or if the squelch operates (it usually operates at the threshold value, so that the conditions are equivalent).

The interruption percentage for each section can be calculated as follows:

(a) Calculate the difference between the mean attenuation and the attenuation corresponding to $\rho = 10$ dB in equation (A.39). This difference is called the 'section margin'.

(b) In the line-of-sight case, enter this margin on curve $\sigma = 0$ of Fig. 185 and read the value of Q.

(c) In the case of diffraction or scattering, enter in the same manner in either Fig. 98 or Fig. 99 the values of the margin and of σ, and read off Q.

Reliability is defined by:

$$R = 1 - \sum Q$$

where ΣQ = sum of values of Q found for the different sections.

REFERENCES

1. GENERAL WORKS

1. A. ANGOT. *Compléments de Mathématiques à l'usage des ingénieurs de l'électrotechnique et des télécommunications.* Editions de la revue d'optique. Paris, 1949.
2. E. T. WHITTAKER and G. N. WATSON. *A course of modern analysis.* Cambridge University Press, 1950.
3. F. E. TERMAN. *Radio Engineers' handbook.* McGraw-Hill, New York and London 1943.
4. L. BLOCH. *Précis d'électricité théorique.* Gauthier-Villars, Paris, 1933.
5. H. BREMMER. *Terrestrial radio waves.* Elsevier's Publishing Co. Inc., New York Amsterdam, London, Brussels, 1949.
6. E. BLOCH. *Théorie cinétique des gaz.* Armand Colin, Paris, 1921.
7. NATIONAL BUREAU OF STANDARDS. Circular 462. Ionospheric Radio Propagation. Government Printing Office, Washington, 1949.
8. G. BOREL and M. DE MIRBECK. *Cours de propagation de l'E.S.E.*, Paris. 1° fascicule, 1950; 2° fascicule, 1951.
9. R. MESNY. *Radio-électricité générale.* Etienne Chiron, Paris, 1935.
10. L. DE BROGLIE. *Problémes de propagation guidée des ondes électromagnétiques.* Gauthier-Villars, Paris, 1941.
11. H. POINCARÉ. *Oeuvres.* Tome X. Gauthier-Villars, Paris.
12. F. N. DAVID. *Probability theory for statistical methods.* Cambridge University Press, 1949.
13. J. L. PAWSEY and R. N. BRACEWELL. *Radio Astronomy.* Clarendon Press, Oxford, 1954.
14. DR. WALDMEIER. *Ergebnisse und Probleme der Sonnenforschung.* Akademie Verlagsgesellschaft. Leipzig, 1941.
15. E. DURAND. *Electrostatique et magnétostatique.* Masson, Paris, 1953.
16. J. ORTUSI. *Propagation des ondes électromagnétiques de haute fréquence.* Société Française de documentation électronique. Paris, 1957.
17. GEORGES BOUDOURIS. *Propagation troposphérique.* Centre de Documentation Universitaire, Paris, 1957.
18. S. M. OSTROW. Handbook for CRPL Ionospheric Predictions. N.B.S. Handbook 90, Washington, 1962.
19. KENNETH DAVIES. *Ionospheric Radio Propagation.* N.B.S. Monograph 80, Washington, 1965.
20. PAUL O. LAITINEN and GEORGE W. HAYTON. Analysis and prediction of sky-wave field intensities in the high-frequency band. *Tech. Rep.* No. 9—U.S. Dept. of Commerce, Washington, 1963.
21. B. R. BEAN and E. J. DUTTON. *Radio Meteorology.* Dover Publications, New York, 1968.

II. TROPOSPHERIC PROPAGATION

101. K. BULLINGTON. Radio propagation at frequencies above 30 megacycles. *P.I.R.E.*, **35,** pp. 1122–1136, October 1947.
102. G. GOUDET and J. VOGE. Rayonnement et propagation des ondes électromagnétiques de courte longueur d'onde. Deuxième partie: Propagation des ondes électromagnétiques de courte longueur d'onde, par J. Voge. *Annales des télécom.*, **3,** pp. 155–179, May 1948; pp. 182–208, June 1948; pp. 233–256, July 1948.

103. S. MATSUO. The method of calculating the v.h.f. field intensity, and research on its variation. The reports of the development of the Electrical Communication Laboratory, No. 5, Tokyo, 1950.
104. H. G. BOOKER and W. E. GORDON. A theory of radio scattering in the troposphere *P.I.R.E.*, **38,** pp. 401–412, April 1950.
105. E. C. S. MEGAW. Scattering of electromagnetic waves by atmospheric turbulence *Nature*, **166,** pp. 1100–1104, December 1950.
106. D. K. BAILEY, R. BATEMAN *et al.* A new kind of radio propagation at very high frequencies observable over long distances. *Phys. Rev.*, **86,** April 1952.
107. K. BULLINGTON. Radio transmission beyond the horizon in the 40–4000 Mc. band. *P.I.R.E.*, **41,** pp. 132–135, January 1953.
108. E. C. S. MEGAW. Waves and fluctuations. *P.I.R.E.*, **100,** Part III, pp. 1–8, January 1953.
109. C. M. CRAIN, A. P. DEAM and J. R. GERHARD. Measurement of tropospheric index-of-refraction fluctuations and profiles. *P.I.R.E.*, **41,** pp. 284–290, February 1953.
110. J. C. SCHELLENG, C. R. BURROWS and E. B. FERRELL. Ultra short wave propagation. *P.I.R.E.*, **21,** pp. 427–463, March 1953.
111. F. VILLARS and V. F. WEISSKOPF. The scattering of electromagnetic waves by turbulent atmospheric fluctuations. *Phys. Rev.*, **94,** pp. 232–240, April 1954.
112. J. VOGE. Problèmes d'actualité dans l'étude de la transmission des ondes ultra-courtes. *Onde Electrique*, **34,** pp. 487–498, June 1954.
113. F. DU CASTEL and P. RIVET. Problèmes de propagation et conditions d'emploi des ondes ultra-courtes. Note préliminaire du *L.N.R.*, No. 180, 1955.
114. B. R. BEAN and F. N. MEANY. Some applications of the monthly median refractivity gradient in tropospheric propagation. *P.I.R.E.*. **43,** pp. 1419–1431, October 1955.
115. T. J. CARROLL and R. M. RING. Propagation of short radio-waves in a normally stratified troposphere. *P.I.R.E.*, **43,** pp. 1384–1390. October 1955.
116. C. M. CRAIN. Survey of airborne microwave refractometer measurements. *P.I.R.E.* **43,** pp. 1405–1411, October 1955.
117. I. H. GERKS. Factors affecting spacing of radio terminals in a u.h.f. link. *P.I.R.E.*, **43,** pp. 1290–1297, October 1955.
118. K. A. NORTON, P. L. RICE and L. E. VOGLER. The use of angular distance in estimating transmission loss and fading range for propagation through a turbulent atmosphere over irregular terrain. *P.I.R.E.*, **43,** pp. 1488–1526, October 1955.
119. F. VILLARS and V. F. WEISSKOPF. On the scattering of radio-waves by turbulent fluctuations of the atmosphere. *P.I.R.E.*, **43,** pp. 1232–1239, October 1955.
120. H. G. BOOKER and J. T. DE BETTENCOURT. Theory of radio transmission by tropospheric scattering using very narrow beams. *P.I.R.E.*, **43,** pp. 281–290, March 1955.
121. H. G. BOOKER. A theory of scattering by non-isotropic irregularities with applications to radar reflections from the aurora. *J. Atm. & Terr. Phys.*, **8,** pp. 204–221, May 1956.
122. R. A. SILVERMAN. Turbulent mixing theory applied to radio scattering. *J. of Appl. Phys.*, **27,** pp. 699–705, July 1956.
123. H. STARAS and A. D. WHEELON. Theoretical research on the troposcatter propagation in the U.S., 1954–1957. *U.R.S.I.*, Boulder 1957, Doc. 302.
124. B. M. FANNIN and K. J. JEHN. A study of radar elevation—angle errors due to atmospheric refraction. *I.R.E. Trans.*, **AP 5,** pp. 71–77, January 1957.
125. A. D. WHEELON. Spectrum of turbulent fluctuations produced by convective mixing of gradients. *Phys. Rev.*, **105,** pp. 1766–1710. March 1957.
126. R. A. SILVERMAN. Fading of radio waves scattered by dielectric turbulence. *J. of Appl. Phys.*, **28,** pp. 506–511, April 1957.
127. H. STARAS. Antenna-to-medium coupling loss. *I.R.E. Trans.*, **AP 5,** pp. 228–231, April 1957.
128. B. R. BEAN. Sur l'utilisation des observations météorologiques courantes en propagation radioélectrique. *Onde Electrique*, **37,** pp. 411–415, May 1957.
129. T. J. CARROLL and M. R. RING. Propagation des micro-ondes dans la zône d'ombre à

travers une couche d'air dont l'indice décroit de façon monotone. *Onde Electrique*, **37,** pp. 471–479, May 1957.

130. H. T. FRIIS, A. B. CRAWFORD AND D. C. HOGG. A reflection theory for propagation beyond the horizon. *B.S.T.J.*, **36,** pp. 627–644, May 1957.
131. J. B. SMITH and L. J. ANDERSON. L'importance du processus de réflexion dans les communications au-delà de l'horizon. *Onde Electrique*, **37,** pp. 485–490. May 1957.
132. A. D. WHEELON. Relation of radio measurements to the spectrum of tropospheric dielectric fluctuation. *J. of Appl. Phys.*, **28,** pp. 684–693, June 1957.
133. F. DU CASTEL and P. MISME. Réflexion d'une onde électromagnétique par une couche d'atmosphère présentant une variation d'indice de réfraction. *C.A. Acad. Sc. de Paris*, **246,** pp. 1838–1840, March 1958.
134. F. DU CASTEL, P. MISME and J. VOGE. Réflexions partielles dans l'atmosphère et propagation à grande distance. 1° partie. *Ann. Téléc.*, **13,** p. 209, 1958.
135. F. DU CASTEL, P. MISME and J. VOGE. Etude physique du feuilletage dans l'atmosphère. Congrès International de Propagation, Liège, October 1958.
136. C.C.I.R. Définition d'une atmosphère fondamentale de référence (Avis 369–1). Atmosphères de référence (Rapport 231–1) constantes de l'équation donnant l'indice de réfraction radioélectrique (Rapport 232). Oslo, 1966.
137. C.C.I.R. Mode de présentation des données obtenues au cours de l'étude de la propagation troposphérique des ondes (Avis 311). Oslo, 1966.
138. C.C.I.R. Courbes de propagation sur ondes métriques et décimétriques dans la gamme de fréquences comprise entre 30 et 1000 MHz (Avis 370–1). Résultats statistiques relatifs à la propagation dans le service de radiodiffusion et dans le service mobile dans la gamme de fréquences de 30 à 1000 MHz (Rapport 239–1). Oslo, 1966.
139. C.C.I.R. Estimation de l'affaiblissement de transmission de l'onde troposphérique (Rapport 244–1). Oslo, 1966.
140. C.C.I.R. Influence des régions non-ionisées de l'atmosphère sur la propagation des ondes (Rapport 233–1). Oslo, 1966.
141. H. BREMMER. Méthodes mathématiques appliquées dans la theorie de la propagation des micro-ondes. Conf. del Seminario de Matematica dell'Universitá de Bari 45–46 —Bologna, 1959.
142. J. A. SAXTON. Quelques réflexions sur la propagation des ondes radioélectriques à travers la troposphère. *Onde Electrique*, **40,** July–August, 1960.
143. LEANG-P-YEH. Simple methods for designing troposcatter circuits. *I.R.E. Trans.*, **CS 8,** No. 3, pp. 193–198, September 1960.
144. K. F. WRIGHT and J. E. COLE. Measured distribution of the duration of fades in tropospheric scatter transmission. *I.R.E. Trans.*, **AP 8,** pp. 594–598, November 1960.
145. B. R. BEAN. *Atmospheric bending of radio waves. Electromagnetic wave propagation.* Academic Press, London and New York, p. 163, 1960.
146. E. DU CASTEL, P. MISME and J. VOGE. *Sur le rôle des phénomènes de réflexion dans la propagation lointaine des ondes ultracourtes. Electromagnetic wave propagation.* Academic Press, London and New York, p. 671, 1960.
147. H. BREMMER. On the theory of wave propagation through a concentrically stratified troposphere with a smooth profile. I—Discussion of the extended WKB approximation. *J. Res. of the N.B.S. Div. Radio Propagation*, **64D,** pp. 31–52, September–October, 1960. II—Expansion of the rigorous solution. *Loc. cit.*, **66D,** pp. 31–52, January–February, 1962
148. M. W. GOUGH. *Diurnal influence in tropospheric propagation. Electromagnetic wave propagation.* Academic Press, London and New York, p. 557, 1960.
149. R. E. GRAY. Tropospheric scatter propagation and meteorological conditions in the Caribbean. *I.R.E. Trans.*, **AP 9,** pp. 492–496, September 1961.
150. I. BENOIEL. Interdependence between hourly median transmission loss and surface refractivity index observed at 900 Mc on a 232-mile far-beyond-the-horizon path. *I.R.E. Trans.*, **CS 9,** pp. 445–450, December 1961.

151. BRADFORD R. BEAN. The radio refractive index of the air. *P.I.R.E.*, **50,** pp. 260–273, March 1962.
152. A. W. STRAITON. Spectra of radio refractive index between ground level and 5000 ft above ground. *I.R.E. Trans.*, **AP 10,** pp. 732–737, November 1962.
153. J. H. CHISHOLM *et al.* Properties of 400 Mcps long-distance tropospheric circuits. *P.I.R.E.*, **50,** pp. 2464–2482, December 1962.
154. H. BREMMER. *Scattering by a perturbed continuum.* Symposium on electromagnetic theory and antennas, Copenhagen, 1962. Pergamon Press, New York, 1963.
155. C. D. BEACH and J. M. TRECKER. A method for predicting interchannel modulation due to multipath propagation in f.m. and p.m. tropospheric radio systems *B.S.T.J.*, **42,** pp. 1–36, January 1963.
156. DAG T. GJESSING and F. IRGENS. On the scattering of electromagnetic waves by a moving tropospheric layer having sinusoidal boundaries. *I.E.E.E. Trans.*, **AP 12,** pp. 51–64, January 1964.
157. P. L. RICE, A. G. LONGLEY and K. A. NORTON. Prediction of the cumulative distribution of ground wave and tropospheric wave transmission loss (Part I), N.B.S. Techn. Note No. 15, PB 151374, June 1959.
158. PAUL D. SHAFT. Information bandwidth of tropospheric scatter system. *I.R.E. Trans.*, **CS–9,** pp. 280–287, September 1961.
159. A. P. BARSIS, K. A. NORTON and P. L. RICE. Predicting the performance of tropospheric communication links, singly and in tandem. *I.R.E. Trans.*, **CS 10,** pp. 2–22, March 1962.
160. J. BATTESTI and LUCIEN BOITHIAS. Faisceaux hertzions transhorizon de faible longeur. *Ann. Téléc.*, **18,** pp. 72–77, March–April, 1963.
161. KAZUO TOKUNAGA and TOSHIO TANAKA. Experimental results of microwave attenuation due to rain along a path. *Electronics and Comm. in Japan*, **39,** pp. 63–70, February 1964.
162. JEAN BATTESTI and LUCIEN BOITHIAS. Etude des sections longues dans les faisceaux hertziens en visibilité. *Ann. Téléc.*, **19,** pp. 173–187, July–August 1964.
163. LUCIEN BOITHIAS and JEAN BATTESTI. Etude expérimentale de la baisse de gain d'antenne dans les liaisons transhorizon. *Ann. Téléc.*, **19,** pp. 221–229, September–October 1964.
164. L. BOITHIAS and P. MISME. Limites d'utilisation de l'indice de réfraction au sol (pour les liaisons troposphériques). *Ann. Téléc.*, **19,** pp. 241–244, November–December 1964.
165. CHARLES R. BURROWS. Ultra-short-wave propagation in the jungle. *I.E.E.E. Trans.*, **AP 14,** pp. 386–388, May 1966.
166. LUCIEN BOITHIAS and JEAN BATTESTI. Les faisceaux hertziens transhorizon de haute qualité. Affaiblisement de propagation at calcul des équipements. *Ann. Téléc.*, **20,** pp. 138–150, July–August 1965.
167. LUCIEN BOITHIAS and JEAN BATTESTI. Les faisceaux hertziens transhorizon de haute qualité (suite). *Ann. Téléc.*, **20,** pp. 237–254, November–December 1965.
168. D. TURNER, B. J. EASTERBROOK, C. ENG and G. E. GOLDING. Experimental investigation into radio propagation at 11–11·5 Gc/s. *P.I.E.E.*, **113,** pp. 1477–1479, September 1966.
169. R. W. CANNON, D. W. WILKINSON and G. C. RIDER. Operational experience with a tropospheric-scatter radio-relay link. *P.I.E.E.*, **113,** pp. 1490–1494, September 1966.
170. H. BREMMER. Semi-geometric-optical approaches to scattering phenomena. Symposium on quasi-optics. *Pol. Inst. of Brooklyn*, pp. 415–435, June 1964.
171. L. BOITHIAS and J. BATTESTI. Protection contre less évanouissements sur les faisceaux hertziens en visibilité. *C.N.E.T.*, Etude 821T, February 1967.
172. J. BATTESTI, J. BOITHIAS and P. MISME. Calcul des affaiblissements en propagation transhorizon à partir des paramètres radiométéorologiques. *C.N.E.T.*, Etude 859T, February 1968.
173. T. W. HARROLD. Attenuation of 8·6 mm wavelength radiation in rain. *P.I.E.E.*, **114,** pp. 201–203, February, 1967.

174. TADASHI AKIYAMA, SHOZO AYOGASHI and HARUIKO YOSHIDA. Variability of the angle of arrival of microwaves. *Electronics and Comm. in Japan*, **50,** pp. 60–67, February 1967.
175. J. BELL. Propagation measurements at 3·6 and 11 GHz over line-of-sight radio paths. *P.I.E.E.* **114,** pp. 545–549, May 1967.
176. A. NEJAT INCE and H. PAUL WILLIAMS. Design studies for reliable long-range ground-to-air communication. *I.R.E. Trans.*, **COM-15,** pp. 680–688, October 1967.
177. B. M. HICKIN. Atmospheric attenuation of radio signals above 10 GHz. *G.E.C.-A.E.J. Journal*, **35,** pp. 133–136, No. 3, 1968.
178. J. A. LANE. Small-scale variations of radio refractive index in the troposphere. *P.I.E.E.*, **115,** pp. 1227–1239, September 1968.
179. K. C. YEH and C. H. LIU. Displacement of rays in a turbulent medium. *I.E.E.E. Trans.*, **AP-16,** pp. 678–683, November 1968.
180. ARVIDS VIGANTS. Space-diversity performance as a function of antenna separation. *I.E.E.E. Trans.*, **COM-16,** pp. 831–836, December 1968.
181. ANTONY J. MONDOLOCH. Overwater propagation of millimeter waves. *I.E.E.E. Trans.*, **AP-17,** pp. 82–85, January 1969.
182. H. LAKE and J. F. ROCHE. Reliability of an 11 GHz communication system in a tropical environment. *Telecommunications*, January 1969.
183. PHILLIP A. BELLO. A troposcater channel model. *I.E.E.E. Trans.*, **COM-17,** pp. 130–137, April 1969.
184. M. P. M. HALL and C. M. COMER. Statistics of radio-refractive-index soundings taken over a 3-year period in the United Kingdom. *P.I.E.E.*, **116,** pp. 685–689, May 1969.

III. PROPAGATION THROUGH DIFFRACTION

200. H. POINCARÉ. Sur la diffraction des ondes électriques: à propos d'un article de M. MacDonald. *Proc. Royal Society*, **72,** pp. 42–52, 1904.
201. T. L. ECKERSLEY. On the connection between the ray theory and dynamics. *Proc. Royal Soc.*, Sect. A., **132,** pp. 83–98, 1931.
202. B. VAN DER POL. Über die Ausbreitung elektromagnetischer Wellen. *Zeitschr. für Hochfrequenztechnik und Elektroakustik*, **39,** pp. 152–156, 1931.
203. T. L. ECKERSLEY. Radio transmission problems treated by Phase Integral methods, *Proc. Royal Soc.*, Sect. A., **136,** pp. 499–527, 1932.
204. B. VAN DER POL and H. BREMMER. The diffraction of electromagnetic waves from an electrical point source round a finitely conducting sphere with application to radiotelegraphy and the theory of rainbows. *Phil. Mag.*, serial 7, **24,** pp. 141–176. July 1937, November supplement 1937, pp. 825–864, pp. 817–834, June 1939, **27,** pp. 261–275, March 1939.
205. K. A. NORTON. The calculation of ground wave field intensity over a finitely conducting spherical earth. *P.I.R.E.*, **29,** pp. 623–639, December 1941.
206. G. MILLINGTON. Ground wave propagation over an inhomogeneous smooth earth. *P.I.E.E.*, **96,** Part III, January 1949. *P.I.E.E.*, **97,** Part III, pp. 209–222, July 1950.
207. K. A. NORTON. Transmission loss of space waves propagated over irregular terrain. *I.R.E. Trans.*, **AP 3,** pp. 152–166, August 1952.
208. S. O. RICE. Diffraction of plane radio waves by a parabolic cylinder. *B.S.T.J.*, **33,** pp. 417–504, March 1954.
209. J. A. SAXTON. Basic ground-wave propagation characteristic in the frequency band 50–800 MHz. *P.I.E.E.*, **101,** Part III, pp. 211–214, July 1954.
210. J. A. SAXTON and B. N. HARDEN. Ground wave field—strength surveys at 100 and 600 MHz. *P.I.E.E.*, **101,** Part III, pp. 215–224, July 1954.
211. K. BULLINGTON. Reflection coefficient of irregular terrain. *P.I.R.E.*, **42,** pp. 1258–1262, August 1954.
212. H. BREMMER. The propagation over an inhomogeneous earth considered as a two-dimensional scattering problem. Electromagnetic wave propagation international conference—pp. 253–260, Brussels, 1958.

213. I. P. SHKAROFSKY, M. P. BACHYNSKI and H. E. NEUGEBAUER. Electromagnetic wave propagation over mountains. *I.R.E.* 1958 *Canadian Conv. Rec.*, pp. 115–120, Toronto, October 1958.
214. C.C.I.R. Courbes de propagation pour l'onde de sol aux fréquences inférieures à 10 MHz (Avis 368). Oslo, 1966.
215. ALBERT W. BIGGS. Radiation fields from a horizontal electric dipole in a semi-infinite conducting medium. *I.R.E. Trans.*, **AP 10,** pp. 358–362, June 1962.
216. RABINDRA N. GHOSE. The long-range subsurface communication system. *I.R.E. Trans.*, **CS 9,** pp. 590–596, December 1961.
217. GEORGES H. GRENIER. Obstacle gain and shadow loss. *Microwave Journal*, **V,** pp. 60–68, July 1962.
218. I.E.E.E. Transactions on Antennas and Propagation, **AP 11,** May 1963. (Special issue on electromagnetic waves in the earth.)
219. A. D. WATTS, F. S. MATTHEWS and E. L. MAXWELL. Some electrical characteristics of the earth's crust. *P.I.R.E.*, **51,** pp. 897–910, June 1963.
220. S. UGAY, S. AOYAGI and S. NAKAHARA. Microwave transmission across mountain ridges by using diffraction grattings. *Electronics and Comm. in Japan*, **46,** pp. 7–17, May 1963.
221. H. T. DOUGHERTY and L. J. MALONEY. Application of diffraction by convex surfaces to irregular terrain situation. *Radio Sci. Journal of Research N.B.S.*, **68D,** pp. 239–250, February 1964.
222. M. TAKADA and M. SHINJI. An application of the diffractor grating to the 11 Gc/s microwave system. *I.E.E.E. Trans.*, **AP 13,** pp. 532–541, July 1965.
223. R. J. KING, S. W. MALEY and J. R. WAIT. Ground-wave propagation along three-section mixed path. *P.I.E.E.*, **113,** pp. 747–751, May 1966.
224. JACQUES DEYGOUT. Multiple knife-edge diffraction of microwaves. *I.E.E.E. Trans.*, **AP 14,** pp. 480–489, July 1966.
225. A. B. CARLSON. Microwave propagation over mountain-diffraction paths. *I.E.E.E. Trans.*, **AP 14,** pp. 489–496, July 1966.
226. E. SOFAER and J. W. STARK. Tropospheric radio-wave propagation over mixed land and sea paths. *P.I.E.E.*, **113,** pp. 1291–1298, August 1966.
227. C.C.I.R. Détermination des caractéristiques électriques de la surface de la terre (Rapport 229). Oslo, 1966.
228. C.C.I.R. Propagation de l'onde de sol sur terrain non homogène (Rapport 230). Oslo, 1966.
229. JAMES R. WAIT. Some factors concerning electromagnetic wave propagation in the earth's crust. *P.I.E.E.*, **54,** pp. 1020–1025, August 1966.
230. P. KNIGHT and R. D. C. THODAY. Influence of the ground near transmitting and receiving aerials on the strength of medium-frequency sky waves. *P.I.E.E.*, **116,** pp. 911–919, June 1969.
231. R. EDWARDS and J. DURKIN. Computer prediction of service areas for mobile radio networks. *P.I.E.E.*, **116,** pp. 1493–1500, September 1969.

IV. IONOSPHERIC PROPAGATION

301. S. CHAPMAN. The absorption and dissociative or ionizing effect of monochromatic radiation in an atmosphere on a rotating earth. *Proc. Phys. Soc.*, **43,** pp. 26–45, January 1931.
302. M. MAYOT. La prévision des taches solaires. *Annales d'Astrophysique*, **10,** pp. 222–236, 1947.
303. M. MAYOT. Sur la prévision des taches solaires. *C.R. Acad. Sc. de Paris*, **224,** pp. 1699–1701, 1947.
304. J. A. RATCLIFFE. Diffraction from the ionosphere and the fading of radio waves. *Nature*, **162,** p. 9, July 1948.

305. R. GALLET and K. RAWER. La relation a longue période entre l'ionisation de la couche F, et l'activité solaire sur l'ensemble du globe. *Ann. de géophysique*, **6**, pp. 104–114 and 211, 1950.
306. E. ARGENCE, M. MAYOT and K. RAWER. Contribution à l'étude de la distribution électronique de l'ionosphère et de l'absorption des ondes courtes. *Annales d'Astrophysique*, **13**, 242–285, 1950.
307. D. LEPECHINSKY. Effects of temperature variations of the upper atmosphere on the formation of ionospheric layers. *J. of Atm. & Terr. Phys.*, **1**, pp. 278–285, 1951.
308. M. MAYOT. La prévision du nombre de Wolf et l'analyse linéaire. *Annales d'Astrophysique*, **14**, pp. 232–235, 1951.
309. C. W. ALLEN. World-wide diurnal variations in the F_2 region. *J. of Atm. & Terr. Phys.*, **4**, pp. 53–67, 1953.
310. E. ARGENCE and M. MAYOT. Méthode de détermination des hauteurs vraies des couches de l'ionosphère, compte-tenue de l'action du champ magnétique terrestre. *J. Geoph. Res.*, **58**, pp. 147–169, June 1953.
311. G. PILLET. Vérification des prévisions du B.I.F. par les enregistrements de W.W.V. et W.W.V.H. à Paris et en terre Adélie. Note préliminaire du *L.N.R.*, No. 166, 1953.
312. L. R. O. STOREY. An investigation of whistling atmospherics. *Phil. Trans. Roy. Soc.*, A, **246**, pp. 113–141, July 1953.
313. D. LEPECHINSKY. *L'ionosphère et la propagation des ondes radioélectriques. Annuaire du bureau des longitudes pour l'an* 1954. Gauthier-Villars, Paris, 1954.
314. J. M. WATTS and J. N. BROWN. Some results of sweep-frequency investigation in the low frequency band. *J. Geoph. Res.*, **59**, pp. 71–86, March 1954.
315. M. NICOLET. Meteor ionization and the night time E layer. *J. of Atm. & Terr. Phys.*, special supplement on meteor physics, **2**, pp. 99–110, 1955.
316. O. G. VILLARD, V. R. ESHELMAN, L. A. MANING and A. M. PETERSON. The role of meteors in extended-range v.h.f. propagation. *P.I.R.E.*, **43**, pp. 1473–1480, October 1955.
317. D. LEPECHINSKY. On the existence of QL and QT transition level in the ionosphere and its experimental evidence and effect. *J. of Atm. & Terr. Phys.*, **8**, No. 6, pp. 297–304, June 1956.
318. D. LEPECHINSKY. The QL and QT transition level. *J. of Atm. & Terr. Phys.*, **10**, No. 4, pp. 243–244, 1957.
319. J. A. SAXTON. La physique de la diffusion ionosphèrique sur ondes métriques. *Onde Electrique*, **37**, pp. 450–455, May 1957.
320. K. J. BUDDEN. The 'waveguide' mode theory of the propagation of v.l.f. radiowaves. *P.I.R.E.*, **45**, pp. 772–774, June 1957.
321. J. R. WAIT. The attenuation *vs.* frequency characteristics of v.l.f. radiowaves. *P.I.R.E.*, **45**, pp. 768–771, June 1957.
322. J. R. WAIT. The mode theory of v.l.f. ionospheric propagation for finite ground conductivity. *P.I.R.E.*, **45**, pp. 760–767, June 1957.
323. A. H. WAYNICK. The present state of knowledge concerning the lower ionosphere. *P.I.R.E.*, **45**, pp. 741–749, June 1957.
324. C.C.I.R. Propagation des ondes métriques, par l'intermédiaire de la région E sporadique ou par d'autres phénomènes d'ionisation anormale (Rapport 259–1). Oslo, 1966.
325. C.C.I.R. Evanouissement des signaux se propageant par l'ionosphère (Rapport 266–1). Oslo, 1966.
326. C.C.I.R. Disponibilité et échange de données de base pour les prévisions concernant la propagation (Rapport 248–1). Oslo, 1966.
327. E. V. APPLETON. The normal E region of the ionosphere. *P.I.R.E.*, **47**, pp. 155–159, 1959.
328. W. W. BERNING. Earth satellite observations of the ionosphere. *P.I.R.E.*, **47**, pp. 280–288, February 1959.
329. L. BIERMANN and R. LUST. Radiation and particle precipitation upon the earth from solar flares. *P.I.R.E.*, **47**, pp. 209–210, February 1959.

330. H. FRIEDMAN. Rocket observations of the ionosphere. *P.I.R.E.*, **47,** pp. 272–280, February 1959.
331. R. M. GALLET. The very-low-frequency emissions generated in the earth's exosphere. *P.I.R.E.*, **47,** pp. 211–231, February 1959.
332. R. A. HELLIWELL and M. G. MORGAN. Atmospheric whistlers. *P.I.R.E.*, **47,** pp. 200–208, February 1959.
333. V. I. KRASSOUSKY. Exploration of the upper atmosphere with the help of the third soviet sputnik. *P.I.R.E.*, **47,** pp. 289–296, February 1959.
334. K. I. MAEDA and T. SATO. The F region during magnetic storms. *P.I.R.E.*, **47,** pp. 232–239, February 1959.
335. L. A. MANNING and V. R. ESHLEMAN. Meteors in the ionosphere. *P.I.R.E.*, **47,** pp. 186–199, February 1959.
336. D. F. MARTYN. The normal F region of ionosphere. *P.I.R.E.*, **47,** pp. 147–155, February 1959.
337. M. NICOLET. The constitution and composition of the upper atmosphere. *P.I.R.E.*, **47,** pp. 142–147, February 1959.
338. M. PETERSON, R. D. EGAN and D. S. PRATT. The IGY three-frequency backscatter sounder. *P.I.R.E.*, **47,** pp. 300–314, February 1959.
339. C.C.I.R. Propagation par diffusion ionosphérique (Rapport 260–1). Oslo, 1966. Systèmes radioélectriques employant la propagation par diffusion dans l'ionosphère (Rapport 109–1). Oslo, 1966.
340. W. B. JONES and R. M. GALLET. Ionospheric mapping by numerical methods. *Journal U.I.T.*, **27,** pp. 260e–264e, December 1960.
341. KENNETH A. NORTON. *Low and medium frequency radio propagation. Electromagnetic wave propagation*, pp. 375–444. Academic Press, New York, 1960.
342. J. S. GREENHOW and E. L. NEUFELD. *Turbulence in the lower E-region from meteor echo observations. Electromagnetic wave propagation*, p. 493. Academic Press, New York, 1960.
343. G. A. DESCHAMPS and W. L. WEEKS. Charts for computing the refractive index of a magneto-ionic medium. *I.R.E. Trans.*, **AP 10,** pp. 305–317, May 1962.
344. R. NAISMITH. A new method of ionospheric forecasting. *P.I.E.E.*, **109,** Part B, pp. 125–130, March 1962.
345. J. RALPH JOHLER. Propagation of the low-frequency radio signal. *P.I.R.E.*, **50,** pp. 404–427, April 1962.
346. JAMES R. WAIT. Introduction to the theory of v.l.f. propagation. *P.I.R.E.*, **50,** pp. 1624–1647, July 1962.
347. H. GREENBERG *et al.* Optimum h.f. prediction. *I.R.E. Trans.*, **AP 10,** pp. 325–327, May 1962.
348. PIERRE HALLEY and ANNE-MARIE GERVAISE. Essai d'une prévision à long terme de l'activité solaire (paramètres du 20eme cycle). *Ann. Téléc.*, **18,** pp. 94–105, May–June 1963.
349. T. LAASPERE, M. G. MORGAN and W. C. JOHNSON. Chorus, hiss and other audio-frequency emissions at stations of the whistlers east-network. *P.I.E.E.*, **52,** pp. 1331–1348, November 1964.
350. P. R. ARENDT, A. PAPAYOANOU and H. SOICHER. Determination of the ionospheric electron content utilizing satellite signals. *P.I.E.E.*, **53,** pp. 268–277, March 1965.
351. A. LEBEAU. Matière ionisée et courant électroniques dans l'environnement terrestre. *Onde Electrique*, No. 471, pp. 690–695, June 1966.
352. C. RENARD. Détermination des paramètres constitutifs de l'ionosphère entre 78 et 100 km d'altitude par la mesure locale du champ TBF rayonné par un émetteur au sol. *Ann. Téléc.*, **21,** pp. 117–135, May–June 1966.
353. C. RENARD. Détermination de la densité électronique de l'ionosphère au-desus de 100 km d'altitude par la mesure locale du champ TBF rayonné par un émetteur au sol. *Ann. Téléc.*, **27,** pp. 169–183, July–August 1966.
354. C.C.I.R. Choix d'indices d'activité solaire pour la propagation ionosphérique (Avis 371). Choix des indices fondamentaux de la propagatio n ionosphérique (Rapport 246–1). Oslo, 1966.

355. C.C.I.R. Sondages ionosphériques sous incidence oblique (Rapport 249–1). Propagation troposphérique à grande distance sans réflexions intermédiaires sur le sol (Rapport 250–1). Oslo, 1966.
356. C.C.I.R. Evaluation de l'intensité du champ et de l'affaiblissement de transmission de l'onde d'espace pour les fréquences comprises entre les limites approximatives de 1,5 et 40 MHz (Rapport 252–1). Oslo, 1966.
357. C.C.I.R. Propagation des ondes myriamétriques dans l'ionosphère et à travers l'ionosphère (Rapport 262–1). Oslo, 1966.
358. M. JOACHIM. Progrès récents dans la prévision à long terme de la propagation ionosphérique des ondes radioélectriques. Conférence prononcée à l'U.I.T., 25 January, 1967 (H.C.).
359. L. M. MUGGLETON. Dependence of ionospheric absorption on solar zenith angle. *P.I.E.E.*, **113**, pp. 1909–1912, December 1966.
360. H. RISBETH. A review of ionospheric F region theory. *P.I.E.E.*, **55**, pp. 16–35, January 1967.
361. W. C. BAIN and B. R. MAY. D region electron-density distribution data. *P.I.E.E.*, **114**, pp. 1593–1597, November 1967.
362. GUY VASSEUR and ROBERT FELSTEIN. Calcul des profils d'ionisation à partir de sondages ionosphériques en contre-haut et en contre-bas. *Ann. Télécom.*, **23**, July–August 1968.
363. P. J. D. GETHING, J. G. MORRIS, E. G. SHEPHERD and D. V. TIBBLE. Measurement of elevation angles of h.f. waves. *P.I.E.E.*, **116**, pp. 185–193, February 1969.
364. T. MURAKAMI and G. S. WICKIZER. Ionospheric phase distortion and Faraday rotation of radio waves. *R.C.A. Review*, pp. 475–503, September 1969.
365. H. H. INSTON. Dispersion of h.f. pulses by ionospheric reflection. *P.I.E.E.*, **116**, pp. 1789–1793, November 1969.
366. T. B. JONES and W. KEENLISIDE. Comparison of measured and calculated oblique-incidence radiowave propagation characteristics. *P.I.E.E.*, **117**, pp. 16–22, January 1970.
367. C.C.I.R. Atlas d'ionisation. Rapport spécial No. 340.
368. C.C.I.R. Interim method for estimating sky-wave field strength and transmission loss at frequencies between the approximate limits of 2 and 30 MHz. *C.C.I.R. Report 252–2*, New Delhi, 1970.

V. NOISE—STATISTICAL DAMPING

401. LORD RAYLEIGH. On the resultant of a large number of vibrations of the same pitch and arbitrary phase. *Phil. Mag.*, 5° série, **10**, p. 73, August 1880.
402. H. A. THOMAS and R. E. BURGESS. Survey of existing information and data on radio noise over the frequency range 1–30 Mc. Dept. of scientific and industrial research, special report No. 15. H.M. Stationery Office, London, 1947.
403. R. J. PIERCE. Noise in resistances and electron stream. *B.S.T.J.*, **27**, pp. 158–174, January 1948.
404. S. O. RICE. Mathematical analysis of random noise. *B.S.T.J.*, **23**, No. 3, pp. 272–332, July 1944, **24**, No. 1, pp. 46–156, January 1945, **27**, pp. 109–157, January 1948.
405. M. LAFFINEUR. Le rayonnement radioélectrique du soleil et de la voie lactée. *Onde Electrique*, No. 272, pp. 402–407, November 1949.
406. R. BUREAU and R. BOST. Sur les foyers d'atmosphériques. Notes préliminaires du *L.N.R.*, Nos. 152 and 154, 1951.
407. H. V. COTTONY and J. R. JOHLER. Cosmic radio noise intensities in the v.h.f. band. *P.I.R.E.*, **40**, p. 1053, September 1952.
408. F. CARBENAY. Correspondence entre le niveau moyen des atmosphériques et le degré d'intelligibilité d'une liaison radioélectrique sur onde kilométrique. *C.R. Ac. Sci. de Paris*, **235**, pp. 423–425 and p. 652, 1952.
409. K. A. NORTON. Transmission loss in radio propagation. *P.I.R.E.*, **41**, pp. 146–152, January 1953.

410. S. O. RICE. Statistical fluctuations of radio field strength far beyond the horizon. *P.I.R.E.*, **41**, pp. 274–281, February 1953.
411. J. C. SIMON. Quelques problèmes de fluctuation en radioélectricité. *Ann. Radioélectricité*, **X**, pp. 4–19, January 1955.
412. D. G. BRENNAN. On the maximum signal-to-noise ratio realizable from several noisy signals. *P.I.R.E.*, **43**, p. 1530, October 1955.
413. K. A. NORTON, L. E. VOGLER, M. W. MANSFIELD and P. J. SHORT. The probability distribution of a constant vector plus a Rayleigh distributed vector. *P.I.R.E.*, **43**, pp. 1354–1361. October 1955.
414. B. B. JACOBSEN. Thermal noise in multi-section radiolink. *P.I.E.E.*, Part C, **105**, pp. 139–150, March 1958.
415. C.C.I.R. Measurement of field strength, power flux density (field intensity), radiated power, available power from the receiving antenna and transmission loss (Report 227). Genève, 1963.
416. C.C.I.R. Largeur de bande et rapport signal/bruit dans l'ensemble du circuit (Avis 339–1). Oslo, 1966.
417. C.C.I.R. Marges contre les évanouissements pour les diverses classes d'émission (Avis 340). Oslo, 1966.
418. C.C.I.R. Utilisation des données sur les bruits atmosphériques radioélectriques (Avis 372). Oslo, 1966.
419. C.C.I.R. Répartition mondiale et caractéristiques des bruits atmosphériques radioélectriques (Rapport 322). Genève, 1964.
420. C.C.I.R. Faisceaux hertziens de téléphonie. Bruits tolérables pendant de très courtes périodes de temps sur les liaisons en visibilité directe (Rapport 130). Oslo, 1966.
421. HAROLD E. CURTIS. Probability distribution of noise due to fading on multi-section f.m. microwave systems. *I.R.E. Trans.*, **CS 7**, pp. 161–167, September 1959.
422. C. CLARKE. Atmospheric radio-noise studies based on amplitude-probability measurements at Slough, England, during the IGY. *Proc. I.E.E.E.*, **109**, Part B, pp. 393–404, September 1962.
423. BRUCE B. BARROW. Diversity combination of fading signals with unequal mean strengths. *I.R.E. Trans.*, **CS 11**, pp. 73–78, March 1963.
424. LUCIEN BOITHIAS and JEAN BATTESTI. Puissance moyenne de bruit dans les faisceaux hertziens transhorizon à modulation de fréquence. *Ann. Téléc.*, **18**, pp. 88–93, May–June 1963.
425. B. SHEFFIELD. Nomograms for the statistical summation of noise in multihop communications systems. *I.E.E.E. Trans.*, **CS 11**, pp. 285–288, September 1963.
426. P. A. BRADLEY and C. CLARKE. Atmospheric radio noise and signals received on directional aerials at high frequencies. *P.I.E.E.*, **111**, pp. 1534–1540, September 1964.
427. D. TURNER. Results of noise measurements on an operational s.h.f. radio-link. *P.I.E.E.*, **111**, pp. 1541–1545, September 1964.
428. K. W. PEARSON. Method for the prediction of the fading performance of a multi-section microwave link. *P.I.E.E.*, **112**, pp. 1291–1300, July 1965.
429. OLU IBUKUN. Structural aspects of atmospheric radio noise in the tropics. *P.I.E.E.*, **54**, pp. 361–366, March 1966.
430. CHARLES A. PARRY. The maximum capacity of tandem link multichannel troposcatter system. *I.E.E.E. Trans.*, **COM 14**, pp. 130–139, April 1966.
431. A. PICQUENARD. A combinação das distribuições estatísticas na propagação das ondas radioelétricas. 1° Congresso Nacional de Engenharia Electrônica, São José dos Campos—January 1965 (à paraître).
432. A. PICQUENARD. Os calculos dos circuitos telefônicos sôbre micro-ondas. Monografia INBELSA No. 1—São Paulo, 1965.
433. AVID VIGANTS. Number and duration of fades at 6 and 4 GHz. *B.S.T.J.*, **50**, pp. 815–841, March 1971.
434. W. Y.-S. CHEN. Estimated outage in long-haul radio-relay systems with protection switching. *B.S.T.J.*, **50**, pp. 1455–1485, April 1971.

INDEX